Vol. 288, No. 3, April 11, 1994
Completing Volume 288

ISSN 0003-2670

ANALYTICA CHIMICA ACTA

An international journal devoted to all branches of analytical chemistry

ELSEVIER

ANALYTICA CHIMICA ACTA

Scope. *Analytica Chimica Acta* publishes original papers, rapid publication letters and reviews dealing with every aspect of modern analytical chemistry. Reviews are normally written by invitation of the editors, who welcome suggestions for subjects. Letters can be published within **four months** of submission. For information on the Letters section, see inside back cover.

Submission of Papers

Americas

Prof. Harry L. Pardue
Department of Chemistry
1393 BRWN Bldg, Purdue University
West Lafayette, IN 47907–1393
USA

Tel:(+1-317) 494 5320
Fax:(+1-317) 496 1200

Computer Techniques

Prof. J.T. Clerc
Universität Bern
Pharmazeutisches Institut
Baltzerstrasse 5, CH-3012 Bern
Switzerland

Tel:(+41-31) 6314191
Fax:(+41-31) 6314198

Prof. Sarah C. Rutan
Department of Chemistry
Virginia Commonwealth University
P.O. Box 2006
Richmond, VA 23284-2006
USA
Tel:(+1-804) 367 1298
Fax:(+1-804) 367 7517

Other Papers

Prof. Alan Townshend
Department of Chemistry
The University
Hull HU6 7RX
Great Britain

Tel:(+44-482) 465027
Fax:(+44-482) 466410

Prof. Willem E. van der Linden
Laboratory for Chemical Analysis
Department of Chemical Technology
Twente University of Technology
P.O. Box 217, 7500 AE Enschede
The Netherlands
Tel:(+31-53) 892629
Fax:(+31-53) 356024

Prof. Paul Worsfold
Dept. of Environmental Sciences
University of Plymouth
Plymouth PL4 8AA
Great Britain

Tel:(+44-752) 233006
Fax:(+44-752) 233009

Submission of an article is understood to imply that the article is original and unpublished and is not being considered for publication elsewhere. *Anal. Chim. Acta* accepts papers in English only. There are no page charges. Manuscripts should conform in layout and style to the papers published in this issue. See inside back cover for "Information for Authors".

Publication. *Analytica Chimica Acta* appears in 16 volumes in 1994 (Vols. 281–296). *Vibrational Spectroscopy* appears in 2 volumes in 1994 (Vols. 6 and 7). Subscriptions are accepted on a prepaid basis only, unless different terms have been previously agreed upon. It is possible to order a combined subscription (*Anal. Chim. Acta* **and** *Vib. Spectrosc.*).
Our p.p.h. (postage, packing and handling) charge includes surface delivery of all issues, except to subscribers in the U.S.A., Canada, Australia, New Zealand, China, India, Israel, South Africa, Malaysia, Thailand, Singapore, South Korea, Taiwan, Pakistan, Hong Kong, Brazil, Argentina and Mexico, who receive all issues by air delivery (S.A.L.–Surface Air Lifted) at no extra cost. For Japan, air delivery requires 25% additional charge of the normal postage and handling charge; for all other countries airmail and S.A.L. charges are available upon request.

Subscription orders. Subscription prices are available upon request from the publisher. Subscription orders can be entered only by calendar year and should be sent to: Elsevier Science B.V., Journals Department, P.O. Box 211, 1000 AE Amsterdam, The Netherlands. Tel: (+31-20) 5803 642, Telex: 18582, Telefax: (+31-20) 5803598, to which requests for sample copies can also be sent. Claims for issues not received should be made within six months of publication of the issues. If not they cannot be honoured free of charge. Readers in the U.S.A. and Canada can contact the following address: Elsevier Science Inc., Journal Information Center, 655 Avenue of the Americas, New York, NY 10010, U.S.A. Tel: (+1-212) 6333750, Telefax: (+1-212) 6333990, for further information, or a free sample copy of this or any other Elsevier Science journal.
Advertisements. Advertisement rates are available from the publisher on request.

US mailing notice – Analytica Chimica Acta (ISSN 0003-2670) is published 3 times a month (total 48 issues) by Elsevier Science B.V. (Molenwerf 1, Postbus 211, 1000 AE Amsterdam). Annual subscription price in the USA US$ 3035.75 (valid in North, Central and South America), including air speed delivery. Second class postage paid at Jamaica, NY 11431. *USA Postmasters*: Send address changes to Anal. Chim. Acta, Publications Expediting, Inc., 200 Meacham Av., Elmont, NY 11003. Airfreight and mailing in the USA by Publication Expediting.

ANALYTICA CHIMICA ACTA

An international journal devoted to all branches of analytical chemistry

(Full texts are incorporated in CJELSEVIER, a file in the Chemical Journals Online database available on STN International; Abstracted, indexed in: Aluminum Abstracts; Anal. Abstr.; Biol. Abstr.; BIOSIS; Chem. Abstr.; Curr. Contents Phys. Chem. Earth Sci.; Engineered Materials Abstracts; Excerpta Medica; Index Med.; Life Sci.; Mass Spectrom. Bull.; Material Business Alerts; Metals Abstracts; Sci. Citation Index)

VOL. 288 NO. 3 APRIL 11, 1994

CONTENTS

(Continued overleaf)

Contents (continued)

ELSEVIER

Analytica Chimica Acta 288 (1994) 131–139

ANALYTICA CHIMICA ACTA

Methods for kinetic analysis of simultaneous, first-order reactions in waters: the kinetic model and methods for data analysis

Yanjia Lu [a], C.L. Chakrabarti [a,*], M.H. Back [b], D.C. Grégoire [c], W.H. Schroeder [d], A.G. Szabo [e], L. Bramall [e]

[a] *Ottawa-Carleton Chemistry Institute, Department of Chemistry, Carleton University, 1125 Colonel By Drive, Ottawa, Ontario K1S 5B6, Canada*

[b] *Ottawa-Carleton Chemistry Institute, Department of Chemistry, University of Ottawa, Ottawa, Ontario K1N 6N5, Canada*

[c] *Geological Survey of Canada, 601 Booth St., Ottawa, Ontario K1S 0E8, Canada*

[d] *Atmospheric Environment Service, Environment Canada, 4905 Dufferin Street, Downsview, Ontario M3H 5T4, Canada*

[e] *Institute for Biological Sciences, National Research Council of Canada, Ottawa, Ontario K1A 0R6, Canada*

(Received 8th September 1993; revised manuscript received 17th November 1993)

Abstract

The graphical method and the iterative method for analysing kinetic data for metal speciation in waters are described. The graphical method involves successive subtractions of one component from the total concentration of the metal remaining, beginning with the slowest component. The iterative method uses nonlinear regression of the experimental data assuming different numbers of components to obtain the weighted residuals. The number of components which gives a minimum to the sum of squares of the weighted residuals represents the number of kinetically distinguishable components. The weighted residuals should also have a normal distribution throughout the course of the reaction. These methods were applied to simulated data for systems containing three components whose rate constants differed by a factor of two and for some cases by a factor of three. When the concentrations of each component were equal and the ratio of the rate constants equal to two, the values of the rate constants obtained by these analyses ranged from 2 to 19% of the assigned values, but the values for the initial concentrations were as much as 40% different from the assigned values. When the concentration of one component was altered the reliability of its recovered rate constant and initial concentration decreased. The advantage of the iterative method is that no prior knowledge of the number of components, rate constants and initial concentrations is required. It is demonstrated that both of these methods provide simple, reliable ways of analysing kinetic data for characterization of metal species in waters.

Key words: Ion exchange; Kinetic methods; Metal speciation; Waters

* Corresponding author.

SSDI 0003-2670(93)E0699-4

1. Introduction

Kinetic determinations of multicomponent systems are well established [1–5]. Kinetic analysis applied to metal speciation has been studied by a number of authors [6–11]. The main purpose of those studies was the estimation of the number of components and the kinetic parameters associated with each component. A graphical method [9], also called the Guggenheim method [12], and the kinetic spectrum method [8] (Laplace transform) have both been used to obtain values for the kinetic parameters. Non-linear regression methods were then used for further refinement of the parameters. When the difference between the rate constants was small or when the data were noisy, the graphical method could not supply readily distinguishable linear segments in the graph of ln(concentration) as a function of time and interpretation was difficult. The kinetic spectrum method suffered from the same problems and for the best resolution the rate constants should differ by a factor of 40, as indicated by Olson and Shuman [8]. Furthermore, the use of higher order derivatives in performing the Laplace transform requires an accuracy not available with most experimental data.

The purpose of the present study is to examine and compare these two methods, the graphical method and the iterative method, for the analysis of a sequence of consecutive first-order reactions to determine the number of components, the rate constants for each individual process and the initial concentration of each process. The graphical method is simple and direct and has been widely used for analysis of kinetic data [13,14]. Although its success rests heavily on the judgment of the analyst, it is useful to compare the results from this method with those from a more objective method, the iterative method. The iterative method is based on non-linear regression analysis [15–20] and has been used extensively in fluorescence decay kinetics [21]. The methods were tested using simulated data for a system containing three components with ratios of rate constants $k_1/k_2 = k_2/k_3 = 2$, using at first equal concentrations of each component. A factor of two may be considered a reasonable limit to the difference between rates for which resolution of components of a mixture may be achieved. The relative concentration of components is also an important factor in the accuracy of resolution and is illustrated by the results obtained on altering the concentration of each component by a factor of ten. The methods were also tested with a set of experimental data collected from a synthetic solution of aluminum. The advantages and limitations will be assessed.

2. The kinetic model

In studies of the kinetics of dissociation of naturally occurring metal complexes Chelex-100 cation exchange resin is frequently used as an efficient metal complexing agent. Chelex-100 resin is a co-polymer of styrene and divinylbenzene containing paired iminodiacetate ions which act as chelating groups in binding polyvalent metal ions. Its structure changes with pH as shown below [22]:

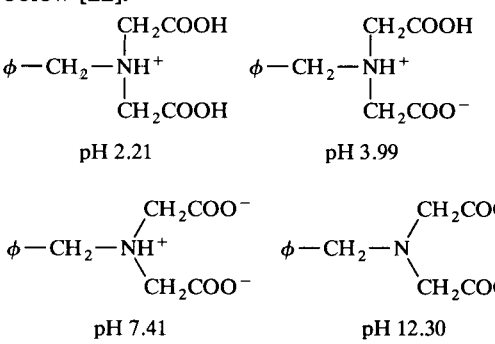

Chelex-labile metal includes free metal ion, as well as metal ion bound in complexes weaker than the Chelex–metal complex. In addition, metal complexes stronger than the Chelex–metal complex may appear as Chelex-labile if Chelex resin is present in large excess, as was the case in our experiments. The advantage of using Chelex resin for kinetic studies of metal speciation is that no other reagents are added and therefore perturbation of the system is small.

Following earlier work by Olson and Shuman [8], a kinetic model has been developed to describe the dissociation kinetics [6] of ML_i, where M is a metal ion and L_i stands for the ith ligand

(simple inorganic or organic ligand), or for the ith binding site on a polyfunctional ligand, such as humic materials. The model assumes that all these species dissociate independently and simultaneously at a rate that depends on the nature of the ligands, the functional group, its position on the macromolecule, and the residual charge. In this paper, we apply this model to the analysis of freshwater samples.

Consider a freshwater sample containing a mixture of n components in which each component, designated ML_i, exists in equilibrium with its dissociation products:

$$ML_i \rightleftharpoons M + L_i \quad (1)$$

For simplicity, the charge signs on metal ions are omitted. When a large excess of the Chelex-100 resin is added to this system, metal ions are taken up by the Chelex resin:

$$\text{Chelex} + M \rightleftharpoons \text{Chelex–M} \quad (2)$$

where Chelex stands for Chelex-100 resin. As the metal ion is removed from solution by this process the equilibrium 1 shifts to restore M. If the rate of uptake of M by Chelex is fast compared to the dissociation of the metal–ligand complex, ML_i, then the rate of loss of M from the solution is determined by the slower rate of dissociation of ML_i:

$$ML_i \xrightarrow{k_i} M + L_i \quad (3)$$

where k_i is the rate constant for the dissociation of component ML_i. The model therefore describes a system of simultaneous, first-order (or pseudo-first-order) reactions involving the various metal complexes present in the sample. The sum of the concentrations of all metal species remaining in the sample can be measured as a function of time. In freshwaters the metal complexes may be positively charged and these cationic species can be taken up directly by the Chelex resin without pre-dissociation. The rates, therefore, can also be described mechanistically as

$$ML_i + \text{Chelex} \xrightarrow{k_i} \text{Chelex–}ML_i \quad (4)$$

If the uptake for each component occurs simultaneously and independently, the rate constant measured for each component is the rate constant of the complexation reaction between metal complex and the Chelex resin. Since the Chelex resin is added in large excess, the reactions described by Eq. 4 are pseudo-first-order. Therefore, in both cases, the sum of the concentrations of all components in the sample at time t can be described as:

$$C(t) = \sum_{i=1}^{n} C_i^0 \exp(-k_i t) \quad (5)$$

where C_i^0 is the initial concentration of ML_i, the ith metal complex component. In the case of freshwater samples, the number of metal complexes, their initial concentrations and rate constants for dissociation are unknown. The methods of analysis to be adopted must be able to find the best values for each of these unknown quantities in an appropriately objective manner.

3. Methods for data analysis

The two methods mentioned earlier will be used to illustrate the analysis of the data without any prior knowledge or assumption about the number of components or the rate constants for dissociation. First, the simple graphical method, described by Saltzman [13], and second, the iterative method, a direct non-linear regression analysis of Eq. 5 following the method outlined by McKinnon et al. [21] will be examined for the conditions under which the number of components may be determined and reliable values for the kinetic parameters may be obtained. Two sets of data were analyzed. The first set was simulated using a mixture of three components according to the following equation:

$$C(t) = C_1^0 \exp(-k_1 t) + C_2^0 \exp(-k_2 t) + C_3^0 \exp(-k_3 t) \quad (6)$$

where $k_1/k_2 = k_2/k_3 = 2$. The initial concentrations, C_1^0, C_2^0 and C_3^0 were varied by factors of 10. Poisson noise was added to the simulated data. The second set was experimental measurements of the rate of uptake of aluminum by Chelex-100 resin from a synthetic solution. The computer programm used in this study is a non-linear regression package [23] (an on-line interactive routine on the computer network at Carleton Uni-

versity) which uses the Levenberg-Marquardt method for computing parameter estimates.

3.1. The graphical method

If metal ions are lost from solution by first-order processes a plot of ln(concentration of metal ion) as a function of time will have curvature if dissociation of more than one metal complex contributes to the total loss of metal ion. The rates of dissociation of each complex must be separated by a series of subtractions of the concentration of each component from the total concentration remaining, beginning with the component with the slowest rate. At sufficiently long times all but the final (the slowest component) will have decayed and a linear segment will be unambiguously observed from which its rate constant may be obtained. The initial concentration is obtained by extrapolation to zero time. The concentration of this species is then subtracted from the total concentration, leaving a clear linear segment corresponding to the second slowest component in the mixture. The procedure may be repeated as many times as required. The values of the rate constants obtained by this procedure may be further refined by non-linear regression analysis of Eq. 5. The results of the analysis for the system containing equal concentrations of each component by the graphical method is illustrated in Fig. 1. The first inset (curve b) shows the logarithmic curve for the decay for all three components, clearly showing curvature, and the second inset (curve c) shows the curve for the remaining two components after subtraction of the slowest. The curvature is much less, but discernible. Concentrations lower than 0.01 μg/l ($\ln C = -4.6$), the detection limit of the measurement, were not included in the fitting process. Values for k_1, k_2 and k_3 and C_1^0, C_2^0 and C_3^0 were thus determined by the graphical method for each set of conditions. The actual values and the values obtained by this analysis are summarized in Table 1.

3.2. The iterative method

The iterative method is based on non-linear regression analysis of kinetic data. Eq. 5 is fitted

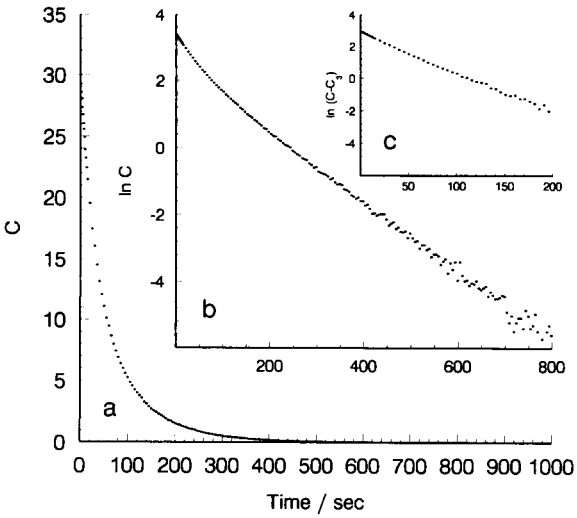

Fig. 1. Graphical method for the determination of the kinetic parameters for a simulated system with $k_1/k_2 = k_2/k_3 = 2$, $k_1 = 0.04$, $C_1 = C_2 = C_3 = 10$. (a) Plot of C as a function of time; (b) plot of ln C as a function of time; (c) plot of $\ln(C - C_3)$ as a function of time.

by non-linear regression assuming a number of components, starting with one and increasing until the sum of squares of the weighted residuals, defined as

$$\text{Sum of squares of weighted residuals} = \sum \left[\frac{C(t) - C_T(t)}{C(t)^{1/2}} \right]^2 \quad (7)$$

achieves a minimum value.

The plot of weighted residuals over the course of the reaction gives a visual indication of the adequacy of fitting for each point. With the correct number of components the plot of the weighted residuals should be randomly and uniformly distributed about zero throughout the course of the reaction. Non-uniform distribution of residuals, observed as curvature, indicates missing terms in the model [24].

The values of the sum of squares of the weighted residuals for the simulated data for equal concentration of all three components and for the cases when C_2 was reduced to one and increased to 100 are given in Table 2. In each system the sum of squares of the weighted residuals showed no change in increasing the number of components from 3 to 4 and three components only are kinetically distinguishable. The weighted

Table 1
Kinetic parameters determined for the simulated data ($k_1/k_2 = k_2/k_3 = 2$) by the graphical method and the iterative method

System	Parameter	Values assigned	Values determined	
			Graphical method	Iterative method
I	C_1	10.0	5.86	11.2
	C_2	10.0	13.3	8.66
	C_3	10.0	10.8	10.1
	k_1	0.0400	0.0475	0.0375
	k_2	0.0200	0.0231	0.0192
	k_3	0.0100	0.0102	0.0100
II	C_1	1.00	1.48	0.245
	C_2	10.0	10.5	10.4
	C_3	10.0	9.60	10.4
	k_1	0.0400	0.0536	0.0207
	k_2	0.0200	0.0185	0.0214
	k_3	0.0100	0.0100	0.0101
III	C_1	100	90.9	101
	C_2	10.0	19.9	9.13
	C_3	10.0	9.94	9.49
	k_1	0.0400	0.0423	0.0390
	k_2	0.0200	0.0226	0.0184
	k_3	0.0100	0.0100	0.0099
IV	C_1	10.0	10.7	10.6
	C_2	1.0		0.0845
	C_3	10.0	10.0	10.4
	k_1	0.0400	0.0365	0.0390
	k_2	0.0200		0.0394
	k_3	0.0100	0.0100	0.0100
V	C_1	10.0	106	9.09
	C_2	100	13.9	101
	C_3	10.0		10.1
	k_1	0.0400	0.0211	0.0414
	k_2	0.0200	0.0106	0.0201
	k_3	0.0100		0.0100
VI	C_1	10.0	7.24	10.4
	C_2	10.0	12.9	9.91
	C_3	1.00	1.02	0.690
	k_1	0.0400	0.049	0.0391
	k_2	0.0200	0.0215	0.0194
	k_3	0.0100	0.0100	0.0093
VII	C_1	10.0	14.8	2.24
	C_2	10.0		16.0
	C_3	100.0	105	102
	k_1	0.0400	0.0404	0.629
	k_2	0.0200		0.0278
	k_3	0.0100	0.0101	0.0100

Table 2
Sum of squares of the weighted residuals of iterative non-linear regression for the simulated 3-component systems

C_2	Number of component fitted	Sum of squares of the weighted residual
10.00	1	10.3
	2	0.0740
	3	0.0530
	4	0.0530
1.00	1	9.56
	2	0.0620
	3	0.0602
	4	0.0602
100.00	1	8.11
	2	0.133
	3	0.0646
	4	0.0646

residuals as a function of time for the simulated system where all components are of equal concentration are shown in Fig. 2. The distribution of the residuals with 3 components is better than with 2 components. Increasing the number of components to four generally caused no significant change in the distribution of the weighted

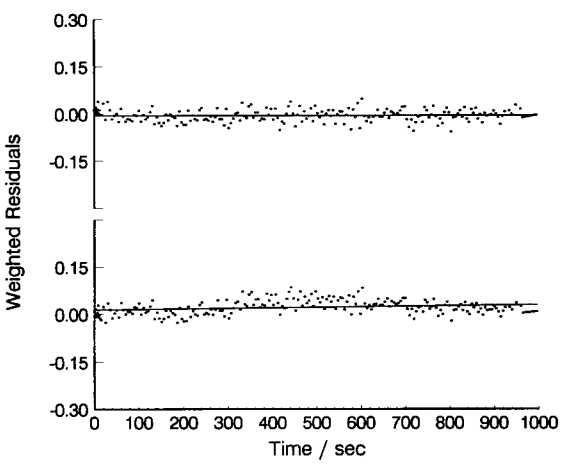

Fig. 2. Plots of the weighted residuals as a function of time for kinetic analysis of a simulated system with $k_1/k_2 = k_2/k_3 = 2$, $k_1 = 0.04$, $C_1 = C_2 = C_3 = 10$. Bottom trace: 2-component-fitting; top trace: 3-component-fitting.

residuals. Analysis by non-linear regression using four components, however, gave unrealistic and in some cases negative kinetic parameters.

When the choice is made of the number of components non-linear regression yields the kinetic parameters. The values of the rate constants and initial concentrations obtained by the iterative method are given in Table 1, where they may be compared with the values obtained by the graphical method. The values for the rate constants and initial concentrations determined by the iterative method were usually better but sometimes worse than those obtained by the graphical method. In the graphical method a component was sometimes missed completely, whereas the iterative method always gave values for the rate constant and initial concentration of each component chosen.

The accuracy of the analyses varied considerably among the three components. In general, rate constants and initial concentrations of the third component (the slowest) were determined within a few percent of the assigned values, except when $C_2/C_3 = 10$. The first component was the most poorly analyzed, the values having been obtained following two subtractions. Also, when the concentration of the component being subtracted was greater than that of the next slowest component by a factor of 10, the analysis for the latter was unreliable and sometimes indeterminate. As an example, analysis by the graphical method for the case where C_2 was reduced by a factor of ten is shown in Fig. 3. The second inset shows no curvature, indicating that the second component was effectively lost between the first and the third. Values for C_2 and k_2 were not obtained for this case by the graphical method. Fig. 4 shows the distribution of the weighted residuals for the same system. The fit with three components is not an improvement over that with two components. The iterative method therefore does not necessarily provide a more reliable indication of the number of components than the graphical method, even though kinetic parameters were evaluated from the non-linear regression analysis with three components.

The limitations in the relative ratio of concentration of each species which may be resolved from the other components and for which kinetic parameters may be obtained are important in analysis of freshwaters because concentrations of complexes may vary widely. The concentration range may be extended if there is a greater difference in the values of the rate constants.

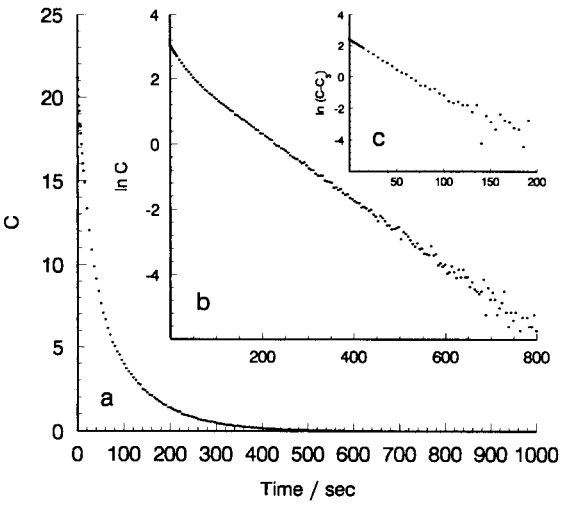

Fig. 3. Graphical method for the determination of the kinetic parameters for a simulated system with $k_1/k_2 = k_2/k_3 = 2$, $k_1 = 0.04$, $C_1 = C_3 = 10$, $C_2 = 1$. (a) Plot of C as a function of time; (b) plot of ln C as a function of time; (c) plot of $\ln(C - C_3)$ as a function of time.

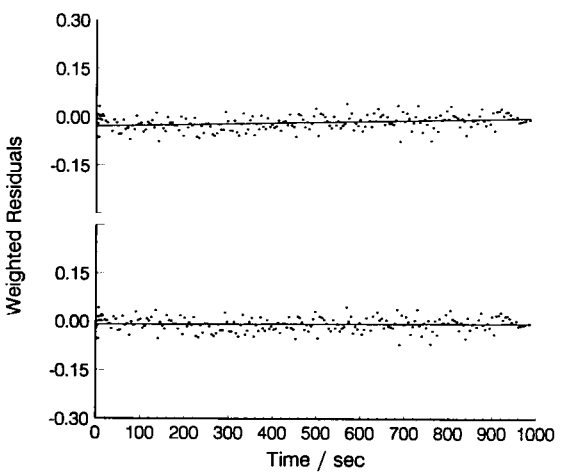

Fig. 4. Plots of the weighted residuals as a function of time for kinetic analysis of a simulated system with $k_1/k_2 = k_2/k_3 = 2$, $k_1 = 0.04$, $C_1 = C_3 = 10$, $C_2 = 1$. Bottom trace: 2-component-fitting; top trace: 3-component-fitting.

Table 3
Kinetic parameters determined for the simulated data ($k_1/k_2 = k_2/k_3 = 3$) by the graphical method and the iterative method

System	Parameter	Value assigned	Values determined	
			Graphical method	Iterative method
VIII	C_1	10.0	9.82	10.0
	C_2	10.0	10.2	9.94
	C_3	10.0	10.3	9.96
	k_1	0.0900	0.0918	0.0885
	k_2	0.0300	0.0302	0.0298
	k_3	0.0100	0.0101	0.00998
IX	C_1	10.0	10.5	8.96
	C_2	1.00		1.94
	C_3	10.0	10.1	10.1
	k_1	0.0900	0.0811	0.0948
	k_2	0.0300		0.0452
	k_3	0.0100	0.0100	0.0100
X	C_1	10.0		9.71
	C_2	100	108	100
	C_3	10.0	10.5	10.2
	k_1	0.0900		0.0902
	k_2	0.0300	0.0313	0.0301
	k_3	0.0100	0.0101	0.00100

The resolution of the three components is significantly improved when the ratio of rate constants is increased to three. The values of the rate constants and initial concentrations obtained by both the graphical method and the iterative method for the simulated data for equal concentration of all three components and for the cases when C_2 was reduced by a factor of 10 and increased by a factor of 10 are given in Table 3. The kinetic parameters for the system where all components are of equal concentration were obtained with errors less than 3%. For the systems where the concentration of C_2 was altered, the iterative method gave better results than the graphical method. When the concentration of one component was 10 times larger than the next faster component, the graphical method failed to detect the faster component.

These limitations to the analysis by the graphical method arise mainly from the difficulty in choosing the range of time over which the logarithmic function is linear. The degree of noise in the data clearly contributes to this difficulty. There is no objective method for this and success depends heavily on the judgment of the analyst. The iterative method has the advantage of being entirely objective but its limitations are nevertheless apparent in the values of Table 1.

3.3. Analysis of an aqueous sample of aluminum

A synthetic sample of aluminum was prepared by spiking ultrapure water with an appropriate volume of an aqueous solution of aluminum standard (1000 μg l^{-1} Al prepared from pure Al powder (SPEX), dissolved in 2% (v/v) HNO_3). The uptake of aluminum in the Chelex batch technique was measured as a function of time. The sum of the concentrations of all the kinetically distinguishable components of aluminum remaining in the sample was monitored as a function of time using inductively-coupled plasma mass spectrometry with the solution nebulization sample delivery technique.

The two methods were applied to experimental data collected from the synthetic aqueous solution of aluminum. Aluminum ions are equilibrated in water according to the following reactions:

$$Al^{3+} + OH^- \rightleftharpoons Al(OH)^{2+} \quad (9)$$

$$Al(OH)^{2+} + OH^- \rightleftharpoons Al(OH)_2^+ \quad (10)$$

$$Al(OH)_2^+ + OH^- \rightleftharpoons Al(OH)_3 \quad (11)$$

At pH 5, an aqueous solution of aluminum contains 37% of Al^{3+}, 35% of $Al(OH)^{2+}$, 23% of $Al(OH)_2^+$ and 5% of dissolved $Al(OH)_3$ (there was no precipitation of $Al(OH)_3$ under our experimental conditions) [25]. Fig. 5 shows a logarithmic plot of the uptake of Al(III) by Chelex resin from the aqueous solution of aluminum as a function of time. The application of the graphical method to this set of the experimental data given in Fig. 5 shows three kinetically distinguishable components, as indicated in the insets. The kinetic parameters are listed in Table 4.

The results of the application of the iterative method to the synthetic solution of aluminum are shown in Table 5. When the number of components in the model was increased from 1 to 3, the

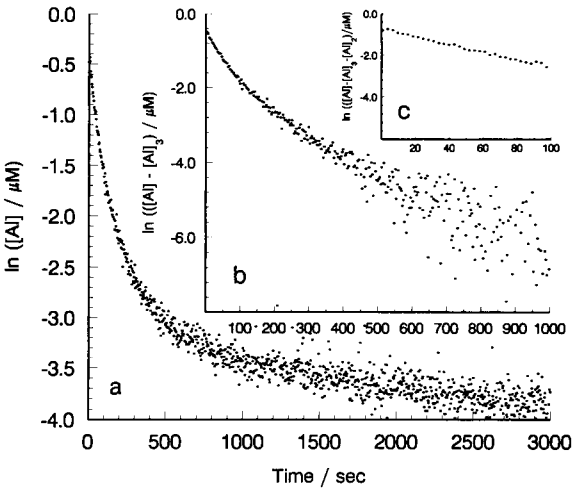

Fig. 5. Logarithmic plots of uptake of Al(III) by Chelex-100 from a synthetic, aqueous solution of aluminum. [Al(III)] = 6.5 μM, [Chelex] = 1% (w/w), pH 5.0, ionic strength = 3.9×10^{-5}, temperature = 20°C. (a) Plot of ln[Al(III)] as a function of time; (b) after the first subtraction; (c) after the second subtraction.

values of sum of squares of the weighted residuals decreased sharply, but when the number of components were increased from 3 to 4, no change occurred. The number of components in this synthetic solution is, therefore, 3, in agreement with the number obtained by the graphical method.

Fig. 6 shows the plots of the weighted residuals vs. time for the data from the analysis of aluminum in a synthetic solution. With a 3-component system, a random and normal distribution about zero was observed. The number of components of aluminum in the synthetic solution is, therefore, three, in agreement with that obtained by using the graphical method and by using the

Table 4
Kinetic parameters determined by the graphical method and the iterative method for a synthetic solution containing [Al(III)] = 0.65 μM, pH 5.0

Parameter	Graphical method	Iterative method
C_1^0, μM	0.45	0.43
C_2^0, μM	0.13	0.18
C_3^0, μM	0.039	0.039
k_1, s^{-1}	1.7×10^{-2}	2.1×10^{-2}
k_2, s^{-1}	4.5×10^{-3}	5.4×10^{-3}
k_3, s^{-1}	2.2×10^{-4}	2.2×10^{-4}

Table 5
Sum of squares of the weighted residuals of iterative non-linear regression for the kinetic data from a synthetic solution containing [Al(III)] = 0.65 μM, pH 5.0

Number of component fitted	Sum of squares of the weighted residuals
1	10.9
2	0.637
3	0.374
4	0.374

sum of squares of the weighted residuals. The initial concentrations and the rate constants of these components determined by non-linear regression are listed in Table 4. Both methods indicate three kinetically distinguishable components, and the rate constants of the components are in good agreement. The fact that three components with different rates of removal are distinguished in the aqueous solution indicates that the ionic species are not rapidly equilibrated. Since the ions (mononuclear species) represented in Eqs. 9–11 would most certainly be rapidly equilibrated, the species governing the removal of Al^{3+} are not these simple ions but must be of a more complex nature, probably, polynuclear species. However, the limited amount of data available

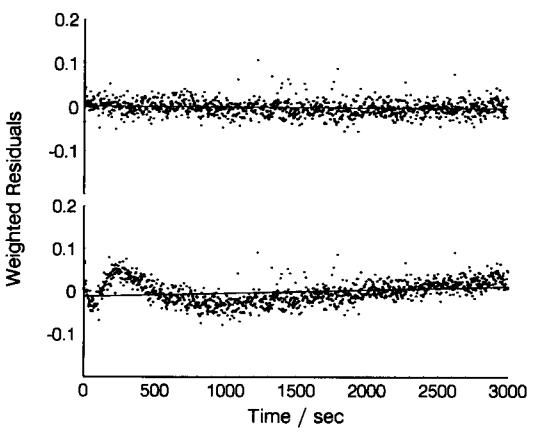

Fig. 6. Plots of the weighted residuals as a function of time for kinetic analysis of uptake of Al(III) by Chelex-100 from a synthetic, aqueous solution of aluminum. [Al(III)] = 6.5 μM, [Chelex] = 1% (w/w), pH 5.0, ionic strength = 3.9×10^{-5}, temperature = 20°C. Bottom trace: 2-component-fitting; top trace: 3-component-fitting.

does not justify further characterization of these species.

4. Conclusions

The analysis of the simulated data shows the reliability and the limitations of the two methods. The iterative method does not rely on a subjective assessment for the determination of the kinetic parameters but is still limited in the power to resolve reactions whose rate constants are close. The simple graphical method can often provide reasonable values for the kinetic parameters and is a useful complement to the iterative method. When the rate constants are as close as separated by a factor of two, analysis by both methods seems desirable. For both methods the quantity and the quality of the experimental data are of prime importance.

5. Acknowledgements

The authors are grateful to the Natural Sciences and Engineering Research Council of Canada and Environment Canada Atmospheric Environment Service for financial support of this research project.

6. References

[1] H.L. Pardue, Anal. Chim. Acta, 216 (1989) 69.
[2] R.G. Garmon and C.N. Reiley, Anal. Chem., 34 (1962) 600.
[3] R.G. Willis, W.H. Woodruff, J.R. Frysinger, D.W. Margerum and H.L. Pardue, Anal. Chem., 42 (1970) 1350.
[4] I. Schechter, Anal. Chem., 64 (1992) 729.
[5] H.A. Mottola, Kinetic Aspects of Analytical Chemistry, Wiley, New York, 1988.
[6] C.L. Chakrabarti, Y. Lu, J. Cheng, M.H. Back and W.H. Schroeder, Anal. Chim. Acta, 276 (1993) 47.
[7] J.G. Hering and F.M.M. Morel, Environ. Sci. Technol., 24 (1990) 242.
[8] D.L. Olson and M.S. Shuman, Anal. Chem., 55 (1983) 1103.
[9] M.K.S. Mak and C.H. Langford, Inorg. Chim. Acta, 70 (1983) 237.
[10] J.A. Lavigne, C.H. Langford and M.K.S. Mak, Anal. Chem., 59 (1987) 2616.
[11] C.H. Langford and D.W. Gutzman, Anal. Chim. Acta, 256 (1992) 183.
[12] E.A. Guggenheim, Philos. Mag., 2 (1926) 5328.
[13] B.E. Saltzman, Anal. Chem., 31 (1959) 1914.
[14] S. Siggia and J.G. Hanna, Anal. Chem., 33 (1961) 896.
[15] H.A. Spang, Soc. Indust. Appl. Math. Rev., 4 (1962) 343.
[16] D.W. Marquardt, Soc. Indust. Appl. Math., 11 (1963) 431.
[17] H. Smith and S.D. Dubey, Indust. Qual. Control., 21 (1964) 64.
[18] Y. Bard, Nonlinear Parameter Estimation, Academic Press, New York, 1974.
[19] D.W. Marquardt, F.R. Bennett and E.J. Burnell, J. Mol. Spectrosc., 7 (1961) 269.
[20] R.M. Alcock, F.R. Hartley and D.E. Rogers, J. Chem. Soc. Dalton Trans., (1978) 123.
[21] A.E. McKinnon, A.G. Szabo and D.R. Miller, J. Phys. Chem., 81 (1977) 1564.
[22] Chelex 100 Chelating Ion Exchange Resin Instruction Manual, Bio-Rad Laboratories, Richmond, 1990, p. 2.
[23] SPSS Reference Guide, SPSS Inc., Chicago, IL, 1990.
[24] N.R. Draper and H. Smith, Applied Regression Analysis, Wiley, New York, 2nd edn., 1981.
[25] E. Courtyn, M. Nagels, C. Vandecasteele, Z.-Q. Yu and R. Dams, Bull. Soc. Chim. Belg., No. 96 (1987) 635.

ELSEVIER

Analytica Chimica Acta 288 (1994) 141–156

ANALYTICA CHIMICA ACTA

Chemical speciation of Cu, Zn, Pb and Cd in rain water

Jianguo Cheng [a], C.L. Chakrabarti [a,*], M.H. Back [b], W.H. Schroeder [c]

[a] *Ottawa-Carleton Chemistry Institute, Department of Chemistry, Carleton University, Ottawa, Ontario K1S 5B6, Canada*
[b] *Ottawa-Carleton Chemistry Institute, Department of Chemistry, University of Ottawa, Ottawa, Ontario K1N 6N5, Canada*
[c] *Atmospheric Environment Service, Environment Canada, 4905 Dufferin Street, Downsview, Ontario M3H 5T4, Canada*

(Received 8th September 1993; revised manuscript received 17th November 1993)

Abstract

A scheme for metal speciation which combines physical characterization by size fractionation and chemical characterization by dissociation kinetics has been used to characterize trace metal species in a sample of rain water. The lability of the metal species in each size fraction of ultrafiltration was determined by differential pulse anodic stripping voltammetry and by ion-exchange with Chelex-100 resin, using both the column and the batch technique. Most of the Pb, Cd, Cu and Zn soluble species were ASV-labile and Chelex-labile, and fell in the small size fractions (< 1000 molecular weight cut off). Kinetic analysis of the rain water sample (multi-component system) revealed the presence of the following kinetically distinguishable components (other than the very labile metal aqua ions) undergoing first-order (or pseudo-first-order) dissociation: three for copper, two for zinc, two for lead and one for cadmium. The lability of metal species found in the rain water sample ranged from labile, moderately labile, slowly labile to inert species, the half-lives range from less than one minute to more than seven days. The results of the kinetic analysis of rain water sample were very similar to those of a snow sample collected at the same site about 8 months earlier. The observed difference between the kinetically distinguishable components in the rain water sample and in the snow sample may be due to differences in the pH of the samples.

Key words: Anodic stripping voltammetry; Ion exchange; Kinetic Methods; Metal speciation; Size fractionation; Rain water; Waters

1. Introduction

One important environmental compartment and stage of the biogeochemical cycle of heavy metals is the atmosphere, where the heavy metals occur as aerosols and are bound to dust particles [1]. These metals can be deposited to the surface of water or land via dryfall (dust) or precipitation such as rain, snow and hail. Nguyen et al. [2] determined the total concentrations of Cu, Pb, Cd, Zn and Se in rain water and snow samples by stripping voltammetry and emphasized the significance of rain and snow in the transport of toxic trace metals from atmosphere to terrestrial and marine biota. The influences of toxic metals in precipitation on the quality of natural waters has been reported by several authors [3–7]. However, very little has been published on chemical speciation of heavy metals in precipitation until recently [8,9].

* Corresponding author.

SSDI 0003-2670(93)E0689-5

An understanding of chemical speciation is important for at least two reasons [10]. First, the toxicity caused by ingestion and inhalation of a metal is dependent on its chemical form. Secondly, chemical speciation strongly influences environmental pathways, transport and fate of a metal. In recent years, environmental scientists are becoming increasingly aware of the need for methods yielding detailed information on various physical and chemical forms of heavy metals in precipitation to determine the sources, transport, transformation and removal processes of the heavy metals in the atmosphere, the influences of chemical speciation of heavy metals on the quality of land and natural waters, and bioavailability of heavy metal species.

Development and application of various schemes for study of metal speciation in the aquatic environment have been reported and critically evaluated in the literature [8–27]. The theoretical background for kinetic studies of metal speciation has been developed and discussed in several publications [28–33]. Several techniques and methods such as solvent extraction, ultrafiltration, dialysis, gel permeation chromatography, adsorption, ion-exchange, UV-irradiation, ion-selective electrode potentiometry and stripping voltammetry have been used in chemical speciation schemes to distinguish between metal forms in natural waters [17]. However, only a few applications of these schemes and techniques for chemical speciation of heavy metals in precipitation have been reported in the literature, and only sporadic interest has been shown hitherto in systematic research on toxic metals in rain and snow [8,34]. Lum et al. [35] studied the bioavailable Cd, Pb and Zn in wet and dry deposition. Rain water over the North Atlantic Ocean was analyzed by Lim and Jickells [34] for particulate, dissolved and acid-leachable trace metals. Other studies showed that Pb and Cd concentrations in rain water decreased with increasing rainfall intensity. The highest enrichment of Cd, Pb and Cu was observed in ice-accretion deposition [36].

We have developed a scheme for metal speciation based on size fractionation by ultrafiltration and chemical characterization of each size fraction by dissociation kinetics of its metal species, and applied the scheme to samples of rain, snow and river surface water [8]. In this paper, we discuss results of further work done by applying this scheme to a sample of rain water, in which the speciation of Zn, Cu, Pb and Cd has been determined. The results are compared with the previous results for these metals in a snow sample collected from the same site about 8 months earlier.

2. Dissociation kinetics of metal complexes

2.1. ASV-lability

Differential pulse anodic stripping voltammetry (DPASV) has been used by many researchers to determine ASV-labile species in aqueous samples [8,9,11,12,19–24,32]. ASV-labile species are defined as those that can be reduced at and deposited into a hanging mercury drop electrode (HMDE) from a stirred solution. Therefore, ASV-labile species comprise free metal ions and those metal complexes which are dissociated to free metal ions and are reduced at HMDE within the time scale of measurement in ASV which is in the order of 10^{-3} s [37]. The ASV-labile species are therefore operationally defined.

The dissociation of a 1:1 complex formed between a divalent metal ion, M, and ligand, L, and the subsequent reduction of the metal ion at a HMDE may be expressed as:

$$ML \underset{k_f}{\overset{k_d}{\rightleftharpoons}} M^{2+} + L^{2-} \qquad \text{(slow)} \qquad (1)$$

$$M^{2+} + 2e^- \longrightarrow M \qquad \text{(fast)} \qquad (2)$$

When the complex, ML, is not itself reducible at the applied voltage, the electrodeposition is due to reduction of M^{2+} ions generated by dissociation of ML, and the stripping current is due to subsequent oxidation of M. If the dissociation of ML (Eq. 1) is slow and the reduction of M^{2+} (Eq. 2) is fast, the rate constant measured will be the dissociation rate constant k_d of the metal complex (equation 1). Turner and Whitfield [38] reported that the lability of the complex could be indicated by the ratio of the kinetic current i_k to

the diffusion current i_d (the current observed for the same concentration of the metal ion as that in the sample, but in the absence of ligand), i_k/i_d, which is related to the rate constant k_f and k_d, the concentration of the ligand, thickness of the diffusion layer and the diffusion coefficient of the metal ion in the medium, and the radius of the mercury drop. An implicit assumption in the above relationship is that the metal complex, ML, is not directly reducible at the applied voltage, in other words, the metal ion is formed by the dissociation of the metal–ligand complex before it is reduced at and deposited into the HMDE. If the applied voltage is too high, the metal complex ML may be reduced directly instead of undergoing dissociation prior to the reduction of the metal ion at the HMDE (Route 1). There is also the possibility, that even at the lower applied voltage, only the organic ligand part of ML is reduced to form ML_{red} (Route 2). The ML_{red} does not yield metal ions for reduction at the HMDE, and hence does not give stripping current, making the ML species ASV-nonlabile. Hence, ASV-nonlability may be also due to causes other than slowness of the metal–ligand dissociation.

$$ML + ne^- \underset{k_o}{\overset{k_r}{\rightleftharpoons}} M + L^{n-} \qquad \text{(Route 1)} \qquad (3)$$

$$ML + ne^- \underset{k'_o}{\overset{k'_r}{\rightleftharpoons}} ML_{red} \qquad \text{(Route 2)} \qquad (4)$$

In order to reduce or eliminate direct reduction of the metal complex, the deposition potential is generally set just sufficiently negative to yield the maximum peak current for the free metal ion in that medium.

2.2. Chelex-100 lability

Chelex-100 is a styrene–divinylbenzene copolymer resin incorporating iminodiacetic acid chelating groups:

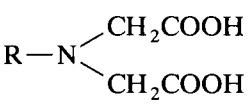

When fully ionized, Chelex can be represented as $Chelex^{2-}$. Chelex-100 resin is very useful for chemical speciation due to its two properties – moderate ion-exchange reactivity, and exclusion of large molecules and colloidal particles by virtue of the size of its beads. Chelex-100 resin used in this work had a pore size of about 1.5 nm. Copper and lead species adsorbed on colloidal ferric hydroxide in solutions are rejected by this resin [29]. Because the external surface area of the resin beads contributes little to their total surface area, Chelex-100 resin provides not only a suitable material for the differentiation of metal complexes based on the affinity between the metal ion and the iminodiacetic acid chelating group, but also a rapid method for separation of small metal species from macromolecular or colloidally-associated metal species.

In rain water, snow and other natural waters, complexant such as organic and inorganic ligands, or colloidal matters are present. Metals may be bound to different complexants or to different bonding sites of such complexant (polyfunctional), or adsorbed on or entrapped into colloidal matter. If dissociation of metal ions from such different bonding sites is thermodynamically favourable and the dissociation processes are independent and occur simultaneously, the dissociation rates will depend on the nature of the functional groups, their position on the macromolecular complexants and the residual charge on the complexants.

The reaction between a metal complex, ML (where L is a polyfunctional ligand) and Chelex can be expressed as (the charge on the ions are omitted for simplicity):

$$ML \underset{k_{-1}}{\overset{k_1}{\rightleftharpoons}} M + L \qquad \text{(slow)} \qquad (5)$$

$$M + Chelex \underset{k_{-2}}{\overset{k_2}{\rightleftharpoons}} M\text{–}Chelex \qquad \text{(fast)} \qquad (6)$$

When Chelex is present in sufficient excess (as in the present experiment) reaction 6 is pseudo-first-order. The rate constant k_2 is quite large as determined in this laboratory by measuring the rate of uptake of the metal M by Chelex-100 using inductively coupled plasma mass spectrometry. Because $k_2[Chelex] \gg k_{-1}[L]$, the overall reaction

$$ML + Chelex \longrightarrow M\text{–}Chelex + L \qquad (7)$$

is irreversible. The rate of decrease in the concentration of the complexed metal species due to the metal complex dissociation in the presence of a sufficient excess of Chelex-100 resin can be expressed by:

$$-\frac{d[ML]}{dt} = k_1[ML]$$

$$[ML] = [ML]_o e^{-k_1 t}$$

$$\frac{d[M]}{dt} = k_1[ML] - k_2[M]$$

$$[M] = [M]_o e^{-k_2 t} + \frac{k_1[ML]_o}{k_2 - k_1}(e^{-k_1 t} - e^{-k_2 t})$$

Because $k_2 \gg k_1$ and k_2 is large

$$[M] \simeq \frac{k_1}{k_2}[ML]_o e^{-k_1 t}$$

$$= \frac{k_1}{k_2}[ML]$$

Thus the rate of formation of M–Chelex in the above reaction (Eq. 6) can be represented by:

$$\frac{d[M\text{–Chelex}]}{dt} = k_2[M]$$

$$= k_2\frac{k_1}{k_2}[ML]$$

$$= k_1[ML] \quad (8)$$

where k terms are the first-order or pseudo-first-order rate constants of the respective reactions, [ML] is the concentration of the metal complex ML, and the subscript o stands for reaction time zero. Hence, the rate of formation of M–Chelex is determined by the rate of dissociation of ML in reaction 5.

For free metal (aqua) ions or other very labile species, the metal ion can directly and rapidly exchange with the sodium ion which is bound to the Chelex resin, following a pseudo-first-order reaction (reaction 6). A large value for the rate constant for dissociation is associated with "labile" complexes, a lower value with "moderately labile" complexes, a still lower value with "slowly labile" complexes. Thermodynamically highly stable species, or species which are trapped by colloidal matter so that they cannot react with Chelex-100 resin, or species which react with Chelex-100 resin extremely slowly are grouped together as the "inert" or nonlabile species.

3. Experimental

3.1. Reagents

Stock solutions (1000 μg ml^{-1}) of Cd, Cu, Pb were prepared by dissolving an appropriate quantity of CdO (Baker, Analytical Reagent), copper metal (99.9% pure) and $Pb(NO_3)_2$ (Fisher, A.C.S. reagent), in ultrapure nitric acid (Ultrex II) with heating and diluting to appropriate volume with ultrapure water; the final solutions contained 1% (v/v) ultrapure HNO_3. A reagent solution (1000 μg ml^{-1}) of Zn was purchased from BDH. Stock solutions (1000 μg ml^{-1}) of aluminium and iron were prepared separately by dissolving 0.5000 g aluminium and iron powder (SPEX) in 20 ml HCl (Ultrex)–H_2O (1 : 1) respectively, with heating and diluting to 500 ml with ultrapure water. Ultrapure water of resistivity of 18.2 megohm cm was obtained directly from a Milli-Q-plus water purification system (Millipore). Ultrapure HNO_3 (Ultrex II) was manufactured by Baker (Phillipsburg, NJ).

A stock solution of 2.0 M sodium acetate solution was prepared by dissolving an appropriate quantity of sodium acetate (BDH) in ultrapure water. This solution then was purified by electrolysis at −1.4 V versus SCE for at least 48 h and the electrolysis continued till the solution was needed.

3.2. pH and conductivity measurements

The pH was measured with an Accumet 925 pH/ion Meter (Fisher Scientific), using a AccupHast Combination glass electrode with an internal calomel reference electrode. The conductivity was measured with a conductivity bridge, model 31 (Yellow Springs Instrument).

3.3. Cleaning procedure

Nalgene Teflon FEP™ (fluorinated ethylene propylene) bottles and flasks fitted with screwed-

on caps were used exclusively except where stated otherwise. The following cleaning procedure was rigorously applied [40]. The bottles and flasks were pre-cleaned by soaking with $HCl-H_2O$ (1 : 1) (HCl was AR grade) for one week at room temperature, then with HNO_3-H_2O (1 : 1) (HNO_3 was AR grade) for one week at room temperature, followed by rinsing with ultrapure water until the pH of the water after rinsing was about 6. Finally, they were filled with ultrapure water and allowed to stand for two or more weeks until they were used. The soaking water was periodically changed to ensure continued cleaning. The final pH of the two-day-long filled water at the last time must be $\geqslant 6$. Before use, the containers were rinsed five times with ultrapure water.

The filters were also cleaned before use. 0.45-μm filter papers were cleaned by soaking in 0.5% ultrapure HNO_3 (Ultrex II) for 24 h and rinsing them ten times with ultrapure water, followed by soaking them in ultrapure water for two or more weeks until they were used (the soaking water was changed periodically to ensure continued cleaning). Ultrafiltration membranes were preconditioned by successive soaking in NaOH solution (pH < 11), 0.5% ultrapure HNO_3 (Ultrex II), and finally in ultrapure water [24]. The ultrafilters were stored in a 10% (v/v) ethanol in water solution in cleaned PTFE containers at 4°C. Before use, the filters were stirred with ultrapure water, with frequent changes of water, to remove added ethanol.

3.4. Sample collection and treatment

A sample of rain water was collected in a cleaned Nalgene C.P.E. (conventional polyethylene) bottle (2 l) in one hour at a site on the roof top of the Steacie Building at Carleton University. As soon as the sample collection was completed, three small portions (50 ml) were taken out, one in a polytetrafluoroethylene (PTFE) beaker for the measurements of pH and conductivity (at room temperature), one in the pre-cleaned PTFE chamber of a digestion bomb for wet digestion in the high-pressure bomb for the determination of the total metal, and one for analysis by DPASV. The remaining rain water sample was filtered through a 0.45-μm filter. Three 50-ml aliquots of the filtrate were taken for analysis as follows: one aliquot for DPASV, one aliquot for pH and conductivity, and one aliquot for total soluble metal. The total soluble metal was determined by graphite platform furnace atomic absorption spectrometry after the filtrate was acidified to contain 1% (v/v) nitric acid (Ultrex II). Another aliquot of the filtrate was taken for the Chelex-100 column study and 200 ml of the filtrate was taken for the Chelex-100 batch study. The remaining filtrate was then passed through various ultrafiltration membrane filters having different molecular weight cut off (MWCO), and different size fractions were obtained. The dissociation kinetics of the metal species in different size fractions were studied by DPASV and by ion-exchange with Chelex-100 resin. All of the above filtrates and ultrafiltrates were collected directly into pre-cleaned Nalgene Teflon FEP™ 250-ml flasks.

3.5. Filtration and ultrafiltration

The rain water sample was filtered with a Gelman filtration assembly fitted with a GA-6 filter (pore size 0.45 μm, diameter 47 mm). Before the filtration of the sample, 200 ml of ultrapure water was filtered and the middle portion of the eluted water was taken as the blank for the determination of total concentration of the soluble species. The rain water sample was filtered through a pre-cleaned 0.45-μm filter (GA-6) immediately after collection and the first 50 ml of the filtrate was discarded. The filtrate was collected directly into the pre-cleaned Nalgene Teflon FEP™ 250 ml flasks. The filter paper with the retained particulate matter was used for the determination of the metal species in particulate phase. Another filter paper was used, following the same procedures as above but ultrapure water instead of the rain water sample as the blank in the measurement of the metal species in the particulate phase.

Ultrafiltration for the soluble phase was performed with the Amicon ultrafiltration assembly (W.R. Grace, Beverly, MA), Model 8200, fitted with the Amicon disc membrane filters (diameter

62 mm). The MWCO values of the membrane filters were 100000, 50000, 30000, 10000, 5000, 1000 and 500. Each time 160 ml of the sample was filled, the initial 20 ml and the last 80 ml were discarded, and only the middle fraction was collected, since the initial 20 ml could contain a reduced concentration of species in the ultrafiltrate because of dilution by water trapped in the filter and the last 80 ml of the ultrafiltrate often contained higher concentrations of organic carbon because of leakage of high-molecular-weight substances occurring as the concentration of filtered species above the membrane increased [41]. Before ultrafiltration of the rain water sample, 160 ml of Ultrapure water was filtered through the ultrafilter using the same procedure as mentioned above and the filtered water was used as the blank in the determination of the metal species in that size fraction.

3.6. DPASV measurement

DPASV measurements were performed with a PAR Polarographic Analyzer (Princeton Applied Research), Model 174A, connected to an Omnigraphic recorder (Houston Instrument, Bellaire, TX), Model 3000. The voltammetric cell made of Pyrex glass was equipped with three electrodes. A Methrohm E405 microfeed HMDE was used as the working electrode. The auxiliary electrode was a Pt-coil and the reference electrode was a saturated calomel electrode (SCE). Before each voltammetric measurement, the solution was deaerated by bubbling pure nitrogen (99.995%) through it for 10 min. During the measurement, the inert nitrogen atmosphere blanket over the solution was maintained by flushing nitrogen over the solution. The plating step was carried out at a potential of -0.07, -0.45, -0.80 and -1.15 V versus SCE for Cu, Pb, Cd and Zn, respectively, with stirring for 60 s, followed by a 30-s quiescent period. In the stripping step, the sweep rate was 50 mV/s with an imposed pulse of 10 mV every 0.5 s, and the scan range was 0.75 V. An aqueous solution of 0.040 M sodium acetate, which had been prepared using the 2.0 M sodium acetate stock solution and the pH of which was adjusted to that of the sample, was used. The sodium acetate had been purified by electrolysis at -1.4 V versus SCE for at least 48 h, and the electrolysis continued till the solution was used. The final pH of the rain water sample was measured.

3.7. Cation-exchange with Chelex-100 resin

The Chelex-100 resin was 100–200 mesh size in Na-form (Bio-Rad Labs.) and was used in both the Chelex-100 column and the Chelex-100 batch technique for study of chemical kinetics. Before use, the Chelex-100 ion-exchange resin was washed and soaked with ultrapure water until the pH of the water suspension was the same as that of the sample and remained unchanged in two hours, then the resin suspension was filtered through a pre-cleaned 0.45-μm filter. This Chelex-100 resin will be called "pre-treated". In the Chelex column technique, 5 g of the pre-treated Chelex-100 resin was filled into a plastic cylindrical column with 1 cm inner diameter. The void volume of the packed Chelex-100 resin in this column was 1.7 ml. The sample passed through the column with a flow rate of 2 ml min^{-1}. One portion of the effluent was collected for the determination of the Chelex-column-nonlabile species. The amount of the Chelex-column-labile species was obtained either by the subtraction of the Chelex-column-nonlabile species from the total metal concentration in that fraction or by the determination of the metal concentration in the eluted sample after heating it with a small volume of 3.0 M HCl (Ultrex). In the Chelex batch technique, the pre-treated Chelex-100 resin (1%, w/v) was added to the ultrafiltrate of each size fraction or the Chelex column effluent, and the mixture was shaken with a wrist-action mechanical shaker. At the specific times, 1 ml of the clear supernatant solution was withdrawn with a syringe fitted with a microfilter, and the solution was acidified to contain 1% (v/v) HNO_3 (Ultrex II) for determination of the total metal concentration remaining in the solution after uptake by the Chelex-100 resin as a function of the reaction time. The determination of metal concentration was done by graphite platform furnace atomic absorption spectrometry.

The initial and the final pH of the Chelex-100 batch test solutions were measured.

3.8. Determination of the total metal concentration

The total metal concentration was determined as the sum of the metal concentration in the particulate phase and the metal concentration in the soluble phase, both of which were determined by graphite platform furnace atomic absorption spectrometry. For determination of the metal concentration in the particulate phase, the filter paper containing the particulate phase was acid-digested in a pre-cleaned PTFE-lined metal bomb, and then the product was further digested with 20 ml of 10% (v/v) HNO_3 (Ultrex II) in an air oven for four hours at 150°C. The product was then diluted to 200 ml with ultrapure water. A blank was prepared by digesting a pre-cleaned filter paper following the above procedure for the determination of the metal species in the particulate phase. An aliquot of the filtrate, or the ultrafiltrate in each size fraction was acidified to contain 1% (v/v) HNO_3 (Ultrex II) for the determination of the total soluble metal species, or soluble metal species in each size fraction of the ultrafiltrate.

A Perkin-Elmer Zeeman atomic absorption spectrometer, Model 5000, fitted with a computer-controlled HGA-500 graphite furnace, a pyrolytic graphite-coated tube, and a pyrolytic graphite platform, was used for determination of the total metal concentrations. Hollow-cathode lamps of Pb, Cd, Cu, Zn, Al and Fe (Fisher) were operated at 6, 4, 6, 6, 8 and 6 mA, respectively. A spectral bandpass of 0.7 nm was used for all these elements except Fe, for which a 0.2 nm spectral bandpass was used. Argon was used as the purge gas with a flow rate at 300 ml min^{-1}, which was interrupted during the atomization step. The optimum furnace temperature program for dry/pyrolysis/atomization cycle for Pb, Cd, Cu, Zn, Al and Fe is given in Table 1.

3.9. The speciation scheme

The speciation scheme was presented in detail previously [8] and will only be briefly summarized here. Fig. 1 presents an outline of the scheme. Measurements of pH, conductivity and DPASV

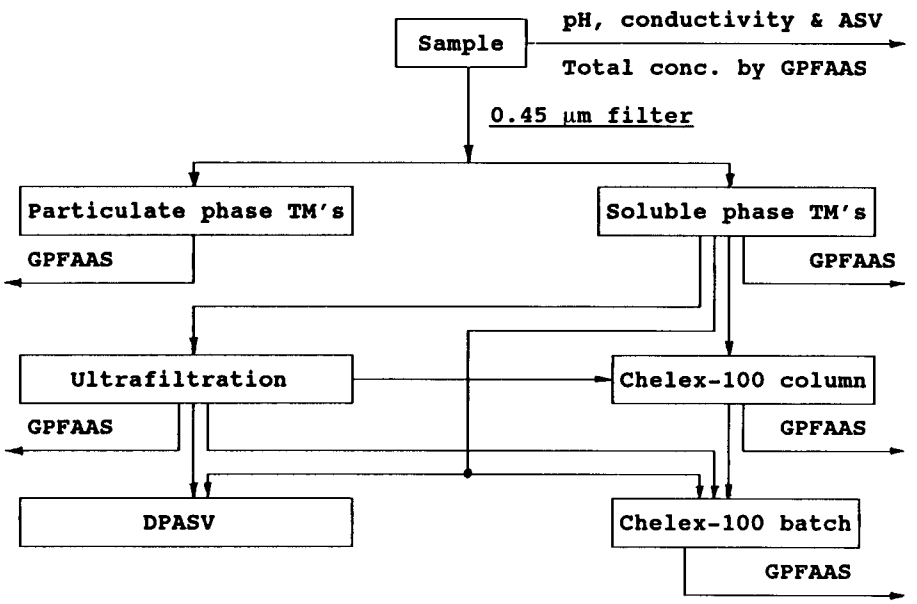

Fig. 1. Scheme for metal speciation. TM = Total metals; DPASV = differential pulse anodic stripping voltammetry; GPFAAS = graphite platform furnace atomic absorption spectrometry. The pH was measured before and after each run.

Table 1
Analysis lines and instrumental conditions for graphite platform furnace atomic absorption spectrometry

Element	Analysis line (nm)	Pyrolysis temp. (°C)	Atomization parameters	
			Temp. (°C)	Duration (s)
Al	309.2	1300	2400	7
Cd	228.8	400	1600	4
Cu	324.8	900	2300	5
Fe	248.3	900	2500	6
Pb	283.3	500	1900	5
Zn	213.9	500	2000	5

were made directly (i.e. without any pre-treatment) on the sample. The remaining sample was filtered to remove the particulate phase (> 0.45 μm). The concentration of total soluble species was determined by graphite platform furnace atomic absorption spectrometry. Aliquots of the filtrate were used for kinetic studies, using DPASV, Chelex column and Chelex batch techniques. The remaining filtrate was subjected to ultrafiltration for determining the size distribution of the soluble metal species. Each size fraction was studied for total metal concentration and for kinetics of dissociation of the metal species in that size fraction.

The above speciation scheme combines physical size fractionation by ultrafiltration of the soluble species, with chemical characterization (dissociation kinetics) by anodic stripping voltammetry, and by the Chelex-100 column and the Chelex-100 batch technique. This results in a measurement timescale for dissociation kinetics ranging about 8 orders of magnitude. Although the results it generates are operationally defined and are therefore difficult to interpret in terms of bioavailability, it provides information for possible correlation of chemical characterizations of metal species with their bioavailability and toxicity.

4. Results and discussion

4.1. pH and conductivity

The pH and the conductivity of the rain water sample measured at room temperature immediately after its collection (on August 26, 1992) were 5.3 and 20.5 μS cm^{-1}, respectively. These values may be compared with those measured previously for the snow sample (collected on January 10, 1992) for which the pH and conductivity

Table 2
Size fractionation of zinc, copper, lead and cadmium species by ultrafiltration

	Zn (μg l^{-1})	Cu (μg l^{-1})	Pb (μg l^{-1})	Cd (μg l^{-1})
August 26, 1992, rain water (pH 5.3)				
Total metal conc.:	24.1	7.10	3.92	0.236
In the particulate phase:	2.97	2.03	1.05	0.038
In the soluble phase (< 0.45 μm):	21.1	5.07	2.87	0.198
Ultrafiltration (MWCO):				
> 10000	0	0	0	0
10000–5,000	1.66	1.12	0.10	0
5000–1000	3.82	2.46	0.37	0
1000–500	6.28	0.57	1.04	0.083
< 500	9.24	0.95	1.23	0.115
January 10, 1992, snow (pH 3.9) [8]				
Total metal conc.:	9.0	5.7	5.5	0.11
In the particulate phase:	0.90	1.08	1.00	0.005
In the soluble phase (< 0.45 μm):	8.13	4.7	4.4	0.11
Ultrafiltration (MWCO):				
> 10000	0	0	0	0
10000–1000	2.5	2.0	2.3	0.035
< 1000	5.6	2.7	2.1	0.075

Table 3
Aluminium and iron in the rain water sample (pH 5.3) and the snow sample (pH 3.9)

	Rain water (pH 5.3) August 26, 1992		Snow (pH 3.9) [8] January 10, 1992	
	Al ($\mu g\,l^{-1}$)	Fe ($\mu g\,l^{-1}$)	Al ($\mu g\,l^{-1}$)	Fe ($\mu g\,l^{-1}$)
Total metal concentration:	389.8	608.7	400.9	375.2
in the particulate phase:	378.4	601.3	388.7	366.2
in the soluble phase ($< 0.45\ \mu m$):	11.4	7.4	12.2	9.0

were 3.9 and 28.8 $\mu S\ cm^{-1}$, respectively. The pH and the conductivity are important parameters of atmospheric precipitation quality. The pH is related to the possible forms and charge of the chemical species, and the conductivity reflects the ion concentration of the soluble species. The pH and the conductivity of the filtrate from filtration through a 0.45-μm filter was also measured and compared with that of the unfiltered sample. No significant difference was observed.

4.2. Ultrafiltration and size distribution

Table 2 shows the size distribution of the metal species in each size fraction of the rain water sample. The results of the analysis of the snow sample published earlier [8] are included for comparison. Most of the Cu, Pb, Cd and Zn species in the rain water sample and the snow sample were in the soluble phase. The amount of Al and Fe, both in the particulate and the soluble phase, were also determined and the results are given in Table 3. At the natural pH of the rain water sample (pH 5.3), the Al and Fe may exist as oxy-hydroxo colloids or as hydrous oxides adsorbed on other colloidal matter containing Cu, Pb, Cd and Zn as adsorbed or occluded species. Most of the Cu, Pb, Cd and Zn in the soluble phase were in the small size fractions. In the rain water sample (pH 5.3), > 70% of these metals were present as soluble species. As the predominant metal species in the soluble phase, 44.0% of the zinc, 44.9% of the lead and 51.1% of the cadmium passed through the ultrafiltration membrane with MWCO 500, and were probably present as metal aqua ions and/or as small inorganic complexes such as metal bicarbonates, whereas 48.2% of the copper was in the range with MWCO from 5000 to 1000, and was probably present as larger complexes of organic ligands, or metals adsorbed on or occluded by col-

Table 4
ASV-lability of Cu, Zn, Pb and Cd species in the rain water sample (pH 5.3) and the snow sample (pH 3.9)

	ASV-labile ($\mu g\,l^{-1}$)				ASV-nonlabile ($\mu g\,l^{-1}$)			
	Cu	Pb	Cd	Zn	Cu	Pb	Cd	Zn
August 26, 1992, rain water (pH 5.3)								
Unfiltered sample:	4.9	1.8	0.2	–	2.2	2.1	0	–
In the soluble phase ($< 0.45\ \mu m$):	3.3	1.5	0.2	–	1.8	1.4	0	–
Ultrafiltration (MWCO):								
> 10000	0	0	0	0	0	0	0	0
10000–5000	0	0.2	0	0.8	1.1	0	0	0
5000–1000	0.3	0.2	0	1.9	0.7	0	0	1.9
1000–500	1.9	0	0.2	4.7	0	1.1	0	1.6
< 500	1.1	1.1	N.D. [a]	7.9	0	0.1	0.1	1.3
January 10, 1992, snow (pH 3.9) [8]								
In the soluble phase ($< 0.45\ \mu m$):	2.0	4.7	N.D.	7.5	2.7	N.D.	N.D.	0.6

[a] N.D. = Not detectable

loidal matter. For the Zn, Pb and Cu, the species retained by the ultrafiltration membrane with MWCO 10 000, and for the Cd, the species retained by MWCO 1000 were below the limits of detection. In the snow sample, > 80% of these metal species were in the soluble phase. As the predominant species in the soluble phase, 69.1% of the zinc, 57.4% of the copper and 68.2% of the cadmium passed through the ultrafiltration membrane with MWCO 1000, and were probably present as metal aqua ions and/or small inorganic complexes such as metal bicarbonates, whereas 52.3% of the lead was in the size range with MWCO from 10 000 to 1000, and were probably present as larger complexes of organic ligands, or metals adsorbed on or occluded by colloidal matter.

In atmospheric precipitation there are many naturally-occurring substances such as inorganic and organic compounds, and hydrous oxides. Many of them can behave as complexant for heavy metals. Adsorption of metal ions on hydrous oxides or occlusion inside colloidal matter, ion-exchange with clay materials (flying dust), binding by organically-coated particulate matter or organic matter, or adsorption of metal complexes by colloidal matter are common. All of these processes are related to the size (also shape and charge) distribution of aerosols.

4.3. ASV-labile species

Table 4 shows ASV-lability of the metal species. The values of the previous measurements [8] for the snow sample (pH 3.9) are also given for comparison. The ASV measurements for Cu, Pb, Cd and Zn were sequentially made at the pH 5.3 of the sample at the applied potential −0.07, −0.45, −0.80 and −1.15 V versus SCE, respectively. It was found that in the soluble phase 64.7% of the copper, 51.7% of the lead, 100% of the cadmium and 76.1% of the zinc in the rain water sample were ASV-labile, whereas 42.6% of the copper, 100% of the lead and 92.6% of the zinc in the snow sample were ASV-labile. Cadmium in the snow sample was not detectable because of its low concentration. It can also be seen from Table 4 that there was no significant difference in the ASV-labile fraction of the species between the filtered and the unfiltered samples.

In rain water, snow and other natural waters, excess complexing ligands, if present, will complex the metal added as spikes. Therefore, for standardizing ASV measurements, it is important to use an analytical calibration curve prepared using peak height of standard solutions of metal ion rather than an analytical calibration curve obtained by adding spikes of metal ions to the sample, i.e. by a standard addition curve [42]. In this work, the analytical calibration curve was obtained by adding standard solutions of metal ions (taken as the nitrate) to the blank which was ultrapure water containing 0.04 M sodium acetate and adjusted to the pH of the samples with ultrapure nitric acid.

4.4. Chelex-100-labile species

Chemical speciation based on the reactivity between metal species and Chelex-100 cation-ex-

Table 5
Chelex-100-column-lability of metal species in the rain water sample (pH 5.3)

	Chelex-column-labile ($\mu g\ l^{-1}$)				Chelex-column-nonlabile ($\mu g\ l^{-1}$)			
	Zn	Cu	Pb	Cd	Zn	Cu	Pb	Cd
August 26, 1992, rain water (pH 5.3)								
Total soluble species (< 0.45 μm):	20.5	2.67	2.56	0.19	0.06	2.40	0.31	0.082
Ultrafiltration (MWCO):								
> 10 000	0	0	0	0	0	0	0	0
10 000–5000	1.2	0.82	0	0	0	0.27	N.D.	0
5000–1000	3.9	0.33	0.29	0	0	2.13	N.D.	0
1000–500	6.2	0.57	1.4	0.089	0.05	N.D.	N.D.	0
< 500	9.2	0.95	1.23	0.040	0.03	N.D.	N.D.	0.075

change resin was investigated in this work, in which both column and batch techniques were used.

The Chelex column technique was used to study labile and moderately labile metal species. Because the amount of Chelex resin that had to be used with the column technique was large and the contact time was short, it can be considered that the uptake rate of the metal species in the sample by Chelex-100 resin was diffusion-limited. Under the experimental conditions of this study (flow rate was 2.0 ml min^{-1} and the void volume of the packed Chelex-100 resin in the column was 1.7 ml), the contact time of the sample with the resin was about 51 s. This timescale corresponds to moderately labile metal species in the sample.

Table 5 shows the Chelex-100 column lability of metal species in the soluble phase of the rain water sample. It can be seen that 99.7% of the zinc, 52.7% of the copper, 89.2% of the lead and 61.1% of the cadmium species were Chelex-column-labile. Table 5 also shows the size distribution of the Chelex-column-labile species. The predominant Chelex-column-labile species of copper, zinc and lead in the rain water sample were in the small size fractions, whereas the predominant Chelex-column-labile species of cadmium was in the range with MWCO from 1000 to 500, and were probably small inorganic complexes of cadmium. The size fractions of all metals in the MWCO < 500 probably contained metal aqua ions, or small inorganic metal complexes. Chelex-column-nonlabile species of zinc and cadmium were in the small size fraction, whereas the Chelex-column-nonlabile copper species mainly existed in the size range with MWCO from 5000 to 1000, and were probably larger metal complexes of organic ligands. For lead, the concentrations of the Chelex-column-nonlabile species in different size fractions were too low to be detected.

Table 6 shows the Chelex-100 batch lability of the metal species. For comparison, Table 6 also shows our previous results [8] for the Chelex-100 batch lability of metal species in a snow sample. The symbol $C_{i,o}$ stands for the initial concentration of each kinetically distinguishable component of the metal species. 100% of the lead and cadmium, 77.0% of the copper and 99.7% of the zinc species in the rain water sample, and 100% of the lead and cadmium, 65.0% of the copper and 98% of the zinc in the snow sample were labile or moderately labile species. In the rain water sample, three kinetically distinguishable components for copper, two for zinc, two for lead and one for cadmium were observed, whereas in the snow sample, four kinetically distinguishable components for copper, two for zinc, one for lead and one for cadmium were observed. However, the kinetically distinguishable metal components in both the rain water and the snow sample are similar. The only difference was that the labile component of copper in the snow sample was not observed in the rain water sample, and the rain

Table 6
Chelex-100-batch-lability of the metal species in the rain water sample[a] (pH 5.3) and the snow sample[b] (pH 3.9)

Metal	$C_{i,o}$ ($\mu g\ l^{-1}$)		Rate constant (s^{-1})		Half-life (s)	
	This work [a]	Previous work [b]	This work [a]	Previous work [b]	This work [a]	Previous work [b]
Cu		2.4		$(3.1 \pm 0.5) \times 10^{-2}$		22.4
	3.98	0.7	$(2.3 \pm 0.1) \times 10^{-3}$	$(1.6 \pm 0.1) \times 10^{-3}$	3.0×10^{2}	4.33×10^{2}
	0.29	0.9	$(3.3 \pm 0.3) \times 10^{-5}$	$(6.2 \pm 1.1) \times 10^{-5}$	2.1×10^{4}	1.12×10^{4}
	0.90	0.8	$(8.5 \pm 0.2) \times 10^{-6}$	$(8.8 \pm 0.3) \times 10^{-6}$	~ 1 day	~ 1 day
Zn	23.27	7.8	$(4.7 \pm 0.1) \times 10^{-3}$	$(4.0 \pm 0.1) \times 10^{-3}$	1.5×10^{2}	1.73×10^{2}
	0.07	0.15	$< 4.0 \times 10^{-7}$	$< 2.8 \times 10^{-6}$	> 20 days	> 6 days
Pb	1.97	4.4	$(1.3 \pm 0.1) \times 10^{-2}$	$(1.0 \pm 0.3) \times 10^{-2}$	53	69.3
	0.94		$(3.3 \pm 0.1) \times 10^{-3}$		2.1×10^{2}	
Cd	0.168	0.11	$(4.9 \pm 0.1) \times 10^{-3}$	$(8.2 \pm 0.7) \times 10^{-3}$	1.4×10^{2}	84.5

[a] Rain water sample collected on August 26, 1992.
[b] Snow sample collected on January 10, 1992 [8].

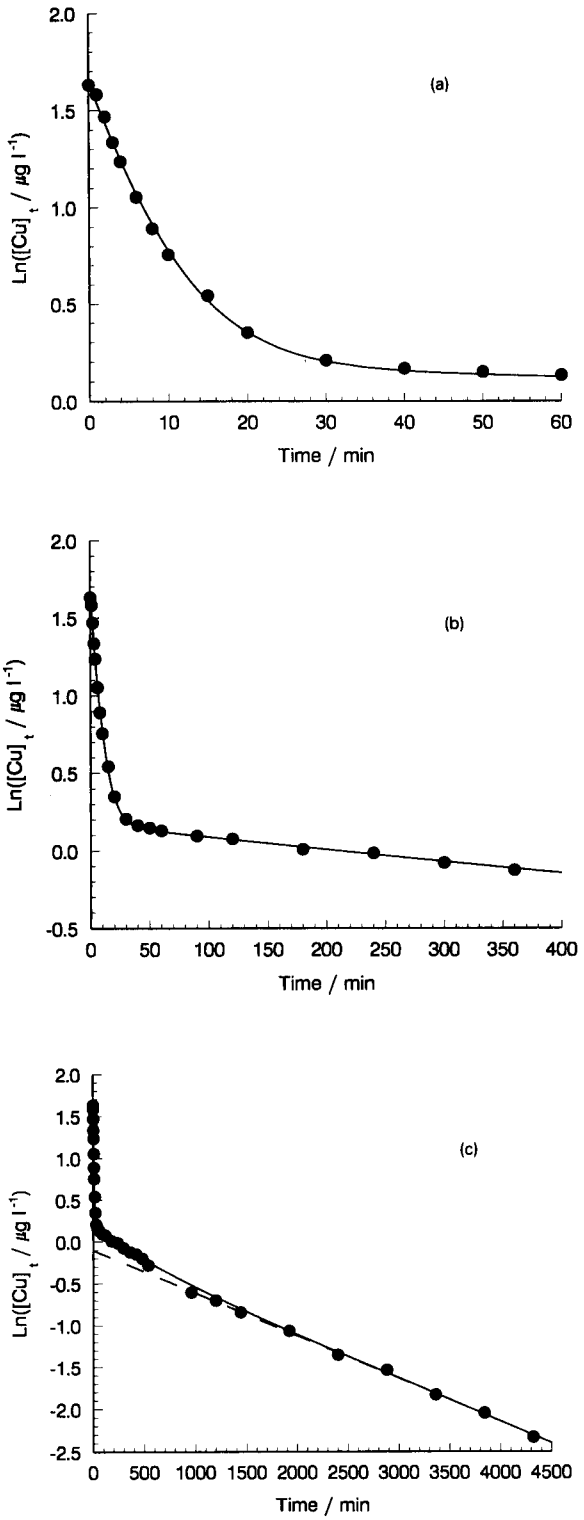

water sample had one more kinetically distinguishable lead component than the snow sample. The difference may be due to the sample pH. At pH lower than 4, the predominant species of both lead and copper were free aqua ions rather than other hydroxo species, whereas at pH 5.3 and in the presence of dissolved carbon dioxide, some of the lead aqua ions and most of the copper ions were present as carbonato species or hydroxo species, specially hydrolyzed copper ion $CuOH^+$.

In the rain water and the snow sample, the concentration of organic matter such as humic materials are relatively low [43]; therefore, in an acidic medium, most of these metals are present as metal aqua ions, hydroxo species, carbonato species and other small inorganic metal complexes, i.e. the main factors that affect the distribution of the metal species are inorganic ligands and colloidal matter. The oxy-hydroxide colloids of Fe(III), Al(III) and Mn(IV)) may take up heavy metal ions such as Cu, Zn, Pb and Cd by simple adsorption, surface complexation or occlusion.

4.5. Method of data analysis for the Chelex-100 batch process

We adopted the kinetic model for kinetic analysis of multi-component systems developed in our earlier paper [8], and by Olson and Shumam [22]. In dealing with a metal associated with a polyfunctional complexant, or with different ligands, each kinetically distinguishable component of a metal was assumed to dissociate independently and simultaneously by a first-order or a pseudo-first-order rate process. Hence, the reaction between Chelex-100 resin and the kinetically distin-

Fig. 2. Copper remaining in the rain water sample as a function of time after uptake by Chelex-100 resin in the Chelex batch technique. (a) and (b) are the expansions of (c) in the specific time ranges. The concentration of Chelex-100: 1% (w/v). ● = experimental data; solid line = calculated value; broken line = experimental plot for the most slowly dissociating copper component.

guishable components of the metal species can be treated as parallel reactions:

$$A + R \xrightarrow{k_1} Z$$
$$B + R \xrightarrow{k_2} Z$$
$$\vdots$$
$$N + R \xrightarrow{k_n} Z$$

where A, B,..., N are the kinetically distinguishable components of the metal bound to different ligands or different sites of a polyfunctional complexant, R is the Chelex-100 resin and Z is the Chelex-bound metal. If the concentration of Chelex-100 resin is much higher than the total concentration of all the metal species and the binding capacity of the Chelex-100 resin for the metal ions is infinite, then we have pseudo-first-order conditions, and hence, $C_A = C_{A,o}\exp(-k_1 t)$, $C_B = C_{B,o}\exp(-k_2 t)$, . . . , and $C_N = C_{N,o}\exp(-k_n t)$. The mass balance expression is:

$$C_T = C_{A,o} + C_{B,o} + \ldots + C_{N,o} = C_A + C_B + \ldots + C_N + C_Z \quad (9)$$

$$C_t = C_T - C_Z = C_{A,o}\exp(-k_1 t) + C_{B,o}\exp(-k_2 t) + \ldots + C_{N,o}\exp(-k_n t) = \sum C_{i,o}\exp(-k_i t) \quad (10)$$

where C_T is the total concentration of the metal species in the rain water sample, $C_{A,o}$, $C_{B,o}$ and $C_{N,o}$ are the initial concentrations of the kinetically distinguishable components A, B, and N, respectively, C_A, C_B, C_N and C_Z are the concentrations of the kinetically distinguishable components A, B, N and the Chelex-bound metal component Z at time t, respectively, and C_t is the total concentration of the metal species remaining in the test solution at time t after uptake by Chelex-100 resin. Obviously, a plot of ln C_t versus time is non-linear (except for the special case $k_1 = k_2 = \ldots = k_n$). However, if $k_1 \gg k_2 \gg \ldots \gg k_n$ or $C_{A,o}\exp(-k_1 t) \gg C_{B,o}\exp(-k_2 t) \gg \ldots \gg C_{N,o}\exp(-k_n t)$, then at some finite time essentially all of the reactants except N will be exhausted, and the function of Eq. 10 can be reduced to:

$$\ln C_t \approx \ln C_{N,o} - k_n t \quad (11)$$

so that the terminal part of a plot of ln C_t versus t should be linear. For the remaining components, a linear plot occurs when the value of $C_{i,o}\exp(-k_i t)$ is much greater than those of the remaining components of the metal species during that period of time. Figs. 2–4 show the experimental results and the calculated plots of the metal species in the rain water sample. The data

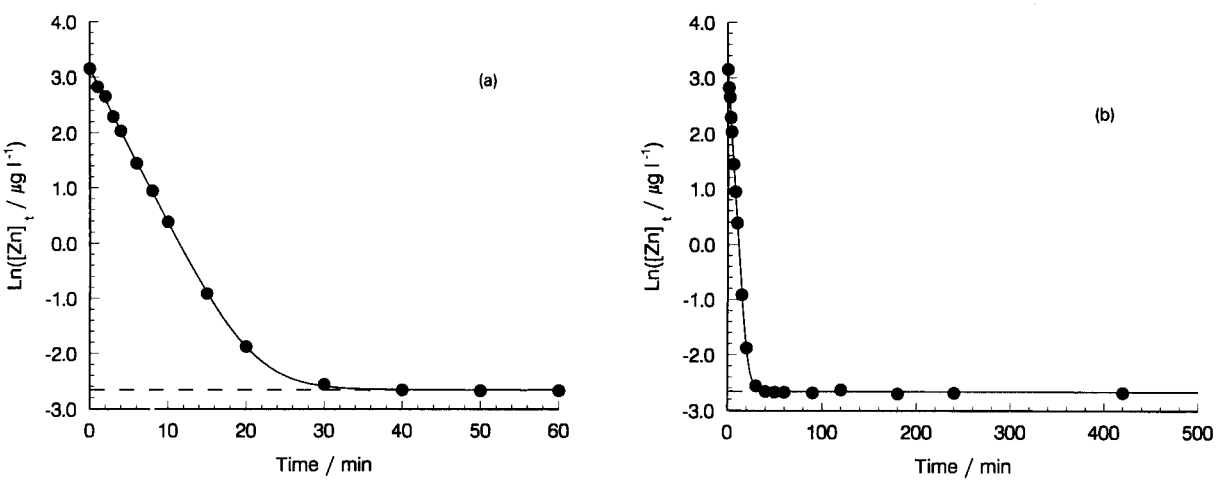

Fig. 3. Zinc remaining in the rain water sample as a function of time after uptake by Chelex-100 resin in the Chelex batch technique. (a) is the expansion of (b) in the specific time range. The concentration of Chelex-100: 1% (w/v). • = experimental data; solid line = calculated value; broken line = experimental plot for the most slowly dissociating zinc component.

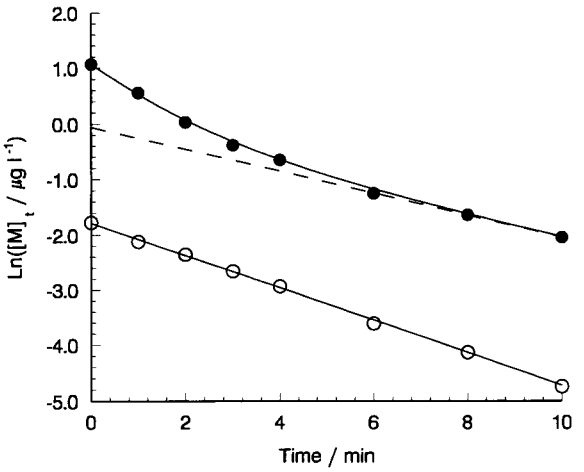

Fig. 4. Lead and cadmium remaining in the rain water sample as a function of time after uptake by Chelex-100 resin in the Chelex batch technique. The concentration of Chelex-100: 1% (w/v). ● = Pb experimental data; ○ = Cd experimental data; solid line = calculated value; broken line = experimental plot for the most slowly dissociating Pb component.

for all species were fitted by non-linear regression analysis to the function of Eq. 10.

The accuracy of the kinetic analysis depends to a great extent on the degree of adherence of the process to the kinetic model. The most crucial decision concerns the number of exponentials required in the function of Eq. 10 to fit the data. In this work, we adopted the method of weighted residuals [44] to assess the "goodness of fit" for the kinetic parameters.

$$r_e(t) = \frac{C_e(t) - C_c(t)}{[C_e(t)]^{1/2}} \qquad (12)$$

where $r_e(t)$ is the weighted residual, $C_e(t)$ is the concentration of metals remaining in the test solution measured at time t after uptake by Chelex-100 resin, $C_c(t)$ is the calculated concentration obtained from the derived model parame-

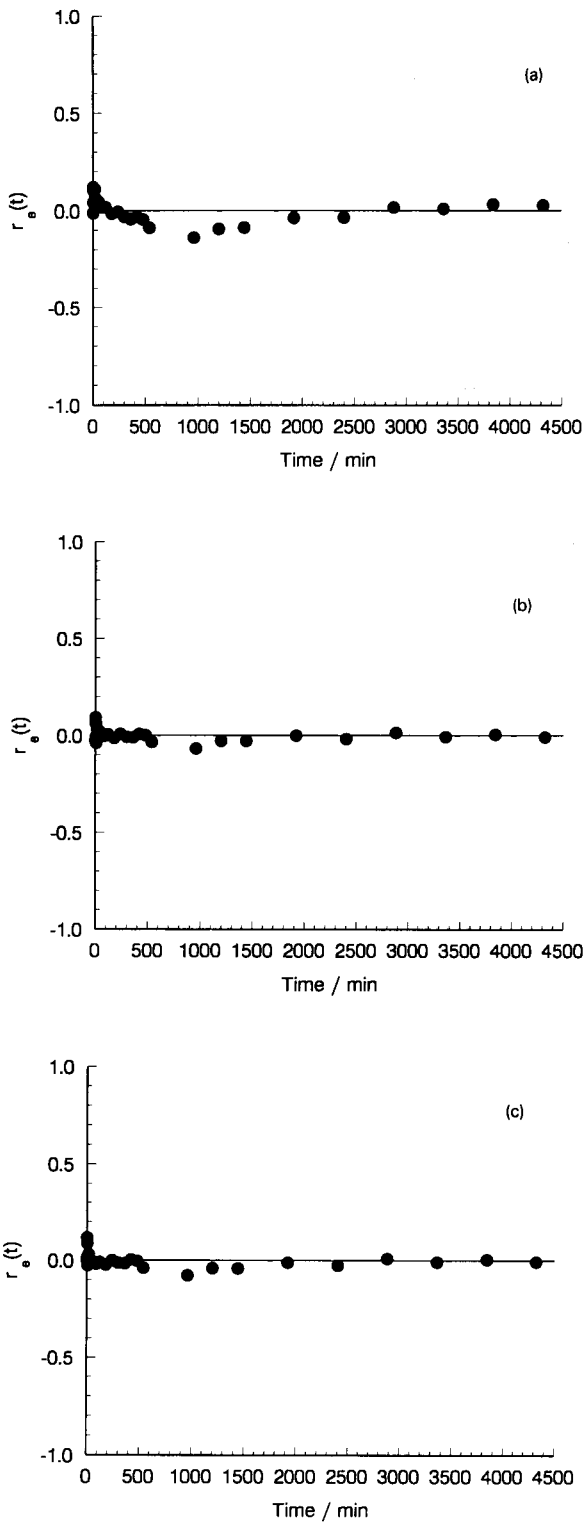

Fig. 5. Plots of weighted residuals versus time for copper species in the rain water sample. (a) 2-component-fitting with rate constants of 2.4×10^{-3} and 9.9×10^{-6}; (b) 3-component-fitting with rate constants of 2.3×10^{-3}, 3.3×10^{-5} and 8.5×10^{-6}; (c) 4-component-fitting with rate constants of 2.3×10^{-3}, 5.2×10^{-5}, 1.7×10^{-5} and 8.5×10^{-6}.

ters by non-linear regression analysis. If the model is adequate, the plot of the weighted residuals, $r_e(t)$, versus time, t, should appear to be randomly and normally distributed about zero. Fig. 5a–c shows the data fitting of the copper species in the soluble phase of the rain water sample. These figures clearly show that the 2-component-fitting gives a large error in the early reaction time region and the 4-component-fitting does not improve the results compared with the 3-component-fitting. Therefore, this data reduction method shows that three components of the copper species were kinetically distinguishable in the soluble phase of the rain water. Similar assessments were also made of the Zn, Pb and Cd species. The results of kinetic analysis suggest that in the rain water sample, the kinetically distinguishable components of the metal species were as follows: three for copper, two for Zn and Pb, and one for Cd. The values for the rate constants and $C_{i,o}$ obtained by non-linear regression analysis for each first-order or pseudo-first-order process are summarized in Table 6. The values of $C_{i,o}$ indicate the initial concentrations of each kinetically distinguishable component of the metal species which dissociated at a rate corresponding to the respective rate constant.

5. Conclusions

Our speciation scheme can accommodate an unknown number of components corresponding to different complexants or different binding sites in a polyfunctional complexant covering a wide range of rate constants. The half-lives of the first-order rate of dissociation of the metal complexes by the ASV and the Chelex-100 resin both column and batch techniques, can be identified and/or measured over the time range of milliseconds to days, covering about 8 orders of magnitude. By combining with ultrafiltration, more informative estimates of free and bound metal species based on size fractionation can be made. An important feature of this kinetic analysis scheme is that information about the lability of the metal species in aqueous environmental samples can be obtained not only qualitatively (i.e. "very labile", "moderately labile", "slowly labile" and "inert"), but also quantitatively, yielding meaningful values for kinetic parameters. Although the emphasis of this scheme is on the soluble phase, some information on the metal in the particulate phase can also be obtained by comparing the ASV measurement results of filtered and unfiltered samples. Use of graphite platform furnace atomic absorption spectrometry allows direct determination (i.e. without pre-concentration) of trace metals in rain water samples to be done rapidly with excellent accuracy and precision.

Comparing the results obtained by this kinetic analysis of the rain water sample with the previous results of the snow sample, we found that most of the metal species were similar in both the rain water and the snow sample. Since the distribution of metal species in aqueous media is pH-dependent the difference between the species in the rain water and the snow sample may be due to the difference in the pH of these samples. Most of Pb, Cd, Cu and Zn species in both the rain water sample and the snow sample were both ASV- and Chelex-column-labile, and fell in small size fractions. In rain water and snow samples, the concentration of organic complexing agents such as humic materials is generally low. Therefore, at an acidic pH of the samples the metal species in these samples are expected to be mainly metal aqua ions, hydroxo species, carbonato species and other small inorganic metal species which are present in small size fractions (MWCO < 1000).

6. Acknowledgements

The authors are grateful to the Natural Sciences and Engineering Research Council of Canada and Environment Canada: Atmospheric Environment Service for financial support of this research project. The authors thank Dr. A.G. Szabo, Institute of Biological Sciences, National Research Council of Canada, Ottawa, Canada, for valuable suggestions and discussion on the kinetic data analysis.

7. References

[1] J.J. Dulka and T.H. Risby, Anal. Chem., 48 (1976) 640A.
[2] V.D. Nguyen, P. Valenta and H.W. Nürnberg, Sci. Total Environ., 12 (1979) 151.
[3] A.W. Andren and S.E. Lindberg, Water Air Soil Pollut., 8 (1977) 199.
[4] P.P. Betson, Water Resources Research, 14 (1978) 1165.
[5] D.P. Dethier, Water Resources Research, 15 (1979) 787.
[6] S.J. Eiseneich, Water Air Soil Pollut., 13 (1980) 287.
[7] D.S. Jeffries and W.R. Synder, Water Air Soil Pollut., 15 (1981) 127.
[8] C.L. Chakrabarti, Y. Lu, J. Cheng, M.H. Back and W.H. Schroeder, Anal. Chim. Acta, 276 (1993) 47.
[9] T.M. Florence, G.M. Morrison and J.L. Stauber, Sci. Total Environ., 125 (1992) 1.
[10] R.M. Harrison, in J.O. Nriagu and C.I. Davidson (Eds.), Toxic Metals in the Atmosphere, Vol. 17, Wiley, New York, 1986, p. 319.
[11] R.D. Guy and C.L. Chakrabarti, in Proceedings of International Conference on Heavy Metals in Environment, Toronto, October 27–31, 1975, p. 275.
[12] R.D. Guy and C.L. Chakrabarti, Chemistry in Canada, 28 (1976) 26.
[13] C.H. Langford and D.W. Gutzman, Anal. Chim. Acta, 256 (1992) 183.
[14] J.A. Lavigne, C.H. Langford and M.K.S. Mak, Anal. Chem., 59 (1987) 2616.
[15] C.H. Langford and M.K.S. Mak, Comments Inorg. Chem., 2 (1983) 127.
[16] P.G.C. Campbell and A. Tessier, in J.-P. Vernet (Ed.), Heavy Metals in the Environment, Vol. 1, CEP Consultants, 1989, p. 516.
[17] P.G.C. Campbell and A. Tessier, in J.W. Patterson and R. Passino (Eds.), Metals Speciation Separation, and Recovery, Lewis Publishers, 1987, p. 201.
[18] P.G.C. Campbell and A. Tessier, Water Air Soil Pollut., 30 (1986) 1023.
[19] P. Figura and B. McDuffie, Anal. Chem., 52 (1980) 1433.
[20] P. Figura and B. McDuffie, Anal. Chem., 51 (1979) 120.
[21] D.L. Olson and M.S. Shuman, Geochim. Cosmochim. Acta, 49 (1985) 1371.
[22] D.L. Olson and M.S. Shuman, Anal. Chem., 55 (1983) 1103.
[23] T.M. Florence, Talanta, 29 (1982) 345.
[24] D.P.H. Laxen and R.M. Harrison, Sci. Total Environ., 19 (1981) 59.
[25] J.R. Kramer, P. Brassard, P.V. Collins, T. Clair, J. Guo and M. LeBeuf, Book of Abstracts XXVII-CSI Post-Symposium: Speciation of Elements in Environmental and Biological Sciences, June 16–18, 1991, Loen, Norway, p. I-1.
[26] Y.K. Chau, Analyst, 117 (1992) 551.
[27] G.E. Batley (Ed.), Trace Element Speciation: Analytical Methods and Problems, CRC Press, Boca Raton, FL, 1989, pp. 43–76.
[28] S.E. Cabaniss, Environ. Sci. Technol., 24 (1990) 583.
[29] M.K.S. Mak and C.H. Langford, Inorg. Chim. Acta, 70 (1983) 237.
[30] M.S. Shuman, B.J. Collins, P.J. Fitzgerald and D.L. Olson, in R.F. Christman and E.T. Gjessing (Eds.), Aquatic and Terrestrial Humic Materials, Ann Arbor Science, Ann Arbor, MI, 1983, p. 349.
[31] D.S. Gamble, A.W. Underdown and C.H. Langford, Anal. Chem., 52 (1980) 1901.
[32] J. Buffle, Complexation Reactions in Aquatic Systems: an Analytical Approach, Ellis Horwood, Chichester, 1988.
[33] J.G. Hering and F.M.M. Morel, Environ. Sci. Technol., 24 (1990) 242.
[34] B. Lim and T.D. Jickells, Global Biogeochem. Cycles, 4 (1990) 445.
[35] K.R. Lum, E.A. Kokotich and W.H. Schroeder, Sci. Total Environ., 63 (1987) 161.
[36] R. Kral, M. Mejstrik and J. Velicka, Sci. Total Environ., 111 (1992) 125.
[37] W. Davison, J. Electroanal. Chem. Interface Electrochem., 87 (1978) 395.
[38] D.R. Turner and M.J. Whitfield, Electroanal. Chem., 103 (1979) 73.
[39] G.E. Batley (Ed.), Trace Element Speciation: Analytical Methods and Problems, CRC Press, Boca Raton, FL, 1989, p 62.
[40] J.R. Moody and R.M. Lindstrom, Anal. Chem., 49 (1977) 2264.
[41] J.R. Wheeler, Limnol. Oceanogr., 21 (1976) 846.
[42] T.M. Florence, in G.E. Batley (Ed.), Trace Element Speciation: Analytical Methods and Problems, CRC Press, Boca Raton, FL, 1989, p. 83.
[43] D.I. Welch and C.D. Watts, Int. J. Environ. Anal. Chem., 38 (1990) 185.
[44] A.E. McKinnon, A.G. Szabo and D.R. Miller, J. Phys. Chem., 81 (1977) 1564.

ELSEVIER

Analytica Chimica Acta 288 (1994) 157–166

ANALYTICA CHIMICA ACTA

Adsorptive cathodic stripping voltammetric determination of ultra-trace concentrations of vanadium on a glassy carbon mercury film electrode

Samuel B.O. Adeloju *, Fleurdelis Pablo

Centre for Electrochemical Research and Analytical Technology, Department of Chemistry, University of Western Sydney, Nepean, P.O. Box 10, Kingswood, NSW 2747, Australia

(Received 2nd July 1993; revised manuscript received 2nd November 1993)

Abstract

The determination of trace and ultra-trace concentrations of vanadium(V) by adsorptive cathodic stripping voltammetry on a glassy carbon mercury film electrode is described. The method involves a controlled preconcentration of the element by interfacial accumulation as vanadium–pyrogallol complex on the electrode followed by cathodic stripping voltammetric measurement. The optimum analytical conditions for the measurement of vanadium by this method include the use of 0.20 M acetate buffer at pH 5.6 to 5.8, 5×10^{-4} M pyrogallol, an accumulation potential of -0.30 V vs. Ag/AgCl and a rotated electrode at 1920 rpm. The study of inorganic interference indicated that metal ions generally do not interfere with the vanadium determination, except for Pb(II) ions. However, the effect of this interference is eliminated by the addition of EDTA into the solution. The interference of surface-active substances, e.g., Triton X-100, is overcome by UV irradiation of the sample. For a 3-min accumulation, the linear concentration range obtained is 0–75 $\mu g\, l^{-1}$ ($R^2 = 0.948$) and lowest detectable amount is 1.0 $\mu g\, l^{-1}$ (R.S.D. = 9.5%). The use of the adsorptive voltammetric technique after dry-ashing and UV treatment of the samples is successfully demonstrated for the determination of vanadium in standard biological and environmental reference materials.

Key words: Stripping voltammetry; Glassy carbon mercury film electrode; Vanadium

1. Introduction

Vanadium is an important trace element which is known to be essential for some animals, but can also be toxic at high concentrations. Studies have shown that vanadium interferes with many biochemical processes. For example, it oxidizes L-ascorbate to form vanadium(IV) and dehydroascorbic acid, and it inhibits the activity of (Na, K)-ATPase, dynein ATPase, LAD-1, monoamine oxidase [1]. However, its physiological role is not yet fully understood. Vanadium is also used as an alloy additive for many steel products, and as a catalyst in the production of plastics and other chemicals. A common source of vanadium in the

* Corresponding author.

SSDI 0003-2670(93)E0631-G

environment include smoke from industrial stack, fly ash and thermometallurgical wastes.

Owing to its toxic and essential nature in biological systems, there has been a considerable interest in the determination of vanadium in various sample materials. The common methods used for the determination of vanadium are neutron activation analysis, spark-source spectrometry, atomic absorption spectrometry, colorimetry and electrochemical methods. The first two methods are relatively expensive and require specialized equipment which are often not accessible to most laboratories. Although spectrophotometric methods are available for the routine analysis of the element, the refractory oxides of vanadium are often difficult to dissociate in the flame or other heat-source used in these methods [1]. Other spectrophotometric methods involve a prior preconcentration such as complexation, solvent extraction, flotation separation or adsorption on a cationic exchange or chelating resin [2–11] which are often time-consuming. The stripping voltammetric methods which are similarly accurate, sensitive and relatively cheaper, have also been explored for the determination of vanadium using the hanging mercury drop electrode (HMDE) [12–14]. In particular, the use of adsorptive cathodic stripping voltammetry on HMDE has been successfully demonstrated for the determination of ultra-trace concentrations of the element. However, the use of a glassy carbon mercury film electrode (GCMFE) as a basis for improving the sensitivity of the technique and for enabling its use in flowing sample stream has never been explored. Furthermore, the use of the technique for the determination of ultra-trace concentrations of vanadium in biological materials has not been previously reported. Also, in view of the current lack of an accepted standard method for the determination of vanadium in biological and environmental materials, there is a need for further investigation in this area.

In this study, the determination of trace and ultra-trace concentrations of vanadium in biological and environmental materials by adsorptive cathodic stripping voltammetry (ACSV) on a glassy carbon mercury film electrode is explored. The method involves a controlled preconcentration of the element by interfacial accumulation as vanadium–pyrogallol complex on the electrode. This is followed by a subsequent cathodic potential scan to reduce the complex during the stripping step. Particular considerations include characterization of the electrode processes, optimization of the analytical conditions, study of the effects of inorganic and organic interferences. The utilization of the method for the determination of vanadium in biological and environmental materials by use of a dry-ashing procedure is also investigated.

2. Experimental

2.1. Apparatus

Stripping voltammograms were obtained using a Metrohm 646 Processor coupled with a 647 VA Stand. A 3-mm diameter rotating glassy carbon electrode filmed in situ with mercury from a 5×10^{-5} mol l^{-1} Hg(II) solution was employed as working electrode; a Ag/AgCl ([KCl] = 3 mol l^{-1}) and a 2 mm-diameter Pt rod were employed as reference and auxiliary electrode, respectively. Cyclic voltammograms were obtained using a BAS 100B coupled with BAS cell stand and plotter. pH measurements were made with an Activon digital pH/mV meter. Dry ashing of samples was carried out using the Heraeus Laboratory Muffle Furnace M 110. UV irradiation of samples was performed using a Raytech Model LS-7 UV equipment (0.2 A, 230 V, 50 Hz) in the shortwave region (2800–100 Å).

2.2. Reagents

Analytical-reagent grade chemicals (Ajax Chemicals) were used unless indicated otherwise. All solutions were prepared with Ultrapure water from Barnstead NANOpure and ULTROpure reverse osmosis systems. A stock (1 g l^{-1}) vanadium was prepared from ammonium metavanadate dissolved in 1 M hydrochloric acid. Dilute working standard solutions were prepared weekly from the stock solution by diluting with 0.1 M HCl solution. Stock (1 g l^{-1}) mercury was prepared

from mercuric chloride dissolved in 0.1 M HCl. Stock acetate buffer (2 M) was prepared from sodium acetate and acetic acid. Pyrogallol solution (0.1 M) was prepared daily from laboratory grade reagent and kept in the dark to prevent decomposition. Ethylenediaminetetraacetic acid disodium salt solution (1 g l^{-1}) was also prepared from laboratory grade reagent. The solutions for the interference studies were prepared from the corresponding metals dissolved in either HCl or HNO_3.

2.3. Procedures

Voltammetric measurement

Appropriate volumes of the supporting electrolyte (acetate buffer solution), Hg(II), pyrogallol, EDTA and vanadium standard solutions are placed into the polarographic cell. The voltammetric analyzer is then programmed to deaerate the solution with nitrogen for 5 min, while rotating the working electrode at 1920 rpm, apply the accumulation potential for the required period, allow 15 s for solution equilibration, and record the voltammogram under the following conditions: mode, differential-pulse; potential range, −0.30 V to −0.80 V vs Ag/AgCl; scan rates, 10 mV s^{-1}; pulse amplitude, 50 mV; duration between pulses, 600 ms; and potential step between pulses, 6 mV. The same instrumental parameters are used throughout the paper unless otherwise indicated. The cyclic voltammograms are obtained within a potential range of +0.30 and −1.30 V.

Analysis of samples

Sample preparation. Standard reference materials from National Institute of Standards and Technology, U.S. Department of Commerce (Gaithersburg, MD 20899) (bovine liver, apple leaves, peach leaves and urban particulate matter) were digested by a dry ashing method adapted from previously reported work [15–17]. The method involves dry ashing an accurately weighed sample in cleaned silica crucible in a muffle furnace using a programmed heating of 2 h at 100°C, 1 h at 150°C, 1 h at 250°C, 1 h at 350°C and at least 20 h at 450°C or until only a white residue is left. The cooled residue is dissolved in 3 ml 1 M HCl and UV irradiated for 8 h. The resulting

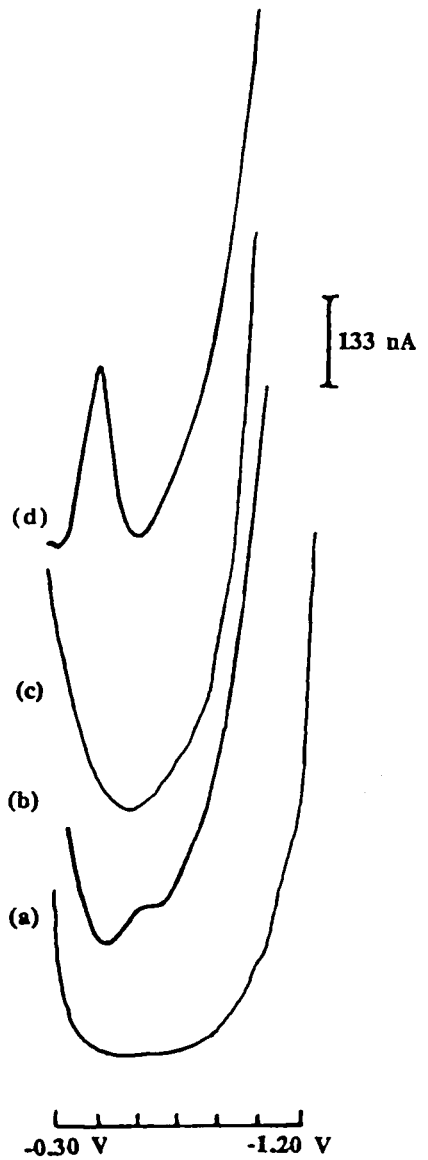

Fig. 1. Cathodic stripping voltammograms obtained on a GCMFE (rotated at 1920 rpm) to demonstrate the influence of pyrogallol on the reduction of vanadium for a 3-min accumulation at −0.30 V. (a) Blank consisting of 0.20 M acetate buffer at pH 5.7, 5×10^{-5}M Hg(II), 250 μg l^{-1} EDTA; (b) solution (a) with 25 μg l^{-1} V(V); (c) solution (a) with 5×10^{-4} M pyrogallol; (d) solution (a) with 25 μg l^{-1} V(V) and 5×10^{-4} M pyrogallol.

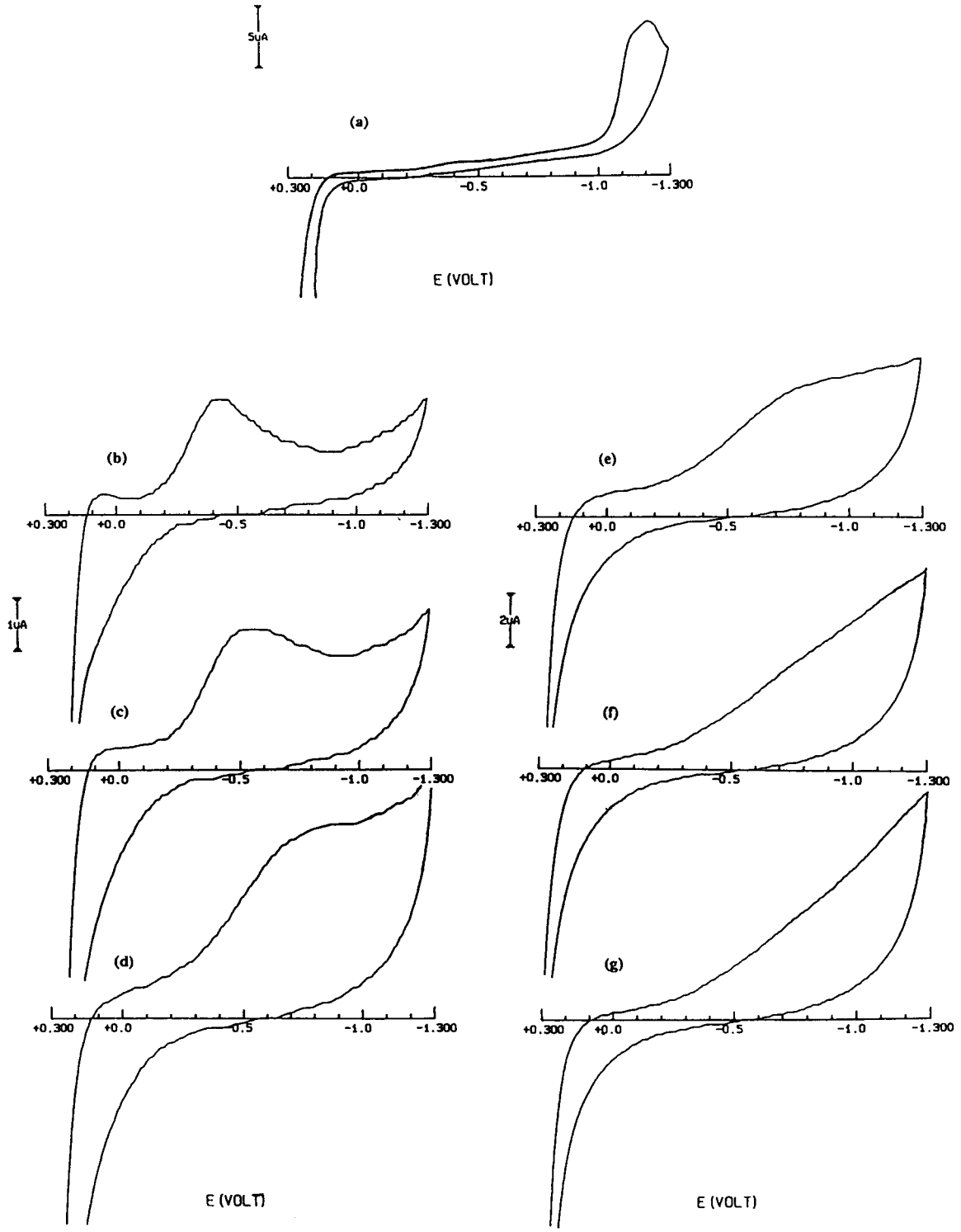
5uA
(a)
+0.300
+0.0
-0.5
-1.0
-1.300
E (VOLT)
(b)
(c)
(d)
1uA
(e)
(f)
(g)
2uA

solution is transferred into a volumetric flask and made up to the final volume with 1 M HCl.

Determination of vanadium. Appropriate volumes of the digested sample are taken for analysis by adsorptive CSV. The amount of vanadium is determined by the standard additions method based on 4 consecutive additions of vanadium within the linear concentration range for a 3-min accumulation period.

3. Results and discussion

3.1. Characterization of electrode processes

The utilization of various buffer systems such as ammonia–ammonium acetate, potassium hydrogen phthalate, phosphate, oxalate, borate and acetic acid–sodium acetate was investigated for the adsorptive cathodic stripping voltammetry of vanadium. Also, the effectiveness of complexing agents such as 8-hydroxyquinoline, catechol and pyrogallol was investigated. These complexing agents are known to form stable complexes with vanadium [18] and, of these, catechol has been previously used for the adsorptive cathodic stripping voltammetric determination of vanadium on a HMDE [12].

In this study, the optimum peak sensitivity and resolution for vanadium was obtained on the GCMFE with pyrogallol in the acetic acid–sodium acetate buffer electrolyte. The response obtained with the other buffer systems were either broad, unresolved or much less sensitive. The poor response obtained in the other buffer systems appeared to be due to their higher pH. The optimum pH for the formation and adsorption of the vanadium–pyrogallol complex lies within 5 and 6, as demonstrated later in this study. The acetate buffer provides the ideal pH for this purpose. In this buffer, the response obtained for vanadium with the use of pyrogallol was much more resolved and more than 7 times more sensitive than those obtained with catechol or 8-hydroxyquinoline.

Fig. 1 illustrates the effect of pyrogallol on the cathodic stripping behaviour of vanadium on GCMFE in acetate buffer. No peak was obtained for the blank solution (Fig. 1a), but in the presence of vanadium (Fig. 1b) a small peak was evident at −0.56 V due to the reduction of vanadium(V). Likewise, there was no response when pyrogallol was added to the blank (Fig. 1c), but the addition of vanadium(V) resulted in a considerable enhancement of the peak (Fig. 1d). This indicates that an interfacial accumulation process is involved during the preconcentration step. The application of an accumulation potential therefore enables the in situ formation of the mercury and the adsorption of vanadium–pyrogallol complex on the electrode surface:

$$V^{5+}_{(aq)} + nPG_{(aq)} \rightleftharpoons V(PG)^{(5-2n)+}_{n(aq)} + 2nH^+$$

$$V(PG)^{(5-2n)+}_{n(aq)} \rightleftharpoons V(PG)^{(5-2n)+}_{n(ads)}$$

where PG and n represent pyrogallol and number of pyrogallol reacting with V^{5+}, respectively. This view is supported by the lack of a vanadium response in the absence of mercuric ions in solution. The stripping step involves the reduction of the adsorbed vanadium–pyrogallol complex:

$$V(PG)^{(5-2n)+}_{n(ads)} + e^- \rightleftharpoons V(PG)^{(4-2n)+}_{n(aq)}$$

$$E_p = -0.51V$$

The formation of V(IV)–pyrogallol complex in aqueous media has been previously reported [18].

Fig. 2 shows the cyclic voltammograms for vanadium(V) on the GCMFE at various scan rates. The voltammograms were obtained without prior preconcentration in order to investigate the reversibility of the reduction process with spontaneous accumulation of vanadium–pyrogallol complex. Fig. 2a shows that in the absence of pyrogallol, a cathodic peak at −1.22 V corresponding to

Fig. 2. Cyclic voltammograms obtained on a GCMFE of 5.77×10^{-4} M V(V) in 0.20 M acetate buffer at pH 5.7 without prior preconcentration (a) without pyrogallol at 10 mV s^{-1} scan rate; and (b–g) with 2×10^{-2} M pyrogallol at scan rates 5, 10, 20, 30, 40 and 50 mV s^{-1}, respectively.

the reduction of V(V) to V(IV) is evident. However, in the presence of the complexing agent, a cathodic peak which corresponds to the reduction of vanadium(V)–pyrogallol to vanadium(IV)–pyrogallol is obtained (Fig. 2b–e). The peak potential shifted towards more negative values from −0.47 V to ca. −0.70 V with increasing scan rate between 5 and 30 mV s^{-1}, while the peak current decreased and the peak broadened. With further increase in the scan rate from 30 to 50 mV s^{-1} (Fig. 2e–g), the cathodic peak gradually disappeared. These observations indicate that the reversibility of the spontaneous accumulation–reduction process decreased with increasing scan rate. Also, it is apparent that within the scan rate studied, no corresponding anodic peak was obtained, indicating an overall irreversible process. Furthermore, the broadness of the cathodic peak indicates that the desorption/reduction of the vanadium complex involves a slow electron transfer. This view is consistent with the rather broad vanadium stripping response. Hence, the use of pyrogallol, a prior accumulation of vanadium–pyrogallol complex and a slow scan rate are desirable for the reliable determination of vanadium.

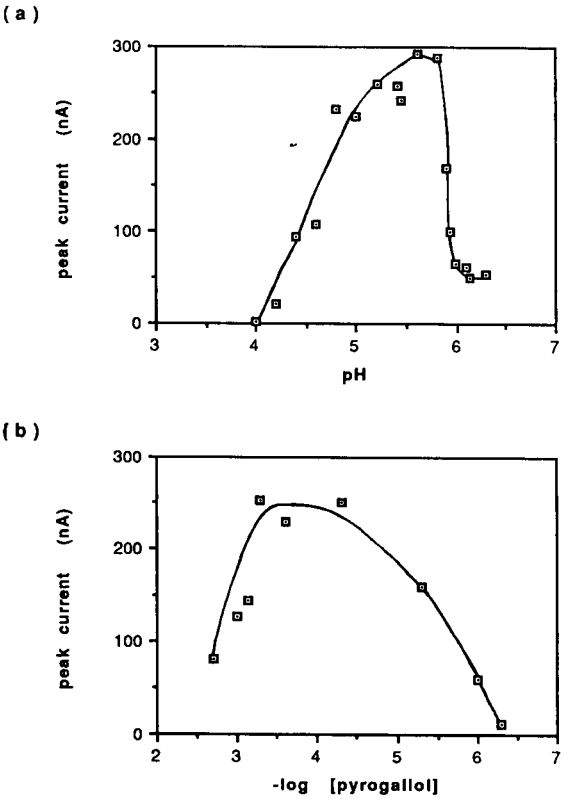

Fig. 3. Influence of (a) pH of 0.20 M acetate buffer electrolyte containing 5×10^{-4} M pyrogallol; (b) concentration of pyrogallol on the peak currents of 25 $\mu g\ l^{-1}$ (5×10^{-7} M) V(V) for an accumulation at −0.30 V for 300 s and 1920 rpm rotation of GCMFE.

3.2. Optimization of measurement conditions

Influence of pH and concentration of supporting electrolyte

The measurement of vanadium by adsorptive CSV is very much dependent on pH because of the involvement of hydronium ions in the complexation of vanadium and in maintaining the proper form of the complexing agent for reaction with vanadium. Thus, the pH and concentration of the acetate buffer electrolyte must be carefully chosen to give optimum sensitivity for the vanadium measurement.

The peak potential obtained for the adsorptive stripping voltammograms for vanadium(V) in the presence of pyrogallol shifted to more negative values and the peaks became more symmetrical with increasing pH. This observation suggests that the reduction of vanadium–pyrogallol complex is pH-dependent. Fig. 3a shows the influence of pH on the vanadium peak current and indicates that the best working pH range for the adsorptive CSV determination of the element is 5.6 to 5.8. Outside this pH range, the sensitivity is low and the stripping peak is poorly-shaped. At low pH (< 4), the pyrogallol is protonated making it inactive for complexation with vanadium. On the other hand, no response was obtained for vanadium at high pH (> 7) due to the tendency for vanadium(V) and vanadium(IV) to undergo complex hydrolysis–polymerization reactions in basic media [19].

The variation of the acetate buffer concentration from 0.05 to 0.50 M did not influence the sensitivity of the vanadium response significantly. This suggests that the buffer concentration range has sufficient buffering capacity to maintain the desired pH for the adsorptive accumulation.

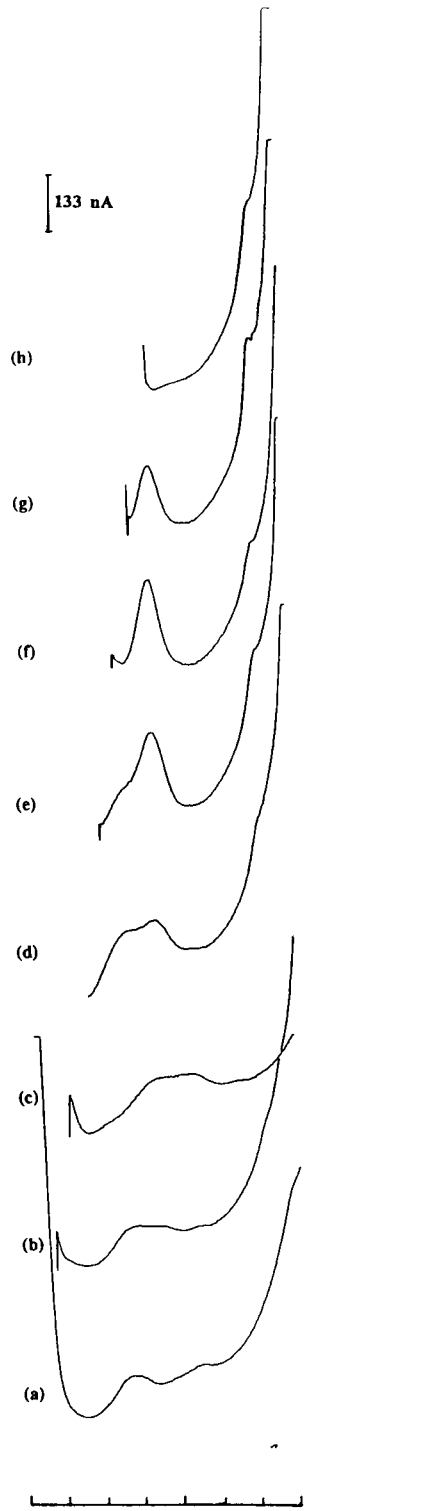

Hence, 0.20 M acetate buffer of pH 5.7 was used for all subsequent measurements.

Influence of concentration of pyrogallol

Fig. 3b shows the influence of pyrogallol concentration on the vanadium stripping peak currents. It is apparent that a concentration of the complexing agent of about 2 to 3 orders of magnitude higher than the concentration of vanadium is required to obtain good sensitivity for the measurement of vanadium. The excess pyrogallol seems to be useful in ensuring complete complexation of vanadium. However, the presence of a larger excess of pyrogallol (greater than 3 orders of magnitude compared to vanadium) resulted in decreased sensitivity, possibly due to competition between the excess pyrogallol and vanadium–pyrogallol complex for adsorption sites on the electrode. Hence, 5×10^{-4} M pyrogallol was used for all other work.

Influence of accumulation potential

Fig. 4 illustrates the influence of various accumulation potentials on the vanadium stripping peaks. It is apparent from the voltammograms that the use of an accumulation potential of −0.30 V gives optimum peak current and resolution. At less negative accumulation potentials (Fig. 4a–e), the sensitivity of the vanadium peak was low and the response was not well resolved from the pyrogallol peak which appears at the more positive potential. Accumulation of pyrogallol and vanadium–pyrogallol complex resulted in stripping peaks that overlap, indicating that these species are not interdiffusible [20]. Furthermore, the low peak currents obtained for the poorly-resolved peaks suggest that there is competition between the pyrogallol and vanadium–pyrogallol complex for accumulation onto the working electrode. The peak current for the pyrogallol response, which occurred at the more positive potential, increased

Fig. 4. Cathodic stripping voltammograms obtained on a GCMFE of 25 $\mu g\ l^{-1}$ V(V) for 3-min preconcentration on a GCMFE rotated at 1920 rpm at different accumulation potentials: (a) +0.20 V; (b) +0.10 V; (c) 0.00 V; (d) −0.10 V; (e) −0.20 V; (f) −0.30 V; (g) −0.40 V; and (h) −0.50 V vs. Ag/AgCl.

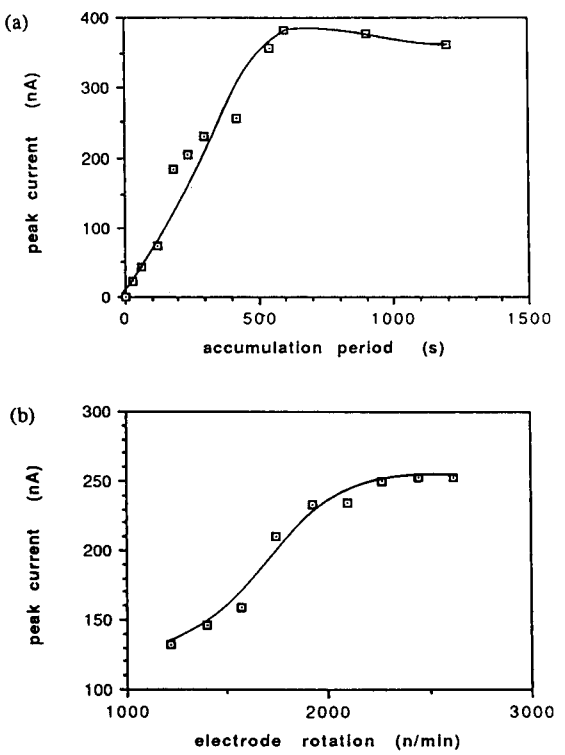

Fig. 5. Influence of (a) accumulation period; and (b) electrode rotation rate for a 5-min accumulation on the stripping peak currents of 25 $\mu g\ l^{-1}$ V(V).

with the increasing concentration of the complexing agent. However, the selective accumulation of the vanadium–pyrogallol complex was accomplished by the use of an accumulation potential more negative or equal to −0.30 V (Fig. 4f–h). The use of an E_{acc} more negative than −0.30 V (Fig. 4g–h) resulted in decreased peak current. Hence, an accumulation potential of −0.30 V was used for all subsequent measurements.

Influence of accumulation time and rate of electrode rotation

Fig. 5a shows the influence of accumulation period on the vanadium stripping peak currents. The peak currents increased with increasing accumulation period up to 600 s, but showed little variation at longer accumulation periods. This confirms the involvement of adsorption as the resulting saturation of the electrode surface at the long accumulation periods limits the stripping peak current.

The influence of the rate of electrode rotation on the vanadium peak currents is shown in Fig. 5b. The curve shows that the peak currents increased when electrode rotation rate between 1220 and 1920 rpm was used and the reproducibility of the results was good. Further increase in the rotation rate from 1920 to 2620 rpm resulted only in a slight increase in peak currents. Evidently, the peak current increased with the rate of electrode rotation until limited by saturation of the electrode surface. Moreover, the high rates of rotation caused strain on the drive belt rotating the electrode, resulting in poor reproducibility of the hydrodynamic conditions during the accumulation step. Hence, on the basis of sensitivity and reproducibility the electrode rotation rate of 1920 rpm was chosen.

3.3. Analytical applications

Inorganic and organic interferences

The interference effects of Cd, Pb, Cu, Zn, Mg, Cr, As, Fe, Co, Sn, Al and Ni ions were investigated in solutions containing equal amounts of the interferant and vanadium; and tenfold more interferant than vanadium. Except for Cd and Pb, the other metal ions did not interfere with the vanadium response, even when present at 10× the concentration of vanadium. On the other hand, cadmium gave a sharp, fairly resolved peak from vanadium at −0.67 V (180 mV more negative than the vanadium peak). A 10-fold increase in cadmium concentration caused about 50% suppression of the vanadium response. In contrast, lead gave a reduction peak which coincides with the vanadium response at −0.50 V. The addition of EDTA was effective in eliminating the Cd and Pb interference by forming complexes which are not readily adsorbed onto the electrode under the optimum experimental conditions. The required amount of EDTA for this masking effect is at least equal (in moles) or slightly more than the amount of interfering ions in solution, but not exceeding 1.2 ppm.

The addition of 250 $\mu g\ l^{-1}$ of Triton X-100, cetyl trimethyl ammonium bromide and sodium

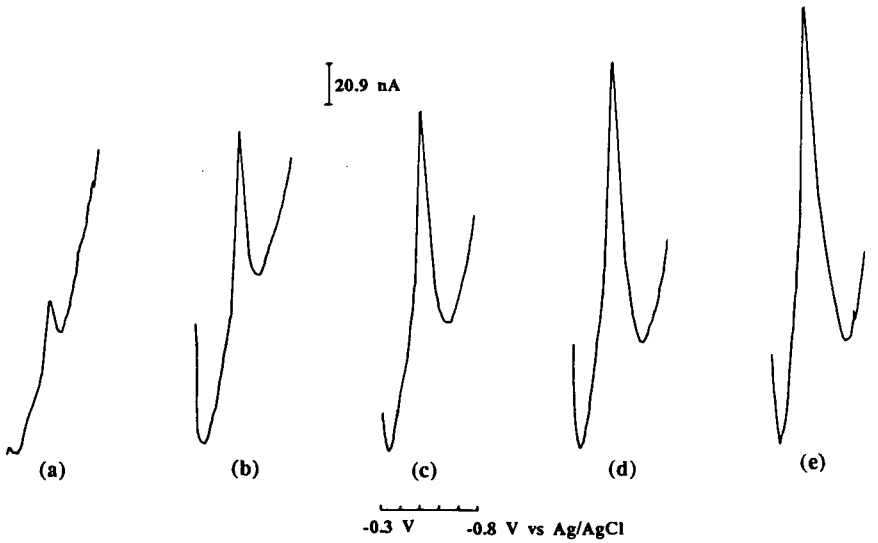

Fig. 6. Measurement of vanadium in dry-ashed sample of urban particulate matter by standard additions method. (a) sample only; (b–e) sample spiked with 5, 10, 15 and 20 $\mu g\ l^{-1}$ V(V), respectively.

dodecyl sulphate to a solution containing 25 $\mu g\ l^{-1}$ vanadium resulted in peak current suppression of 72.6, 46.5 and 71.4%, respectively. This is due to a competitive adsorption of the organic substance and vanadium–pyrogallol complex on the GCMFE. The results indicate that the organic substance is preferably adsorbed on the GCMFE. The organic interferences can be removed by sample digestion or UV treatment. In a previous work [15], it was shown that UV irradiation of the solution for at least 2 h enabled the breakdown of the organic substance and thus, improve the sensitivity of the desired complex.

Table 1
Linear concentration range and detection limit for different accumulation periods (t_{acc})

t_{acc} (s)	Linear concentration range ($\mu g\ l^{-1}$)	Lowest detectable concentration ($\mu g\ l^{-1}$) [a]
180	0–75 ($R^2 = 0.948$, $n = 18$)	1.0 (R.S.D. = 9.5%)
300	0–50 ($R^2 = 0.976$, $n = 12$)	0.5 (R.S.D. = 10.4%)
600	0–40 ($R^2 = 0.972$, $n = 10$)	0.25 (R.S.D. = 15.6%)

[a] $n = 10$; lowest detectable concentration based on signal-to-noise ratio of 3.

Linear concentration range and detection limit

Table 1 shows the achievable linear concentration range and lowest detectable concentration based on a signal-to-noise ratio of 3 for vanadium(V) at different accumulation period under the optimum analytical conditions obtained above.

Table 2
Analysis of standard reference materials

Reference material	Vanadium concentration	
	Adsorptive CSV [a]	Certified value
Urban particulate matter 1648	137.3 $\pm$ 7.7 $\mu g\ g^{-1}$	140 $\pm$ 3 $\mu g\ g^{-1}$
Peach leaves 1547	0.34 $\pm$ 0.04 $\mu g\ g^{-1}$	0.37 $\pm$ 0.03 $\mu g\ g^{-1}$
Apple leaves 1515	0.25 $\pm$ 0.05 $\mu g\ g^{-1}$	0.26 $\pm$ 0.03 $\mu g\ g^{-1}$
Bovine liver 1577b	0.117 $\pm$ 0.020 $\mu g\ g^{-1}$	0.123 $\mu g\ g^{-1}$ [b]

[a] Mean $\pm$ mean deviation ($n = 3$).
[b] Non-certified value.

Generally, a wider linear concentration range is achieved with shorter accumulation period, but the detection limit achieved under this condition is higher. Although the detection limit of 0.3 nM (0.015 $\mu g\ l^{-1}$) obtained by van den Berg and Huang for a 2-min accumulation of vanadium–catechol complex on a HMDE [12] is better than the 0.30 $\mu g\ l^{-1}$ (based on 3σ) obtained in this study with the GCMFE, the present method is still adequate for the determination of vanadium in most biological and environmental materials. A major advantage of this method is that it does not involve excessive use of mercury and it is more amenable for use in flow injection systems. Even in samples containing low concentrations of vanadium, the use of 3-min accumulation period is sufficient for the reliable determination of the element.

Analysis of reference materials

Fig. 6 shows typical voltammograms recorded for vanadium in dry-ashed sample of urban particulate matter under the optimum analytical conditions obtained above. As can be seen, the peak height increased with increasing concentration of vanadium. Table 2 summarizes the results obtained for the adsorptive stripping voltammetric determination of vanadium in the reference materials. The results show good agreement between the experimental and certified values. This indicates that the use of dry-ashing and UV-irradiation treatment of the sample, coupled with the adsorptive cathodic stripping voltammetric method is adequate for the reliable determination of vanadium in the samples.

4. Conclusion

The determination of ultra-trace concentrations of vanadium by adsorptive cathodic stripping voltammetry on a glassy carbon mercury film electrode has been successfully demonstrated. The use of the technique in conjunction with dry ashing and subsequent UV treatment enabled the reliable determination of vanadium in biological and environmental materials. The achievable limit of detection of 1 $\mu g\ l^{-1}$ with 3-min accumulation period, under the optimum analytical conditions, is sufficient for the analysis of the biological and environmental materials.

5. Acknowledgements

The authors are grateful to the University of Western Sydney, Nepean, for the provision of research support and a postgraduate research award for this project.

6. References

[1] UNEP-ILO-WHO, Environmental Health Criteria 81: Vanadium, WHO, Geneva, 1988.
[2] Z. Marczenko and R. Lobinski, Talanta, 35 (1988) 1001.
[3] K. Satyanarayana and R. Mishra, Anal. Chem., 46 (1974) 1609.
[4] R. Lobinski and Z. Marczenko, Anal. Sci., 4 (1988) 629.
[5] I. Mori, Y. Fujita, K. Fujita, T. Tanaka, Y. Nakahashi and A. Yoshii, Anal. Lett., 20 (1987) 747.
[6] C. Agarwal, M.K. Deb and R.K. Mishra, Anal. Lett., 23 (1990) 2063.
[7] O. Budevsky and L. Johnova, Talanta, 12 (1965) 291.
[8] F. Uchida, S. Yamada and M. Tanaka, Anal. Chim. Acta, 83 (1976) 427.
[9] S. Bhattacharya, S.K. Roy and A.K. Chakraburtty, Anal. Chim. Acta, 257 (1992) 123.
[10] R.R. Rao and S.M. Khopkar, Fresenius' Z. Anal. Chem., 343 (1992) 475.
[11] V. Dupont, Y. Auger, C. Jeandel and M. Wartel, Anal. Chem., 63 (1991) 520.
[12] C.M.G. van den Berg and Z.Q. Huang, Anal. Chem., 56 (1984) 2383.
[13] J. Wang, B. Tian and J. Lu, Talanta, 39 (1992) 1273.
[14] J. Lu, W. Jin and S. Wang, Anal. Chim. Acta, 238 (1990) 375.
[15] S.B.O. Adeloju and F. Pablo, Anal. Chim. Acta, 270 (1992) 143.
[16] A.R. Byrne and J. Kucera, Fresenius' Z. Anal. Chem., 340 (1991) 48.
[17] S.B.O. Adeloju and F. Pablo, Electroanalysis, (1994) submitted for publication.
[18] G. Wilkinson, R.D. Gillard and J.A. McCleverty (Eds.), Comprehensive Coordination Chemistry: The Synthesis, Reactions, Properties and Applications of Coordination Compounds, Vol. 3, Pergamon, Oxford, 1987.
[19] J.C. Bailar, H.J. Emeleus, Sir R. Nyholm and A.F. Trotman-Dickenson (Eds.), Comprehensive Inorganic Chemistry, Vol. 3, Pergamon, Oxford, 1973.
[20] A. Bond, Modern Polarographic Methods in Analytical Chemistry, Dekker, New York, 1980, p. 446.

ELSEVIER

Analytica Chimica Acta 288 (1994) 167–177

ANALYTICA CHIMICA ACTA

Investigation of nematic liquid crystals as surface acoustic wave sensor coatings for discrimination between isomeric aromatic organic vapors

Samuel J. Patrash, Edward T. Zellers *

The University of Michigan, School of Public Health, Department of Environmental and Industrial Health, Ann Arbor, MI 48109-2029, USA

(Received 23rd August 1993; revised manuscript received 15th October 1993)

Abstract

The use of thermotropic nematic liquid crystals (LC) as surface acoustic wave (SAW) vapor sensor coatings was investigated. Responses to four pairs of isomeric aromatic organic vapors were measured using two LC coatings and four isotropic polymer coatings. In most cases, the LC coatings showed higher sensitivity toward the more rod-like isomer within a pair due to the anisotropic nature of the deposited LC films. However, the importance of vapor-coating functional-group interactions as mediating factors in the sensor responses was evident in several cases. Incorporation of an LC coating into a four-sensor array improved the discrimination between isomers relative to an array employing only isotropic coatings. A persistent decline in the sensor baseline signal and vapor sensitivity observed over time with both LC coatings could be attributed to evaporative loss and/or changes in the elastic stiffness of the coatings.

Key words: Acoustic methods; Sensors; Liquid crystal; Vapor sensor; Surface acoustic wave sensor

1. Introduction

The development and characterization of surface coatings continues to be a major focus of research on coated bulk acoustic wave (BAW), surface acoustic wave (SAW) and related piezoelectric vapor sensors [1–4]. The type of coating material employed and the nature of the interactions that occur between the coating and the analyte vapor(s) are key determinants of sensor sensitivity and selectivity. With sorptive coatings, such as high-boiling liquids and rubbery polymers, responses vary directly with the extent of equilibrium vapor partitioning into the bulk of the coating. As a result, sensitivity is generally higher for less volatile vapors and for vapors capable of stronger intermolecular interactions with the coating [5]. The coating-vapor interaction strength, in turn, is determined principally by the relative polarities, polarizabilities, and hydrogen-bond donor/acceptor properties of the functional groups present in the interacting species [5–7]. Selective measurement of certain vapors is

* Corresponding author.

SSDI 0003-2670(93)E0609-B

possible by employing an array of sensors overlayed with different functionalized coating materials and then analyzing the response pattern obtained upon vapor exposure [8–10]. However, isomeric or structurally homologous vapors, which have very subtle differences in chemical properties, would not likely to be reliably discriminated from each other using conventional isotropic coating materials.

The use of coating materials capable of differentiating between vapors on the basis of molecular size and shape constitutes an alternative approach to achieving selectivity with BAW or SAW sensors and sensor arrays. Examples include zeolites, cyclodextrins, cyclophanes, calixarenes, and other so-called cavitands that are characterized by the presence of well-defined cavities or pores. Gases and vapors not able to fit within the cavities are not sorbed as strongly. Although a number of preliminary reports have appeared on the behavior of such materials as acoustic-wave sensor coatings [11–15], a systematic study demonstrating size/shape selectivity, while accounting for differences in vapor volatility and functional-group interactions with the coating material, has yet to be performed.

In this paper, we present results of an initial investigation of thermotropic nematic liquid crystals (LC) as SAW sensor coatings for discriminating between isomeric and structurally similar organic vapors. LCs are materials that exhibit properties intermediate between those of crystalline solids and isotropic liquids, either over a range of temperatures (as in thermotropic LCs) or due to the presence of solvent (as in lyotropic LCs) [16]. LCs can also be classified by the nature of their structural anisotropy: *nematic* LCs are characterized by anisotropic domains wherein the molecules are aligned parallel to one another; *smectic* LCs also exhibit domains of parallel alignment in addition to a well-ordered layered structure; and *cholesteric* LCs have a spiral anisotropy due to the presence of chiral centers in the constituent molecules.

The LC anisotropy gives rise to solvent properties that differ from those of isotropic liquids [16]. With nematic LCs, for example, solute vapors having more rod-like or planar shapes are often preferentially dissolved. This feature has been exploited in gas chromatography by using LC stationary phases to separate structural isomers (e.g., substituted aromatic compounds) that could not be resolved using standard isotropic stationary phases [17–19].

The first report on the use of LCs as acoustic wave sensor coatings was published by Mierzwinski and Witkiewicz [20]. In that study, responses from an 8-MHz quartz BAW resonator coated with each of four different nematic LCs were examined upon exposure to several vapors. Included in the set of vapors were the *o*- and *p*-isomers of diethylbenzene. For most of the vapors, sensor responses varied inversely with vapor boiling point as expected for isotropic coatings. In contrast, the responses for *p*-diethylbenzene were 1–21% greater than those for *o*-diethylbenzene, even though these isomers have the same boiling point. The differences in responses between these isomers were attributed to the preferential solubility of the more rod-like *p*-isomer in the LC coatings due to the LC anisotropy. Unfortunately, no data were provided on the responses to these isomers using isotropic coatings, and the possibility that the response differences could be accounted for wholly or partly by slight differences in polarity or polarizability between the isomeric vapors was not considered.

In the work described here, SAW sensor responses to several pairs of isomeric aromatic organic vapors are examined using LC coatings and then compared to those obtained using isotropic coatings that span a wide range of structures and polarities. One of our goals was to determine whether partial selectivity for *p*- or 4-substituted isomers would be observed consistently across different classes of aromatic compounds. In addition, we wanted to assess the relative contributions of structural anisotropy and functional-group interactions to SAW sensor responses using LC coatings. Finally, it was of interest to determine whether inclusion of LC coatings in a SAW sensor array would significantly improve the selective identification of isomeric vapors compared to an array employing only isotropic coating materials.

1.1. SAW sensor response equations

Eq. 1 gives an approximate expression for the change in the frequency of a SAW oscillator, Δf_c, upon deposition of a thin, non-conducting, perfectly elastic, isotropic coating film [21,22],

$$\Delta f_c = (k_1 + k_2) f_o^2 h \rho_c - k_1 f_o^2 h 4\mu[(\lambda + \mu) / (\lambda + 2\mu)] / V^2 \quad (1)$$

where k_1 and k_2 are substrate constants (-8.7×10^{-8} m^2/kg s and -3.9×10^{-8} m^2/kg s, respectively, for ST-quartz) [10], f_o is the frequency of the uncoated device (Hz), h is the coating film thickness (m), ρ_c is the density of the coating material (kg/m^3), V is the acoustic wave velocity (3158 m/s for ST-quartz), and λ and μ are, respectively, the Lamé constant and shear modulus of the film (N/m^2).

The quantity $h\rho_c$ is equivalent to the mass per unit area of the film and the first term on the right-hand side of Eq. 1 reflects the component of the sensor response arising from the addition (or loss) of mass from the surface of the sensor. Since k_1 and k_2 are negative, increases of mass lead to decreases in the output frequency. The second term on the right hand side of Eq. 1 depends primarily on the elastic stiffness or, more specifically, the shear modulus of the coating film, μ. The effective value of μ is frequency dependent and will therefore increase with the operating frequency of the SAW sensor [10,23,24]. For coatings whose shear moduli are in the range of 10^7–10^9 N/m^2, the magnitude of the second term of Eq. 1 will be about 1–10% of that of the first term. However, since k_1 is negative, the second term will lead to a positive shift in frequency, counteracting the effect of mass loading. The net value of Δf_c will then depend on the relative contributions of the first and second terms of the equation. The observation that Δf_c is invariably negative upon coating deposition indicates that the effect of mass loading predominates over that of elastic stiffness.

An equation similar to Eq. 1 can be used to describe the change of frequency upon exposure of a coated SAW sensor to a vapor [24,25]. For sorptive polymer coatings, vapor exposure causes an increase in the coating mass and a decrease in elastic stiffness (i.e., softening). In this case, the second term on the right hand side of Eq. 1 is positive and mass loading, softening, or a combination of the two will cause a negative shift in sensor frequency.

It has been shown, however, that the following simplified equation can describe quite accurately the responses of polymer-coated SAW oscillators to organic vapors [5,24]:

$$\Delta f_v = \Delta f_c K_e C_v / \rho_c \quad (2)$$

where Δf_v is the frequency shift observed upon exposure to a vapor, C_v is the atmospheric vapor concentration, and K_e is the "effective" partition coefficient. For cases where liquid or rubbery-amorphous polymer coatings are used, responses to most vapors are linear over a considerable range of concentration and K_e can be used as a summary measure of sensitivity. Values of K_e are typically higher than the partition coefficients determined from gas chromatographic measurements [5,24] presumably because sensor responses are a function of changes in both the mass and modulus of the coating upon vapor sorption. Thus, while K_e is not a true partition coefficient it nonetheless serves as a useful index with which to compare sensor responses to different vapors.

2. Experimental

Two commercially available LC coating materials, referred to as E38 and ZLI-389 (EM Industries, Hawthorn, NY), were investigated. E38 is a proprietary mixture of 4-cyano-4′-*n*-alkylbiphenyls ($\rho = 1.005$ g/cm^3) that exhibits a stable nematic phase between -9 and 85°C. ZLI-389 is a proprietary mixture of two types of aromatic esters ($\rho = 1.077$ g/cm^3) with a nematic range between -20 and 60°C. Aside from their commercial availability, these particular LCs were chosen for study because they have nematic ranges that bracket normal ambient temperatures and, unlike many common LCs, they are chemically stable in the presence of atmospheric oxygen and water vapor. Their basic structures are shown below.

E38

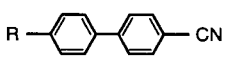

ZLI-389

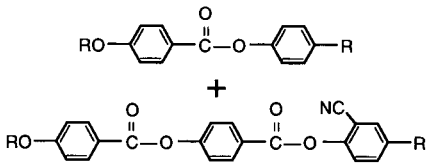

The following isotropic coatings were also examined: poly(bis(cyanoallyl)siloxane) ($\rho = 1.001$ g/cm^3, OV-275), poly(methylphenylsiloxane) (25% methyl, $\rho = 1.15$ g/cm^3, OV-25), poly(phenyl ether) six-rings ($\rho = 1.22$ g/cm^3, PPE), Apiezon-L (a branched hydrocarbon grease, $\rho = 0.892$ g/cm^3, APL) (Anspec, Ann Arbor, MI), and poly(isobutylene) ($\rho = 0.918$ g/cm^3, PIB) (Aldrich, Milwaukee, WI). Solutions of the coatings were prepared in one of several organic solvents and applied to the sensors using an airbrush. For each coating material, the deposition process was monitored via the sensor frequency shift and concluded when Δf_c reached approximately 200 kHz (note: the actual quantity measured was the difference frequency between the coated device and an uncoated reference device, and since the frequency of the coated sensor was initially lower than that of the reference sensor, decreases in the coated sensor frequency correspond to increases in the difference frequency).

The solvents examined are listed in Table 1 along with their respective boiling points [26]. All solvents were obtained from Aldrich and were greater than 98% pure, with the exception of the lutidine (i.e., dimethylpyridine) isomers which were 96% pure.

A dual 158-MHz delay-line oscillator configuration, consisting of a coated oscillator and a sealed uncoated reference oscillator, was employed. The oscillators and associated circuitry (i.e., mixers, amplifiers, frequency counters, etc.) were obtained from Microsensor Systems, Bowling Green, KY. A few initial measurements were collected with an individual sensor pair while the majority were collected with an array of four sensor pairs. In all cases, difference frequencies were collected at 2-s intervals and logged on a personal computer via an RS-232 interface. Coated sensors were fitted with nickel-plated lids each having vapor inlet and outlet ports. The lids were held in place with clamps and a Teflon® gasket was used to seal the lids to the T-08

Table 1
K_e ratios of rod-like to non-rod-like isomers for all coatings

Vapor pair	b.p. (°C)	coating						
		APL	PIB	OV-25	PPE	OV-275	ZLI-389	E-38
p-Xylene/*m*-xylene	138/139	1.04	0.97	1.04	0.97	1.08	1.05	1.16
Standard deviation		0.02	nd	nd	nd	0.03	0.01	0.04
n		5	1	1	1	2	3	8
4-Methylstyrene/α-methylstyrene	169/163	1.25	1.06	1.04	1.01	1.26	1.49	1.65
Standard deviation		0.05	nd	nd	nd	0.02	0.03	0.02
n		2	1	1	1	2	3	3
4-Chlorotoluene/2-chlorotoluene	162/159	1.02	0.91	0.97	1.04	1.09	1.23	1.21
Standard deviation		0.02	nd	nd	nd	0.10	0.04	0.03
n		2	1	1	1	2	3	2
2,5-Lutidine/2,4-lutidine	157/159	0.90	0.87	0.96	0.90	0.86	0.95	0.91
Standard deviation		0.01	nd	nd	nd	0.01	0.05	0.04
n		2	1	1	1	2	3	3

n = Number of determinations, nd = not determined.

headers on which the sensors were mounted. Sensor temperatures were maintained at 25 ± 0.1°C by contacting the lids either with heating tape or with an aluminum block through which thermostatted water was circulated. The temperature was monitored with a thermocouple threaded inside of one of the sensor lids.

Dynamic test atmospheres of each vapor were generated by bubbling nitrogen through the liquid solvent and then diluting with a stream of filtered clean air controlled to 25°C and 50% relative humidity (Model HCS-302 Flow-Humidity-Temperature Controller, Miller-Nelson Research, Carmel Valley, CA). Vapor concentrations were monitored continuously with an infrared gas analyzer (MIRAN 1A, Foxboro, Bridgewood, MA) placed in-line upstream from the sensors. The sensors were connected to the system via stainless steel or Teflon® tubing and a four-port valve was used to expose the sensor(s) alternately to clean air and air containing the test vapor. The flow rates over the sensors were maintained at approximately 0.080 l/min and were monitored with downstream rotameters.

Each measurement sequence consisted of an initial exposure to clean humidified air to establish a stable baseline frequency followed by duplicate 40-s exposures to a pre-set concentration of the test vapor. Each vapor exposure was separated by a 40-s exposure to clean air. Responses and recoveries were quite rapid, with stable readings being attained within 10-20 s of introduction or removal of the vapor stream. Readings from the last 10 s of each exposure period were averaged and the baseline subtracted to obtain the net sensor response at a given vapor concentration. Each vapor was tested at four different concentrations over a 4–10 fold range. Pairs of isomeric vapors were tested over similar concentration ranges.

3. Results and discussion

3.1. Responses to isomeric vapors

Sensor responses to the vapors were linear for all coatings over the concentration ranges tested and yielded calibration plots with linear regression correlation coefficients (r^2) > 0.99. Values of K_e were calculated for each vapor/coating combination from the average of the responses at each concentration (Eq. 2). K_e for the isotropic coatings ranged from about 2000 to 25 000 and calculated limits of detection (LOD) ranged from 10 to 110 μg/l (the LOD is defined here as the concentration producing a signal-to-noise ratio of three, where a noise level of 15 Hz is assumed). Specific values of K_e and LOD for each isotropic coating/vapor combination have been published elsewhere [5]. For the LC coatings, initial K_e values (see below) ranged from 3600 to 21 000 and LODs ranged from about 10 to 60 μg/l. Typical values of K_e for E38 and ZLI-389 were, respectively, 4380 and 4720 (*p*-xylene), 3660 and 4440 (*m*-xylene), 21 400 and 21 300 (4-methylstyrene), 12 900 and 14 500 (α-methylstyrene), 10 700 and 12 200 (4-chlorotoluene), 9030 and 10 300 (2-chlorotoluene), 12 500 and 13 400 (2,5-lutidine), and 13 400 and 14 900 (2,4-lutidine). Intercoating reproducibility, as determined from the average K_e for *m*-xylene from fresh replicate coating films ($n = 2$–5), was within the range of ±15% for the LC coatings.

Since our primary interest is in the relative responses to the various isomers, the average K_e value for each rod-like (i.e., *p*- or 4-substituted) isomer has been divided by that for the corresponding non-rod-like (i.e., *o*-, *m*-, or α-substituted) isomer for each coating (note: for the lutidines, the 2,5-isomer is considered to be more rod-like than the 2,4 isomer). Table 1 presents the ratios of the K_e values for each isomer pair on the isotropic and LC coatings. For sensor responses determined more than once with the same deposited coating film or with different films of that material, the average K_e ratio, standard deviation and number of determinations are provided in Table 1. The calculation of any particular ratio was always based on isomer responses collected on the same day.

For the xylenes, the *p*-isomer to *m*-isomer response ratios observed with the isotropic coatings ranged from 0.97 to 1.08, while that for E38 was 1.16. The ratio for E38 is significantly larger than the highest ratio observed with the isotropic

coatings as determined by a small-sample t-test of the respective average ratios ($p < 0.025$). The ratio for the other LC coating, ZLI-389, was 1.05 which is within the range observed with the isotropic coatings. Although the ratios for the isotropic coatings are all close to one, the fact that three of the five isotropic coatings gave response ratios greater than one belies the fact that the boiling point for the *p*-xylene is slightly lower than that of *m*-xylene. The substantially larger ratio observed for E38 suggests at least some degree of structural anisotropy in the deposited coating film. The failure to observe a larger response ratio with ZLI-389 may be due to the lack of anisotropic alignment in the deposited film, the disruption of alignment upon vapor sorption, and/or the predominance of chemical (i.e., functional group) factors over shape factors in the overall coating-vapor interaction.

For the chlorotoluenes, the 4-isomer to 2-isomer K_e ratios range from 0.91 to 1.09 on the isotropic coatings, whereas both of the LC coatings give ratios of about 1.2. In this case, a higher response was expected for the higher boiling 4-isomer. Statistical comparisons show that the ZLI-389 ratio is significantly larger than that of the highest isotropic-coating ratio ($p < 0.10$), but that the E38 ratio is not ($p > 0.10$) most likely due to the small sample sizes used. The similarity of the ratios for the LC coatings is curious in light of the data for the xylenes: since the chlorine atom is similar in size to the methyl group, the response ratios for the chlorotoluenes with ZLI-389 were expected to be comparable to those for the xylenes. This provides further evidence of the importance of factors other than shape in affecting responses with this LC coating.

For the methylstyrene isomers the isotropic coatings consistently gave 4-isomer to α-isomer ratios > 1 (range = 1.01–1.26), accordant with the order of boiling points. Once again, however, the LC coatings gave ratios significantly larger than those for the isotropic coatings: 1.49 ($p < 0.005$) and 1.65 ($p < 0.005$) for ZLI-389 and E38, respectively. That the larger ratios observed with the LC coatings are attributable principally to differences in shape between these isomers is supported by photoelectron spectroscopic data showing that in α-methylstyrene the ring carbon atoms and pendant ethylene carbon atoms are not coplanar [27], in contrast to styrene (and, presumably 4-methylstyrene). Thus, the α-methylstyrene would not be expected to fit as well into the parallel LC domains.

Finally, for the lutidines the isotropic coatings gave 2,5-isomer to 2,4-isomer response ratios ranging from 0.86 to 0.96, again, consistent with the slightly higher boiling point of the latter isomer. In this case, however, neither LC coating showed preferential response toward the more rod-like 2,5-lutidine, and the response ratios were similar to those for the isotropic coatings (i.e., ZLI-389 = 0.95 and E38 = 0.91). Factors related to chemical interactions with these relatively polar isomers apparently predominate completely over shape factors for both of the LC coatings.

3.2. Responses to other structurally similar vapors

The preceding results indicate that the LC anisotropy can indeed influence the relative responses to isomeric aromatic vapors due to differences in their shapes, but also that functional-group interactions are important mediating factors. To explore this issue further, responses to cyclohexane, cyclohexene and benzene were examined using the same set of coatings as above. These vapors were selected, in part, based on a previous report describing their analysis by gas chromatography using LC stationary phases and several unspecified isotropic stationary phases [17]. The finding that these vapors eluted in the order given above on the LC stationary phases was attributed to the progression in structure from the planar benzene to the non-planar cyclohexane. These results were contrasted to those observed using the isotropic phases, where these vapors eluted in the order of boiling points (i.e., benzene < cyclohexane < cyclohexene).

Table 2 presents normalized values of K_e for these three vapors on each of the coatings examined. To facilitate comparisons between coatings, the three K_e values for a given coating have been normalized by the highest K_e observed. For the non-polar coatings APL and PIB, the order of K_e follows that of the vapor boiling points, as ex-

Table 2
Normalized K_e values for benzene, cyclohexane, and cyclohexene

Vapor	b.p. (°C)	Normalized K_e value					
		APL	PIB	E38	OV-25	PPE	OV-275
Benzene	80	0.69	0.75	1.00	1.00	1.00	1.00
Cyclohexane	81	0.82	0.84	0.27	0.44	0.26	0.12
Cyclohexene	83	1.00	1.00	0.42	0.65	0.52	0.44

pected. For E38, K_e increases from cyclohexane to cyclohexene to benzene ($K_e = 129$, 199, and 475, respectively), consistent with the expectations based on planarity. However, for the more polar coatings OV-25, PPE and OV-275, the order of K_e values also increases with vapor planarity. Furthermore, larger differences in responses are observed between these vapors with OV-275 than with E38 (note: specific values of K_e for these vapors on the isotropic coatings can be found in Ref. 5).

Thus shape differences are not necessarily the overriding factors governing the relative sensor responses (and gas chromatographic retention times) with LC materials. Benzene is not only the most planar vapor, but also the most polar and polarizable, followed in order by cyclohexene and cyclohexane. The presence of the cyano and phenyl functionalities in the E38, alone, could account for the greater affinity for benzene than for the other vapors.

3.3. Aging effects

Baseline frequencies and responses to *m*-xylene were monitored over time to assess coating stability. Table 3 presents some typical Δf_c and K_e values as a function of time for the LC coatings and two of the isotropic coatings. Data were collected for all four coatings simultaneously with the sensor array. Following an initial 5-day test period, the sensor array was allowed to stand at room temperature with the sensors covered for approximately three months and then a final exposure to *m*-xylene was performed. All K_e values were calculated using the initial value of Δf_c obtained directly after deposition of the coatings. This provides a common reference point for comparing the change of K_e to the change of Δf_c.

For OV-275, Δf_c was essentially constant with time, whereas for both of the LCs Δf_c declined substantially (63 and 51% for E38 and ZLI-389, respectively). For APL, Δf_c was quite constant over the initial 5-day period, but was found to have increased slightly (4%) prior to the final exposure to *m*-xylene. The *m*-xylene K_e value for OV-275 did not change significantly, while that for APL increased by about 15% and those for E38 and ZLI-389 decreased by 46 and 34%, respectively. Interestingly, the decreases in Δf_c for the LC coatings were consistently larger than the decreases in their K_e values for *m*-xylene, and the increase in Δf_c for APL was consistently smaller than the increase in K_e.

The most obvious explanation for the decline in Δf_c and K_e for the LC coatings is evaporation of the coatings from the sensor surface. The fact that the decline of K_e is less than that of Δf_c for

Table 3
Values of Δf_c (kHz) and K_e for *m*-xylene over time [a]

Coating	Day	Δf_c	% Change in Δf_c	K_e	% Change in K_e
E38	1	206	–	3660 (110)	–
	3	171	−17	3190 (70)	−13
	4	151	−27	2950 (130)	−19
	5	142	−31	2930 (90)	−20
	135	75	−64	1940 (90)	−47
ZLI-389	1	239	–	4430 (70)	–
	3	216	−10	4290 (90)	−3
	4	207	−13	4200 (50)	−5
	5	198	−17	4260 (60)	−4
	135	118	−51	2940 (90)	−34
OV-275	1	196	–	1890 (110)	–
	3	197	1	1950 (80)	3
	4	196	0	1960 (70)	4
	5	196	0	2020 (60)	7
	135	198	1	1990 (90)	5
APL	1	206	–	5120 (110)	–
	3	207	0	5330 (130)	4
	4	208	1	5350 (120)	4
	5	208	1	5650 (120)	10
	135	215	4	5880 (110)	15

[a] Values in parentheses are standard deviations determined from the K_e values at four exposure concentrations.

both LCs may be due to one component of the LC mixture evaporating to a greater extent than the other(s). If *m*-xylene were more soluble in the less volatile LC mixture component, K_e would not decline as rapidly as Δf_c.

Other aging mechanisms are also possible. According to Eq. 1, a decrease in the coating thickness, h, such as would occur upon slow evaporation of the coating, would lead to a proportional decrease in Δf_c, regardless of the relative contributions of the first and second terms of the equation to Δf_c. Vapor exposure would then yield a proportionally lower K_e value. If, however, the coating evaporation were coupled with an increase in the shear modulus, then K_e might decline to a lesser extent than Δf_c. Even without any loss of coating, a gradual increase in the shear modulus over time would lead to a decrease in the magnitude of Δf_c, and most likely some loss in sensitivity.

The increase in Δf_c for APL can also be explained in terms of modulus changes: a slow relaxation of chain segments in this oligomer could easily account for a decrease in the modulus, and the disproportionate increase in K_e for APL might be due to an increase in vapor sorption capacity accompanying the increased segmental mobility of the coating film.

The data presented in the previous sections indicate that the LC coatings do possess some degree of anisotropy. However, in the absence of an orienting electric field which would align all molecules in the coating in a common direction, deposited LC coating films most likely consist of a series of small domains where the molecules within each domain have a common average alignment but where successive domains are not necessarily aligned with each other [17]. Over time, the degree of orientation of the domains might increase, leading to an increase in the shear modulus of the coating film (note: although the electric field accompanying wave propagation on the SAW device could contribute to such a change, the oscillation of the field is of too high a frequency to cause synchronous "switching" of the LCs [28]). It is known that vapor solubility in the nematic phase of a substance is less than that in the isotropic phase of the same substance due to both entropic and enthalpic factors [17,19]. Thus, an increase in average alignment within the film would lead to a reduction in K_e.

The plausibility of modulus changes accounting for the observed changes in Δf_c can be assessed by using Eq. 1 to estimate the change of modulus required to account for the observed changes in Δf_c for the LC coatings under the assumption that the entire shift in Δf_c is due to shear modulus changes (note: it is recognized that Eq. 1 is strictly applicable to elastically isotropic coatings, but it should still serve as a useful, if only approximate, model). For E38, for example, the net change in Δf_c over 135 days was −63% or 131 kHz out of the total initial value of 200 MHz. If we assume a coating thickness of 60 nm and a value of 0.84 for the quantity $[(\lambda + \mu)/(\lambda + 2\mu)]$ in Eq. 1 (this quantity is constrained to be between about 0.67 and 1.0), then a modulus change of 6.3×10^9 N/m^2 would be required, regardless of the initial value of the shear modulus.

Although the actual value of the shear modulus of this LC coating is not known, shear moduli derived for several organic polymers from ultrasonic velocity measurements in the low-MHz frequency range [23] suggest that a value somewhere in the range of 10^7 to 10^9 N/m^2 would be expected for the LC coatings at a frequency of 158 MHz. Table 4 summarizes the magnitude of the change in μ required for various possible initial values in this range. For an initial modulus of 10^7 N/m^2, μ must increase by a factor of more than 600 to account for the shift in Δf_c, whereas for an initial value of 10^9 N/m^2, only about a 7-fold increase is necessary. Thus, one cannot rule out, a priori, the possibility that the

Table 4
Changes in shear modulus, μ, required to account for the baseline drift of the E38-coated sensor for various initial values of μ (see text)

$\mu_{initial}$ (N/m^2)	μ_{final} (N/m^2)	$\mu_{final}/\mu_{initial}$
10^9	7.3×10^9	7.3
10^8	6.4×10^9	64
10^7	6.3×10^9	630

observed decline in Δf_c is entirely due to modulus changes over time.

Additional insight into this issue was obtained from a separate series of exposures to both *m*- and *p*-xylene performed with the E38 coating over 26 days. Although the sensitivity declined with time, the magnitude of the decline was essentially the same for both vapors. The K_e values obtained with the freshly deposited coating were 4380 and 3660 for *p*- and *m*-xylene, respectively, yielding a ratio of 1.20. After 26 days, the respective K_e values had declined to 2720 and 2270, but the ratio remained constant at 1.20. If the decline in K_e were due to modulus changes associated with an increase in parallel alignment of the LC domains, then one would expect to see an increase in the *p*-xylene to *m*-xylene response ratio. The fact the response ratios did not change suggests that there was no significant change in alignment or modulus. Thus, the observed declines in Δf_c and K_e are most likely due to evaporative loss with perhaps a small contribution from modulus effects.

3.4. Isomer discrimination with a sensor array

Notwithstanding their instability, it was of interest to determine whether inclusion of LC coatings in an array of SAW sensors would improve the capability for differentiating individual isomers from one another. To this end, a comparison was made between response patterns obtained from an array of four SAW sensors employing the isotropic coatings OV-275, PIB, OV-25 and PPE and an array where one of the isotropic coatings was replaced by the LC coating E38. The PPE coating was selected for replacement because it was the most similar to E38 in terms of the absolute and relative magnitudes of responses to the test vapors. Thus, replacing this coating minimized any differences in the overall range of polarities spanned by the two arrays.

The performance of each array was first evaluated using a principal components analysis of the response data after pattern normalizing to remove the effect of concentration (i.e., for each test concentration, the individual sensor response was divided by the sum of responses from all four coatings in the array) [29]. Projection of the resulting response vectors onto the plane defined by the first two principal components provides an indication of the degree to which the responses to each vapor differ from one another.

Fig. 1a and b shows the principal components plots for the two arrays being considered. Each point represents the response projection for an individual vapor at a given concentration. For the all-isotropic array, *m*- and *p*-xylene cluster quite close together while for the array containing E38 the distance between *m*- and *p*-xylene clusters is greatly increased. A similar improvement in separation is observed between 2- and 4-chloro-

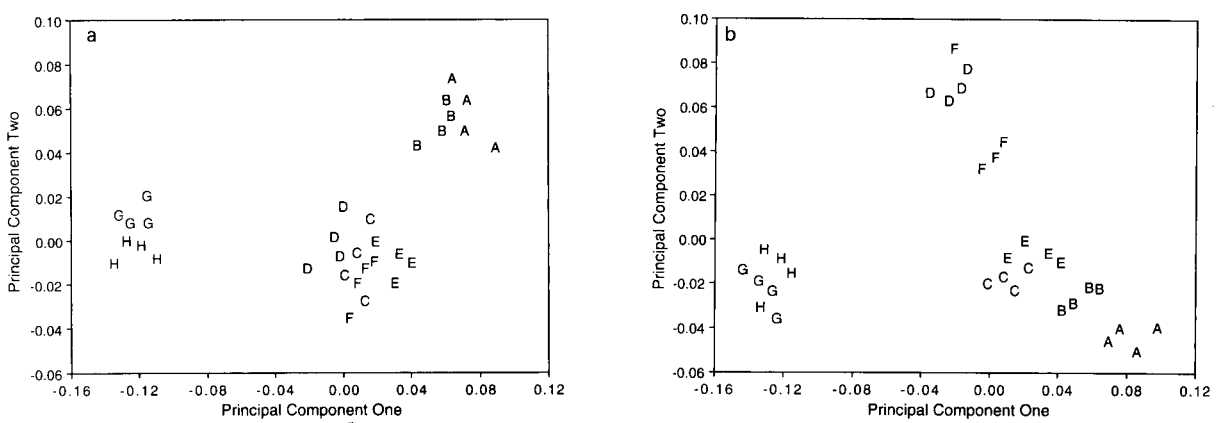

Fig. 1. Principal components analysis projections of response vectors for a four-sensor array with (a) four isotropic coatings and (b) three isotropic coatings and one LC coating (see text). A = *m*-xylene, B = *p*-xylene, C = α-methylstyrene, D = 4-methylstyrene, E = 2-chlorotoluene, F = 4-chlorotoluene, G = 2,4-lutidine, H = 2,5-lutidine.

toluene, and an even greater improvement is seen for the isomeric methylstyrene clusters. For the lutidines, where the K_e ratios were similar for the isotropic and E38 coatings, no increase in separation is observed with the use of the LC in the array. The overall improvement in isomer discrimination with inclusion of the LC coating is apparent, though it is also clear that the isotropic array will show some discrimination between isomers as well.

A more quantitative comparison of the two arrays was then performed using a disjoint principal components regression classification method [30]. In this method the first principal component determined from the array responses to each of the four test concentrations is used to model each vapor. The model created for each vapor is then used in classification procedures. That is, the response vector obtained upon subsequent exposure to a test vapor is compared successively to the principal component vectors of the previously modeled vapors. The test vapor is then identified on the basis of which principal component vector most closely matches that of its response vector.

In lieu of a separate set of response data, a simulated test set was created from the existing calibration set by superimposing Gaussian error (one standard deviation = 5%) on the sensor responses at each concentration and then sampling from the simulated distribution of responses. Each isomer pair was analyzed separately and for each isomer within a pair 40 simulated responses were classified. Error rates were determined from the fraction of incorrect isomer classifications out of the 80 total simulated responses. With the isotropic array error rates of 11, 10, 19 and 14% were obtained for the xylenes, chlorotoluenes, methylstyrenes and lutidines, respectively. As acknowledged above (and as shown in Fig. 1a), the isotropic array is capable of providing some discrimination between the isomers, but the error rates are somewhat higher than one would desire. For the array containing the LC coating there were no misclassifications for the first three pairs of isomers, while for the lutidines the error rate was the same as that for the isotropic array (i.e., 14%). The latter result was expected since the relative responses to the lutidine isomers for E38 were similar to those for PPE (and the other isotropic coatings). The improvement in classification for the other isomers, however, is significant.

4. Conclusions

This brief investigation of LC SAW coatings has yielded several noteworthy results. The importance of the structural anisotropy in as-deposited LC coating films was confirmed. However, it was also shown that the two LC materials investigated here exhibited different behavior and that the ability to discriminate between isomers on the basis of shape alone was not universal. That is, the shape discrimination is mediated by the same types of functional-group interactions that govern responses with isotropic coatings. Nonetheless, inclusion of LC coating materials in a SAW sensor array can enhance the ability to selectively identify certain vapors in the presence of their structural isomers compared to an array containing only isotropic coatings.

The finding that the alkyl cyanobiphenyl LC, E38, gave better discrimination than the aromatic ester LC, ZLI-389, is consistent with previous findings reported by Mierzwinski and Witkiewicz [20] for the one pair of isomers that they examined. It is not clear, however, why the cyanobiphenyl structure generally performs better, i.e., whether it is due to a greater degree of anisotropy or to differences in chemical interaction strengths with the vapors. There is some evidence indicating that cyanobiphenyls show a greater degree of alignment than certain other LC materials under the influence of an electric field [16]. Perhaps they also exhibit a greater degree of spontaneous alignment or are influenced more by interactions with the polar quartz surface of the sensor substrate than are LCs of other structures.

The persistent baseline drifts and losses of sensitivity of sensors coated with the LC materials examined here limit their practical utility. The evidence presented above suggests that evaporative loss of the coating is primarily responsible for these effects, but changes in shear modulus arising from changes in the average alignment of the

LCs over time may also have contributed. It should be possible to find less volatile nematic LCs that would not have this problem. A number of polymeric LCs with nematic ranges in the ambient temperature range are known [16,32] and would appear worth pursuing in light of the results obtained here.

Certain properties of LC materials, which were not investigated in this study, deserve mention. For example, the application of an orienting electric field as a preconditioning step in order to vary, or optimize, the degree of alignment in the LC coatings may be useful. While this will tend to decrease the average sensitivity to all vapors, it should also increase the selectivity for rod-like or planar molecules. Given the rather high sensitivity exhibited by the LCs used here, some loss in sensitivity could be tolerated in exchange for the improved selectivity expected with more highly oriented coating films. Another potentially useful feature of LCs is their susceptibility to abrupt phase transitions (i.e., from nematic to isotropic) in the presence of high concentrations of vapor phase solutes [16]. The large changes in sorbed mass and coating stiffness accompanying such transitions would lead to large changes in sensor response and might be used to trigger alarms in automated vapor monitoring systems. These issues are currently being investigated.

5. Acknowledgment

This work was funded by Grant K01-OHO0077 from the National Institute for Occupational Safety and Health of the Centers for Disease Control.

6. References

[1] M.S. Nieuwenhuizen and A. Venema, Sensors and Materials, 5 (1989) 261.
[2] J.J. McCallum, Analyst, 114 (1989) 1173.
[3] M.D. Ward and D.A. Buttry, Science, 249 (1990) 1000.
[4] R.C. Hughes, A.J. Ricco and M.A. Butler, Science, 254 (1991) 74.
[5] S.J. Patrash and E.T. Zellers, Anal. Chem., 65 (1993) 2055.
[6] D.S. Ballantine, Jr., S.L. Rose, J.W. Grate and H. Wohltjen, Anal. Chem., 58 (1986) 3058.
[7] J.W. Grate and M.H. Abraham, Sensors Actuators, B3 (1991) 85.
[8] S.L. Rose-Pehrrson, J.W. Grate, D.S. Ballantine, Jr. and P. Jurs, Anal. Chem., 60 (1988) 2801.
[9] W.P. Carey, K.R. Beebe and B.R. Kowalski, Anal. Chem., 59 (1987) 1529.
[10] H. Wohltjen, D.S. Ballantine, Jr. and N.L. Jarvis in R.W. Murray, R.E. Dessy, W.R. Heineman, J. Janata and W.R. Seitz (Eds.), Chemical Sensors and Microinstrumentation, ACS Symposium Series 403, American Chemical Society, Washington, DC, 1989, pp. 157–175.
[11] T. Bein, K. Brown, G.C. Frye and C.J. Brinker, J. Am. Chem. Soc., 111 (1989) 7640.
[12] C.S.I. Lai, G.J. Moody, J.D.R. Thomas, D.C. Mulligan, J.F. Stoddart and R. Zarzycki, J. Chem. Soc. Perkins Trans. II, (1988) 319.
[13] F.L. Dickert, Th. Bruckdorfer, H. Feigl, A. Haunschild, V. Kuschow, E. Obermeier, W.-E. Bulst, U. Knauer and G. Mages, Sensors Actuators, B13 (1993), 297.
[14] P. Nelli, E. Dalcanale, G. Faglia, G. Sberveglieri and P. Soncini, Sensors Actuators, B13 (1993) 302.
[15] F.L. Dickert and P.A. Bauer, Adv. Mater., 3 (1991) 436.
[16] G. Meier, E. Sackmann and J.G. Grabmaier, Applications of Liquid Crystals, Springer Verlag, Berlin, 1975.
[17] Z. Witkiewicz, J. Chromatogr., 251 (1982) 311.
[18] G.M. Janini, in J.C. Giddings, E. Grushka, J. Cazes and P.R. Brown (Eds.), Advances in Chromatography, Marcel Dekker, New York, 1979, p. 231.
[19] H. Rotzche, Stationary Phases in Gas Chromatography, Elsevier, Amsterdam, 1991, p. 291.
[20] A. Mierzwinski and Z. Witkiewicz, Talanta, 34 (1987) 865.
[21] H. Wohltjen, Sensors Actuators, 5 (1984) 307.
[22] B.A. Auld, Acoustic Fields and Waves in Solids, Vol. 2, Wiley, New York, 1973, p. 271.
[23] E.T. Zellers, R.M. White and S.W. Wenzel, Sensors Actuators, 14 (1988) 35.
[24] J.W. Grate, M. Klusty, R.A. McGill, M.H. Abraham, G. Whiting and J. Andonian-Haftvan, Anal. Chem., 64 (1992) 610.
[25] D.S. Ballantine, Jr., Anal. Chem., 64 (1992) 3069.
[26] R.C. Weast, D.R. Lide, M.J. Astle and W.H. Beyer (Eds.), CRC Handbook of Chemistry and Physics, 70th edn., CRC Press, Boca Raton, FL, 1989.
[27] J.P. Maier and D.W. Turner, J. Chem. Soc. Faraday Trans. II, 69 (1973) 196.
[28] T. Ikeda, T. Sasaki and K. Ichimura, Nature, 361 (1993) 428.
[29] D.L. Massart and L. Kaufman, The Interpretation of Analytical Chemical Data by the Use of Cluster Analysis, Wiley, New York, 1983.
[30] E.T. Zellers, T.S. Pan, S.J. Patrash, M. Han and S.A. Batterman, Sensors Actuators, B12 (1993) 123.
[31] S. Wold, Pattern Recognition, 8 (1978) 127.
[32] G.W. Gray, J.S. Hill and D. Lacey, Mol. Cryst. Liq. Cryst. Lett., 7 (1990) 47.

ELSEVIER

Analytica Chimica Acta 288 (1994) 179–185

ANALYTICA CHIMICA ACTA

Simultaneous measurement of mass and viscosity using piezoelectric quartz crystals in liquid media

G.L. Hayward *, G.Z. Chu

School of Engineering, University of Guelph, Guelph, Ontario, N1G 2W1 Canada

(Received 10th August 1993; revised manuscript received 8th October 1993)

Abstract

An inexpensive mass and viscosity sensor can be constructed from a quartz crystal microbalance using an automatic gain control oscillator. The gain control voltage, which maintains a constant oscillation amplitude, is shown to be affected only by the energy loss to the liquid medium and the crystal mounting. The frequency shift between a loaded and an unloaded crystal operating in the same medium is shown to closely follow the Sauerbrey equation. A viscosity or density correction based on the gain control voltage can be applied to the measured frequency shift to obtain the mass loading. Errors due to the oscillator phase shift and the crystal mounting losses can be removed by calibration.

Key words: Sensors; Piezoelectric methods; Mass and viscosity sensor; Quartz crystals; Viscosity

1. Introduction

The quartz crystal microbalance was originally used in vacuum to measure the mass of surface deposits [1]. The bulk wave devices commonly used were AT cut quartz crystals which oscillate in a thickness shear mode. The resonant frequency of the crystal, which depends on its mass, was measured by connecting the crystal as the frequency determining part of an electrical oscillator. As shown by Sauerbrey [1], the resonant frequency of a quartz crystal decreases linearly as mass is deposited onto its surface:

$$\Delta f = -2.26 \times 10^{-6} f_o^2 \Delta m/A \qquad (1)$$

where Δf is the frequency shift due to the added mass in Hz, f_o is the resonant frequency of the quartz crystal in Hz and $\Delta m/A$ is the surface mass loading in g cm^{-2}. This model predicts that a mass loading of 5.5 ng cm^{-2} gives a 1 Hz frequency shift with a crystal operating at 9 MHz, which is easily measured. More recently, the use of the quartz crystal microbalance in liquid media has received increasing attention. Applications include such diverse areas as biosensors for antigens or DNA [2], electrochemical deposition sensors [3], liquid chromatography detectors [4,5] and titration end-point indicators [6,7].

In liquid media, the acoustic coupling between the liquid and the quartz surface causes an additional frequency shift. This frequency shift has been modelled by Bruckenstein and Shay [8], who used a dimensional analysis of a diffusion anal-

* Corresponding author.

SSDI 0003-2670(93)E0608-A

ogy, by Kanazawa and Gordon [9] as a viscous shear wave propagating into the liquid and by Shana et al. [10], who included a piezoelectric term in the crystal stiffness. These three models were of the form:

$$\Delta f = -k f_o^{3/2} (\mu\rho)^{1/2} \quad (2)$$

where μ is the liquid viscosity, ρ is the liquid density and k is a constant. The form of this equation agrees with experimental data [11–13] although some deviation in very viscous media has been observed [14].

The viscous impedance has been calculated from an electrical analogy of mechanical shear [15,16] and from a solution of Stokes viscous shear wave propagating into the liquid [17,18]. All of these models were of the form:

$$Z_{\text{VISCOUS}} = 2\pi\sigma f_o^{1/2} (\mu\rho)^{1/2} (1+j) \quad (3)$$

where Z_{VISCOUS} is the viscous impedance, σ is a coupling coefficient and j is the square root of -1. Beck et al. [16] pointed out that the $(1+j)$ term breaks the viscous impedance term into a resistance or energy dissipation and an inductance or energy storage as fluid inertia. These, with an inductance corresponding to the inertia of mass deposited onto the crystal surface may be added to the Butterworth-van Dyke (BVD) electrical equivalent model of a quartz crystal [19] as shown in Fig. 1b. Since the resistance and induc-

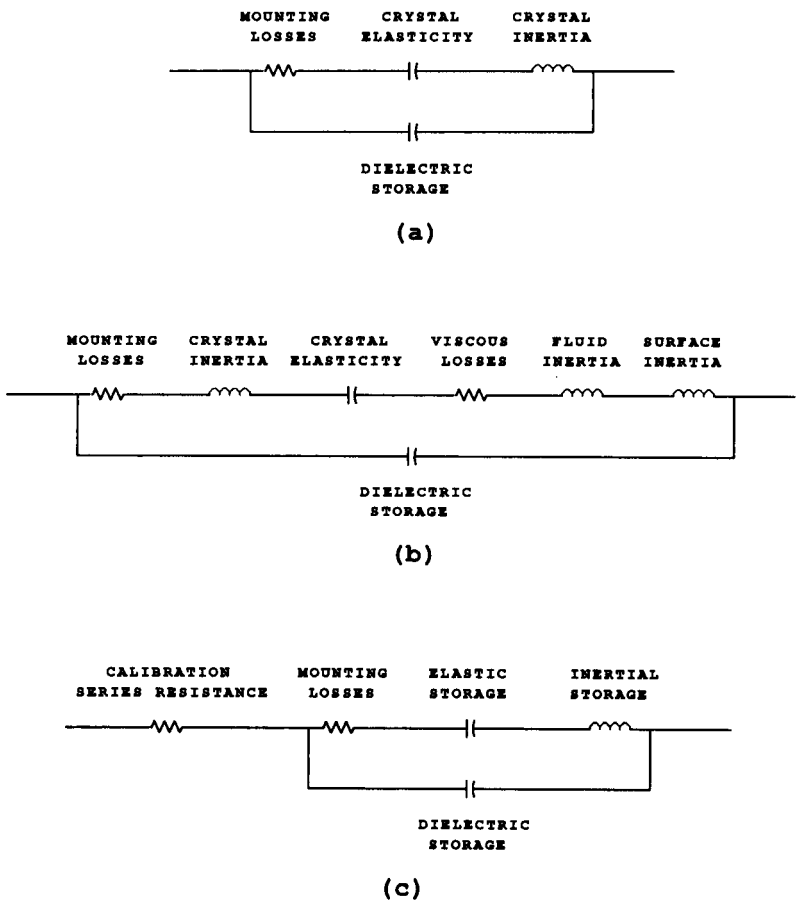

Fig. 1. Quartz crystal equivalent circuits. (a) Butterworth-van Dyke quartz crystal equivalent circuit. (b) Extended quartz crystal equivalent circuit. (c) Equivalent circuit with calibration resistor.

tance terms are additive, the individual values can not be determined from a single frequency measurement.

Network analysis provides a means to determine the values of the BVD parameters [14,17,20]. As before, the individual inductance and resistance components can not be resolved, but shifts from those of a dry, clean crystal can be attributed to viscous and mass loading. The increase in the resistance is due to viscosity, and since the viscous impedance contains the $(1+j)$ term, the viscous inductance can be calculated from [16]:

$$R_{\text{VISCOUS}} = 2\pi f_o L_{\text{VISCOUS}} \quad (4)$$

The remaining inductance increase may be attributed to the mass deposited on the crystal surface [20]. A mass determination, therefore, requires three measurements to resolve the three inductances of Fig. 1b. These are the unperturbed crystal inductance, the viscous inductance from Eq. 4 and the measured overall inductance.

An alternative to the network analyzer, which is a large and expensive research tool, is the automatic gain control (AGC) oscillator. This has been used in several studies [15,18,21,22] to measure the energy dissipation as well as the resonant frequency shift. Since the resistance is the only energy loss element, the AGC voltage required to maintain the oscillator output level may be calibrated against the resistance [18]. The measured frequency shift may be used to calculate the overall inductance change, and the mass calculated by subtracting the viscous inductance from Eq. 4. The mass and liquid loadings can, therefore, be obtained simultaneously from data provided by an AGC oscillator.

2. Experimental

The AGC oscillator used in the present study was designed by Simpson [15]. The oscillator section consists of a Motorola MC1350 amplifier and an NPN transistor. A biased comparator and an integrator form the AGC feedback loop. When the output amplitude decreases due to energy loss from the crystal, the duty cycle of the comparator output decreases, reducing the output of the integrator which is connected to the AGC input of the oscillator. At lower AGC voltages, the gain of the MC1350 increases restoring the amplitude of the oscillator output.

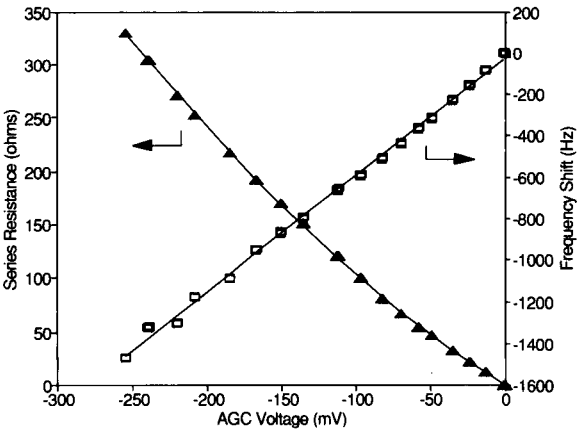

Fig. 2. Crystal resistance vs. AGC voltage calibration. Solid lines are regression fits.

The oscillation frequency was measured with a Hewlett Packard 5330B frequency counter. To improve the stability, a Raltron TF65010B oven controlled external time base was used. A bias amplifier was used to set the AGC reading to zero with a dry crystal connected to the oscillator.

Fig. 2 presents a calibration relating the crystal resistance to the AGC voltage. A series of fixed resistors were placed in series with dry crystals and the AGC voltage change and frequency shift were measured. These resistances were outside the BVD network as shown in Fig. 1c. The difference between the real part of the impedances of the BVD and calibration networks increased with the resistance, giving a maximum error of 2.5 Ohm for the present study. Using this circuit, Hager [21] and Simpson [15] report that the AGC voltage is linear with the viscous loss, however the gain of the MC1350 changes non-linearly with the AGC voltage [23]. Their AGC voltage changes were of the order of 0.045 V, which were small enough to approximate a linear relationship. A second order AGC calibration equation was obtained by a least squares fit. The correlation coefficient (R^2) was 0.9999 and the standard error of the resistance estimated from the AGC

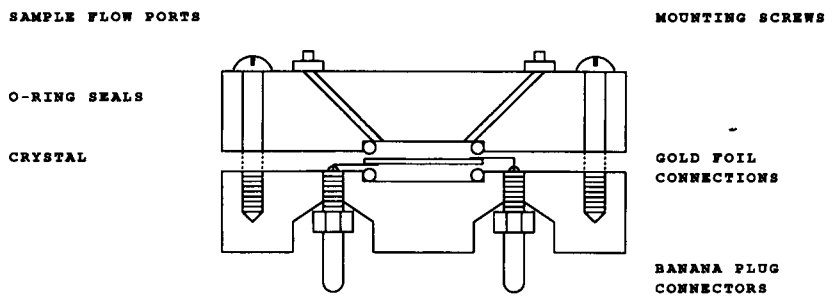

Fig. 3. Crystal support assembly.

voltage was 1.3 Ohm. Both of these errors were less than the dry crystal mounting resistance of approximately 4.9 Ohm, measured using a Hewlett Packard 4195A network analyzer.

The crystals used were 9.00 MHz AT-cut crystals 1.4 cm in diameter with 7 mm diameter gold electrodes (Lap-Tech, Bowmanville). The support assembly, made of a clear acrylic plastic, is shown in Fig. 3. The crystal was clamped between two O-rings with gold foil connections to the crystal electrodes. The entire assembly plugged directly into the oscillator module to reduce the length of the lead wiring. Liquid was passed across the top of the crystal. The entire system, including liquid samples and syringes was placed in a temperature controlled box at 30°C (±0.5°C). Five liquids were used, water and 5, 10, 15 and 20% glycerol (ACS grade, Fisher Scientific Co., Fair Lawn, NJ) by weight in water. The density and viscosity of these solutions were taken from Miner and Dalton [24].

The crystal surface mass was increased in steps by plating silver onto the wet electrode. The plating was performed by passing approximately 100 μA from a silver wire anode through a 0.01 M silver nitrate (ACS reagent grade, Aldrich, Milwaukee, WI) electrolyte. The crystal was not removed from the support assembly during the plating. The plating current was obtained from the voltage drop across a sense resistor and the plating time measured by a stopwatch. The deposited mass was calculated from the total charge passed through the cell.

Two crystals were plated. Each experiment was performed by measuring the frequency and AGC signal for each liquid. Sufficient liquid was passed across the crystal to ensure the glycerol concentration and the frequency was allowed to stabilize before data were recorded. After the five liquids were used, the cell was flushed with deionized water followed by silver nitrate solution and the plating was done. The silver wire anode was passed through one of the sample tubes to the space near the crystal. After plating, the crystal was again flushed with deionized water. This process was repeated 15 times for the first crystal and 18 times for the second.

3. Results

The resistance data obtained from the two plating experiments are shown in Fig. 4. The data

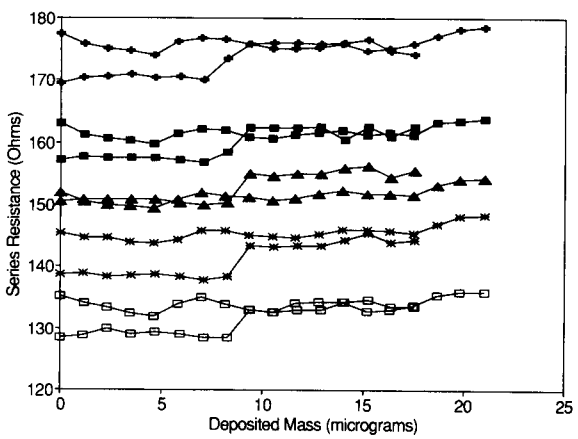

Fig. 4. Series resistance data. □, Water. *, 5% Glycerol. ▲, 10% Glycerol. ■, 15% Glycerol. +, 20% Glycerol.

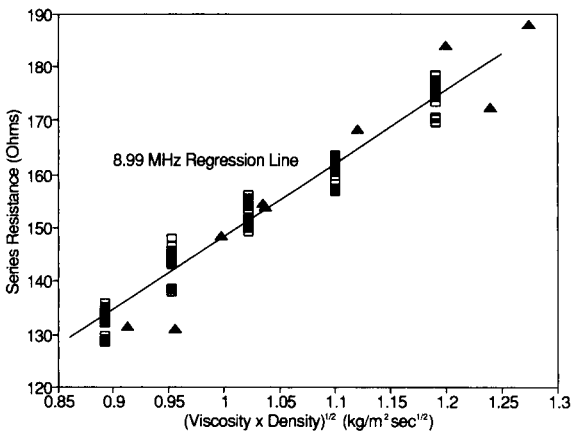

Fig. 5. Series resistance vs. liquid properties. □, Present data. ▲, Previous data [18].

are grouped as 5 horizontal lines, each corresponding to a different liquid medium. It is apparent from this that the amount of mass plated onto the crystal electrode has little effect on the viscous resistance. The increase at 9 μg observed in the data from one of the crystals can be attributed to surface roughness. At the end of each experiment, the crystal was examined. The silver was not deposited uniformly, but rather was concentrated in a few active areas on each crystal. Yang et al. [25] have shown that surface roughness increases the viscous resistance.

Fig. 5 presents these data as a function of the liquid properties. The data are linear in $(\mu\rho)^{1/2}$. The regression gave $R^2 = 0.968$ with a standard error of the resistance estimate of 2.6 Ohm. This is in agreement with equation 3. An electrode area correction from the resistance model derived by Hayward [18] was applied to data from that study. These data, also shown in Fig. 5, agree well with the present data.

The effect of deposited mass on the frequency shift is shown in Fig. 6. Here the frequency shift is the difference between the operating frequency of a plated crystal and that of the unplated crystal operating in the same liquid medium. The relationship is linear ($R^2 = 0.998$) and is in reasonable agreement with the Sauerbrey equation [1]. The difference in slopes suggests that the plating current efficiency was about 96%. This may be due to current leakage across the plating cell, or to the decomposition of water. The plating voltage was not controlled. No effect of the medium viscosity was noted in these data.

These plating experiments have shown that the equivalent resistance of a crystal is related to the viscosity and density of a liquid medium. The deposition of mass onto a crystal causes a frequency shift, but does not affect the equivalent resistance of the crystal. Moreover, when the frequency shift caused by mass loading is calculated from the frequency of a crystal operating in a particular medium, the properties of the medium do not affect the relationship between the mass and the frequency shift. These conditions are necessary, but not sufficient for the design of a mass and viscosity sensor to operate in an unknown medium.

The resistance of the crystal in an unknown solution can be used to obtain the frequency shift from a crystal operating in air by calculating $(\mu\rho)^{1/2}$ from the regression of Fig. 5 and then applying Eq. 2. To test this, data from 5 crystals, including those used in the plating experiments, are presented in Fig. 7. Two complicating factors emerge from these data.

The first factor is the oscillator phase shift. At high phase shifts, the crystal operating frequency is greatly affected by the crystal resistance [18]. The oscillator used in this study had a phase shift

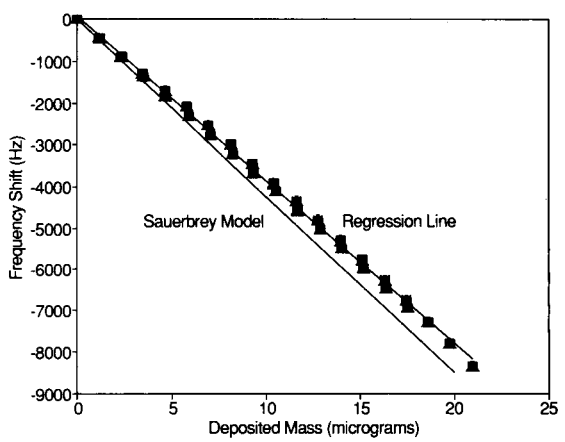

Fig. 6. Frequency shift due to deposited mass. □, Water. *, 5% Glycerol. ▲, 10% Glycerol. ■, 15% Glycerol. +, 20% Glycerol.

of +77.8 degrees. This value was obtained by measuring the operating frequency of three calibrated reference crystals and is in good agreement with the frequency response measurement reported previously [18]. The frequency shifts calculated from the model of Kanazawa and Gordon [8] were corrected by adding the frequency shifts calculated from the BVD equivalent circuit with resistances taken from Fig. 5. The result overpredicts the frequency shift by about 1500 Hz.

The second complicating factor is the mounting resistance. When a crystal is clamped between two O-rings, the energy lost to the O-ring depends on the orientation of the O-ring on the crystal and on the clamping pressure. The effect of these is enhanced when liquid increases the coupling between the O-ring and the crystal. From the BVD model at 77.8 degrees phase shift, a resistance of 30.4 Ohm will give a 1500 Hz frequency shift. This resistance is not unreasonable for mounting since the reference crystals mounted with two small spring clips had a measured resistance of 8 to 10 Ohm. Much more energy may be expected to be dissipated by O-ring mountings. The discrepancy between the curves shown in Figure 7 may, therefore, be attributed to mounting losses.

By changing the reference frequency to that of an unplated crystal operating in pure water, the subtraction to get frequency shift values compensates for the mounting resistance. These frequency shift data are shown in Fig. 8. Since the absolute values of the frequency shift are smaller, the nonlinearity of the oscillator phase shift component of the frequency shift is emphasized. A quadratic equation fitted the data well ($R^2 = 0.987$ with a standard error of frequency shift estimate of 40.2 Hz).

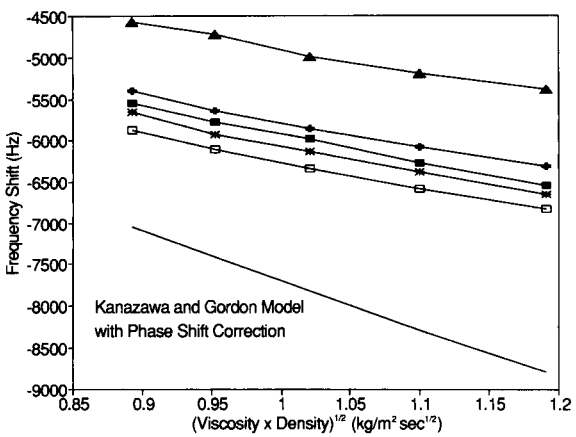

Fig. 7. Frequency shift from dry crystal operation. ▲, Crystal 1 (before plating). ■, Crystal 2 (before plating). *, Crystal 3. +, Crystal 4. □, Crystal 5.

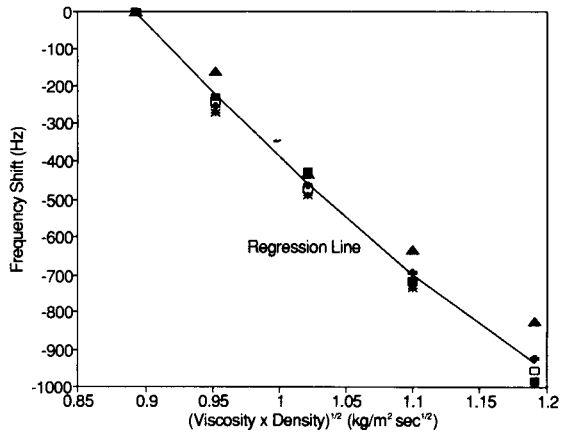

Fig. 8. Frequency shift from operation in water. ▲, Crystal 1 (before plating). ■, Crystal 2 (before plating). *, Crystal 3. +, Crystal 4. □, Crystal 5.

The unplated frequency in an unknown medium can be obtained from $(\mu\rho)^{1/2}$ which in turn is related to the resistance or to the AGC voltage. This may then be subtracted from the measured oscillation frequency to obtain the mass loading. As in the network analyzer method, three measurements are required, the unplated frequency in water, the AGC voltage and the oscillation frequency.

4. Conclusions

An inexpensive mass and viscosity sensor based on an AGC oscillator can be designed to operate in an unknown medium. The AGC voltage is affected only by the liquid medium so that a viscosity or density correction can be applied to the measured frequency shift to obtain the mass loading from the Sauerbrey equation [1]. Errors due to the oscillator phase shift and the crystal mounting losses can be removed by calibration.

5. List of symbols

A	Crystal electrode area, cm^2
f_o	Crystal frequency, Hz
j	Square root of -1
k	Frequency shift constant, $cm^2\ g^{-1}$
$L_{VISCOUS}$	Viscous inductance, Henry
R^2	Correlation coefficient from linear regression
$R_{VISCOUS}$	Viscous resistance, Ohm
$Z_{VISCOUS}$	Viscous impedance, Ohm
Δf	Frequency shift, Hz
Δm	Change in surface mass, g
μ	Liquid viscosity, $g\ cm^{-1}\ s^{-1}$
ρ	Liquid density, $g\ cm^{-3}$
σ	Acoustic coupling coefficient, Ohm $cm^2\ g^{-1}$

6. Acknowledgement

The authors would like to thank Dr. M. Thompson at the University of Toronto for allowing the use of the Hewlett Packard network analyzer. The financial support of the National Science and Engineering Research Council of Canada is gratefully acknowledged.

7. References

[1] G. Sauerbrey, Z. Phys., 155 (1959) 206.
[2] M. Thompson, A.L. Kipling, W.C. Duncan-Hewitt, L.V. Rajakovic, and B.A. Cavic-Vlasak, Analyst, 116 (1991) 881.
[3] R. Schumacher, R., Angew. Chem. Int. Ed. Engl., 29 (1990) 329.
[4] P.L. Konash and G.J. Bastiaans, Anal. Chem., 52 (1980) 1929.
[5] T. Nomura, T. Yanagihara and T. Mitsui, Anal. Chim. Acta., 248, (1991) 329.
[6] S.-Z. Yao, Z.-H. Mo and L.-H. Nie, Anal. Chim. Acta, 229 (1990) 205.
[7] S.-Z. Yao, Z.-H. Mo and L.-H. Nie, Anal. Chim. Acta, 230 (1990) 51.
[8] S. Bruckenstein and M. Shay, Electrochim. Acta, 30 (1985) 1295.
[9] K.K. Kanazawa and J.G. Gordon, Anal. Chim. Acta, 175 (1985) 99.
[10] Z.A. Shana, D.E. Radtke, U.R. Kelkar, F. Josse and D.T. Haworth, Anal. Chim. Acta, 231, (1990) 317.
[11] T. Nomura and A. Minemura, Nippon Kagaku Kaishi, 1980 (1980) 1621.
[12] T. Nomura and M. Okuhara, Anal. Chim. Acta, 142 (1982) 281.
[13] S.-Z. Yao and T.-A. Zhou, Anal. Chim. Acta, 212 (1988) 61.
[14] A.L. Kipling and M. Thompson, Anal. Chem., 62 (1990) 1514.
[15] R.L. Simpson, Ph.D. Thesis, University of Washington, 1985.
[16] R. Beck, U. Pittermann and K.G. Weil, K.G., Ber. Bunsenges. Phys. Chem., 92 (1988) 1363.
[17] H. Muramatsu, E. Tamiya and I. Karube, Anal. Chem., 60 (1988) 2142.
[18] G.L. Hayward, Anal. Chim. Acta, 264 (1992) 23.
[19] V.E. Bottom, Introduction to Quartz Crystal Unit Design, Van Nostrand Reinhold, New York, 1982.
[20] J. Martin, V.E. Granstaff and G.C. Frye, Anal. Chem., 63 (1991) 2272.
[21] H. Hager, Chem. Eng. Commun., 43 (1986) 25.
[22] M. Thompson, C.L. Arthur and G.K. Dhaliwal, Anal. Chem., 58 (1986) 1206.
[23] Motorola Inc., Linear and Interface Integrated Circuits, Motorola Inc., Phoenix, 1983.
[24] C.S. Miner and N.N. Dalton, Glycerol, Reinhold, New York, 1953.
[25] M. Yang, M. Thompson and W.C. Duncan-Hewitt, Langmuir, 9 (1993) 802.

ELSEVIER

Analytica Chimica Acta 288 (1994) 187–192

ANALYTICA CHIMICA ACTA

Direct electrochemical sensing of insecticides by bilayer lipid membranes

Dimitrios P. Nikolelis [a], Ulrich J. Krull *,[b]

[a] *Laboratory of Analytical Chemistry, Department of Chemistry, University of Athens, Panepistimiopolis-Kouponia, 15771 Athens, Greece,* [b] *Chemical Sensors Group, Department of Chemistry, Erindale Campus, University of Toronto, 3359 Mississauga Road North, Mississauga, Ontario L5L 1C6, Canada*

(Received 18th August 1993; revised manuscript received 29th October 1993)

Abstract

This work describes the use of bilayer lipid membranes (BLMs) as sensitive detectors for the direct electrochemical monitoring of the organophosphate and carbamate insecticides monocrotofos and carbofuran, respectively. Egg phosphatidylcholine (PC) and dipalmitoylphosphatidic acid (DPPA) were used for the formation of BLMs. The interactions of monocrotofos and carbofuran with BLMs produced a transient current signal with a duration of seconds, which reproducibly appeared within 3 to 5 min after exposure of the membranes to the insecticides. The sensitivity of response was maximized by use of high concentrations of the charged lipid, and by alteration of the phase distribution within membranes by the introduction of calcium ions in bulk solution. The mechanism of signal generation is related to the absorption of the lipophilic insecticide molecules with a consequent rapid reorganization of the membrane electrostatics. The magnitude of the transient current signal was linearly related to the concentration of monocrotofos or carbofuran in bulk solution with sub-micromolar detection limits.

Key words: Sensors; Bilayer lipid membranes; Carbofuran; Insecticides; Monocrotofos

1. Introduction

Organophosphate and carbamate insecticides are used on a large scale in agricultural and public health applications, and have toxicological effects associated with the inhibition of cholinesterases. Insecticides such as carbofuran have been shown to accumulate and contaminate both ground and surface water. It is therefore desirable to develop sensitive and rapid screening methods for monitoring these toxic pollutants.

A number of analytical methods have been developed in the past decade to quantitatively detect organophosphate and carbamate insecticides. Liquid chromatographic (LC) procedures are used extensively with very low detection limits; for example, carbofuran can be determined by these methods with a fluorescence detector to a level of ca. 5×10^{-9} M [1]. LC methods require sample preparation steps which extend analysis times, and this in addition to the size and cost of

* Corresponding author.

SSDI 0003-2670(93)E0625-H

LC instrumentation limits the use of this technology for screening applications in the field.

A number of electrochemical and optical sensors for the determination of insecticides have been developed recently, which are based on the inhibition of immobilized cholinesterases using various substrates such as acetylcholine, butyrylthiocholine and butyrylcholine [2–5]. A major drawback of these sensors is the long preincubation time of the enzyme with an insecticide for achieving inhibition which can reach to ca. 30 min. Furthermore efforts to reuse the chemically-selective membranes which contained immobilized enzyme resulted in a decrease of the sensitivity and further increase of the response time [2].

Sensors based on lipid membranes can transduce chemical composition into a measurable physical signal by means of selective interactions of the stimulant (analyte) with a membrane or membrane-embedded receptor [6]. The transduction can be designed to result from alterations of the electrostatic fields and/or phase structure of the lipid membrane. Biosensors based on lipid membranes for taste/odorous compounds [7,8] or eye-irritants [9] were reported previously. Investigations of the direct interaction of insecticides with membranes are generally limited to absorption and permeability studies using natural cell membranes [10]. Recently such studies have been extended beyond insecticide–acetylcholinesterase interactions to include receptors [11,12], and modulation of ion channel activity by insecticides [13]. Reports on direct interactions of insecticides with artificial lipid membranes for sensor development have not yet appeared in the literature, though other biological entities including antibodies have been used as selective binding agents to detect pesticides and pollutants [14].

In the present work the analytical utility of bilayer lipid membranes (BLMs) as electrochemical biosensors for direct monitoring of some insecticides such as monocrotofos and carbofuran is presented. The structure of the BLMs was tailored to contain conductive zones so that direct membrane/insecticide interactions could provide enhanced transient current signals. The transduction was a result of alterations of the electrostatics of BLMs based on the lipophilicity and dipole electrostatics of the insecticide.

2. Experimental

2.1. Materials and apparatus

The lipids used throughout this study were lyophilized egg phosphatidylcholine (PC; Avanti Polar Lipids, Birmingham, AL) and dipalmitoylphosphatidic acid (DPPA; Sigma, St. Louis, MO). HEPES (*N*-[2-hydroxyethyl]piperazine-*N'*-[2-ethanosulfonic acid]) was used for preparation of buffer and was supplied from Sigma. Stock solutions of insecticides were kindly donated by Benaki Phytopathological Institute (Athens, Greece) and included aldicarb and carbofuran in acetone (5.2×10^{-3} and 4.5×10^{-3} M, respectively), methyl parathion in methanol (1.9×10^{-3} M) and monocrotofos in acetone (4.5×10^{-5} M). These solutions were capped with parafilm and stored at −4°C in amber vials. Small volumes of the stock solutions were removed daily to be used for the experiments. Water was obtained from a Milli-Q cartridge purification system (Millipore, El Paso, TX) with a minimum resistivity of 18 Mohm cm, and all other chemicals were of analytical reagent grade.

The equipment for the formation of solventless BLMs has been described in detail elsewhere [15,16]. The membranes were formed in an aperture of 0.32 mm diameter in a Saran-Wrap™ partition (10–15 μm thickness) that separated two identical plexiglass chambers, each with a volume of 10 ml and an air/water interface of 3 cm^2. A 25-mV dc voltage was applied across the membrane between two Ag/AgCl reference electrodes. A digital electrometer (Model 614, Keithley Instruments, Cleveland, OH) was used as a current-to-voltage converter. The electrochemical cell and electronic equipment were isolated in a grounded Faraday cage.

2.2. Procedures

Stock solutions of PC and DPPA each containing 2.5 mg ml^{-1} in a mixture of *n*-hexane and

absolute ethanol (80 + 20, v/v) were used for the preparation of lipid solutions containing 35 and 60%, w/w, DPPA (0.2 mg ml^{-1} total lipid). The dilute lipid solutions were freshly prepared and the stock solutions were stored in a nitrogen atmosphere at −4°C. The BLMs were supported in a 0.1 M KCl electrolyte solution buffered with 10 mM HEPES at pH 7.5 and contained 0.5 or 1.0 mM calcium ions.

Solventless BLMs were prepared as previously described [15,16]. A volume of ca. 10 μl of dilute lipid solution was applied onto the electrolyte surface in one cell compartment, and then over a period of a few seconds, the water level in one solution compartment was brought below the aperture and then raised again with a disposable syringe. When the ion current stabilized (over a period of about 5 min), the insecticide solution was injected in one solution compartment using continuous gentle stirring. All experiments were done at 20 ± 1°C.

3. Results and Discussion

The interactions of hydronium and calcium ions with BLMs prepared from mixtures of egg PC and DPPA have been previously examined by conductivity measurements [17,18]. A critical transition concentration of about 25%, w/w, DPPA has been identified for BLMs in the presence of calcium ions. Below this DPPA content the conduction mechanism is associated with minimized surface charge and ion permeation. Above 25%, w/w, DPPA the ion permeation occurs through conductive zones formed by the acidic lipid which maximizes ion current magnitudes. The ability to control conductivity can be used to adjust the sensitivity of transducers based on BLMs [6]. For example, it is possible for a selective interaction between an analyte and a membrane embedded receptor to alter the phase structure and/or electrostatics of a BLM. Recent studies included alterations of the phase structure and/or electrostatic fields of BLMs by pH changes which were caused by an enzyme reaction at one surface of the membranes without disturbing the opposing leaflet [16]. An extension of this work included surface charge alterations caused by an immunological reaction which could be used for antigen determination [19]. A transient current signal was obtained in the latter case after a relatively constant delay time of about 2 min (independent of antigen concentration), while in the former enzyme experiments the time of appearance of the transient signal was related to the substrate concentration. The magnitude of the ion current signal can be maximized by controlling the factors which affect ion permeation, which can be adjusted by selection of the lipid composition used for BLM formation and the hydronium and calcium ion activity in bulk electrolyte solution. The most significant factors which affect ion permeation and therefore the magnitude of signal are the phase structure and surface potential of the lipid membranes. Generally the signal magnitude is maximized for more fluid BLMs and minimized surface potential when the signal is the result of surface charge alterations [19].

Some typical insecticides were chosen for our studies and included monocrotofos, carbofuran, aldicarb and methyl parathion (Fig. 1). Monocrotofos and methyl-parathion are organophosphorus insecticides, carbofuran is a carbamate derivative, whereas aldicarb is an aliphatic carbamoyl oxime. These toxicants are expected to adsorb and partition into the lipid membrane as determined by solubility parameters [10,20]; the degree of such an interaction depends largely on the chemical structure of the insecticide [10].

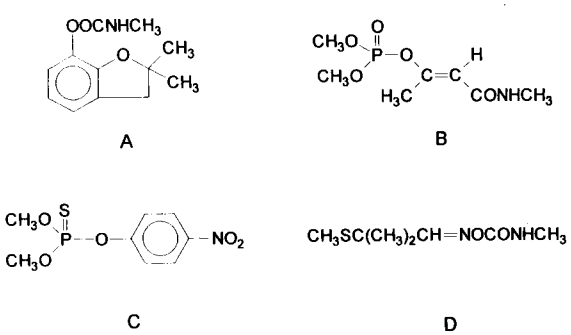

Fig. 1. Chemical structure of insecticides used. (A) Carbofuran, (B) monocrotofos, (C) methyl parathion, (D) aldicarb.

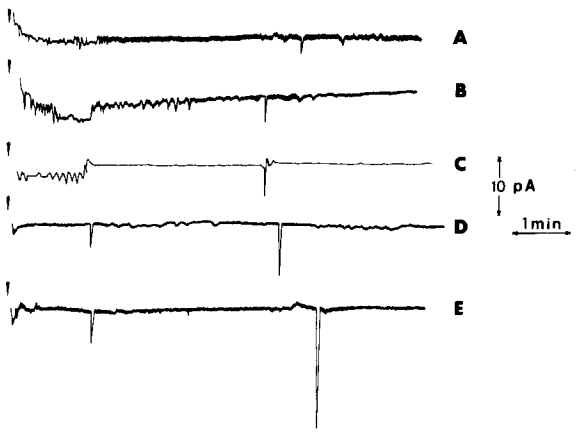

Fig. 2. Experimental results obtained with BLMs composed of 35%, w/w, DPPA in the presence of 1.0 mM of calcium ions and the following carbofuran concentrations in bulk electrolyte solution: (A) 9.02×10^{-7} M; (B) 1.35×10^{-6} M; (C) 2.70×10^{-6}; (D) 4.48×10^{-6} M; (E) 9.02×10^{-6} M. Arrow indicates injection of insecticide in bulk solution.

Fig. 2 shows recordings of the signals obtained at pH 7.5 with BLMs composed of 35% DPPA in the presence of 1.0 mM Ca^{2+} for different concentrations of carbofuran. It can be seen that a transient current response appears at a relatively constant time after exposure of the membrane to carbofuran (4.8 ± 0.51 min, $n = 5$). A similar constant delay time of current transients was obtained when using a constant concentration (4.48×10^{-6} M) of carbofuran (4.9 ± 0.40 min, $n = 5$), indicating that the reproducibility of the time of appearance of the signal is on the order of ca. $\pm 9\%$ (4.8 ± 0.44 min, $n = 10$). The magnitude of the transient of current increases with an increase of the concentration of insecticide. Further transients of similar size were not observed over periods of 30 min after the large transient signal. Similar transient current signals were obtained when using monocrotofos, and the transient signals appeared with a relatively constant delay time which was shorter than that for carbofuran (3.3 ± 0.30 min, $n = 5$). The magnitude of the transient signals can be used to quantify the concentrations of carbofuran and monocrotofos as the heights of the transients are linearly related to the concentration of insecticide as shown in Fig. 3. The reproducibility of chemical sensing of the two insecticides by use of the height of transients is on the order of about $\pm 10\%$. It should be noted that the presence of the insecticides results in a permanent increase of ion current values (increase appearing within 2 min after insecticide injection in bulk solution, e.g. Fig. 2C). Therefore the residual ion current can be larger than previously reported values [17,18] (up to 6 pA for the experimental conditions of Fig. 2) at the time of appearance of the current signal of interest. Control experiments involved injections of similar volumes of acetone and methanol which were used as solvents to carry the insecticides, and no transient responses were obtained. The process of formation of BLMs requires variable times, and insecticide additions have been made at different times after membrane formation and

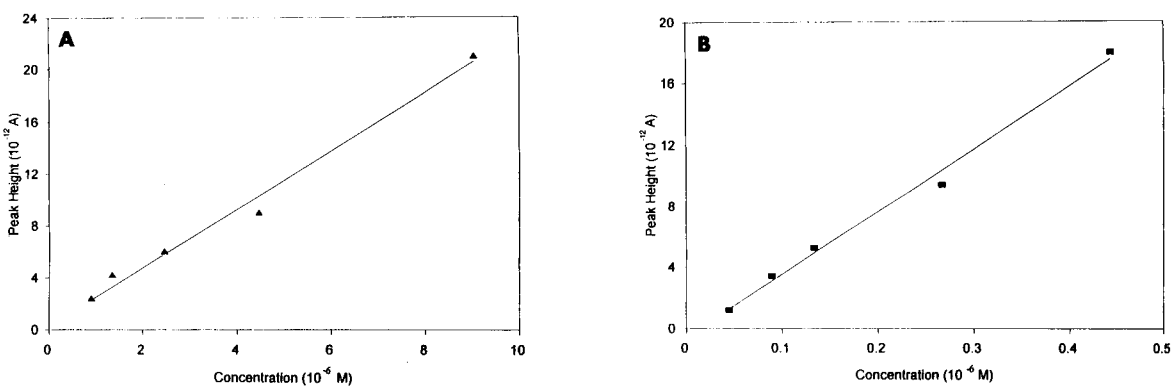

Fig. 3. Calibration of the analytical signal from the experiments with BLMs composed of 35% DPPA and in the presence of 1.0 mM calcium ions. (A) Carbofuran and (B) monocrotofos.

stabilization. Only after addition of insecticides were the transient currents of Fig. 2 observed.

The transient signals have a duration of seconds or less and are indicative of alterations of the electrostatic fields of BLMs. These alterations include membrane double layer and hydrogen bonding network reorganizations owing to the adsorption of monocrotofos and carbofuran onto the membranes. These insecticides have a hydrophilic character (i.e. the partition coefficient of monocrotofos in benzene–water is 0.61 [21]) which contributes to their adsorption onto membranes [20]. Monocrotofos has a structure similar to that of phosphatidic acid but the methoxy moieties (Fig. 1) impart substantial lipophilicity to the molecule [20]. Both phosphatidic acid and monocrotofos can form a hydrogen bonding network at the membrane surface by interactions with the oxygen atoms [20,22,23], and alterations of such hydrogen bonding networks are associated with reorganization of the double layer at one side of the BLM [23,24]. A rapid reorganization would be observed as a phenomenon such as a transient signal. The adsorption and perturbation caused by the insecticide in the BLM is revealed by the initial permanent increase of ion current values.

The appearance of a rapid transient current after a relatively constant delay time suggests that the appearance of signal is governed by the kinetics of insecticide adsorption and incorporation into the BLM. The time of appearance of the transient responses is different for monocrotofos and carbofuran indicating that the insecticide–lipid interaction at the BLM surface depends on the chemical structure of the stimulant and phenomenically appears to be controlled by the adsorption rates and partitioning of the insecticides into the BLM. It is known that monocrotofos is highly soluble in water, while carbofuran is only moderately soluble in water [25]; consistent with the earlier electrostatic response of monocrotofos when compared to carbofuran. Differences in adsorption times between bitter substances and odorants resulting in differences of electrical response times were also noticed in biosensors based on lipid films for detection of bitter or odorous substances [7].

Table 1
Signal magnitudes for different compositions of BLMs and electrolyte solutions. Concentration of carbofuran used for these experiments was 4.48×10^{-6} M

%, w/w, DPPA in BLMs	$[Ca^{2+}]$ (mM)	Signal magnitude (pA)
35	None	1.2
35	0.5	6.4
35	1.0	9.0
60	None	1.6
60	0.5	15

The magnitude and sensitivity of the signal for insecticide determination depends on the quantity of DPPA in the BLM structure and the concentration of calcium ions in bulk solution (Table 1). It can be seen in Table 1 that the signal magnitude is increased when the quantity of the charged lipid in the BLM is increased and/or in the presence of calcium ions in bulk electrolyte solution.

The detection limit for monocrotofos and carbofuran determination measured in these experiments can be set to be three times the noise level of 0.4 pA. Such a detection limit in our experiments will be 4.5×10^{-8} M and 4.8×10^{-7} M for monocrotofos and carbofuran, respectively. These detection limits are similar in magnitude to those obtained by electrochemical methods based on the inhibition of cholinesterases [2–4], but monocrotofos and carbofuran can be determined much more quickly when using detection based on BLMs.

Selectivity studies of the recognition of monocrotofos and carbofuran involved injections of aldicarb and methyl parathion into the bulk electrolyte solution. It is known that phosphorothionates such as methyl parathion have much poorer electrophilic character than their oxygen analogs and provide much weaker hydrogen-bond formation [20]. Aldicarb was found not to cause any transient signals even at concentrations of ca. 10^{-5} M. Injections of methyl parathion gave small transient responses of ca. 1 pA for concentrations larger than 1×10^{-5} M. Therefore detection by means of direct interaction of insecticides with BLMs prepared from PC/DPPA offers some se-

lectivity for monitoring carbofuran and monocrotofos, and these species can be further distinguished by means of the time of appearance of the transient signal. The kinetics of partitioning, and the mechanism of signal generation indicate that simultaneous determinations of mixtures of the two insecticides would be difficult. The use of two BLMs where each is based on a different chemical composition of DPPA/PC, may make simultaneous determinations possible (i.e. simultaneous mathematical solution for two unknowns with two systems). This approach to simultaneous determinations of the insecticides remains to be evaluated.

The results exhibit the potentiality of these devices to transduce the membrane–insecticide interaction, and suggests the basis for the construction of one-shot biosensors for direct monitoring of such environmental pollutants in protein-free water samples; waste water samples containing proteins should be purified and proteins should be eliminated from the samples prior to analysis, as these macromolecules can cause a non-selective interference with BLMs [19]. The signal profile provides an interesting opportunity for the development of chemically-selective modulators or switching devices. Lipid membrane systems of greater stability are required for practical biosensor implementation. Biosensors based on physical adsorption or covalent attachment of ordered lipid films onto metal electrodes have been reported recently [26,27]. The basic principles of signal generation that are described herein can now be further applied in stable BLM devices.

4. Acknowledgements

We are grateful to the Natural Sciences and Engineering Research Council of Canada for some financial support, and to Manolis G. Loukakis (University of Athens) for assistance with some of the experimental work.

5. References

[1] USEPA Office of Drinking Water, Reviews of Environmental Contamination and Toxicology, 104 (1988) 35.
[2] J.-L. Marty, K. Sode and I. Karube, Electroanalysis, 4 (1992) 249.
[3] P. Skladal, Anal. Chim. Acta, 252 (1991) 11.
[4] S. Kumaran and C. Tran-Minh, Electroanalysis, 4 (1992) 949.
[5] Optrodes for Measuring Enzyme Activity and Inhibition, O.S. Wolfbeis; Immobilized Biomolecules for Detection of Environmental Pollutants, K.R. Rogers and M.E. Eldefrawi, in Uses of Immobilized Biological Compounds for Detection, Medical, Food and Environmental Analysis, NATO Advanced Research Workshop, Brixen, Italy, May 9–14, 1993.
[6] D.P. Nikolelis and U.J. Krull, Electroanalysis, 5 (1993) 539.
[7] Y. Okahata, G-I. En-na and H. Ebato, Anal. Chem., 62 (1990) 1431.
[8] H. Muramatsu, E. Tamiya and I. Karube, Anal. Chim. Acta, 251 (1991) 135.
[9] Y. Okahata and H. Ebato, Anal. Chem., 63 (1991) 203.
[10] Y.-P. Sun, Residue Reviews, 94 (1985) 101.
[11] S.H. Zaman, R.J. Harvey, E.A. Barnard and M.G. Darlison, FEBS Lett., 307 (1992) 351.
[12] L.S. Katz and J.K. Marquis, Neurotoxicology, 13 (1992) 365.
[13] L.D. Brown and T. Narahashi, Brain Research, 584 (1992) 71.
[14] L. Rajakovic, V. Ghaemmaghami and M. Thompson, Anal. Chim. Acta, 217 (1989) 111.
[15] D.P. Nikolelis and U.J. Krull, Talanta, 39 (1992) 1045.
[16] D.P. Nikolelis, M.G. Tzanelis and U.J. Krull, Anal. Chim. Acta, 281 (1993) 569.
[17] D.P. Nikolelis J.D. Brennan, R.S. Brown and U.J. Krull, Anal. Chim. Acta, 257 (1992) 49.
[18] D.P. Nikolelis and U.J. Krull, Anal. Chim. Acta, 257 (1992) 239.
[19] D.P. Nikolelis, M.G. Tzanelis and U.J. Krull, Anal. Chim. Acta, 282 (1993) 527.
[20] G.H. Cocolas, Cholinergic Drugs and Related Agents, in R.F. Doerge (Ed.), Wilson and Gisvold's Textbook of Organic Medicinal and Pharmaceutical Chemistry, J.B. Lippincott, Philadelphia, PA, 1982, 8th edn., p. 448.
[21] C.-F. Yang and Y.-P. Sun, Arch. Environ. Contam. Toxicol., 6 (1977) 325.
[22] J.W. Grate, M. Klusty, W.R. Barger and A.W. Snow, Anal. Chem., 62 (1990) 1927.
[23] J.M. Boggs, Biochim. Biophys. Acta, 906 (1987) 353.
[24] P. Yeagle, The Structure of Biological Membranes, CRC Press, Boca Raton, FL, 1992.
[25] P.N.K. Moorthy, Bull. Environ. Contam. Toxicol., 32 (1984) 59.
[26] M. Otto, M. Snejdarkova and M. Rehak, Anal. Lett., 25 (1992) 653.
[27] J.D. Brennan, R.S. Brown, V. Ghaemagghami, K.M. Kallury, M. Thompson and U.J. Krull, Immobilization of Amphiphilic Membranes for Development of Optical and Electrochemical Biosensors, in Chemically-Modified Surfaces, H. Mottola and G. Steinmetz (Eds.), Elsevier, Amsterdam, 1992, p. 275.

ELSEVIER

Analytica Chimica Acta 288 (1994) 193–196

ANALYTICA CHIMICA ACTA

Glucose biosensor based on the incorporation of Meldola Blue and glucose oxidase within carbon paste

Juozas Kulys *[,a], Henrik E. Hansen [a], Thomas Buch-Rasmussen [a], Joseph Wang *[,b], Mehmet Ozsoz [b]

[a] *Novo Nordisk A / S, Roskildevej 56, 3400 Hillerod, Denmark,* [b] *Department of Chemistry and Biochemistry, New Mexico State University, Las Cruces, NM 88003, USA*

(Received 31st August 1993; revised manuscript received 18th October 1993)

Abstract

The phenoxazine compound Meldola Blue (MB) is shown to efficiently mediate the electron transfer from reduced glucose oxidase to a conventional carbon paste electrode. The mediation process is exploited for developing an amperometric biosensor for glucose, which yields a linear response to 0–25 mM glucose at an operating potential of 50 mV (vs. SCE), where interfering reactions do not occur. Experimental variables such as enzyme loading or operating potential are explored. A stable response is observed over several months.

Key words: Biosensors; Glucose; Glucose oxidase; Meldola Blue mediator

1. Introduction

Enzyme electrodes have become a useful analytical tool, because of the unique combination of enzyme specificity and the sensitivity and simplicity of electrochemical transducers [1–3]. In particular, amperometric glucose sensors have received considerable attention in connection with the treatment and control of diabetes. Traditionally, such devices have relied on the immobilization of glucose oxidase (GOx) onto various metallic or carbon surfaces, and on the use of oxygen as the natural electron acceptor for the enzyme. The glucose level has been related to the current associated with the oxidation of the liberated hydrogen peroxide. However, because of the fairly high operating potential and a strong dependence on the oxygen level, "second generation" glucose probes based on non-physiological redox mediators have been developed in recent years [4]. Various mediators have thus been used to shuttle electrons from the redox center of GOx to the surface of the working electrode. Useful sensors based on ferrocene derivatives [5,6], various quinones [7], tetrathiafulvalene [8], ruthenium complexes [9], viologen derivatives [10] or *N*-methylphenazinium ion [11] have thus been developed.

In this article the utility of 7-dimethyl-amino-1,2-benzophenoxazinium salt (Meldola Blue, MB) as an effective electron acceptor for glucose oxi-

* Corresponding authors.

SSDI 0003-2670(93)E0610-J

dase in a carbon paste configuration is described. Phenoxazine derivatives, and particularly MB, have been widely used for fabricating dehydrogenase-based biosensors, because of their ability to mediate the oxidation of dihydronicotinamide adenine dinucleotide (NADH) [12–14]. The low redox potential of MB has been particularly attractive for circumventing problems associated with the detection of NADH. Useful sensors based on various NAD^+-dependent dehydrogenases have thus been developed, including glucose probes utilizing glucose dehydrogenase [12,14]. Meldola Blue has also been shown recently to mediate the electron transfer between lactate oxidase and carbon paste surfaces [15]. In the following sections we illustrate that MB can open a charge-transfer path from the active center of glucose oxidase and carbon paste, and that such mediation greatly facilitates the amperometric biosensing of glucose.

2. Experimental

Glucose oxidase from *Aspergillus niger* with activity 211 U/mg (Sigma) was immobilized on graphite powder using glutaraldehyde. 20 ml of glucose oxidase solution (20 mg/ml) in 0.1 M phosphate buffer pH 7.4 was added to 10 g of graphite powder (Fluka) and mixed. To this mixture, 5 ml of 2.5% glutaraldehyde (Serva) in the same buffer solution was added, and the composite was incubated overnight at room temperature and then dried in vacuum using a rotating vacuum evaporator.

The activity of the immobilized glucose oxidase was determined at 25°C using an oxygen electrode and a 9.8-ml thermostated glass cell. The weighed amount (1.0–1.5 mg) of immobilized enzyme was incubated with extensive mixing by a rotating PTFE bar for 5 min in 0.1 M phosphate buffer solution (pH 7.0) containing 0.1 M sodium chloride and 0.1% of Tween-80 (Merck). The reaction was started after the introduction of 0.5 ml of 1 M glucose solution in the same buffer. The final glucose concentration in the cell was 48 mM. The solution was equilibrated to air and for enzyme activity calculation the concentration of oxygen of 0.25 mM was used. Glucose oxidase activity determined in these conditions and expressed as 1 μmol of oxygen consumption per min and per 1 mg of enzyme (U/mg) was 2.24 times lower than that described by "Sigma". The calculated yield of activity of immobilized enzyme was 35.3%.

The carbon paste was prepared by stirring 2 g of prepared immobilized enzyme with activity of 1.33 U/mg or the mixture of this enzyme with graphite powder together with 1 g of paraffin oil (Fluka) and 50 mg of Meldola Blue (Aldrich). To prepare the homogeneous paste, 1 ml of pentane was added which was allowed to evaporate at room temperature.

To prepare the glucose sensitive electrodes two channels (i.d. 2.3 mm), of rods (o.d. 6 mm, length 4 cm) prepared from high density polyethylene, were filled by carbon paste at 1 Pa pressure.

The electrode current was measured using a new renovated surface of electrodes. The renovation of the surface was performed by cutting slices (thickness 0.3 mm) of polyethylene rod together with carbon paste with special mechanical device comprising of a stainless steel knife.

The electrode current was determined using a computerized self made potentiostat at room temperature. The program is written in "C" for IBM compatible computers. A/D converter resolution is 16 bits, integration time of sampling is 20 ms. Platinum wire of thickness 0.2 mm and length 3 cm was used as an auxiliary electrode and SCE was used as the reference electrode. The procedure of electrodes calibration includes dropping (about 0.04 ml) of glucose solution on the surface of the vertically orientated electrode following a 10 s delay, applying potential to the working electrodes followed again by a 10 s delay and measuring the current in the period of 30 s. The current in this period was integrated; 5 independent measurements from both channels were averaged and displayed in graphs as "integrated current". The sensor temperature was monitored using a thermoresistor mounted in the electrode frame and the electrode response was recalculated to 25°C using the temperature coefficient 1.034.

The electrode calibration was done using a glucose solution in 0.1 M sodium phosphate buffer (pH 7.4) containing 0.1 M NaCl and 2% PEG (20 kD).

3. Results and Discussion

Meldola Blue is known for its low redox potential. Such potential has allowed a low-potential detection of NADH and related substrates [12–14]. The efficient electron transfer between glucose oxidase and the graphite (transducing) particles of carbon pastes, mediated by Meldola Blue, allows a similar biomonitoring of glucose. Fig. 1 displays the dependence of the integrated current upon the operating potential for blank (●) and 1×10^{-2} M glucose (○) solutions. A small background response, associated with the MB redox process, is observed at potentials higher than +0.05 V. The addition of the glucose substrate results in a significant analytical response. The response, which starts at +0.05, increases slowly up to +0.11 V, and then it levels off. Such results are consistent with the cyclic voltammetric behavior of MB in carbon paste matrices [14], for which a formal potential ($E°$) of −0.07 V was obtained. Potentials more positive than the $E°$ value are thus sufficient for reoxidizing and detecting the mediator. Such low operating potentials are very attractive for glucose sensing, because most common GOx mediators require fairly higher potentials (between 0.1 and 0.4 V) [10].

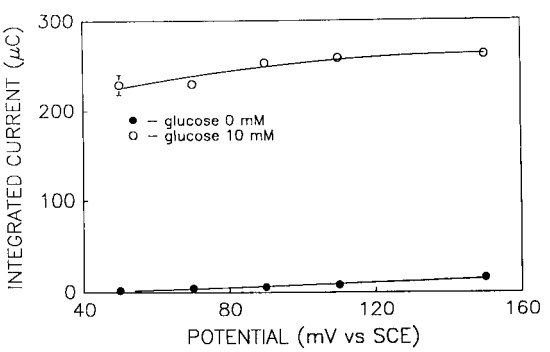

Fig. 1. The dependence of the response of the GOx/MB biosensor on electrode potential. Enzyme activity 1.33 U/mg; aerobic phosphate buffer (pH 7.4).

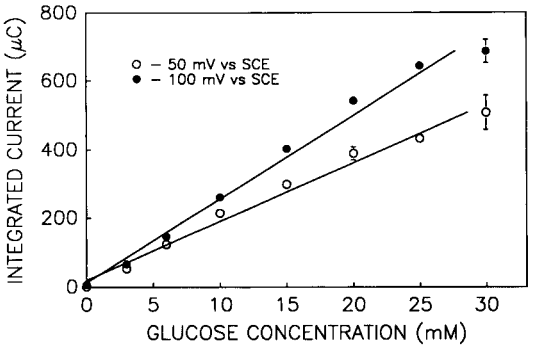

Fig. 2. Dependence of the response of the electrode based on the Meldola Blue on glucose concentration in aerobic phosphate buffer pH 7.4. Enzyme activity 1.33 U/mg; operating potential, 0.05 (○) and 0.10 (●) V; standard error represent bars or was less than circle radius.

Similar to other "second-generation" glucose probes, MB appears to shuttle electrons from the redox center of the enzyme to the graphite surface, in accordance with the following reaction scheme:

$$\text{glucose} + \text{GOx(FAD)} \rightarrow \text{gluconolactone} + \text{GOx(FADH}_2\text{)} \quad (1)$$

$$\text{GOx(FADH}_2\text{)} + \text{MB}^+ \rightarrow \text{GOx(FAD)} + \text{MBH} + 2\text{H}^+ \quad (2)$$

where MB^+ and MBH denote the oxidized and reduced forms of MB, respectively. The liberated MBH is then electrochemically detected by reoxidation:

$$\text{MBH} \rightarrow \text{MB}^+ + \text{H}^+ + 2\text{e}^- \quad (3)$$

thus regenerating the oxidized form.

Calibration plots for glucose, obtained at +0.05 and 0.10 V, are shown in Fig. 2. At both operating potentials, the plots are linear over the entire range (0–2.5×10^{-2} M) examined. The correlation lines are $y = 20 + 17.1C$ (for 0.05 V) and $y = 12.8 + 24.3C$ (for 0.10 V), with $r = 0.9932$ and 0.9931, respectively.

The enzyme activity has a profound effect on the response of the GOx/MB carbon paste electrode. Fig. 3 displays calibration plots for glucose

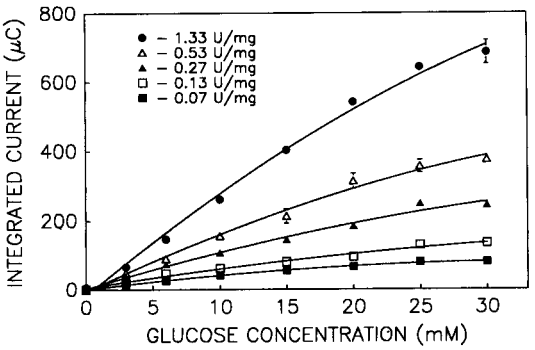

Fig. 3. Dependence of the response of the electrode based on the Meldola Blue on enzyme activity. Conditions as in Fig. 1.

(between 0 and 3×10^{-2} M) for enzyme activities ranging between 0.07 – and 1.33 U/mg. A 7-fold increase in the sensitivity is observed over this region.

The low operating potential accrued from the MB mediation process greatly minimizes the interference of co-existing electroactive species. In particular, endogenous compounds such as ascorbic and uric acids commonly display significant current contributions when "first-generation" (unmediated) glucose sensors are employed. In contrast, only 4 and 7% increases of the 1×10^{-2} M glucose response were observed at the membrane-free GOx/MB biosensor (operated at +0.1 V) upon additions of 5×10^{-4} M ascorbic or uric acids, respectively.

Long term stability is another important requirement of biosensors, in general, and of self-testing glucose devices, in particular. The response for 1×10^{-2} M glucose remained highly stable over a 3-month period (with storage at room temperature, and measurement every 5th day on a fresh surface, using +0.1 V). Such stability is attributed to the new scheme for immobilizing the enzyme, to the protective action of carbon paste matrices [16] and to the renewable (by cutting) character of the GOx/MB device. Similarly, these data indicate no apparent stability and leaking problem for the mediator.

In conclusion, we have demonstrated that MB can shuttle electrons between the reduced flavin adenine dinucleotide of glucose oxidase and the carbon paste surfaces. While the work presented here is within the context of the MB mediator, other phenoxazine derivatives and structurally-related phenothiazines are expected to display a similar performance. The use of such compounds as electron transfer mediators forms the basis for a recent patent [17]. Similar advantages are anticipated for other carbon-transducing surfaces. Such mediation capability offers great potential for glucose sensing in various clinical, food and biotechnological samples. The renewable nature of the carbon paste configuration appears to be particularly attractive for self monitoring of diabetes mellitus.

4. References

[1] A.P. Turner, I. Karube and G. Wilson (Eds.), Biosensors: Fundamental and Applications, Oxford Scientific, Oxford, 1987.
[2] J. Wang, Electroanalytical Techniques in Clinical Chemistry and Laboratory Medicine, VCH, New York, 1988.
[3] J. Czaban, Anal. Chem., 57 (1985) 345A.
[4] P.N. Bartlett, P. Tebbutt and R.G. Whitaker, Progress in Reactions Kinetics, 16 (1991) 55.
[5] A. Cass, G. Francis, H. Hill, W. Aston, I. Higgins, E. Plotkin, L. Scott and A.P. Turner, Anal. Chem., 56 (1984) 667.
[6] J. Wang, L. Wu, Z. Lu, R. Li and J. Sanchez, Anal. Chim. Acta, 228 (1990) 251.
[7] J. Hu and A.P. Turner, Anal. Lett., 24 (1991) 15.
[8] H. Gunashingham and C. Tan, Analyst, 115, (1990) 35.
[9] N. Morris, M. Cardosi, B. Birch and A.P. Turner, Electroanalysis, 4 (1992) 1.
[10] P. Hale, L. Boguslavsky, H. Karan, H. Lan, H. Lee, Y. Okamoto and T. Skotheim, Anal. Chim. Acta, 248 (1991) 155.
[11] G. Jönsson and L. Gorton, Biosensors, 1 (1985) 355.
[12] G. Marko-Varga, R. Appelqvist and L. Gorton, Anal. Chim. Acta 179 (1986) 371.
[13] M. Polasek, L. Gorton, R. Appelqvist, G. Marko-Varga and G. Johansson, Anal. Chim. Acta, 246 (1991) 283.
[14] G. Bremle, B. Persson and L. Gorton, Electroanalysis, 3 (1991) 77.
[15] J. Kulys, W. Schuhmann and H.L. Schmidt, Anal. Lett., 25 (1992) 1011.
[16] A. Amine and J.M. Kauffmann, Bioelectrochem. Bioenerg., 28 (1992) 117.
[17] Use of Benzene Derivatives as Charge Transfer Mediators, International Publication Number WO 92/07263.

ELSEVIER

Analytica Chimica Acta 288 (1994) 197–203

ANALYTICA CHIMICA ACTA

Glucose sensitive conductometric biosensor with additional Nafion membrane: reduction of influence of buffer capacity on the sensor response and extension of its dynamic range

A.P. Soldatkin *[a,b], A.V. El'skaya [b], A.A. Shul'ga [a,c], A.S. Jdanova [a], S.V. Dzyadevich [c], N. Jaffrezic-Renault [a], C. Martelet [a], P. Clechet [a]

[a] *LPCI, URA CNRS 404, Ecole Centrale de Lyon, BP 163, 69131 Ecully cedex, France*
[b] *Institute of Molecular Biology and Genetics, Ukrainian Academy of Sciences, 150 Zabolotny St., Kiev 252143, Ukraine*
[c] *Sector of Bioelectronics, Kiev University, P.O.Box 152, Kiev 252001, Ukraine*

(Received 26th July 1993)

Abstract

Glucose-sensitive enzyme conductometric biosensors based on interdigitated gold electrodes were prepared by cross-linking glucose oxidase with bovine serum albumin in a saturated glutaraldehyde vapour on the sensor chips. Nafion membranes were deposited on top of the glucose sensor by a spin-coating procedure. The effects of buffer concentration and ionic strength were examined for the glucose sensors with and without Nafion membranes. Additional Nafion membranes resulted in a substantial reduction of the effect of buffer concentration on the sensor response and in an extension of the dynamic range of the sensor up to a glucose concentration of more than 10 mM Moreover the comparison of the properties of the developed conductometric glucose biosensors (operational and storage stability, reproducibility of measurements) demonstrates better performance of the sensor with an additional Nafion membrane.

Key words: Biosensors; Conductimetry; Nafion membranes; Glucose sensitive biosensor; Permselectivity

1. Introduction

In recent years considerable research efforts were directed to the development of integrated microbiosensors based on ion sensitive field effect transistors (ISFETs), thin-film metal and carbon electrodes. The interest has been spurred by the attractive qualities of microsensors such as small size, ruggedness and low power consumption. The developed thin-film biosensors were mainly based on potentiometric or amperometric detection modes, while only a small number of publications deal with a conductometric mode [1–6]. The major advantage of the conductometric detection mode is that a large number of enzymatic reactions involve either consumption or production of charged species and therefore lead to a change in ionic composition of the reacting solution [7]. Moreover, one of the attrac-

* Corresponding author.

SSDI 0003-2670(93)E0627-J

tive features of the conductometric biosensors is their suitability for miniaturisation using inexpensive thin-film technology. It is also worth noting that such biosensors compared to other electrochemical biosensors have no light sensitivity, do not need any reference electrode and the driving voltage can be sufficiently small to decrease substantially the sensor power consumption and to reduce safety problems when used in living organisms.

However, conductometric biosensors having a number of essential advantages have also disadvantages common with that of enzyme field effect transistors (ENFETs). One is a strong dependence of the sensor response on the buffer capacity of a sample [5,6]. In fact, increase of the buffer concentration from 2 to 20 mM decreases the sensor response by factors of 10 and 3 for glucose and urea biosensors, respectively. One can conclude that in spite of quite different sensing mechanisms for conductometric transducers and ISFETs, the basic features of the physico-chemical processes inside of the enzymatic film determining the response of the both biosensors seem to be very similar, i.e., the response of the conductometric enzyme biosensors is mainly due to protons generated by a biocatalytic reaction inside the layer of immobilized enzyme.

It was shown earlier, that in the case of ENFETs the application of additional permselective membranes on top of an enzyme membrane reduces substantially the dependence of the sensor response on the buffer concentration [8–10].

Here results are presented concerning the application of additional Nafion membranes in order to reduce the influence of buffer concentration on the response of the conductometric glucose biosensor and to extend its dynamic range.

2. Experimental

2.1. Materials

Glucose oxidase (EC 1.1.3.4) from *Penicillium vitale* (specific activity 168 U mg^{-1}) was obtained from the Cosarsky alcohol plant (Cherkassy, Ukraine), bovine serum albumin (BSA) was purchased from Sigma and 25% aqueous solution of glutaraldehyde (GA) was from Merck. Nafion perfluorinated ion-exchange powder (5%, w/v, in a mixture of lower aliphatic alcohols and 10% water, product No. 27, 470–4) was from Aldrich. All other reagents were of purum analytical grade.

2.2. Enzyme immobilization

Glucose oxidase (GOD) was immobilized using a modified procedure described earlier [6]. 10% (w/w) solutions of GOD and BSA were prepared in 5 mM phosphate buffer (KH_2PO_4–NaOH), pH 7.4. Prior to the deposition on the sensor chip these solutions were mixed in defined proportions and glycerol was added. The mixture composition used was: 5% GOD, 5% BSA and 10% glycerol. The use of glycerol prevents a loss of enzyme activity during the immobilization process and also results in a better homogeneity of the membrane and its better adhesion to the surface of the sensor. As a differential experimental set-up was used, a drop of the enzyme-containing mixture was deposited on the sensitive area of the measuring pair of electrodes while only a mixture containing 10% BSA and 10% glycerol was deposited on the reference pair of electrodes. Then the sensor was placed for 30 min in a saturated GA vapour. After exposure to GA, the membranes were dried at room temperature for 15 min. Before use the membranes were soaked in a 5 mM phosphate buffer, pH 7.5, for at least 30 min to equilibrate the membrane system.

2.3. Formation of additional membranes

Additional Nafion membranes were formed on the top of both enzyme and reference membranes of the glucose sensor by a spin-coating procedure using a 5% Nafion solution (to obtain thicker additional membrane, the procedure of the membrane formation was repeated several times). 5 μl of Nafion solution was deposited on the sensor chip, then the sample was rotated at 500 rpm for 1–2 min. After deposition, membranes were dried at room temperature for 15 min. The thickness of the additional Nafion membranes was estimated by weighing.

2.4. Sensor design and measurements

The conductometric transducers were supplied by Emokon (Kiev, Ukraine). Two identical pairs of gold interdigitated electrodes were photolithographically patterned on a ceramic support with dimensions 5 mm × 30 mm (thickness 0.5 mm). An intermediate layer of chromium (0.1 μm thick) was first deposited to get a better gold adhesion. Each rod was 10 μm wide and 1 mm long with 10 μm spacing between the fingers. The sensitive area for one pair of electrodes was about 1 mm × 1.5 mm, it was defined by photolithographic deposition of a polymerized layer of polyimide.

Conventional AC conductance monitoring technique was used to reduce Faradaic processes, double-layer charging and concentration polarisation on the microelectrode surface (Fig. 1).

The internal generator of Stanford Research Systems SR 510 lock-in amplifier was employed to generate a sinusoidal wave with a frequency of 90 kHz and a peak-to-peak amplitude of 10 mV around a fixed potential of 0 V to each pair of electrodes forming a miniaturized conductance cell.

The differential signal between the electrodes covered with the immobilized enzyme and those covered with the "blank" membrane after a low noise differential amplifier was fed into the lock-in amplifier which was supplied with a reference signal from its internal oscillator. Amplification was achieved with a standard inverting operational amplifier. The amplified in-phase differential signal was monitored using a Servotrace chart recorder (Sefram).

Measurements were conducted in an open cell (2 ml) with intensive stirring at room temperature. The glucose concentration was increased stepwise by adding defined volumes of a concentrated stock solution.

3. Results and discussion

3.1. Influence of buffer concentration

Calibration graphs for the glucose biosensors with and without additional Nafion membranes are presented in Fig. 2A and B. When the measurements were performed in test solutions with different buffer concentrations, defined amounts of NaCl were added in order to ensure identical conductivity for all the solutions. The biosensor without additional membrane demonstrates reproducible response to the addition of glucose, with a response time within 1–2 min. However, the dynamic range is very small (it extends to about 1.5 mM only) and the response amplitude is strongly dependent on the buffer concentration

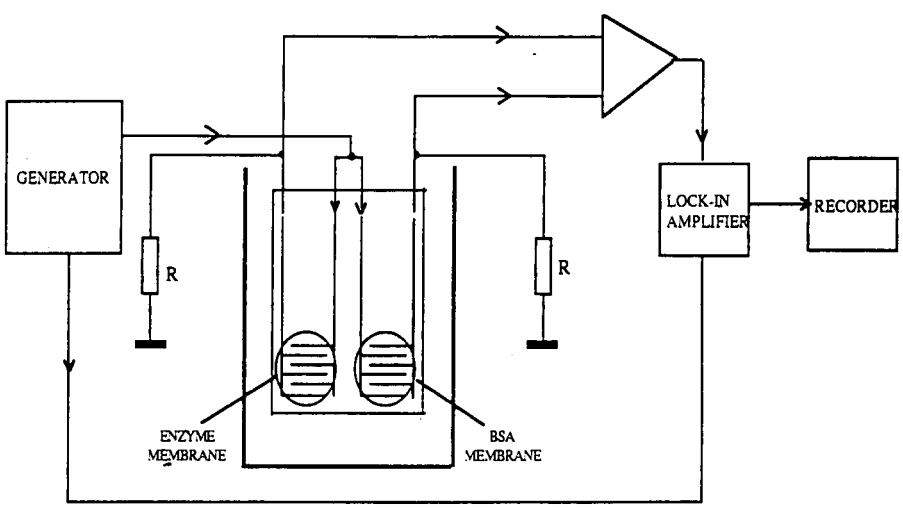

Fig. 1. Experimental set-up used for conductometric measurements.

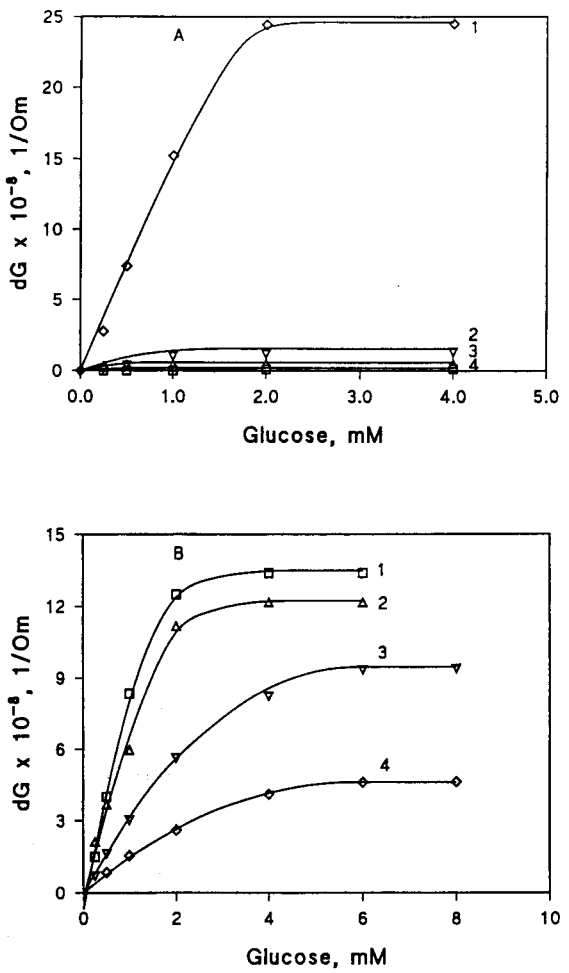

Fig. 2. Calibration graphs for the steady-state response of the glucose sensor without (A) and with one additional Nafion membrane (B) in 1 mM (1), 10 mM (2), 20 mM (3) and 40 mM (4) phosphate buffer, pH 7.4. Before use, the conductivity of the buffer solutions was adjusted to the same constant value by adding NaCl.

in the sample (the response value decreases 20-fold when the concentration of buffer is changed from 1 to 10 mM). Further increase of the buffer concentration up to 20–40 mM makes the measurement of glucose concentration practically impossible. The reason for the limited dynamic range of the glucose sensor is the limitation of the biocatalytic oxidation of glucose by oxygen [11], while the dependence of the response amplitude on the buffer concentration is due to a kind of "carrier-mediated" transport of protons ("facilitated diffusion") out of the enzyme membrane in the presence of mobile buffer species [12]. It means that when the buffer species are present in the solution protons can associate with them and form an additional "channel" of their diffusion out of the enzyme membrane (the first one is the diffusion of protons as free ions).

The application of additional Nafion membranes causes drastic changes of the characteristics of the biosensor: dynamic range, dependence of the response on buffer concentration, response time. As can be seen is Fig. 2B, the use of one Nafion membrane (thickness ca. 3.5 μm) on top of the enzymatic film extends the dynamic range of the sensor up to a concentration of glucose of 4 mM and makes the sensor response nearly insensitive to an increase of buffer concentration of 1–10 mM. The response time of the sensor with the Nafion membrane is within 3–4 min in comparison with 1–2 min for a sensor without additional membrane.

The concentration of the low-molecular-weight components, mainly bicarbonates, that define pH and buffer capacity of blood, is about 25–30 mM [13]. Therefore it was interesting in view of possible biomedical applications to analyse in more detail the response of such a glucose sensor with and without additional membranes in 20 mM and more concentrated solutions of phosphate buffer. The results are presented in Fig. 3. The response of the conductometric sensor without the additional membrane depends strongly on the buffer concentration and about a 50-fold decrease is observed when the latter is changed from 1 to 40 mM (the sensor response in a 1 mM phosphate buffer (pH 7.4), is taken as 100%). In contrast, the sensor with the Nafion membrane shows less influence of the response to the buffer concentration. Its response decreases nearly linearly as the buffer concentration increases and in a 40 mM phosphate buffer the differential output signal is about 25% of its value in a 1 mM buffer.

Such reduction of the buffer capacity influence on the response of the glucose sensor may be explained by taking into account the properties of Nafion as a cationic-exchange membrane. It has been shown that, e.g., the diffusion coefficient

across a Nafion membrane for Na^+ is almost 100 times greater than that for Cl^- [14]. This effect is attributed to negatively charged sulfonate groups inside the Nafion membrane that create a potential barrier for the diffusion of negatively charged ions. In the case of phosphate buffer used in this investigation, the buffer-mediated mechanism of proton diffusion out of the enzyme layer operates due to the movement of neutral and negatively charged buffer species across the membrane. The presence of an additional Nafion membrane effectively blocks the transfer of the negatively charged buffer ions and thus drastically reduces the contribution of the "carrier-mediated" mechanism to the total diffusional flux of protons across the Nafion membrane.

3.2. Influence of ionic strength

It is known that the response of the conductometric glucose biosensor depends on ionic strength [5,6] and that Nafion is a specific ion-exchanging material with different diffusion coefficients for oppositely charged ions also depending on ionic strength of the solution [14]. Therefore it was necessary to study the dependence of the biosensor response (sensor with and without additional membrane) on ionic strength of the solution. The dependence of the glucose sensor response on the concentration of NaCl in the sample is shown in Fig. 4. In principle, an increase of the ionic strength should result in: (i) an increase of the general conductivity of the solution and a decrease of the amplitude of the sensor response value [5,6]; (ii) a greater electrostatic screening of charged functional groups inside the Nafion membrane and, consequently, in a decrease of its barrier properties [14]. In the range of the salt concentrations tested the behaviour of the sensors with and without additional Nafion membrane was similar but differed in the extent to which the magnitude of the response decreased with the increase of the concentration of NaCl. Therefore, the suppression of the response value for the sensor with the Nafion membrane was less pronounced. From a practical point of view it is important to note that for a salt concentration greater than 100 mM the responses of both biosensors are practically independent on the ionic strength.

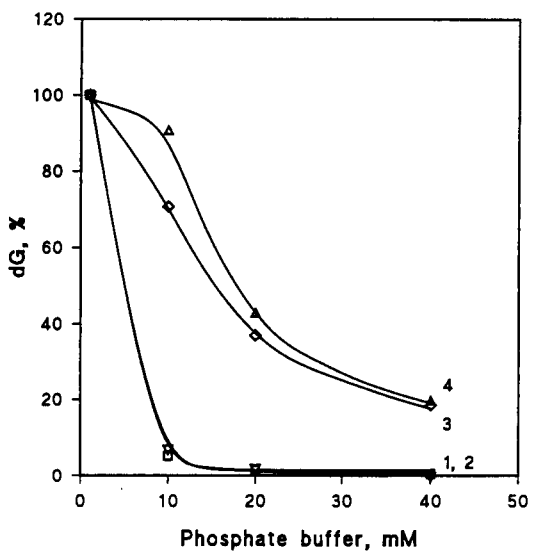

Fig. 3. Dependence of the steady-state sensor response [without (1, 2) and with (3, 4) additional Nafion membrane] on the concentration of phosphate buffer. Measuring conditions: phosphate buffer, pH 7.4, 1 mM and 2 mM glucose concentration for curves 1, 3 and 2, 4 respectively. Before use certain amounts of NaCl were added to the buffer solutions to ensure their identical conductivity. Response: 1 mM phosphate buffer is taken as 100%.

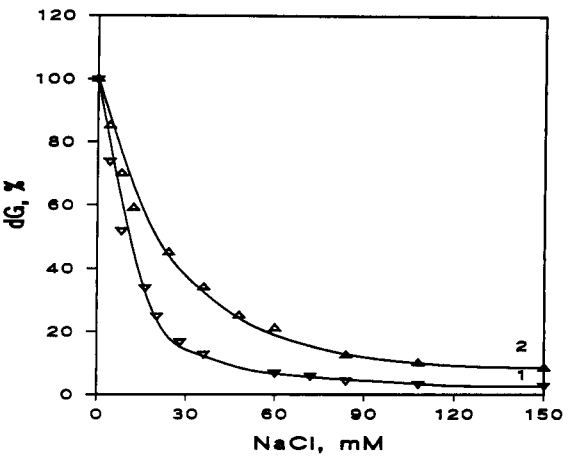

Fig. 4. Dependence of the steady-state sensor response [without (1) and with (2) one additional Nafion membrane] on the concentration of NaCl. Measuring conditions: 5 mM phosphate buffer, pH 7.4, glucose concentration 1 mM.

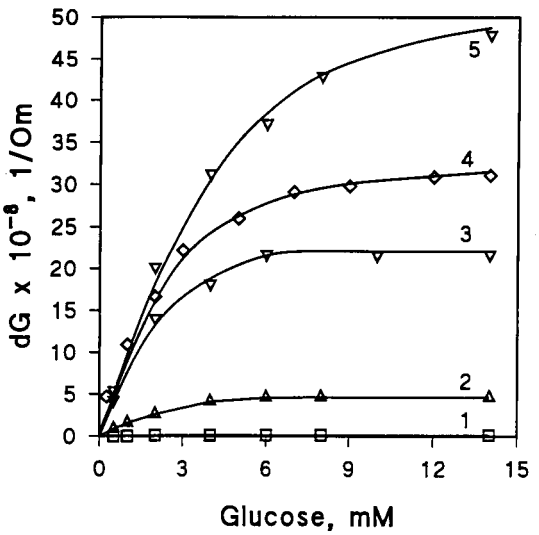

Fig. 5. Calibration graphs for the steady-state response of the glucose sensor without (1) and with one (2), two (3), three (4) and four (5) layers of the additional Nafion membrane. Measuring conditions: 40 mM phosphate buffer, pH 7.4;

3.3. *Influence of the thickness of the additional Nafion membrane*

As can be seen in Fig. 2B the dynamic range for the glucose sensor with a one-step formed additional Nafion membrane is extended only up to a glucose concentration of 4 mM. In the next experiments we have used sensors obtained with several successively deposited layers of Nafion and tested the dependence of the sensor response on the thickness of the formed additional membrane (Fig. 5). With an increase of the thickness of the additional membrane up to 15 μm (4 membrane layers) the value of the sensor response increases, and the dynamic range extends up to 10 mM concentration of glucose. According to the obtained results (Fig. 5) it can be concluded that it is possible to change the sensitivity and the dynamic range of the glucose conductometric biosensor by using additional Nafion membranes with different thickness.

3.4. *Reproducibility and stability of the sensors*

Comparison of the sensor's operational stability and the reproducibility of the sensor response was made for the glucose sensors with and without additional membranes (Fig. 6A and B). Measurements for each sensor were carried out during 6 h and, as can be seen, the amplitude of the responses for both types of the sensors did not change during this time. Standard deviations of the sensor response to concentrations of glucose of 0.5 and 1 mM were 7 and 5%, respectively, for 14 successive measurements using the sensor without the additional membrane. For 15 successive measurements with a sensor having the additional Nafion membrane standard deviations of the sensor response to concentrations of glucose of 0.5, 1.5 and 2 mM were 4, 3 and 2%, respectively. The response of the both types of sensors

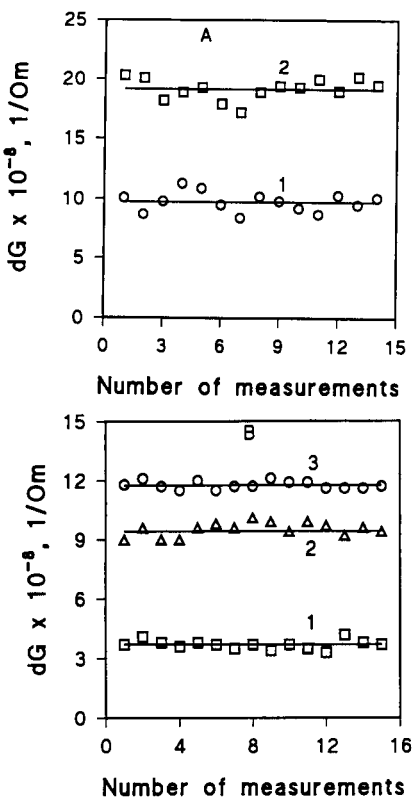

Fig. 6. Reproducibility of the biosensor response. (A) Sensor without additional membrane, 1 mM phosphate buffer (pH 7.4), concentrations of glucose: 0.5 mM (1) and 1 mM (2); (B) Sensor with one additional Nafion membrane, 10 mM phosphate buffer (pH 7.4), concentrations of glucose: 0.5 mM (1), 1.5 mM (2), and 2 mM (3).

was stable for at least 1 month when they were stored in 10 mM phosphate buffer at +4°C.

4. Conclusion

Glucose sensitive conductometric enzyme sensors without and with additional Nafion membrane were developed. It was shown that formation of an additional Nafion membrane on top of the enzyme-containing membrane results in a substantial reduction of the buffer concentration influence on the sensor response and in an extension of its dynamic range up to a concentration of glucose of more then 10 mM. The obtained results are interpreted in terms of permselective properties of the additional membrane formed. The presence of negatively charged groups inside the Nafion membrane blocks a "carrier-mediated" transport of protons through the additional membrane, occurring in the presence of mobile buffer species, thus eliminating their effect on the amplitude of the output signal of the biosensor. The additional Nafion membrane also limits the diffusion of glucose through the membrane more effectively then that of oxygen, which results in an extension of the sensor dynamic range.

The obtained results demonstrate the possibility to improve and to adjust the characteristics (sensitivity to the buffer capacity of the sample, sensor dynamic range, etc.) of the conductometric sensor using additional Nafion membranes with controlled thickness and morphology.

Comparison of properties of the glucose biosensors developed demonstrates a better performance of the sensor with the additional Nafion membrane. The increase of the sensor response time due to the presence of the additional membrane can be overcome by measurements in a kinetic mode.

5. Acknowledgments

A part of this work was supported by a grant from CNRS (contract No. A69/766/92).

6. References

[1] L.D. Watson, P. Maynard, D.C. Cullen, R.S. Sethi, J. Brettle and C.R. Lowe, Biosensors, 3 (1988) 105.
[2] D.C. Cullen, R.S. Sethi and C.W. Lowe, Anal. Chim. Acta, 231 (1990) 33.
[3] B.F.Y. Yon Hin, R.S. Sethi and C.R. Lowe, Sensors Actuators, B1 (1990) 550.
[4] R. Hintsche, B. Moller, I. Dransfeld, U. Wollenberger and F. Sheller, Sensors Actuators, B4 (1991) 287.
[5] A.A. Shul'ga, V.I. Strikha, S.V. Patskovsky, S.V. Dzyadevich, A.V. El'skaya, A.P. Soldatkin and O.A. Bubryak, in: Proceedings of the Second World Congress Biosensors '92, 20–22 May 1992, Geneva, Elsevier Advanced Technology, Oxford, 1992, pp. 81–88.
[6] A.A. Shul'ga, S.V. Dzyadevich, A.P. Soldatkin, S.V. Patskovsky, V.I. Strikha and A.V. El'skaya, Biosensors Bioelectronics, (1993) in press.
[7] C.R. Hill and G. Tomalin, Anal. Biochem., 120 (1982) 165.
[8] A.P. Soldatkin, A.A. Shul'ga, C. Martelet, N. Jaffrezic-Renault, H. Maupas and A.V. El'skaya, Fr. Pat., 93 05 941 (1993).
[9] A.A. Shul'ga, V.I. Strikha, A.P. Soldatkin, A.V. El'skaya, H. Maupas, C. Martelet and P. Clechet, Anal. Chim. Acta, 278 (1993) 233.
[10] A.P. Soldatkin, A.V. El'skaya, A.A. Shul'ga, L.I. Netchiporouk, A.M. Nyamsi Hendji, N. Jaffrezic-Renault and C. Martelet, Anal. Chim. Acta, 283 (1993) 695.
[11] A.A. Shul'ga, A.K. Sandrovsky, V.I. Strikha, A.P. Soldatkin, N.F. Starodub and A.V. El'skaya, Sensors Actuators, B10 (1992) 41.
[12] S. Varansi, S.O. Ogundizan and E. Ruckenstein, Biosensors, 3 (1988) 269.
[13] Yu.V. Chmelevski and O.K. Usatenko, The Main Human Biochemical Constants in a Norm and at a Pathology, Zdorov'e, Kiev, 1987, p. 245.
[14] A. Varebska, S. Koter and W. Kujawski, Desalination, 51 (1984) 3.

ELSEVIER

Analytica Chimica Acta 288 (1994) 205–214

ANALYTICA CHIMICA ACTA

Fiber optic biosensor for fluorimetric detection of DNA hybridization

Paul A.E. Piunno [a], Ulrich J. Krull *,[a], Robert H.E. Hudson [b], Masad J. Damha [c], Huguette Cohen [d]

[a] *Chemical Sensors Group, Department of Chemistry, Erindale College, University of Toronto, 3359 Mississauga Road North, Mississauga, Ontario, L5L 1C6 Canada,* [b] *Biological Chemistry Group, Department of Chemistry, Erindale College, University of Toronto, 3359 Mississauga Road North, Mississauga, Ontario, L5L 1C6 Canada,* [c] *Biological Chemistry Group, Department of Chemistry, McGill University, 801 Sherbrooke Street West, Montréal, PQ, H3A 2K6 Canada,* [d] *Laboratory Services Division, Agriculture Canada, Building No. 22, C.E.F., Ottawa, Ontario, K1A 0C6 Canada*

(Received 30th July 1993; revised manuscript received 18th October 1993)

Abstract

Single stranded deoxyribonucleic acid (ssDNA) thymidylic acid icosanucleotides (dT_{20}) were grown onto optical fibers. The fibers were first derivatized with γ-aminopropyltriethoxysilane (APTES) onto which a spacer arm of 1,10 decanediol bis-succinate terminated with 5′-O-dimethoxytrityl-2′-deoxythymidine was covalently attached. The synthetic route used to grow the ssDNA was the well established solid-phase phosphoramidite methodology. The covalently immobilized oligomers were able to hybridize with available complementary ssDNA (cDNA) which was introduced into the local environment to form double stranded DNA (dsDNA). This event was detected by the use of the fluorescent DNA stain ethidium bromide (EB). The sampling configuration utilized total internal reflection of optical radiation within the fiber, resulting in an intrinsic mode optical sensor. The non-optimized procedure used standard hybridization assay techniques to provide a detection limit of 86 ng ml^{-1} cDNA, a sensitivity of 83% fluorescence intensity increase per 100 ng ml^{-1} of cDNA initially present, with a hybridization analysis time of 46 min. The sensor has been observed to sustain activity after prolonged storage times (3 months) and harsh washing conditions (sonication).

Key words: Biosensors; Fluorimetry; Fibre optic biosensor; DNA hybridization

1. Introduction

The use of DNA as a selective recognition element in biosensor design is a new and exciting area in analytical chemistry. Experiments have been completed wherein ssDNA was covalently immobilized onto quartz optical fibers to successfully demonstrate the basis for development of an optical biosensor for DNA. The non-optimized configuration described herein was able to detect femtomolar concentrations of cDNA with an analysis time of less than 1 h. These experiments indicate that biosensors which can selectively de-

* Corresponding author.

SSDI 0003-2670(93)E0611-A

tect genetic material from biologicals may now be created, with advantages of low detection limits, reasonable analysis times, highly stable biorecognition elements, and regenerability.

Biosensors have been used to selectively detect cells, viruses and other biologically significant materials by using a detection strategy that involves immobilization of enzymes, antibodies or other selective proteins onto solid substrates such as quartz (for piezoelectric and optical sensors) or metal (for electrochemical sensors) [1,2]. However, such sensors are not widely available from commercial sources due to problems associated with the long term stability of the selective recognition elements when immobilized onto solid surfaces [3,4]. An alternative approach which may be used to create biosensors with long term chemical stability takes advantage of the stability of DNA. With the recent advent of DNA probe technology, a number of selective oligomers which interact with the DNA of important biological species, for instance salmonella, have been identified [7–10]. These have been used to provide a new type of selective biorecognition element which is highly selective, stable, and can be easily synthesized in the laboratory [9–11] as compared to other chemically synthesized biorecognition elements, such as catalytic antibodies [12]. As a result, species-specific DNA probes may now be exploited for biosensor development.

DNA biosensors that are presently being developed are largely based on piezoelectric and electrochemical transducers. Two strategies have been employed for piezoelectric biosensors that use DNA. Both strategies begin by immobilizing probe DNA onto the surface of a piezoelectric crystal. The immobilized ssDNA is then allowed to hybridize to cDNA that is introduced to the local environment of the sensor. The first approach relies on observing a change in the resonance frequency of the crystal as a function of a significant mass increase at the surface of the crystal as given by the Sauerbrey equation [13]. This method works provided that the cDNA strands are sufficiently large (> 900 nucleotides) [13,14], or that a high mass metallic chelator may be attached to the target ssDNA strands to ensure a detectable mass change at the surface of the crystal [15]. A second approach involves the simultaneous monitoring of changes in interfacial properties at the surface of the crystal such as microviscosity, elastic modulus, and dielectric, permitting detection of shorter oligomers by piezoelectric sensors based on network analysis [16]. Sensors which respond to interfacial mass changes have been able to detect 1 ng of cDNA, while 0.3 mg of cDNA could be detected by network analysis techniques. Amperometric detection of DNA on the surface of an electrode has been investigated by Millan et al. [17]. This was accomplished by immobilizing probe ssDNA onto the surface of an amperometric electrode, followed by hybridization with cDNA where a redox-active metallo-intercalator present in solution associated with the immobilized dsDNA at the electrode surface and was detected by voltammetry.

The work herein reports one of the first biosensors for direct analysis of DNA hybridization by use of an optical fiber. ssDNA was covalently immobilized onto optical fibers by first activating the surface of the quartz optical fiber with a long chain aliphatic spacer arm terminated in a 5′-*O*-dimethoxytrityl-2′-deoxyribonucleoside, followed by automated solid-phase DNA synthesis. Detection of dsDNA at the fiber surface after hybridization between immobilized ssDNA and cDNA was achieved by exposing the complex to an ethidium bromide solution followed by washings with hybridization buffer solution. The ethidium cation (3,8-diamino-6-phenyl-5-ethyl-phenanthridium) is a fluorescent compound which strongly associates with dsDNA by intercalation into the base stacking region and, in some cases, the major groove of the double helical structure [18]. It is shown that the fluorescence response of the ethidium cation can be monitored in a total internal reflection configuration along an optical fiber to quantify the presence of dsDNA at the surface of the fiber, with the fluorescence intensity being directly proportional to the amount of cDNA initially present in solution. This approach may be refined and used for rapid identification and quantitation of the presence of microorganisms such as pathogenic bacteria and viruses in bodily fluids, food and feed commodities, and

may also find application in screening for genetic disorders.

2. Experimental

2.1. Chemicals

5′-*O*-dimethoxytrityl-2′-deoxythymidine was obtained from Dalton Chemical Labs. (Toronto), N^6-benzoyl-5′-*O*-(dimethoxytrityl)-2′-deoxyadenosine 3′-*N*,*N*-diisopropyl-*O*-cyanoethylphosphoramidite and 5′-*O*-dimethoxytrityl-2′-deoxythymidine 3′-*N*,*N*-diisopropyl-*O*-cyanoethylphosphoramidite were purchased from Applied Biosystems (Mississauga). All other reagents required for use on the DNA synthesizer were prepared as described previously [19]. An oligonucleotide purification cartridge (OPC, Applied Biosystems) with an overall length of 3 cm, internal length of 1.5 cm, and outside diameter of 1 cm was used during oligonucleotide synthesis onto optical fibers. Long-chain alkylamine (LCAA) controlled-pore glass (CPG) beads were obtained from CPG Inc. (Fairfield, NJ) and were derivatized by the method reported by Damha et al. [20]. Ethidium bromide (EB) was obtained from Sigma (St. Louis, MO). *N*-Hydroxysuccinimide, *N*,*N*′-dicyclohexylcarbodiimide (DCC), γ-aminopropyltriethoxysilane (APTES), octadecyltrichlorosilane, hexadecane, 1,10-decanediol, succinic anhydride, *N*,*N*-dimethylformamide (DMF) and 4-dimethylaminopyridine (DMAP) were obtained from Aldrich (Milwaukee, WI). Water was obtained from a Milli-Q five-stage cartridge purification system (Millipore, Mississauga) and had a specific resistance of not less than 18 MΩ cm. Alternatively, sterile water was prepared from glass double-distilled water which was treated with diethylpyrocarbonate (0.1%, v/v; Aldrich) and autoclaved (120°C, 20 min). NaCl and $NaH_2PO_4 \cdot 2H_2O$ were of analytical grade and obtained from BDH (Toronto). 0.2 μm sterile filters (Acrodisc®) were from Gelman Sciences

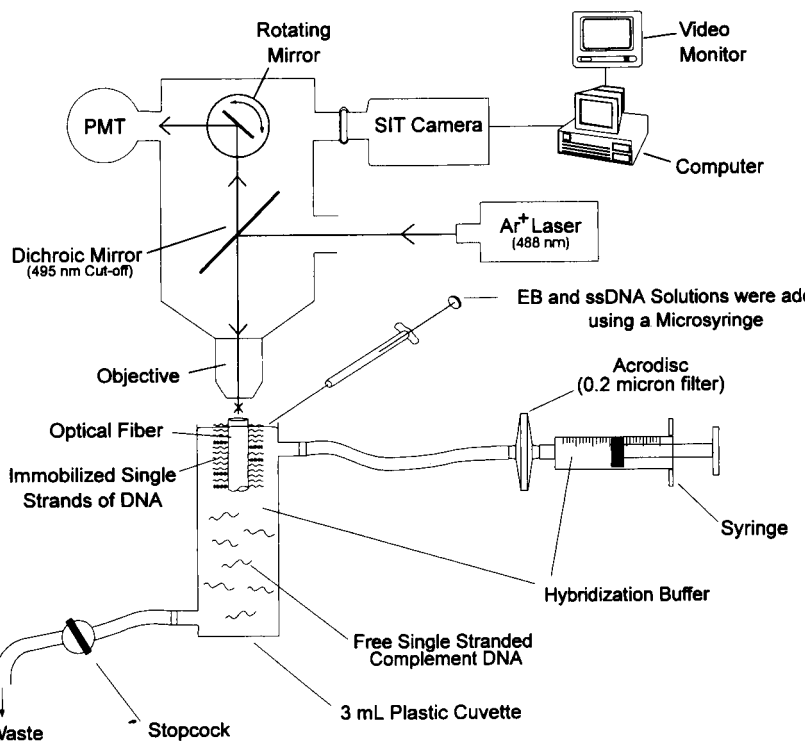

Fig. 1. Schematic diagram of the apparatus used to measure fluorescence intensity from optical fibers coated with immobilized DNA.

(Rexdale). Sephadex G-25 was obtained from Pharmacia (Baie d'Urfé) and C18 Sep-Pak cartridges were purchased from Waters (Mississauga). All polyacryamide gel elecrophoresis reagents and apparatus were purchased from Bio-Rad (Mississauga). All organic solvents were dried and distilled and all other chemicals were of reagent grade or better.

2.2. Equipment

Plastic-clad silica optical fibers with a diameter of 400 μm were purchased from Tasso (Montreal). The cladding on the fibers was mechanically removed and the fibers were cut to lengths of about 1 cm. One face on each fiber was polished by suspending the fiber over (and placing the end

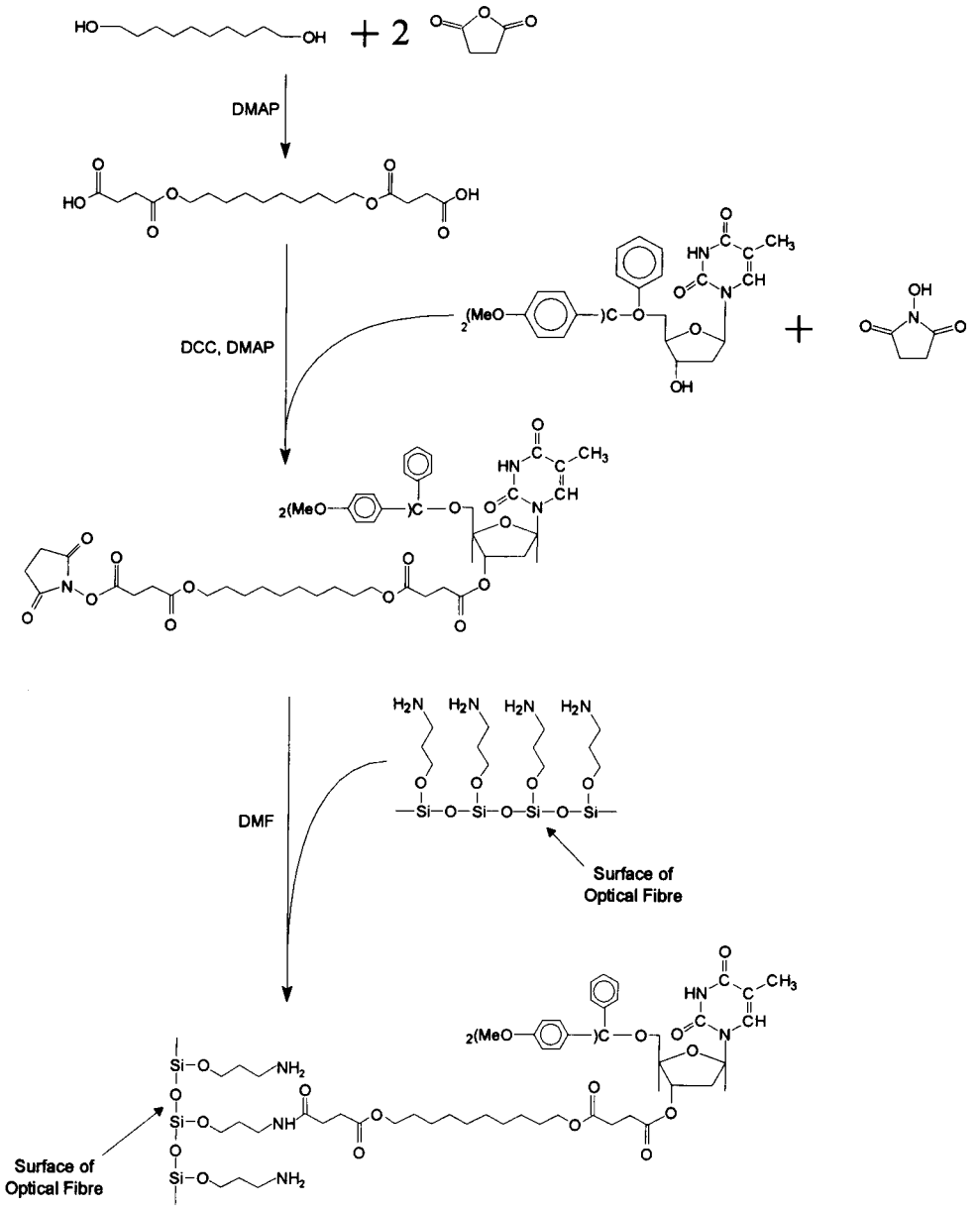

Fig. 2. Synthetic scheme used to activate the surface of the optical fibers with long chain aliphatic spacer molecules terminated with a 5′-*O*-dimethoxytrityl-2′-deoxythimine nucleoside.

face of the fiber in contact with) the rotating plate of a Thermolyne type 37 600 speed controlled mixer (Sybron, Dubuque) onto which 1200 grade emery paper was immobilized. All quartz optical fibers were cleaned using a Harrick PDC-32G plasma cleaner (Harrick Scientific, Ossining) before activation with APTES.

All DNA synthesis was done by the well established β-cyanoethylphosphoramidite method with an Applied Biosystems 381A DNA synthesizer using controlled-pore glass beads or quartz optical fibers. Dimethoxytrityl cation released from each deprotection step of the oligonucleotide synthesis was quantitatively measured by absorption spectroscopy at 504 nm using a Hewlett Packard 8452A diode array spectrometer (Hewlett Packard, Palo Alto, CA) to determine the percent coverage of dT_{20} on the optical fibers. Measurement of absorbance at 260 nm was used to quantify purified oligomers.

The instrument used for fluorescence intensity measurements was based on a fluorescence microscope as is described elsewhere [21] and shown in Fig. 1. A DNA coated fiber was selected at random from the batch of fibers (ca. 25) onto which ssDNA was grown and was positioned under the objective of the microscope. In this orientation the incident laser radiation entered the fiber at one end and was totally internally reflected. The majority of the fiber was submerged in a hybridization buffer solution consisting of 0.9 M NaCl and 50 mM sodium phosphate (pH 7.4) in sterile water. Hybridization buffer was passed through an acrodisc filter immediately prior to introduction into the cuvette.

2.3. Procedures

Preparation of quartz optical fibers derivatized with long chain aliphatic spacer molecules terminated with a 5′-O-dimethoxytrityl-2′-deoxythymidine nucleoside

The protective cladding on the optical fibers was removed and the bare fibers were refluxed in chloroform for 2 h. The fibers were then washed with a 1:1 acetone–methanol mixture and stored in a vacuum desiccator. The optical fibers were plasma cleaned for 5 min at low power (40 W) and were placed in a solution of 1:200 (v/v) APTES in dry toluene. This was done under a nitrogen atmosphere using glassware which was previously treated with octadecyltrichlorosilane. The structure of the APTES coatings on quartz substrates has previously been investigated by Vandenberg et al. [22]. The method of Arnold et al. [23] was used to synthesize an aliphatic spacer arm terminated with 5′-*O*-dimethoxytrityl-2′-deoxythymidine. In this method 1,10-decanediol was condensed with succinic anhydride to form 1,10-decanediol bis-succinate, as illustrated in Fig. 2. The bis-succinate was reacted with *N*-hydroxysuccinimide and 5′-*O*-dimethoxytrityl-2′-deoxythymidine in the presence of DCC and DMAP to yield a nucleoside functionalized spacer molecule. The spacer was then attached to the surface of the APTES treated optical fiber.

2.4. Automated DNA synthesis

Automated solid-phase DNA synthesis is well known and is described in detail elsewhere [24]. The surface-derivatized optical fibers were placed into an emptied Applied Biosystems OPC column with the dead volume being taken up by inert packing material. The end filter papers were replaced (Applied Biosystems) and the column ends were crimped closed using aluminum seals [19]. Synthesis of oligomers onto the optical fibers was carried out at the 0.2-μmol scale with a pulsed-delivery cycle in the trityl off mode. The β-cyanoethylphosphoramidite cycle was used as supplied by Applied Biosystems with the exception of extended nucleoside coupling times (2 min). Deprotection of the phosphate blocking groups from the immobilized oligomer was achieved by standing the fibers in a solution of triethylamine–acetonitrile (2:3) at room temperature for 1.5 h.

Synthesis of dA_{20} was done using a conventional LCAA-CPG support with the β-cyanoethylphosphoramidite cycle supplied by Applied Biosystems. The nonadecamer of random base composition (dR_{19}) was prepared by simultaneously introducing all four phosphoramidite reagents to the column at each coupling step. Standard deprotection with aqueous ammonia

was used to liberate the oligomers from the solid support and remove the base protecting groups. Crude oligomer was purified by polyacrylamide gel electrophoresis and reversed-phase liquid chromatography or size exclusion chromatography.

2.5. Storage and cleaning of fibers

Fibers coated in ssDNA were either stored under vacuum or kept in a solution of ethanol–water (1 : 1). Fibers stored under vacuum were cleaned prior to use by sonication in a solution of ethanol–water (1 : 1) for 5 min in order to remove any fluorescent contaminants adsorbed to the surface of the fibers.

2.6. Detection of cDNA by the optical sensor

100 μl of a 2.75 μg ml^{-1} or various volumes of a 56.8 μg ml^{-1} aqueous solution of purified dA_{20} ssDNA was added to the plastic cuvette containing the suspended fiber in fresh hybridization buffer at 85°C. The solution was allowed to stand and cool to room temperature (25°C) between 30 and 90 min after which the fiber was flushed with 60 ml of hybridization buffer (25°C).

Staining of dsDNA was achieved by injecting 10 μl of a 1 mg ml^{-1} aqueous solution of EB into the cuvette and allowing the solution to stand for 15 min followed by washing the fiber by flushing the cuvette with 60 ml of fresh hybridization buffer (25°C).

Regeneration of ssDNA and removal of EB at the surface of the optical fiber was achieved by washing the fiber in hot (85°C) hybridization buffer. A total of 30 ml of the hot buffer was flushed through the cuvette over a time of about 30 s and the system was allowed to stand for 5 min. An additional 30 ml of hot buffer was then flushed through the cuvette to wash away dissociated cDNA strands.

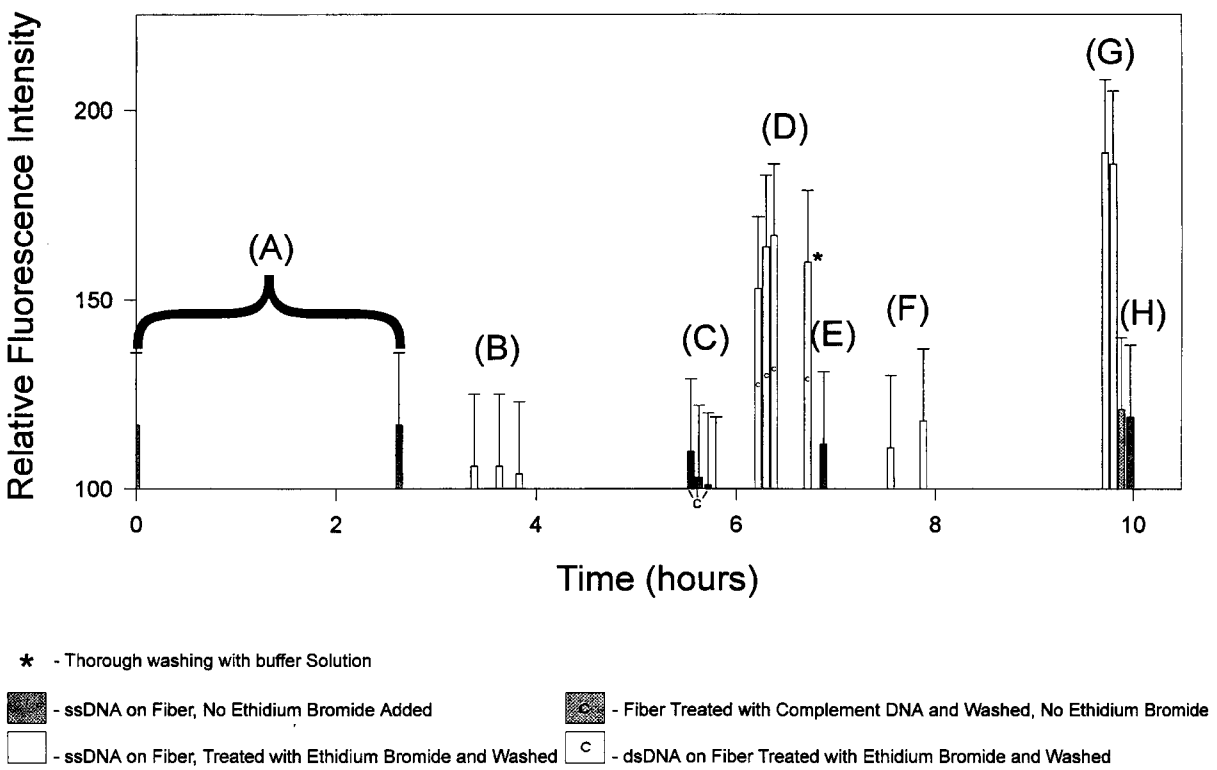

Fig. 3. Response characteristics of a DNA optical biosensor immediately after preparation.

3. Results and Discussion

Triethylamine was used for the removal of β-cyanoethyl protecting groups on the internucleotidic phosphotriester moieties [25]. This procedure causes the loss of the phosphate blocking group via a β-elimination mechanism [26] while not cleaving the ssDNA from the optical fibers.

Determination of the extent of coverage of the optical fibers with DNA was achieved by measuring the amount of dimethoxytrityl cation released during each deprotection step of the DNA synthesis by UV–visible spectrometry. On average 8.8 ± 0.1 nanomoles of dimethoxytrityl cation were released for each deprotection step. This represents $33 \pm 5\%$ coverage of the surface area of the fibers given that the total surface area of all the fibers in the synthesizer was $8 \pm 1 \times 10^{14}$ nm^2.

Fluorescence intensity values are reported as relative quantities obviating the need to control experimental parameters such as laser intensity, optical alignment and PMT gain which are beyond accurate control from day to day. The fluorescent DNA stain EB is a commonly used dye for the detection of DNA [18,27,28]. EB has an absorption maximum of 510 nm, which is sufficiently close to the output wavelength of 488 nm of the Ar^+ laser used in the fluorescence microscope to excite the fluorophore. The dye has an emission maximum of 595 nm when bound to DNA which is well beyond the cut-off wavelength (495 nm) of the dichroic mirror used in the microscope [27].

The response of the fiber optic DNA biosensor to EB and cDNA is shown in Fig. 3. The optical fiber coated with immobilized ssDNA was taken from storage under vacuum, was placed under the fluorescence microscope, and the initial fluorescence intensity with the fiber submerged in the hybridization buffer (25°C) was measured. After two hours the fluorescence intensity from the fiber was measured again, and the results indicated that there was no appreciable drift in the response of the instrument or the amount of fluorescent material present at the surface of the fiber (Fig. 3A). Fluorescence microscopy studies of the surface of fibres which were stored under vacuum indicated the presence of some fluorescent contaminants. The contribution of these fluorescent contaminants was responsible for much of the fluorescence intensity observed in Fig. 3A. As a control experiment, 10 μl of a 1 $mg\text{–}ml^{-1}$ aqueous solution of EB was added to the cuvette (3 ml) in which the fiber was suspended. After 15 min, 60 ml of fresh hybridization buffer (25°C) was flushed through the cuvette in order to remove any non-specifically bound ethidium cation. A decrease in the fluorescence intensity back to baseline values was observed after this washing, as shown in Fig. 3B, due to the removal of fluorescent contaminants from the surface of the optical fiber.

The room-temperature hybridization buffer present in the cuvette was replaced with hot (85°C) hybridization buffer and 257 ng of complementary (dA_{20}) ssDNA was then injected into the cuvette and the system allowed to cool for 90 min. This temperature was chosen as it is sufficiently greater than the 40°C duplex melting temperature (T_m, the temperature at which half of all the duplexes present are dissociated) and is well below the boiling point of the buffer. The duplex melting temperature was calculated using the empirical relation:

$$T_m = 2°C \times (\text{number of A + T residues}) + 4°C \times (\text{number of G + C residues}) \quad (1)$$

for duplexes 11–23 bases long in buffers which are 1 M in Na^+ [29]. Incubation at temperatures below T_m has been shown to cause incomplete hybridization wherein only a fraction of the bases on each strand interact to form partially hybridized complexes [30]. Though covalent immobilization of ssDNA removes one degree of freedom from the oligomer, hybridization at temperatures initially above the duplex T_m ensures the formation of duplexes with the greatest possible extent of overlap. No appreciable intensity change from that of the baseline was observed after the 90 minute incubation period (Fig. 3C). 10 μl of the EB solution was added to the buffer and the solution was allowed to stand for a 15 min incubation time. The fiber was then washed with 60 ml of fresh buffer as described for the blank

experiment. A $50 \pm 20\%$ increase in the fluorescence intensity as shown in Fig. 3D was observed from the fiber which was coated in EB labelled dsDNA. It is interesting to note that 257 ng (4.11 femtomoles) of dA_{20} only amounts to $2 \times 10^{-5}\%$ of the total available ssDNA immobilized onto the fiber. In order to ensure that the ethidium cation that was present was intercalated into the dsDNA, the fiber was washed with an additional 30 ml of buffer solution. After this washing, no appreciable decrease in the fluorescence intensity was observed (Fig. 3D *).

To determine if the DNA sensor could be regenerated, the fiber was washed with 30 ml of hot (85°C) buffer solution over a period of about 30 s and the system allowed to stand for 5 min. After the five minute wait, an additional 30 ml of hot buffer was flushed through the cuvette to wash away the dissociated cDNA strands. This procedure is known to melt DNA duplexes as the buffer temperature was well above the T_m of the dsDNA. The fluorescence intensity returned, within experimental uncertainty, to the initial intensity observed at the beginning of the experiment (Fig. 3E). As a control experiment, EB was introduced into the cuvette, and was then washed out as done previously. The fluorescence intensity remained at the initial value, as shown in Fig. 3F, indicating that the DNA duplexes had indeed been dissociated and the complement strands were removed.

To test the reproducibility of the sensor, another 257 ng of cDNA was added to the cuvette and after 90 min the fiber was treated with EB, was then washed, and the fluorescence intensity was again measured. An increase in fluorescence intensity was observed which was similar in magnitude to that observed from the first dsDNA

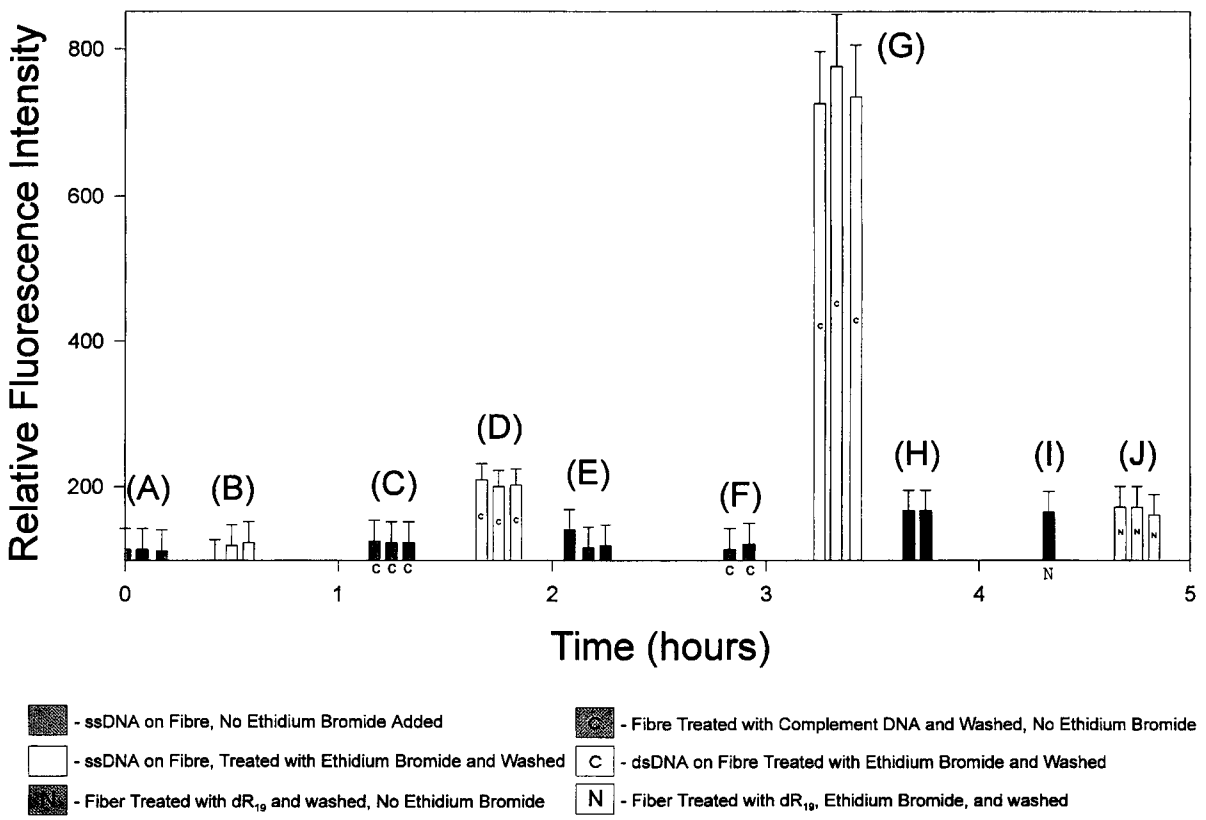

Fig. 4. Response characteristics of a DNA optical biosensor after storage for one month.

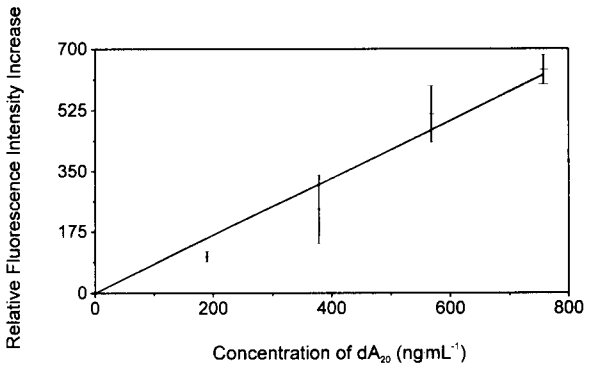

Fig. 5. Relative fluorescence intensity versus concentration of cDNA.

analysis (Fig. 3G). After washing the fiber with hot buffer solution, a baseline intensity within the experimental uncertainty of the results was again observed (Fig. 3H).

A calibration experiment was done to test the analytical response of the DNA biosensor. The procedures used in this experiment were identical to that of the first experiment with the exception that 30 min incubation times for hybridization were used as it was found that only 30 min was required for the 85°C buffer that was added to the cuvette to cool to 25°C. Good reversibility of the signal was observed (Fig. 4) as well as a signal which was linear with the amount of cDNA added to the cuvette (Fig. 5). The regression line shown in Fig. 5 shows a good fit to the data points with an r^2 value of 0.965. From this data, the sensitivity of the sensor was determined to be an increase in fluorescence intensity of 83% per 100 ng ml^{-1} of cDNA with a measured limit of detection of 86 ng ml^{-1}.

The robustness of the fibers, and DNA as a biorecognition element, was made evident by the maintenance of activity after long term storage and stringent cleaning conditions. Fibers that were stored for up to 30 days in vacuo or in ethanol–water (1 : 1) solutions possessed identical response characteristics to freshly prepared fibers. Adsorbed fluorescent contaminants which were accumulated through long term storage were completely removed (as confirmed through fluorescence microscopy) by sonicating the fibers in a solution of ethanol–water (1 : 1) with full maintenance of activity and sensitivity. The response to 86 ng ml^{-1} of cDNA was a 50 ± 20% increase in fluorescence intensity for a freshly prepared sensor (Fig. 3D), which correlates well to the 104 ± 15% intensity increase observed when the 1 month old sensor was treated with 189 ng ml^{-1} of cDNA (Fig. 4D).

A control experiment was also done in which 30 μl of a 60 μg ml^{-1} solution of 19 nucleotide long oligomer with random base composition was injected into the cuvette containing hot (85°C) buffer followed by incubation for 30 min. Washing of the fiber after incubation with dR_{19} and treatment with EB was done as described previously. No change in intensity was observed for this control experiment (Fig. 4H–J) indicating that the sensor was sequence specific.

4. Conclusion

This work has demonstrated that ssDNA may be covalently immobilized with a highly specific orientation onto the surface of quartz optical fibers and can undergo hybridization with cDNA introduced into the local environment of the sensor. Hybridization events may be detected by the use of the fluorescent DNA stain ethidium bromide which is known to intercalate into dsDNA. The detection system was shown to be reproducible, regenerable, long-lived, rugged and to provide a measured detection limit of 86 ng ml^{-1} of cDNA with an increase of fluorescence intensity of 83% per 100 ng ml^{-1}.

Future work will involve the covalent immobilization of a variety of different fluorescent probes directly onto the immobilized ssDNA via 5′ derivatization. The probes will have high quantum yields when intercalated into the base stacking region of dsDNA and near zero quantum yields when in the presence of immobilized ssDNA. The tethered fluorescent probe should provide a reduction in the response time, be unaffected by non-specific absorption and offer greater portability due to the reduced demand for external solution treatment. Washings with hot chaotropic salt solutions shall also be investi-

gated for the removal of cDNA strands from the surface of the fibre. Chaotropic salts are known to decrease duplex stabilities and hence should improve the regenerability of the biosensor [30]. Extensions of this work to the detection of pathogenic bacteria using DNA probe technology are now being investigated.

5. References

[1] D.L. Wise, Bioinstrumentation: Research, Developments and Applications, Butterworth, Stoneham, MA, 1990.
[2] R.P. Buck, William, E. Hatfield, Mirtha Umaña and Edmond F. Bowden, Biosensor Technology: Fundamentals and Applications, Marcel Dekker, New York, 1990.
[3] K.M.R. Kallury, W.E. Lee and M. Thompson, Anal. Chem., 64 (1992) 1062.
[4] U.J. Krull, R.S. Brown, E.T. Vandenberg and W.M. Heckl, J. Electron Microsc. Technique, 18 (1991) 212.
[5] R.H. Symons, Nucleic Acid Probes, CRC Press, Boca Raton, FL, 1989.
[6] L.C. Bock, L.C. Griffin, J.A. Latham, E.H. Vermaas and J.J. Toole, Nature, 355 (1992) 564.
[7] F. Tay, Y.B. Liu, M.J. Flynn and J. Slots, Oral Microbiol. Immunol., 7 (1992) 344.
[8] M.I. Sherman, A.H. Bertelsen and A.F. Cook, Bioorganic and Medicinal Chemistry Letters, 3 (1993) 469.
[9] S.L. Beaucage and M.H. Caruthers, Tetrahedron Lett., 22 (1981) 1859.
[10] G. Alvarado-Urbina, G.M. Sathe, W.-C. Liu, M.F. Gillen, P.D. Duck, R. Bender and K.K Ogilvie, Science, 214 (1981) 270.
[11] R.L. Letsinger and W.B. Lunsford, J. Am. Chem. Soc., 98 (1976) 3655
[12] K.M. Shokat and P.G. Schultz, Methods Enzymol., 203 (1993) 327.
[13] M.E.A. Downs, S. Kobayashi and I. Karube, Anal. Lett., 20 (1987) 1897.
[14] J.C. Andle, J.F. Vetelino, M.W. Lade and D.J. McAllister, Sensors Actuators B, 8 (1992) 191.
[15] J.C. Richards and D.T. Bach, Eur. Pat. Appl., EP295965 A2 21 December 1988.
[16] H. Su, M. Yang, K.M.R. Kallury and M. Thompson, Analyst, 118 (1993) 309.
[17] K.M. Millan, A. Saraullo and S.R. Mikkelsen, 76th Canadian Society for Chemistry Conference and Exhibition, Sherbrooke, PQ, 06/1993, abstract 740.
[18] R.R. Monaco and F.H. Hausheer, J. Biomolecular Struct. Dynamics, 10 (1993) 675.
[19] R.H.E. Hudson and M.J. Damha, J. Am. Chem. Soc., 115 (1993) 2119.
[20] M.J. Damha, P.A. Giannaris and S.V. Zabarylo, Nucleic Acids Res., 13 (1990) 3813; and references cited therein.
[21] J.D. Brennan, R.S. Brown, C.P. McClintock and U.J. Krull, Anal. Chim. Acta, 237 (1990) 253.
[22] E.T. Vandenberg, L. Bertilsson, B. Liedberg, K. Uvdal, R. Erlandsson, H. Elwing and I. Lundstroem, J. Colloid Interface Sci., 147 (1991) 103.
[23] L. Arnold, Z. Tocik, E. Bradkova, Z. Hostomsky, V. Paces and J. Smrt, Collect. Czech. Chem. Commun., 54 (1989) 523.
[24] S.L. Beaucage and R.P. Iyer, Tetrahedron, 48 (1992) 2223; and references cited therein.
[25] V.A. Efimov, S.V. Reverdatta and O.G. Chakhmakhcheva, Tetrahedron Lett., 23 (1982) 961.
[26] G.M. Tener, J. Am. Chem. Soc., 89 (1961) 159.
[27] R.P. Haugland, Molecular Probes: Handbook of Fluorescent Probes and Research Chemicals, 5th edn., Molecular Probes, 1992.
[28] J.B LePecq and C. Paoletti, J. Mol. Biol., 27 (1967) 87.
[29] R.B. Wallace and C.G. Miyada, Methods Enzymol., 152 (1987) 435.
[30] J. Van Ness and L. Chen, Nucleic Acids Res., 19 (1991) 5143.

ELSEVIER

Analytica Chimica Acta 288 (1994) 215–220

ANALYTICA CHIMICA ACTA

Separation of mono-, di- and tributyltin compounds by isocratic ion-exchange liquid chromatography coupled with hydride-generation atomic absorption spectrometric determination

Gerhard Schulze *, Christian Lehmann

Technische Universität Berlin, Institut für Anorganische und Analytische Chemie, Strasse des 17. Juni 135, D-10623 Berlin, Germany

(Received 16th June 1993; revised manuscript received 12th October 1993)

Abstract

A method is described for the speciation determination of *n*-butyltin compounds. The three substances are separated from each other and from inorganic tin ions within 10 min by ion-exchange chromatography using a mixture of citric and oxalic acid in methanol as eluent. They are determined by atomic absorption spectrometry after on-line hydride generation and decomposition of the volatile hydrides in an electrically heated quartz T-tube. The limits of detection were 27, 40 and 31 nmol/l for tributyltin, dibutyltin and monobutyltin, respectively. Linear calibration graphs were obtained between 0.1 and 10 μmol l^{-1}. The method was applied to spiked samples of sea water after enrichment by solid-phase extraction.

Key words: Atomic absorption spectrometry; Ion chromatography; Liquid chromatography; Butyltin compounds; Hydride generation; Sea water; Speciation; Waters

1. Introduction

During the last 12 years, interest has grown in the speciation determination of organotin compounds in the aquatic environment. Because of its widespread use and high aquatic toxicity, tributyltin (TBT) is one of the most investigated organotin compounds. It is used as a biocide in antifouling paints, which contains up to 12% of TBT in the dry paint film. To protect ships, boats or docks against fouling, the substance has to be released continuously into the water [1]. Laughlin and Linden [2] reported concentrations in marinas and harbours of 0.03–9 nmol l^{-1}. Laboratory and field experiments have shown that microorganisms such as algae or bacteria are affected by concentrations well below 0.3 nmol l^{-1} [3]. Therefore, the use of TBT on small boats is prohibited in several countries. TBT is degraded by UV irradiation and microorganisms to dibutyltin (DBT), monobutyltin (MBT) and inorganic tin or is adsorbed on sediment particles. Under optimum conditions (upper 2 m of sunlit water, high plankton density, no sedimentation), the half-life of TBT is 1–3 weeks, but in an anaerobic environment degradation can take months or years [4].

* Corresponding author.

SSDI 0003-2670(93)E0634-J

To examine the status and degradation of TBT, a method is needed to measure all species of butyltin compounds. The separation techniques generally used are gas chromatography (GC) and liquid-chromatography (LC). GC needs derivatization by a Grignard reaction or hydride formation prior to sample injection. LC offers the advantages that the risk of decomposition at high temperatures is avoided and off-line sample derivatization is not necessary. Hence, the eluted compounds can be detected by flame [5], electrothermal [6] or hydride-generation (HG) atomic absorption spectrometry (AAS) [7], inductively coupled mass spectrometry [8], UV spectrophotometry [9] or fluorescence spectrometry [10]. In most instances ion-exchange chromatography is used, but normal-phase [11] and reversed-phase [9] systems have also been suggested. Generally the ion-exchange separations are performed on Partisil SCX a strong cation exchanger with a silica gel core) with methanolic solutions of diammonium citrate or ammonium acetate as eluent. These systems require a pH gradient for the elution of MBT [12]. Nevertheless, the peak shapes are not optimum. Further optimization of the eluent is limited by the low solubility of diammonium citrate in methanolic solutions [13]. For gradient elution, time-consuming re-equilibration of the column after each run and the use of expensive mixing systems are necessary. In addition to these disadvantages, fluorescence detection cannot be applied because of its pH sensitivity.

In this paper, a method is described for separating isocratically MBT, DBT and TBT in the presence of inorganic tin on a cation-exchange column within 10 min. For detection HGAAS is used. In contrast to the arrangement of Ebdon et al. [7] it works without air segmentation and without decomposition of TBT in a postcolumn photoreactor.

2. Experimental

2.1. Apparatus

The equipment illustrated in Fig. 1 is composed of three parts: the LC system, the hydride generator with separator and the AAS detector.

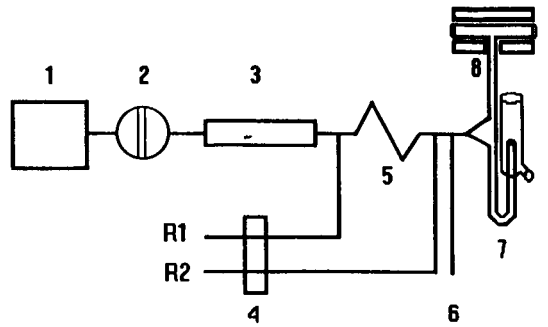

Fig. 1. Schematic diagram of the equipment: 1 = LC pump; 2 = six-port valve; 3 = column; 4 = peristaltic pump; 5 = mixing tube; 6 = carrier gas (nitrogen); 7 = gas–liquid separator; 8 = quartz tube furnace; R1 = 0.1 mol l^{-1} HCl; R2 = 1% (w/v) $NaBH_4$.

2.2. LC systems

The LC system consists of a chromatograph (Model 5000; Varian, Darmstadt) with a pneumatic injector (100-μl sample loop) and a PRP-X 200 column (250 × 4.1 mm i.d.) (Hamilton, Darmstadt). The ion exchanger is sulphonated poly(styrene–divinylbenzene) (exchange capacity 35 μeq/g). The eluent composition was optimized using the low-pressure mixing system of the chromatograph. After the measurements, 80% (w/w) methanol was pumped through the column to replace the eluent solution.

2.3. Hydride generator and separator

The eluate from the column is mixed with 0.1 mol l^{-1} hydrochloric acid (R1) using a Y-shaped connector to lower the pH. After having passed the mixing tube (80 × 0.5 mm i.d.), 1% sodium tetrahydroborate solution (R2) is added to the acidified eluate. The reagents are transported by a peristaltic pump (MS 4 Reglo 8-100; Ismatec, Wertheim). The flow-rates of the reagent streams are given by the inner diameter of the pumping tubes (Table 1).

The separator, based on that proposed by Burns et al. [14], was optimized by Schulze et al. [15] for the determination of butyltin compounds. It works without segmentation of the carrier stream. To avoid adsorption of lipophilic compounds on hydrophobic surfaces, the mixing de-

vice and the separator are fitted into one unit. As the substances react very rapidly, the reaction line can be as short as 4 mm. The mixture is sprayed into the separator with nitrogen. Hence vaporization is favoured by the large surface area of the small droplets. Considering the high boiling points of the hydrides, the connection between the separator and the quartz tube should be kept hot and very short (70 mm × 4 mm i.d.). The optimization of the hydride system has been described in detail elsewhere [16].

2.4. AAS detector

The organotin hydrides are decomposed in an electrically heated, open quartz T-tube (100 mm × 10 mm i.d.) mounted in the AAS device (Pye Unicam SP9; Philips, Kassel). The quartz furnace oven is similar to that proposed by Burns et al. [14], but the firebricks are additionally wrapped with heat-insulating plates (5 mm). The signals are recorded by an integrator (Model C-R3A; Shimadzu, Duisburg).

2.5. Reagents

Analytical-reagent grade chemicals from Merck (Darmstadt) were used unless indicated otherwise.

For eluents appropriate amounts of citric acid, oxalic acid and lithium hydroxide (LAB, 98%) are dissolved in 500 ml of distilled methanol (technical grade). The solutions are filtered through a 0.45-μm membrane (Sartorius, Göttingen). Concentrated hydrochloric acid is diluted to 0.1 mol l^{-1}. For the reduction reagent, 10 g of sodium tetrahydroborate pellets (for synthesis grade) are dissolved in 1 l of potassium hydroxide solution (2 g l^{-1}). To achieve increased stability, the solution is filtered as above.

Stock standard solutions of organotin compounds (Schering, Bergkamen) are prepared by dissolving the substances in methanol containing 0.01 mol l^{-1} hydrochloric acid. These solutions are stable for several months if stored in the dark at room temperature. Working standard solutions are prepared weekly by dilution with the same solvent.

Table 1
Optimum conditions for HGAAS

Hydride generation system	
Acid	0.1 mol l^{-1} HCl; flow-rate 0.29 ml min^{-1}
Reductant	1% (w/v) $NaBH_4$ in 0.2% (w/v) KOH; flow-rate 0.49 ml min^{-1}
Gas stream	nitrogen, flow-rate 350 ml min^{-1}
AAS detector	
Light source	Philips hollow-cathode lamp; 224.6 nm; current 5 mA
Bandpass	0.5 nm; damping 2 s
Furnace	temperature 820°C

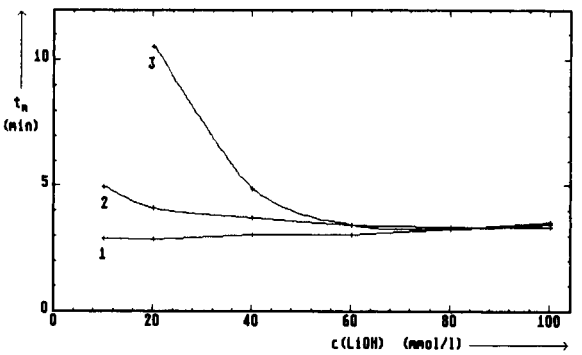

Fig. 2. Retention times of (1) TBT, (2) DBT and (3) MBT vs. LiOH concentration (50 mmol l^{-1} citric acid in methanol).

3. Results and discussion

Problems in the ion-exchange separation of butyltin compounds arise with the ammonium salts used for the eluent (see above). By using citric acid and lithium hydroxide instead of diammonium citrate, it is possible to elute all three species. As shown in Fig. 2, variation of the lithium hydroxide concentration is the most effective for MBT. Without lithium hydroxide, all compounds are retained on the column. At low pH the degree of dissociation of citric acid is low and only small amounts of MBT are complexed. DBT and TBT show a nearly constant behaviour. With the optimized lithium citrate eluent (50 mmol l^{-1} citric acid, 40 mmol l^{-1} lithium hydroxide in methanol) the substances are separated within 6 min (Fig. 3 A). However, it is difficult to

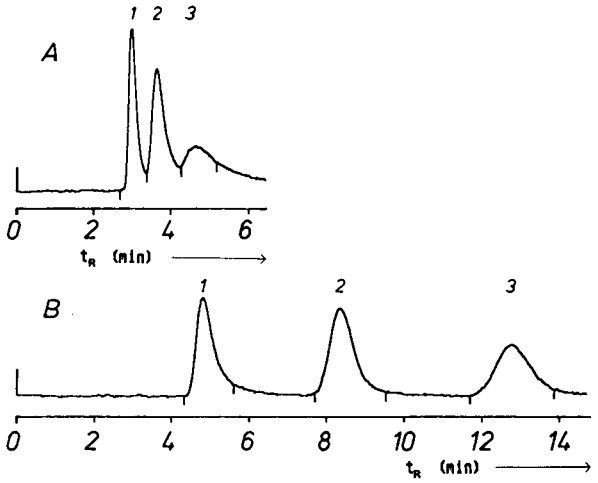

Fig. 3. Separation of (1) TBT, (2) DBT and (3) MBT. (A) 50 mmol l^{-1} citric acid and 40 mmol l^{-1} LiOH in methanol; (B) 80 mmol l^{-1} oxalic acid and 60 mmol l^{-1} LiOH in 80% (w/w) methanol.

evaluate quantitatively the broad MBT elution peak. The peak shape might be improved by increasing the concentrations of the compounds, but then the resolution deteriorates. By using oxalic acid instead of citric acid the separation is also possible, but the peaks are broadened and the retention times are increased as shown for the optimum conditions in Fig. 3B [80 mmol l^{-1} oxalic acid, 60 mmol l^{-1} lithium hydroxide 80% (w/w) methanol]. The low solubility of the substances in methanol–water mixtures with high methanol contents makes further optimization impossible. Increasing the water content of the eluent enhances the solubility, but the retention time of TBT then increases unacceptably.

The determination could be improved by using both acids as complexing agents. The concentration of oxalic acid was varied starting with the optimum lithium and citrate concentrations (50 mmol l^{-1} citric acid, 40 mmol l^{-1} lithium hydroxide in methanol). The addition of oxalic acid caused a decrease in pH. This was compensated for by adding dropwise a saturated solution of lithium hydroxide. The use of oxalic acid is the most effective for DBT, so that the more highly charged MBT is eluted earlier than DBT (Fig. 4). The best results are obtained in the range 4–8

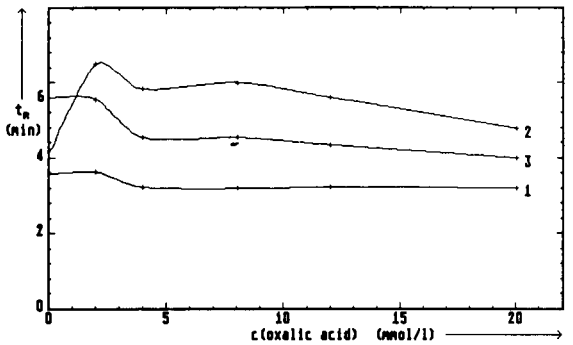

Fig. 4. Effect of oxalic acid on the retention times of (1) TBT, (2) DBT and (3) MBT (50 mmol l^{-1} citric acid, ≥ 40 mmol l^{-1} LiOH in methanol, constant pH).

mmol l^{-1} oxalic acid. The peak shape of MBT and the resolution of the peaks are improved (Fig. 5). Moreover, the peak of inorganic tin appears. The optimum eluent composition obtained for the separation of equimolar amounts of butyltin compounds (1 μmol l^{-1} each) was 50 mmol l^{-1} citric acid, 50 mmol l^{-1} lithium hydroxide and 4 mmol l^{-1} oxalic acid in methanol, with a flow-rate of 1 ml min^{-1}.

The best results were obtained with 100% methanol, in contrast to 70–80% as reported [7,12]. This can be explained by the use of different ion-exchange materials. Most separations have been done on Partisil SCX, a silica gel-based ion exchanger, but the column used here (Hamilton PRP-X 200) is based on poly(styrene–divinylbenzene), which has stronger hydrophobic interactions.

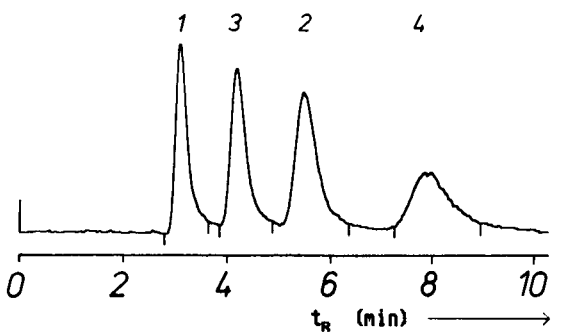

Fig. 5. Separation of (1) TBT, (2) DBT, (3) MBT and (4) SN(IV) (50 mmol l^{-1} citric acid, 50 mmol l^{-1} LiOH and 4 mmol l^{-1} oxalic acid in methanol).

Table 2
Limits of detection and determination for butyltin compounds

Parameter	MBT	DBT	TBT
Limit of detection (nmol l^{-1})	31	40	27
Limit of determination (nmol l^{-1})	102	134	88

Linearity of the calibration graphs was demonstrated by injection of 100 μl of a standard mixture containing of 0.1–10 μmol/l of each butyltin compound in methanol (correlation coefficient > 0.9992). The limits of detection and determination were calculated by the calibration graph method [17] for a confidence level of 99% (Table 2). For a standard mixture of 0.2 μmol l^{-1} of each compound the relative standard deviation is 2–5% (n = 10).

The detection limits are higher than the concentrations that occur in natural waters, so preconcentration is necessary. For enrichment of the organotin compounds mainly liquid–liquid extraction and sometimes solid-phase extraction are used. Here the latter was preferred because online coupling with LC is possible. For retaining MBT, tropolone as a complexing agent is normally used to enhance its hydrophobic character. However, this reagent interferes with the complex equilibria during the ion-exchange separation [12], so it was replaced with kojic acid. For enrichment by solid-phase extraction a 100-mg C_{18} column (ICT, Frankfurt) was used. The column was pretreated by pumping 1.5 ml of methanol [90% (w/w), 10 mmol l^{-1} HCl] followed by 6.5 ml of an aqueous solution of kojic acid (1 mmol l^{-1}). Subsequently, 50 ml of the sample will pass through the column at a flow-rate of 10 ml min^{-1}. The sample was prepared by adding a mixture of butyltin standards (MBT, DBT and TBT, 10 nmol l^{-1} each) to 50 ml of sea water acidified with HCl to pH 1 and containing 0.5 ml of methanol, 0.05 mmol of kojic acid and 0.5 mmol of ascorbic acid. Then 10 ml of doubly distilled water were pumped through the colunm, washing out ionic substances, and the water was then removed by pumping air for 1 min. The butyltin compounds were extracted with 1 ml of methanol [90% (w/w) methanol containing 10 mmol l^{-1} HCl]. This extract was used for the separation. All enrichment steps were controlled automatically by a programmed autosampler (Model 221; Gilson, Villiers-le-Bel). The separation is not disturbed by co-extracted matrix components present in the sea-water extract. The recoveries for the solid-phase extraction of a 50-ml sea-water sample spiked with 10 nmol l^{-1} of each butyltin compound were 84% for TBT, 98% for DBT and 84% for MBT. Recoveries at various concentration level are given in Table 3.

4. Acknowledgements

The authors thank Mr. M. Harnisch (Umweltbundesamt, Berlin) for provision of the chromatograph, Mr. H. Traxler (Hamilton, Darmstadt) for making available the PRP-X 200 column and Schering (Bergkamen) for the organotin compounds. They also thank Mr. Ch. Müller for assistance.

5. References

[1] C.J. Evans and S. Karpel, Journal of Organometallic Chemistry Library, Vol. 16, Elsevier, Amsterdam, 1985, p. 135.
[2] R.B. Laughlin and O. Linden, Ambio, 16 (1987) 252.
[3] K.G. Steinhäuser, W. Amann, A. Späth and A. Polenz, Wasser, 65 (1985) 203.

Table 3
Recoveries (%) for butyltin compounds at different concentration levels (C) in various sample volumes (V)

Compound	V (ml) C (nmol l^{-1})	V (ml) C (nmol l^{-1})	V (ml) C (nmol l^{-1})	V (ml) C (nmol l^{-1})
	5 100	25 20	50 10	100 5
TBT	85.3 ± 1.3	84.6 ± 2.0	84.3 ± 1.4	84.6 ± 3.9
DBT	98.1 ± 2.0	95.4 ± 3.4	98.3 ± 1.3	91.0 ± 2.7
MBT	92.0 ± 2.6	91.8 ± 1.3	83.8 ± 1.3	75.0 ± 0.9

[a] Mean values ± standard deviations (n = 4).

[4] M.D. Müller, L. Renberg and G. Rippen, Chemosphere, 18 (1989) 2015.
[5] L. Ebdon, P. Jones and S.J. Hill, Analyst, 110 (1985) 515.
[6] K.L. Jewett and F.E. Brinkman, J. Chromatogr. Sci., 19 (1981) 583.
[7] L. Ebdon, S.J. Hill and P. Jones, Talanta, 38 (1991) 607.
[8] H. Suyani, J. Creed, T. Davidson and J. Caruso, J. Chromatogr. Sci., 27 (1989) 139.
[9] W.G. Lakata, E.P. Lankmayer and K. Müller, Fresenius' Z. Anal. Chem., 319 (1984) 563.
[10] L. Ebdon and J.J. Garcia Alonso, Analyst, 112 (1987) 1551.
[11] A. Praet, C. Dewaele, L. Verdonck and G.P. Van der Kelen, J. Chromatogr., 507 (1990) 427.
[12] J.W. McLaren, K.W.M. Siu, J.W. Lam, S.N. Willie, P.S. Maxwell, A. Palepu, M. Koether and S.S. Berman, Fresenius' J. Anal. Chem., 337 (1990) 721.
[13] W. Kleiböhmer and K. Cammann, Fresenius' Z. Anal. Chem., 335 (1989) 780.
[14] D.T. Burns, F. Glockling and M. Harriott, Analyst, 106 (1981) 921.
[15] G. Schulze, H. Rybczynski and Ch. Lehmann, Fresenius' J. Anal. Chem., 342 (1992) 192.
[16] G. Schulze and Ch. Lehmann, in B. Welz (Ed.) 6. Colloquium Atomspektrometrische Spurenanalytik, Bodenseewerk Perkin-Elmer, Überlingen, 1991, p. 305.
[17] DIN 32 645, Chemical Analysis; Detection Limit, Identification Limit and Determination Limit (draft), 1991.

ELSEVIER

Analytica Chimica Acta 288 (1994) 221–226

ANALYTICA CHIMICA ACTA

Determination of the six major flavonoids in Scutellariae Radix by micellar electrokinetic capillary electrophoresis

Ying-Mei Liu, Shuenn-Jyi Sheu *

Department of Chemistry, National Taiwan Normal University, Taipei, Taiwan

(Received 20th August 1993; revised manuscript received 9th November 1993)

Abstract

A capillary electrophoretic method for determining the six flavonoids in Scutellariae Radix, i.e., baicalin, baicalein, wogonin 7-*O*-glucuronide, wogonin, oroxylin A 7-*O*-glucuronide and oroxylin A, was developed. A buffer solution composed of 20 mM sodium dodecyl sulphate, 10 mM sodium dihydrogenphosphate and 12.5 mM sodium borate was found to be the most suitable electrolyte for this separation, whereby the contents of the six flavonoids in crude Scutellariae Radix could easily be determined within about 25 min. The effects of surfactant concentration, pH and temperature on the migration behaviour of the solutes were studied.

Key words: Electrophoresis; Flavonoids; Pharmaceuticals; Scutellariae Radix

1. Introduction

Scutellariae Radix is the root of *Scutellaria baicalensis* Georgi and is a commonly used Chinese herbal drug possessing the effects of clearing heat, moistening aridity, purging fire and detoxifying toxicosis and is an anti-abortion agent [1]. Flavonoids are their major components and about 40 kinds have been identified so far [2–8]. These flavonoids are known to have a broad range of physiological activities [9,10]. Several methods have been established to determine some of the flavonoids contained in the crude drug, such as thin-layer chromatography (TLC) [11–13], pulse polarography [14] and liquid chromatography (LC) [15–17].

Micellar electrokinetic capillary chromatography (MECC) was first reported by Terabe et al. in 1984 [18], and since then has been applied successfully to both charged and neutral compounds [19–23]. A negatively charged surfactant such as sodium dodecyl sulphate (SDS) or sodium decyl sulphate was usually added to the background electrolyte to improve the selectivity of the separation. The success of this MECC technique could be largely attributed to the additional partition mechanism between the solutes and the micellar pseudo-stationary phase.

Following previous studies that have shown that capillary electrophoresis could offer satisfactory results in the analysis of some Chinese herbs

* Corresponding author.

SSDI 0003-2670(93)E0629-L

[24–27] and in the separation of flavonoids [28,29], we applied MECC to the determination of the six most abundant flavonoids contained in Scutellariae Radix, i.e., baicalin (BG), baicalein (B), wogonin 7-*O*-glucuronide (WG), wogonin (W), oroxylin A 7-*O*-glucuronide (OG) and oroxylin A (O) (Fig. 1). The effects of the pH of the buffer, the SDS concentration in the electrophoretic medium and the temperature used on the migration times of the flavonoids were studied.

2. Experimental

2.1. Reagents and materials

Sodium dodecyl sulphate was purchased from Sigma (St. Louis, MO) and sodium borate, sodium dihydrogenphosphate and salicylic acid from Osaka (Osaka, Japan). Baicalin, baicalein and wogonin were obtained from Yoneyama (Osaka, Japan). Wogonin 7-*O*-glucuronide, oroxylin A 7-*O*-glucuronide and oroxylin A were isolated from Scutellariae Radix [5–8]. Scutellariae Radix was purchased from the Chinese herbal market in Taipei (Taiwan). Deionized water from a Milli-Q system (Millipore, Bedford, MA) was used to prepare all buffer and sample solutions.

2.2. Preparation of Scutellariae Radix extracts

A 0.1-g sample of pulverized Scutellariae Radix was extracted with 50% aqueous ethanol (7.5 ml) by reflux for 30 min, then centrifuged at 1500 *g* for 5 min. Extraction was repeated three times. The extracts were combined and filtered through a No. 1 filter-paper. After the addition of a 2.5-ml aliquot of internal standard solution (3 mg of salicylic acid in 1 ml of 50% aqueous ethanol), the Scutellariae Radix extract was diluted to 25 ml with 50% aqueous ethanol. This solution was then injected directly into the capillary electrophoresis (CE) system.

2.3. Apparatus and conditions

The analysis was carried out on a BioFocus 3000 capillary electrophoresis system equipped with a UV detector adjusted to 275 nm and a 100 cm × 75 μm i.d. fused-silica capillary tube (Polymicro Technologies, Phoenix, AZ) with the detection window placed at 95.4 cm. The conditions were as follows: injection mode, 3 p.s.i. s (0.6-s injection at 5 p.s.i. pressure); run time, 25 min; applied voltage, 30 kV (constant voltage, positive to negative polarity); and cartridge temperature, 20°C. The electrolyte was a buffer solution consisting of 20 mM SDS, 10 mM sodium dihydrogenphosphate and 12.5 mM sodium borate. Before each run, the capillary was washed with 0.5 M NaOH for 60 s, with nitrogen for 60 s and with buffer for 120 s.

3. Results and discussion

3.1. Analytical conditions

All six flavonoids and salicylic acid (internal standard, S) were successfully determined in a single run by MECC under suitable conditions. The separation was achieved by optimizing the pH of the buffer, the SDS concentration and the cartridge temperature. A 100-cm capillary to

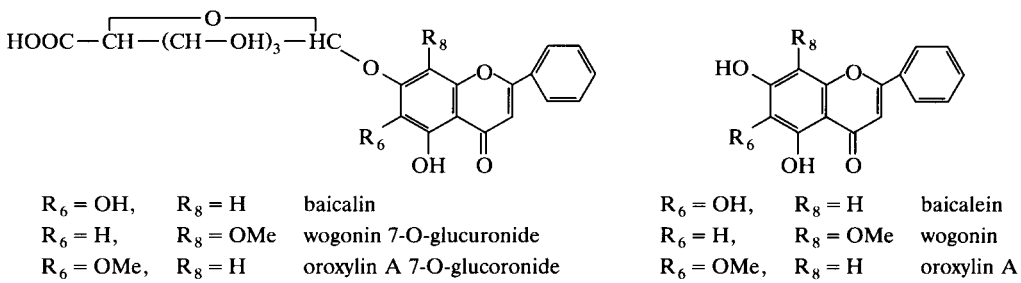

R_6 = OH,	R_8 = H	baicalin	R_6 = OH,	R_8 = H	baicalein
R_6 = H,	R_8 = OMe	wogonin 7-O-glucuronide	R_6 = H,	R_8 = OMe	wogonin
R_6 = OMe,	R_8 = H	oroxylin A 7-O-glucoronide	R_6 = OMe,	R_8 = H	oroxylin A

Fig. 1. Structures of the six flavonoids in Scutellariae Radix.

complete this set-up was chosen, because with a capillary shorter than 100 cm acceptable baseline separation was not obtained.

Preliminary experiments were first conducted at pH 9.6 and 9.9 (10 mM NaH_2PO_4 and 10 mM $Na_2B_4O_7$; 10 mM NaH_2PO_4 and 20 mM $Na_2B_4O_7$) without SDS in the electrophoretic medium, as in conventional CZE. In both instances, BG, WG, OG and S could be separated, but B, W, O overlapped, indicating that all the three aglycones possess similar charges under these pH conditions. The electrophoretic medium in the absence of the micelles does not seem to provide sufficient selectivity to separate the flavonoids. However, with SDS, the components in the mixture sample can be separated on the basis of the relative affinity for the micellar environment or the bulk aqueous phase. A buffer system with suitable amounts of SDS, NaH_2PO_4 and $Na_2B_4O_7$ was chosen. From the foregoing evidence, it was concluded that the more hydrophobic flavonoids would tend to be strongly associated with the micelles and thus be eluted after the hydrophilic species.

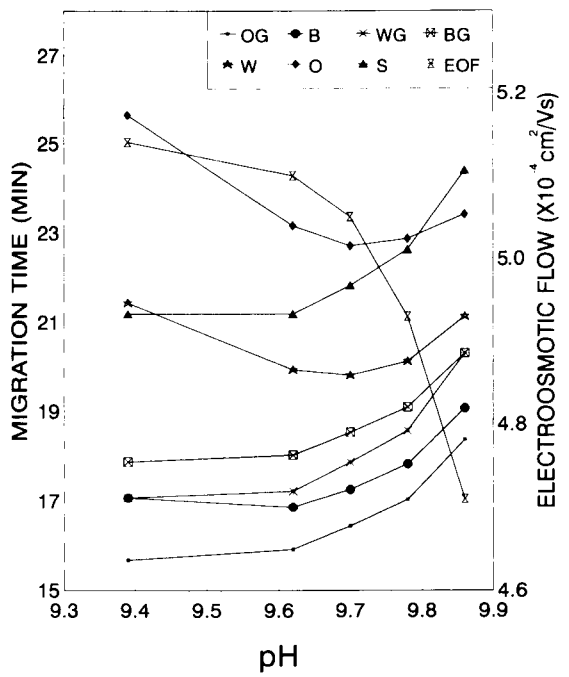

Fig. 2. Effect of pH on migration time. All experiments were conducted at a voltage of 30 kV across the 100 cm×75 μm i.d. separating tube filled with borate–phosphate buffers of different pH values containing 20 mM SDS; cartridge temperature, 20°C; detection wavelength, 275 nm. (■) OG = oroxylin A 7-*O*-glucuronide; (●) B = baicalein; (*) WG = wogonin 7-*O*-glucuronide; (⊠) BG = baicalin; (☆) W = wogonin; (◆) O = oroxylin A; (▲) S = salicylic acid (internal standard); (⧖) EOF = electroosmotic flow.

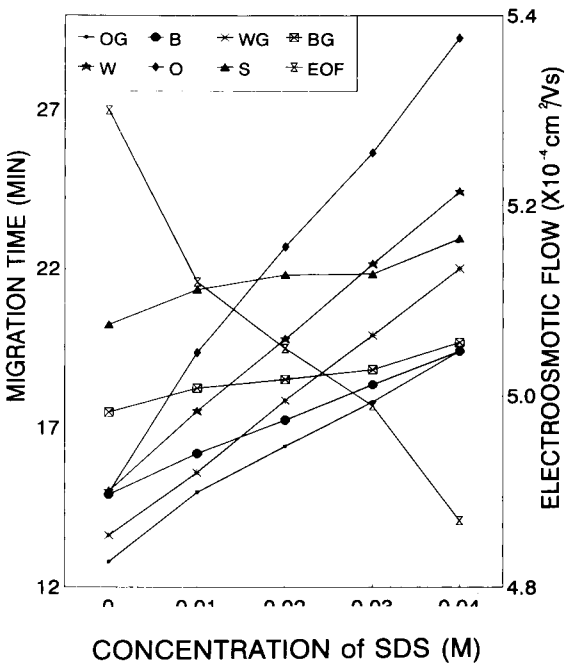

Fig. 3. Effect of SDS concentration on migration time. The carriers were 10 mM NaH_2PO_4–12.5 mM $Na_2B_4O_7$ solutions (pH 9.75) containing 0–40 mM SDS. Other conditions and symbols as in Fig. 2.

Effect of pH

Several electrolyte systems containing 20 mM SDS at different pH values ranging from 9.39 to 9.86 (prepared by mixing 10 mM NaH_2PO_4 with 7.5, 10, 12.5, 15 and 20 mM $Na_2B_4O_7$, respectively) were used in order to study the effect of pH on the selectivity of the separation. In Fig. 2, the migration times for the flavonoids obtained at different pH values are shown. The migration times of these seven compounds varied with the pH of the buffer. From the results, a buffer solution of pH 9.7 was found to produce the best resolution.

Effect of SDS

Five electrolyte systems containing different SDS concentrations ranging from 0 to 40 mM at pH 9.7 (10 mM NaH_2PO_4 and 12.5 mM $Na_2B_4O_7$) were used to study the effect of SDS concentration on the selectivity of the separation. The results obtained are shown in Fig. 3, where the migration times are plotted against SDS concentration. There was an increase in the migration times of the flavonoids when the SDS concentration in the electrophoretic solution increased. This increase can be explained by the fact that at higher SDS concentration the phase ratio of the micelle to the aqueous phase would be larger. Hence the probability of solubilization of the flavonoids by the micelles would be higher, resulting in an increase in the migration times for these compounds. O, W and B were considerably affected by SDS, because they were more hydrophobic than the other compounds. Fig. 3 indicates that the seven compounds were completely separated at 0.01 and 0.02 M SDS, but there were some interferences in the crude drug extract at 0.01 M SDS.

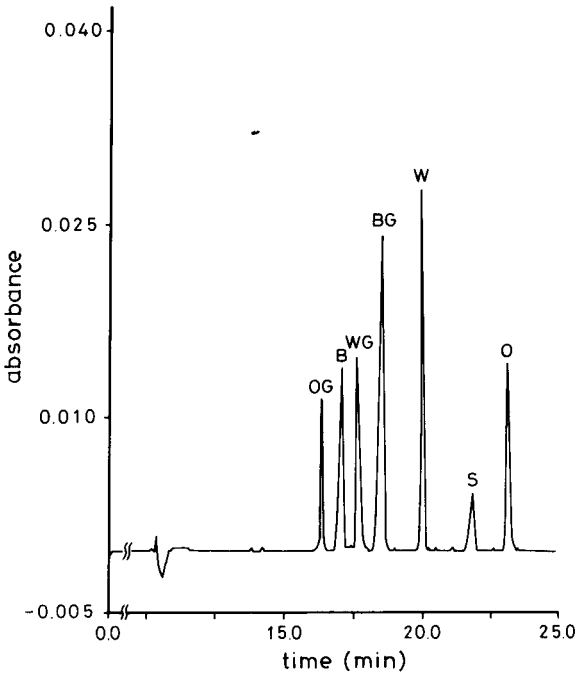

Fig. 5. Capillary electropherogram of a mixture of the six flavonoids present in Scutellariae Radix. Peaks: OG = oroxylin A 7-*O*-glucuronide, 0.098 mg ml^{-1}; B = baicalein, 0.105 mg ml^{-1}; WG = wogonin 7-*O*-glucuronide, 0.182 mg ml^{-1}; BG = baicalin, 0.350 mg ml^{-1}; W = wogonin, 0.105 mg ml^{-1}; O = oroxylin A, 0.070 mg ml^{-1}; S = salicylic acid (internal standard), 0.300 mg ml^{-1}.

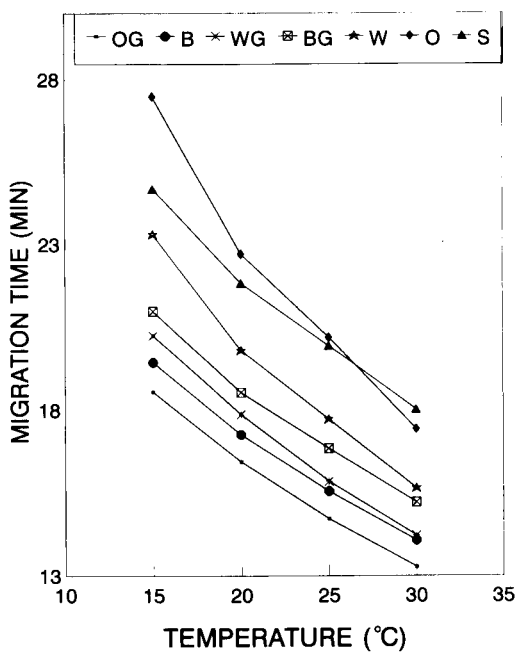

Fig. 4. Effect of cartridge temperature on migration time. The carrier was 10 mM NaH_2PO_4–12.5 mM $Na_2B_4O_7$ solution (pH 9.75) containing 20 mM SDS. The experiments were conducted at cartridge temperatures of 15, 20, 25 and 30°C. Other conditions and symbols as in Fig. 2.

Effect of temperature

The cartridge temperature of the BioFocus 3000 apparatus is controllable. A buffer solution composed of 20 mM SDS, 10 mM NaH_2PO_4 and 12.5 mM $Na_2B_4O_7$ at different cartridge temperatures (15, 20, 25 ,and 30°C) was used to study the effect of temperature on the selectivity of the separation. Migration times were plotted against temperature (Fig. 4). As expected, there was a decrease in the migration times of the flavonoids when the cartridge temperature increased. From Fig. 4 it is clear that analyses carried out at both 15 and 20°C could offer good separations, but with a shorter run time at 20°C.

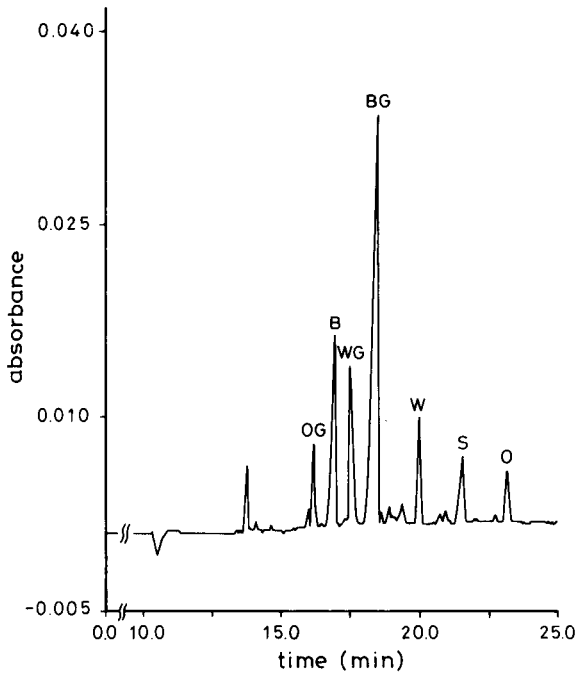

Fig. 6. Capillary electropherogram of the extract of a Scutellariae Radix sample. Peaks as in Fig. 5.

From the above results, the best resolution was obtained with an electrolyte containing 20 mM SDS, 10 mM NaH_2PO_4 and 12.5 mM $Na_2B_4O_7$ and with the cartridge temperature set at 20°C. Fig. 5 presents an electropherogram showing the separation of the six authentic flavonoids with the following migration times: 16.4 min, oroxylin A 7-*O*-glucuronide; 17.3 min, baicalein; 17.9 min, wogonin 7-*O*-glucuronide; 18.5 min, baicalin; 19.8 min, wogonin; 21.8 min, salicylic acid (internal standard); and 22.7 min, oroxylin A. As the ethanol–water extract of Scutellariae Radix sample was injected directly and analysed, the results were as good as those obtained with pure chemical samples without interference, as shown in Fig. 6.

3.2. Calibration graphs for flavonoids

Calibration graphs (peak-area ratio, y, vs. concentration, x, in mg ml^{-1}) were constructed in the range 0.007–0.135 mg ml^{-1} for baicalein, wogonin and oroxylin A 7-*O*-glucuronide, 0.013–0.234 mg ml^{-1} for wogonin 7-*O*-glucuronide, 0.025–0.450 mg ml^{-1} for baicalin and 0.005–0.090 mg ml^{-1} for oroxylin A. The regression equations of these curves and their correlation coefficients were calculated as follows: baicalin, $y = 15.42x - 0.01$ ($r = 0.9998$); baicalein, $y = 23.17x - 0.03$ ($r = 0.9998$); wogonin 7-*O*-glucuronide, $y = 12.60x + 0.02$ ($r = 0.9999$); wogonin, $y = 31.77x + 0.02$ ($r = 0.9999$); oroxylin A 7-*O*-glucuronide, $y = 11.27x + 0.03$ ($r = 0.9991$); oroxylin A, $y = 32.49x + 0.02$ ($r = 0.9998$).

3.3. Determination of flavonoids in Scutellariae Radix

When the test solution was analysed by CE under the selected conditions, the electropherogram shown in Fig. 6 was obtained. The peaks were identified by comparison of the migration times and UV spectra with those obtained from authentic samples of the flavonoids. By substituting the peak-area ratios of the individual peaks for y in the above equations, the contents of the individual flavonoids in the Scutellarriae Radix were obtained: oroxylin A 7-*O*-glucuronide, 14.46 ± 0.35; baicalein, 28.52 ± 0.25; wogonin 7-*O*-glucuronide, 33.01 ± 0.71; baicalin, 122.13 ± 2.15; wogonin, 7.25 ± 0.15; and oroxylin A, 4.58 ± 0.07 mg g^{-1} (mean ± S.D.; $n = 6$)

Suitable amounts (0.10–1.35 mg) of the six flavonoids were added to a sample of Scutellariae Radix of known flavonoid content and the mixture was extracted and analysed using the proposed procedure. The recoveries of the flavonoids were 98.1–102.6% with relative standard deviations of 0.9–2.4% ($n = 6$). The relative standard deviation of the migration time of each compound was below 2% ($n = 6$).

This work has successfully demonstrated that by optimizing parameters such as pH, surfactant concentration of the electrophoretic media and temperature employed, high-resolution separations of a complicated mixture can easily be achieved. It is believed that this technique can be extended to the determination of the bioactive components of other Chinese herbal drugs. Further studies on this technique are in progress.

4. Acknowledgement

Financial support from the National Science Council, Republic of China, is gratefully acknowledged.

5. References

[1] H.Y. Hsu, Y.P. Chen, S.J. Sheu, C.H. Hsu, C.C. Chen and H.C. Chang, Chinese Materia Medica – a Concise Guide, Modern Drug Press, Taipei, 1984, pp. 120–121.
[2] M. Takido, M. Aimi, S. Takahashi, H. Yamauchi, H. Torii and S. Toi, Yakugaku Zasshi, 95 (1975) 108.
[3] S. Takagi, M. Yamaki and K. Inoue, Yakugaku Zasshi, 100 (1980) 1220.
[4] S. Takagi, M. Yamaki and K. Inoue, Yakugaku Zasshi, 101 (1981) 899.
[5] T. Tomimori, Y. Miyaichi and H. Kizu, Yakugaku Zasshi, 102 (1982) 388.
[6] T. Tomimori, Y. Miyaichi, Y. Imoto, H. Kizu and Y. Tanabe, Yakugaku Zasshi, 103 (1983) 607.
[7] T. Tomimori, Y. Miyaichi, Y. Imoto, H. Kizu and Y. Tanabe, Yakugaku Zasshi, 104 (1984) 524.
[8] T. Tomimori, Y. Miyaichi, Y. Imoto, H. Kizu and C. Suzuki, Yakugaku Zasshi, 104 (1984) 529.
[9] M. Kubo, Y. Kimura, T. Odani, T. Tani and K. Namba, Planta Med., 43 (1981) 194.
[10] M. Kubo, H. Masuda, M. Tanaka, Y. Kimura, H. Okuda, N. Higashino, T. Tani, K. Namba and S. Arichi, Chem. Pharm. Bull., 32 (1984) 2724.
[11] M. Liu and W. Gao, Yaowu Fenxi Zazhi, 2 (1982) 134; C.A., 97 (1982) 203289b.
[12] L. Yu, M. Liu and Y. Zhang, Yaowu Fenxi Zazhi, 3 (1983) 18; C.A., 99 (1983) 10922k.
[13] C. Yu, C. Li, Y. Xing, Y. Wang, H. Liu and C. Shen, Zhongguo Shouyi Zazhi, 12 (1986) 41; C.A., 106 (1987) 72993f.
[14] X. Zhang and L. Xu, Zhongcaoyao, 16 (1985) 216; C.A., 103 (1985) 59375z.
[15] E. Katsura and T. Yamagishi, Hokkaidoritsu Eisei Kenkyushoho, 32 (1982) 17; C.A., 101 (1984) 12273h.
[16] T. Tomomori, H. Jin, Y. Miyaichi, S. Toyofuku and T. Namba, Yakagaku Zasshi, 105 (1985) 154.
[17] Y. Takino, T. Miyahara, E. Arichi, S. Arichi, T. Hayashi and M. Karikura, Chem. Pharm. Bull., 35 (1987) 3494.
[18] S. Terabe, K. Otsuka, K. Ichikawa, A. Tsuchiya and T. Ando, Anal. Chem., 56 (1984) 111.
[19] S. Fujiwara and S. Honda, Anal. Chem., 59 (1987) 2773.
[20] C.P. Ong, H.K. Lee and S.F.Y. Li, J. Chromatogr., 542 (1991) 473.
[21] C.P. Ong, C.L. Ng, H.K. Lee and S.F.Y. Li, J. Chromatogr., 547 (1991) 419.
[22] I.K. Sakodinskaya, C. Desiderio, A. Nardi and S. Fanali, J. Chromatogr., 596 (1992) 95.
[23] Q.P. Dang, Z.P. Sun and D.K. Ling, J. Chromatogr., 603 (1992) 259.
[24] Y.M. Liu and S.J. Sheu, J. Chromatogr., 600 (1992) 370.
[25] Y.M. Liu and S.J. Sheu, J. Chromatogr., 623 (1992) 196.
[26] Y.M. Liu and S.J. Sheu, J. Chromatogr., 634 (1993) 329.
[27] Y.M. Liu and S.J. Sheu, J. Chromatogr., 637 (1993) 219.
[28] P.G. Pietta, P.L. Mauri, A. Rava and G. Sabbatini, J. Chromatogr., 549 (1991) 367.
[29] U. Seitz, P.J. Oefner, S. Nathakarnkitkool, M. Popp and G.K. Bonn, Electrophoresis, 13 (1992) 35.

ELSEVIER

Analytica Chimica Acta 288 (1994) 227–235

ANALYTICA CHIMICA ACTA

Enzyme amplified immunoassay for steroids in biosamples at low picomolar concentrations

Ulf Lövgren [a], Karin Kronkvist [b], Gillis Johansson [b], Lars-Erik Edholm *,[a]

[a] *Department of Bioanalytical Chemistry, Astra Draco AB, P.O. Box 34, S-221 00 Lund, Sweden*
[b] *Department of Analytical Chemistry, University of Lund, P.O. Box 124, S-221 00 Lund, Sweden*

(Received 12th July 1993; revised manuscript received 11th October 1993)

Abstract

A competitive enzyme amplified ELISA for steroids was developed using recycling of NADH/NAD^+ between the enzymes diaphorase and alcohol dehydrogenase. The substrate was generated from the steroid-bound enzyme label alkaline phosphatase, which dephosphorylated NADPH or $NADP^+$. Secondary antibodies were partially denatured and adsorbed to the microtitre plates to overcome the inhomogeneity of the plastic material. In the amplified ELISA reported here, amounts down to 1 femtomol per well of the steroid budesonide could be quantified with a relative standard deviation of 30%. Plasma samples were pretreated using a solid phase extraction and a subsequent column liquid chromatography fractionation. Concentrations in blood plasma could be quantified down to 8 pM (5 fmol per well) with a precision of better than 20%. Different detection principles for the alkaline phosphatase label were compared, and the proposed double amplification procedure was found to give a substantial increase in detectability of the enzyme conjugate compared to the conventional detection of *p*-nitrophenol.

Key words: Enzymatic methods; Immunoassay; Alkaline phosphatase; Steroids; Plasma

1. Introduction

Current pharmaceutical research requires very sensitive bioanalytical methods for determination of drugs and drug metabolites in the picomolar or subpicomolar range. This is mainly due to an increasing potency of many modern drugs and a trend towards the use of locally administered drugs [1]. Steroids constitute an important class of drugs and recent work on achieving low detection limits shows that although steroids can be determined in biosamples down to 100 pM with liquid chromatography–mass spectrometry [2], it is still very difficult to reach the desired low detection levels with this technique. Immunoassay, on the other hand, is one of the most powerful analytical techniques when both high sensitivity and high selectivity is required [3]. The selectivity of a direct application, without purification of the sample, may still not be sufficiently high in a matrix containing metabolites or high concentrations of endogenous substances with similar antigenic structure. Cross-reactions with the antibodies can be prevented or reduced by using a

* Corresponding author.

SSDI 0003-2670(93)E0605-7

pre-separation step prior to the immunoassay, for example column liquid chromatography. Other possible interferences from matrix components can also be minimized in this way.

Enzyme labels are attractive in immunoassays because of their ability to amplify the signal. Each turn-over will produce a product molecule which is detectable by itself or which can generate detectable species in a following, amplifying step. Peroxidase, alkaline phosphatase and β-galactosidase are the most commonly used enzyme labels. Horseradish peroxidase has a higher turn-over rate than the others and will thus provide a higher amplification. Alkaline phosphatase (AP) is a widely used enzyme label because of its generally very stable conjugates. It is easily conjugated to many antigens or antibodies and due to its ability to dephosphorylate a variety of different substrates, there are possibilities to utilize different detection techniques such as colorimetry [4], electrochemistry [5–7], fluorimetry [8] or chemiluminescence measurements [9]. Some of these detection techniques permit quantification of the generated product down to fmol levels. The attainable sensitivity will then depend on the affinity constant of the antibody [3].

The sensitivity of an enzyme immunoassay can be enhanced by increasing the number of enzyme molecules per analyte, using biotin–avidin complexes [10,11] or enzyme–anti-enzyme complexes [12], or by the use of enzyme amplification systems. Another signal amplification method in this field is the "catalyzed reporter deposition" (CARD) developed by Bobrow et al. [13].

Enzyme amplification of ELISA can be achieved by coupling of the primary enzyme system to a secondary one in a cascade [14,15], or by using substrate recycling where the product from the enzyme label is shuttled between two other enzymes producing a detectable product in each cycle [16]. The potential of detecting low amounts of enzyme label with the substrate recycling amplification technique in immunoassays has been shown to be very high [16,17], but reported applications for low-molecular-weight substances in real samples are very few.

This work will report on the potential of the amplified enzyme immunoassay for the drug budesonide in blood plasma. Budesonide is a synthetic glucocorticosteroid commonly used in the treatment of asthma and rhinitis and it is chosen as a model substance in the present study.

2. Experimental

2.1. Apparatus

All microtitre plate readings were performed with a Multiskan MCC/340 type 347 (Labsystems, Helsinki) equipped with a 492-nm filter, and the plates were washed with an Ultrawash II MA 56 (Dynatech Laboratories, West Sussex). The dispensing of reagents to the microtitre plates was carried out by a Multidrop type 831 automatic dispenser (Labsystems) and the samples were pipetted with a 8-channel Socorex pipette (Renens).

Evaluations of the immunoassay results were made with Multicalc, a computer program for immunoassay measurements (Pharmacia-Wallac, Turku).

The electrochemical measurements were performed in a flow-injection system consisting of an LKB 2150 LC pump (Pharmacia LKB, Uppsala) and an electric six-port injection valve (Valco, Houston, TX) with a loop volume of 25 μl. The detector was a thin layer, BAS CC-4, flow-through cell (Bioanalytical Systems, West Lafayette, IN) with a glassy carbon working electrode, an Ag/AgCl (3 M NaCl) reference electrode and a stainless steel auxiliary electrode. An Access-Chrom chromatography computer system v. 1.8. (Perkin-Elmer Nelson Systems, Cupertino, CA) was used for integration of the output signals from the BAS LC-4 potentiostat.

The liquid chromatography system for the sample pretreatment consisted of a Waters M510 LC pump, a Waters WISP 710B autosampler, a Waters M440 UV detector (Millipore, Milford, MA) and a Gilson FC 203B fraction collector (Gilson Medical Electronics, Middleton, WI). A column rinsing gradient was performed by injecting 500 μl ethanol from a six-port valve (Valco), where the loop was filled by a FMI RP-G150 lab pump (Fluid Metering, Oyster Bay, NY).

2.2. Materials

Budesonide [11β,21-dihydroxy-16α,17α-(22*R*,*S*)-propylmethylenedioxypregna-1,4-diene-3,20-dione] and budesonide-21-hemisuccinate were synthesized by Astra Draco. Antiserum (from sheep) raised towards budesonide-21-hemisuccinate was obtained from the University of Surrey (UK) [18]. Anti-sheep IgG (from donkey) was obtained from Sigma (St. Louis, MO) and partially denatured by lowering the pH value to 2.5 for 10 min [19].

p-Aminophenyl phosphate was synthesized by Astra Draco according to De Riemer and Meares [20]. AMPAK enzyme amplification kit containing a substrate solution with NADPH, an amplifier solution with the enzymes alcohol dehydrogenase E.C. 1.1.1.1 and diaphorase E.C.1.6.4.3, including the substrates ethanol and INT-violet, was from DAKO Diagnostics (Cambridgeshire). *p*-Nitrophenyl phosphate substrate and buffer solution was purchased as a phosphatase substrate kit from Pierce (Rockford, IL). The Hydropore-EP isolate cartridge from Rainin Instruments (Woburn, MA) was used for the immobilization of budesonide in the affinity purification of antibodies. Alkaline phosphatase (AP) E.C. 3.1.3.1 (from calf intestine), Tween 20, and bovine serum albumin (BSA) fraction V, were purchased from Sigma (St. Louis, MO). All other chemicals were of p.a. grade. Maxisorp microtitre plates were purchased from Nunc (Roskilde). Centricon ultrafiltration tubes were obtained from Amicon (Grace, Beverly, MA) and Bond-Elut columns came from Analytichem (Harbor City, CA).

2.3. Preparation of budesonide-alkaline phosphatase conjugate

1000 units of AP were coupled to 0.22 mg budesonide-21-hemisuccinate at the carboxylic group of the steroid derivative, according to the mixed anhydride method [7,21]. After conjugation the enzyme activity was determined spectrophotometrically at 310 nm with *p*-aminophenyl phosphate as substrate. It was found that 56% of the original enzyme activity was retained.

2.4. Purification of the antisera

Isolation of the IgG fraction from budesonide antiserum

1.5 ml of antiserum and 1.5 ml of 0.15 M NaCl was mixed and cooled. 2.2 ml of cold, saturated ammonium sulphate solution was added and the solution was incubated on a rocker for 2 h at +4°C. After centrifugation the supernatant was discarded and the sediment was washed twice with 1.5 ml of a 1.68 M ammonium sulphate solution. The solid residue was dissolved in 6 ml of water and ultrafiltered in a Centricon tube, MW cut off 30 000 D. Finally, the residue was diluted to 7.5 ml in 0.1 M sodium phosphate buffer, pH 7.3.

The microtitre plates for the comparison of different detection principles were coated with primary antibodies, which were further purified by using a protein G column (MAb-Trap G, Pharmacia) according to the manufacturers instructions.

Affinity purification of the steroid-selective antibody fraction

Budesonide was immobilized in the Hydropore column using BSA as a spacer molecule. 12 mg of budesonide-21-hemisuccinate was coupled to BSA using the mixed anhydride method, similar to the enzyme conjugation procedure [7]. After ultrafiltration of the budesonide–BSA conjugate with 0.05% Tween 20 in the buffer, and diluting it with 1 M potassium phosphate buffer, pH 7.0, a volume of 250 μl was injected into the Hydropore column (preactivated with reactive epoxy groups) according to the description from the manufacturer.

A buffer consisting of 6.7 mM citric acid, 6.7 mM orthophosphoric acid, 11.4 mM boric acid, 68.6 mM sodium hydroxide and 0.05% Tween 20 was used as mobile phase in the affinity chromatography system. Two LC pumps were connected for the generation of a step gradient, where pump A delivered the mobile phase adjusted to pH 7.0 and pump B delivered the mobile phase adjusted to pH 2.2.

The IgG fraction was, after the "salting-out" procedure, diluted to 500 μl in the mobile phase

(pH 7.0) and a volume of 250 μl was injected into the flow. At the time of the injection the flow was 0.05 ml/min using only pump A, and after 20 min the flow was increased to 0.25 ml/min in order to wash out IgG other than anti-budesonide antibodies. A step gradient was generated by pumping 0.05 ml/min with pump A and 0.20 ml/min with pump B, resulting in a pH of 2.5. After another 6 min the pH was decreased even further to 2.2, using only pump B. The high affinity anti-budesonide antibody fraction eluted in this last step was collected and an equal volume of 0.1 M sodium phosphate buffer, pH 7.3 was added to neutralize the solution. After ultrafiltering (Centricon tubes, mol.wt. cut off 30 000 D) the fraction was diluted with 10 ml of 0.1 M sodium phosphate buffer, pH 7.3 containing 0.19 mg/l merthiolate to inhibit bacterial growth.

2.5. Procedure

Sample pretreatment

Plasma samples were spiked in the 7.9–99 pM range by adding budesonide to human blank plasma. The samples were pretreated according to the scheme in Fig. 1. After centrifugation they were purified using a solid-phase extraction with 500 mg C_{18} Bond-Elut columns. Before addition of the plasma sample (2.5 ml) the columns had been treated once with methanol and twice with deionized water. The columns were rinsed with 5 ml portions of water, with 5 mM ammonium acetate buffer, pH 7.0 containing 35% methanol and with water again. Phase reversal was made with 5 ml heptane and budesonide was eluted in 5 ml 35% ethylacetate in heptane. These fractions were dried to completeness in a Savant "Speedvac concentrator" (Savant, Farmingdale, NY). The samples were dissolved in 350 μl of 0.04 mM formic acid containing 25% ethanol, and 300 μl was injected into an LC system with a 50 × 2.1 mm column packed with 3 μm C_{18} Nucleosil (Machery-Nagel, Düren), thermostated to 40°C, and a Guard-Pak Resolve silica column (Waters Millipore). Since the samples were dissolved in a buffer containing less ethanol (25%) than the mobile phase (35%) a relatively large sample volume (300 μl) could be injected due to peak compression [22]. Fractions of 1 ml were collected at a flow rate of 0.5 ml/min and the fraction containing budesonide was evaporated to dryness and redissolved in 180 μl incubation buffer (0.05 M tris(hydroxymethyl)aminomethane, pH 7.3 with 0.1% BSA, 0.05% Tween 20 and 0.15 M sodium chloride). After each chromatogram 500 μl ethanol was injected from a separate 6-port injection valve in order to rinse the column.

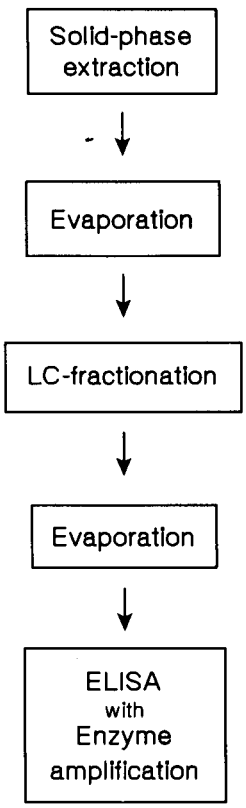

Fig. 1. Scheme of the sample pretreatment and detection.

2.6. ELISA detection

The budesonide was quantified in the competitive enzyme amplified immunoassay shown in Fig. 2. Microtitre plates were coated overnight at room temperature with 75 μl of partially denatured anti-sheep IgG from donkey (10 μg/ml) in 0.05 M sodium carbonate buffer, pH 9.6. The wells were blocked with 300 μl 2% (w/v) BSA and

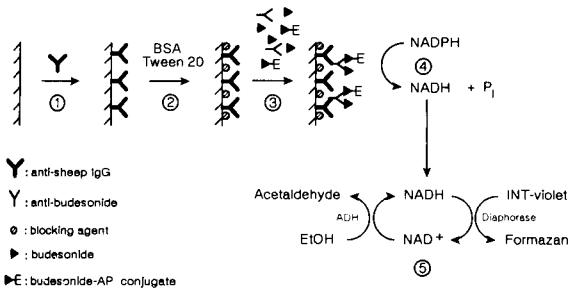

Fig. 2. The ELISA procedure involving (1) coating the wells with secondary antibodies, anti-sheep IgG, (2) blocking with BSA and Tween 20, (3) incubation with sample, anti-budesonide antibodies and enzyme conjugate, (4) incubation with substrate for the labelling enzyme and (5) incubation with amplification enzymes and substrate recycling.

0.05% (v/v) Tween 20 in 0.05 M sodium carbonate buffer, pH 9.6 and kept in room temperature for 2–3 h. Subsequently the wells were washed six times with 0.05 M Tris–HNO_3 buffer, pH 7.3, with 0.05% Tween 20 and 0.15 M sodium chloride. 60 μl of the enzyme-conjugated steroid solution (1:8000 in incubation buffer) and 60 μl of the analyte solution (from the pretreatment step) were added to each well, followed by the addition of 30 μl of affinity-purified anti-budesonide antibody solution (1:175 in incubation buffer). The microtitre plates were incubated overnight at room temperature and then washed four times with the AMPAK wash buffer. The magnesium ion concentration in the AMPAK substrate solution, containing NADPH, was increased by adding $MgCl_2$ corresponding to 1 mM. 100 μl of this solution was added to each well and the plates were incubated for 90 min with slight swivelling at room temperature and in the dark. Thereafter 100 μl of amplifier solution was added to each well and the generated color of formazan was measured in the plate reader at 492 nm after 20 min.

2.7. Comparison of different detection systems

An alternative assay for alkaline phosphatase was developed. Microtitre plates were coated overnight at room temperature with 75 μl anti-budesonide antibody, purified on a protein G column and diluted (1:50) in 0.05 M sodium carbonate buffer, pH 9.6, blocked and washed as described above. 90 μl of incubation buffer was added to each well followed by addition of different dilutions of the enzyme conjugate to each microtitre plate column in the order 1:200, 1:400, 1:800, ..., 1:204 800 and a blank without enzyme conjugate. Each microtitre plate column received a constant enzyme conjugate dilution, yielding eight replicates. The microtitre plates were incubated overnight at room temperature and then washed four times with the AMPAK wash buffer. Evaluation was performed using one of the following detection systems.

Enzyme amplification

100 μl of the AMPAK substrate solution was added to each well and the plate was incubated for 20 or 180 min with slight swivelling at room temperature and in the dark. When the incubation time was longer than 20 min the $MgCl_2$ concentration in the AMPAK solution was increased with 1 mM, according to the manufacturers instructions. Thereafter 100 μl of amplifier solution was added to each well and the generated color of formazan was measured in the plate reader at 492 nm.

p-Nitrophenyl phosphate as enzyme substrate

The enzyme substrate solution was prepared according to the description given in the Phosphatase Substrate kit (10 mg to 20 ml diethanolamine substrate buffer). 200 μl of this solution was added to each well and the plate was incubated with slight swivelling at room temperature and in the dark. The *p*-nitrophenol was measured by the plate reader at 405 nm after different incubation times.

p-Aminophenyl phosphate as enzyme substrate and amperometric detection in a flow system

150 μl of a freshly prepared and deaerated enzyme substrate solution consisting of 2 mM *p*-aminophenyl phosphate (PAPP) in 0.05 M Tris buffer, pH 7.3, with 0.1% BSA, 0.15 M NaCl and 0.05% Tween 20, was added to each well and the plate was incubated for 60 min in the dark. The enzyme reaction was stopped by transferring 100

μl from each well to another plate with 40 μl 0.1 M sodium phosphate buffer, pH 8.0 per well. *p*-Aminophenol, the reaction product, was determined amperometrically at a glassy carbon electrode at 250 mV versus Ag/AgCl, by injections of 25 μl aliquots into the flow system. The carrier solution in the flow system was the same as for the samples injected in order to minimize non-Faradaic currents. A description of the flow injection system has been given previously [7].

3. Results and Discussion

3.1. Immunoassay

Insufficient reproducibility has often limited the application of immunochemical methods of analysis and attempts were therefore made to improve a previously described procedure [7]. In competitive immunoassay the primary antibodies are not in stoichiometric excess with respect to the antigens. It is therefore essential to have the same amount of antibodies present in every sample. Due to inhomogeneity in the microtitre plate material, the adsorption of antibodies differs from well to well and the precision is thus decreased [23]. This can be circumvented by binding the antibodies covalently to the solid support material [24,25] or by coating the support with secondary antibodies or protein A or G, in great excess [26]. This procedure gives a more homogenous solid phase resulting in a more uniform binding of the primary antibody. The orientation of the primary antibodies is also enhanced, so that the antigenic sites are directed out in the solution [26]. The same pre-coated plates can be used for different analytes as long as the primary antibodies originate from the same animal species. In this work the secondary antibodies, anti-sheep IgG, were partially denatured in order to further improve the orientation of the antibodies. This procedure is also thought to increase the adsorption of the antibodies to the solid phase material [19]. Because of the small fraction of specific anti-budesonide in the antiserum obtained, an affinity purification had to take place prior to the assay. The fraction last eluted from the affinity column was used in the ELISA.

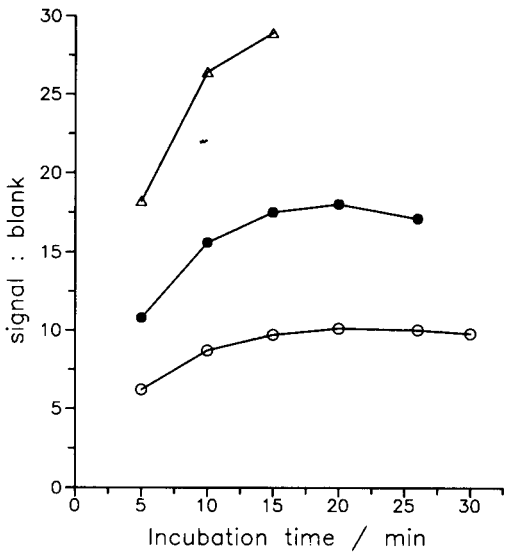

Fig. 3. The signal to blank ratio plotted against the substrate recycling time for different dilutions of enzyme conjugate (△) 1:400, (●) 1:800 and (○) 1:1600.

The detection potential of the assay can be varied extensively by changing the reaction time for the enzyme label. After addition of amplifier solution, the alkaline phosphatase was inhibited and no more NADH was produced. On the other hand, variation of the amplification time has only small influence on the detectability of the enzyme label. The amplification recycling step was optimized with respect to the substrate recycling time. It can be seen in Fig. 3 that 20 min seemed to be optimal, independent of the enzyme conjugate dilution. A further increase in incubation time results in higher absorbance values but does not increase the signal to blank ratio, due to production of formazan in the absence of enzyme label.

A standard curve for budesonide in pure buffer solution is shown in Fig. 4. Amounts down to about 1 fmol per well can be quantified with a relative standard deviation of 30% ($n = 8$), see Table 1. Due to the amplification system, lower amounts of the enzyme conjugate can be used to obtain satisfactory signal to blank ratio. This fact combined with the affinity purification of the anti-budesonide antibodies and the use of mi-

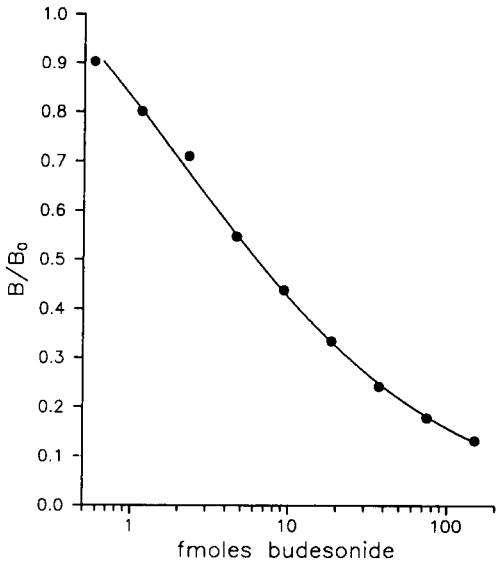

Fig. 4. Standard curve for budesonide in pure buffer solutions using enzyme amplification (90+20 min) and spectrophotometric detection. Each value is a mean of eight determinations.

crotitre plates coated with partially denatured secondary antibodies result in a steep calibration curve. The sensitivity has been increased about 4 times compared to a previously reported ELISA for budesonide with amperometric detection of *p*-aminophenol [7].

3.2. Plasma samples

When working with very low concentrations of analyte, picomolar or even lower, the selectivity of the antibodies towards the antigen is often insufficient. Interferences from cross-reacting substances, mainly endogenous steroids and drug metabolites with similar antigenic structure, can be expected and the sample must be cleaned up before it enters the ELISA. The solid phase extraction removed much of the interfering matrix components as well as some polar steroid metabolites [7,27], and the column liquid chromatography step was used to separate budesonide from other cross-reacting steroids. The selectivity and other characteristics of the chromatography system has been described previously [7].

Table 1
Relative standard deviation (RSD) of the ELISA using pure buffer solutions. Each value is calculated from eight determinations

Amount budesonide (fmol per well)	R.S.D. (%) B/B_0	R.S.D. (%) Conc.
0.6	7.6	35
1.2	7.2	29
2.3	6.9	25
4.7	6.4	20
9.4	5.4	15.8
18.8	4.9	12.5
38	5.0	12.8
75	7.4	14.3
150	5.1	10.5

Table 2
RSD of the complete ELISA procedure for spiked plasma samples. Six intra-assay samples, each analysed in duplicate

Real conc. (pM)	Apparent conc. (pM)	R.S.D. (%)
7.9	8.7	18.1
24.4	22.2	7.8
99.0	94.2	12.8

Budesonide in spiked human plasma could be quantified down to about 8 pM (5 fmol per well) with a precision better than 20%, expressed as intra-assay variation ($n = 6$), see Table 2. It was previously observed that the additional steps in the sample pretreatment procedure resulted in an increase of the relative standard deviation [7]. Special attention to the choice of test tubes and pre-washing of the test tubes used for the fraction collection improved the precision for plasma samples so that it became of the same size as for pure solutions.

3.3. Comparison of different detection principles

Alkaline phosphatase is an enzyme that is able to dephosphorylate a variety of different substrates and different detection techniques can be used to quantify the label. When designing a highly sensitive competitive ELISA, the amount of enzyme conjugate should be as low as possible but still enough to give sufficiently high signal to blank ratio. The signal to blank ratio was studied for varying enzyme conjugate dilutions as an ex-

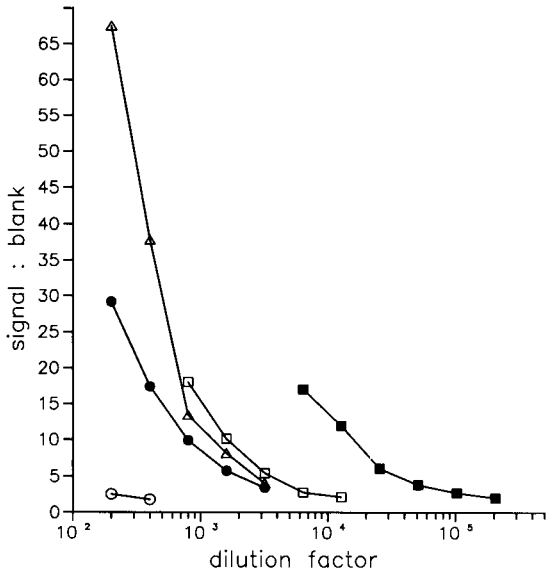

Fig. 5. Comparison of the potential sensitivity of different detection principles. Signal to blank ratios plotted versus the enzyme conjugate dilution factor. Spectrophotometric detection of *p*-nitrophenol at 405 nm with (○) 1 h and (●) 24 h substrate incubation time, (△) electrochemical detection of *p*-aminophenol in a flow-injection system, and spectrophotometric detection of formazan, using the AMPAK kit, after (□) 20+20 min and (■) 180+20 min incubation time.

pression for the sensitivity potential of the different techniques. A plot of the signal obtained against the amount of conjugate gave approximately a linear relationship over the studied range, except for the 1:200 dilution where a deviation of about 20% was observed due to saturation effects of the antibody. Three different techniques were compared; the enzyme amplification technique, spectrophotometric detection of *p*-nitrophenol and amperometric detection of *p*-aminophenol, see Fig. 5.

The *p*-nitrophenyl phosphate system, which is the most commonly used detection system for alkaline phosphatase in ELISA, showed very low signal to blank ratios with 1 h substrate incubation time. An increase of the incubation time to 24 h was necessary to obtain satisfactory values.

Amperometric detection of *p*-aminophenol after 1 h incubation increased the detectability of the enzyme conjugate further. This detection principle is known to be very sensitive with a large dynamic range [6]. A much larger linear range is obtained using electrochemical detection compared to spectrophotometric detection, where the upper value is limited to an absorbance of ca. 2. This may be very useful in non-competitive assays, but in competitive assays like the one reported here the analytical range is limited by the characteristics of the calibration curve.

The enzyme amplification technique gives lower detection limits than the methods discussed above, already at a total incubation time of 40 min (20 + 20). A prolongation to 200 min (180 + 20) resulted in a further, nearly ten-fold, improvement in detection limit. Compared to the *p*-nitrophenyl phosphate system (24 h) an approximately twenty-fold improvement in detectability and a reduction of incubation time to one seventh was achieved.

With both the enzyme amplification and the amperometric detection techniques the relative standard deviation was 4–6% ($n = 8$), within each plate column. The measurements with the *p*-nitrophenyl phosphate system gave in this study a better relative standard deviation, 2–3% ($n = 8$). If the better precision was significant for this technique or due to other factors, such as larger amounts of conjugate per well and differences in experimental conditions was not fully evaluated.

4. Conclusions

Enzyme amplification is a useful technique to enhance the sensitivity of an ELISA. With substrate recirculation it was possible to quantitate very low amounts of alkaline phosphatase conjugate. Compared to the conventional *p*-nitrophenyl phosphate system, a twenty-fold further dilution of the enzyme conjugate could be used with a satisfactory signal to blank ratio. Together with other improvements of the immunoassay, such as affinity purification of the primary antibodies and coating of wells with partially denatured secondary antibodies, it was possible to quantify budesonide down to 1 fmol per well with a relative standard deviation better than 30% ($n = 8$, single determinations).

After coupling of the ELISA with a preseparation system, consisting of a solid phase extraction and a column liquid chromatography fractionation, budesonide could be quantified down to 8 pM in blood plasma with a precision of better than 20% ($n = 6$). The coupling made it possible to use large sample volumes without any noticeable interferences from matrix components and cross-reacting endogenous steroids.

The performance of the proposed method for determination of budesonide should allow for pharmacokinetic studies at low picomolar concentrations. It is anticipated that the technique developed in this work also should be useful in assays of other types of steroids, provided that antibodies with sufficiently high affinity constants can be raised towards them. The performance obtained with the enzyme amplified immunoassay at low picomolar concentrations is similar to that which can be obtained with other analytical techniques but at concentrations at least ten times lower.

5. Acknowledgements

Financial support from the Swedish Natural Science Research Council and Astra Draco AB is gratefully acknowledged.

6. References

[1] P.J. Barnes, New Engl. J. Med., 321 (1989) 1517.
[2] C. Lindberg, A. Blomqvist and J. Paulson, Biol. Mass Spectrom., 21 (1992) 525.
[3] R.P. Ekins, in W.P. Collins (Ed.), Alternative Immunoassays, Wiley, New York, 1985, p. 219.
[4] B. Porstmann and T. Porstmann, in T.T. Ngo (Ed.), Non-isotopic Immunoassay, Plenum Press, New York, 1988, p. 57.
[5] K.R. Wehmeyer, H.B. Halsall and W.R. Heineman, Clin. Chem., 31 (1985) 1546.
[6] H.T. Tang, C.E. Lunte, H.B. Halsall and W.R. Heineman, Anal. Chim. Acta, 214 (1988) 187.
[7] K. Kronkvist, U. Lövgren, L.-E. Edholm and G. Johansson, J. Pharm. Biomed. Anal., 11 (1993) 59.
[8] A. Shalev, A.H. Greenberg and P.J. McAlpine, J. Immunol. Methods, 38 (1980) 125.
[9] I. Bronstein, B. Edwards and J.C. Voyta, J. Bioluminescence Chemiluminescence, 4 (1989) 99.
[10] H.H.D. Meyer, H. Sauerwein and B.M. Mutayoba, J. Steroid Biochem., 35 (1990) 263.
[11] S. de Lauzon, J. El Jabri, B. Desfosses and N. Cittanova, J. Immunoassay, 10 (1989) 339.
[12] A.W. Wognum, P.M. Lansdorp, A.C. Eaves and G. Krystal, Blood, 74 (1989) 622.
[13] M.N. Bobrow, T.D. Harris, K.J. Shaughnessy and G.J. Litt, J. Immunol. Methods, 125 (1989) 279.
[14] D.M. Obzansky, B.R. Rabin, D.M. Simons, S.Y. Tseng, D.M. Severino, H. Eggelte, M. Fisher, S. Harbron, R.W. Stout and M.J. Di Paolo, Clin. Chem., 37 (1991) 1513.
[15] A. Seki, E. Tamiya and I. Karube, Anal. Chim. Acta, 232 (1990) 267.
[16] C.J. Stanley, A. Johannsson and C.H. Self, J. Immunol. Methods, 83 (1985) 89.
[17] A. Johannsson, D.H. Ellis, D.L. Bates, A.M. Plumb and C.J. Stanley, J. Immunol. Methods, 87 (1986) 7.
[18] G.W. Aherne, P. Littleton, A. Thalen and V. Marks, J. Steroid Biochem., 17 (1982) 559.
[19] J.D. Conradie, M. Govender and L. Visser, J. Immunol. Methods, 59 (1983) 289.
[20] L.H. De Riemer and C.F. Meares, Biocemistry, 20 (1981) 1606.
[21] V. Marks, M.J. O'Sullivan, M.N. Al-Bassan and J.W. Bridges, in S.B. Pal (Ed.), Enzyme Linked Immunoassay of Hormones and Drugs, Walter de Gruyter, Berlin, 1978, p. 419.
[22] L-E. Edholm and L. Ögren, in I. Wainer (Ed.), Liquid Chromatography in Pharmaceutical Development, Aster, Springfield, OR, 1986, p. 345.
[23] L.A. Cantarero, J.E. Butler and J.W. Osborne, Anal. Biochem., 105 (1980) 375.
[24] J.D. Place and H.R. Schroeder, J. Immunol. Methods, 48 (1982) 251.
[25] K.L. Brillhart and N.T. Ngo, J. Immunol. Methods, 144 (1991) 19.
[26] W. Hubl, G. Daxenbichler, D. Meißner and H.J. Thiele, Clin. Chem., 34 (1988) 2521.
[27] S. Edsbäcker, P. Andersson, C. Lindberg, J. Paulson, Å. Ryrfeldt and A. Thalen, Drug Metab. Dispos., 15 (1987) 403.

ELSEVIER

Analytica Chimica Acta 288 (1994) 237–245

ANALYTICA CHIMICA ACTA

Flow-injection extraction without phase separation based on dual-wavelength spectrophotometry

Hanghui Liu, Purnendu K. Dasgupta *

Department of Chemistry and Biochemistry, Texas Tech University, Lubbock, TX 79409-1061, USA

(Received 31st August 1993; revised manuscript received 1st November 1993)

Abstract

A new detection technique for flow-injection extraction is introduced. The absorbance is read radially, on the same PTFE tube that constitutes the reaction coil, near its distal terminus. With an effective illuminated detector volume of ~ 60 nl, the optical aperture is much smaller than the segment length, enabling the detector to reliably measure signals for each phase. The detector used is a light emitting diode (LED) based dual-wavelength photometric system utilizing personal computer (PC) based data acquisition and processing. One non-specific wavelength is used to recognize the phases and the other wavelength monitors the analyte concentration. Accurate and reliable phase recognition is achievable with conventional segmentors and peristaltic pumping. Applied to the determination of anionic surfactants by ion-pairing with methylene blue (MB) and extraction into chloroform, a linear response is observed with a limit of detection (LOD) of 0.03 ppm C-12 linear alkylbenzene sulfonate (LAS) for a 65 μl injected sample, compared to an LOD of 0.025 ppm quoted for the standard manual method attainable by subjecting several hundred ml of the sample to extraction.

Key words: Flow injection; Spectrophotometry; Extraction

1. Introduction

Conventional flow-injection extraction (FIE) procedures include mixing and separation of two immiscible liquids. Typically, an aqueous sample is injected into an aqueous carrier stream to which an organic phase is continuously added. The segmented stream then flows through a coil in which extraction occurs. Generally, the organic phase is now separated from the aqueous phase and further led through a flow cell for measurement. One of the most critical aspects of the method is the phase separation [1], with respect to reliability, stability and overall dispersion of the sample zone. Consequently, many refinements on phase separation of solvent extraction in flow systems have been made and some ingenious approaches introduced since FIE systems were first described by Karlberg and Thelander [2] and Bergamin F° et al. [3].

General strategies of performing solvent extraction in continuous flow systems were reviewed in 1989 [4], there had been few fundamen-

* Corresponding author.

SSDI 0003-2670(93)E0621-D

tal developments since. Some salient examples related to performing FIE without phase separation are as follows. Kina and Ishibashi [5] introduced a system in which an analyte that is practically non-fluorescent in aqueous phase but becomes strongly fluorescent in the organic phase could be extracted and fluorometrically measured without phase separation. Unfortunately, such techniques are not generally applicable. Canete et al. [6] placed the detector within the loop of an injection valve and the extraction solvent is loaded into the injection loop and the detector cell. The valve is then switched to inject position and a bi-directional pump moves the segment back and forth without quite drawing the aqueous phase into the cell. Multiple sequential signals generated can be used to provide quantitation. Lei et al. [7] injected the extractant phase into a flowing stream of the sample, to which reagents, if necessary, have been added. The extractant segment, borne by the sample stream, flows through an extraction conduit into the loop of a zone sampling valve. When the loop of this valve is completely full of the extractant phase, the contents of the loop are injected into a miscible carrier where further chemistry may be carried out before detection. The major advantage of the system is its high reliability for phase separation [4,8]. Sahlestrom and Karlberg [9] described a FIE system in which the organic and aqueous streams are separated by a membrane across which the analyte is transferred. The segmentation and the separation step are avoided in the system because the unsegmented recipient stream is led directly into the detector flow cell. However, extraction efficiency is low due to the restricted contact area and time, and long term reliability of the system is limited and is plagued by membrane failure.

Unless some chemistry must be carried out after extraction, phase separation is hardly essential to successfully perform FIE. In the following, we limit our discussion to systems using optical absorption detection, by far the mainstay of FIE. The use of detection cells of volumes of at least several μl (typically too large to be filled completely with a single organic segment of optimum size for FIE), strip-chart recorders with inadequate response speed and manual processing of data greatly deter from performing FIE without phase separation; indeed it is virtually impossible to perform on-line detection and accurately determine the absorbance in each phase. Bold attempts have, nevertheless, been made. Gluck [10] reports that such attempts fail because $\cdots$ the segment length was shorter than the length of the optical aperture and there was never a time when the response would correspond to one phase $\cdots$. His further attempts to keep the segment length longer than the optical aperture by further reducing the diameter of the 1 mm i.d. quartz tube used as the flow cell were unsuccessful due to the formation of adherent films on the wall.

Recently, considerably more sophisticated FIE systems have evolved. Thommen et al. [11] described an arrangement with a capillary flow cell and computer based data acquisition. The small illuminated volume of the detector cell (< 1 μl) and the ability to use measurement frequencies up to 200 Hz made it possible to directly measure each segment. Alternately operated stepper-motor driven syringe pumps are used to achieve uniform segmentation that allows subsequent software based digital phase separation. Individual extractant segments are of 14 μl volume and pass through a tubular glass cell of 0.8 mm i.d., the radial path being used for detection. Individual segments are identified through the location of the spikes that correspond to the phase interfaces. The approach is successful, with obvious advantages. Nevertheless, the reported LOD is > 30 times higher than conventional FIE systems. Additionally, it is difficult to discern whether a given segment is the organic or the aqueous phase if the refractive indices are close and the sample concentration is low. Further, as we shall establish for the extraction system of this paper, the location of the spikes cannot always precisely indicate the positions of the head or the tail of a segment.

An alternative to relying on the spikes to discern segment locations is to make segmentation and flow rates so uniform through the use of high quality pumps and segmentors that an extremely high degree of reproducibility is attained for all aspects of the system. In this vein, Kuban [12]

considered that ··· with adequate control over the segmentation it may even be possible to eliminate phase separation altogether if the (segmentation) repeatability is good enough to allow precise timing of measurement intervals ···. Kuban et al. [12–14] carried out a series of exemplary investigations and obtained very repeatable results. However, it is almost impossible to attain and maintain this degree of repeatability with peristaltic pumps and conventional segmentors. We have felt therefore a persistent need for an affordable (e.g., peristaltic pump based) and reliable FIE system that does not need phase separation.

In this paper, a new FIE system is introduced. The absorbance is read radially, on the same PTFE tube that constitutes the reaction coil, near its distal terminus. With an effective illuminated detector volume of ~ 60 nl, the optical aperture is much smaller than the segment length, enabling the detector to reliably measure signals for each phase. The detector used is a LED-based dual-wavelength photometric system utilizing PC-based data acquisition and processing. One non-specific wavelength is used to recognize the phases and the other wavelength monitors the analyte concentration. Accurate and reliable phase recognition is achievable with conventional segmentors and peristaltic pumping.

2. Experimental

2.1. Reagents

All chemicals were of analytical-reagent grade except as specified and distilled deionized water was used throughout.

MB reagent: MB (100 mg, Baker Analyzed) was dissolved in 100 ml water. A 60 ml aliquot was transferred to a 1000 ml flask and 500 ml water, 41 ml 3 M H_2SO_4 and 50 g $NaH_2PO_4 \cdot H_2O$ were added. After shaking to ensure that dissolution was complete, it was made up to 1000 ml. Stock C12 LAS solution (1 mg/ml): C-12 LAS (56% by weight) and sodium hexadecane sulfonate was obtained as a gift (courtesy S. Dubey, Shell Development Company, Westhollow Research Center, Houston, TX). Other surfactants mentioned were also obtained from the same source. To the appropriately diluted solution, 1% (v/v) formalin was added to prevent microbial degradation. Spectrophotometric grade chloroform was used as the extractant.

2.2. Apparatus

The FIE system for the determination of methylene blue active substances (MBAS) such as anionic surfactants like LAS is shown schematically in Fig. 1. A peristaltic pump (Minipuls-2, 4-channel head, 10 rollers, Gilson International) is used for pumping. An electropneumatically actuated 6-port loop type rotary PTFE valve (type 5701P, Rheodyne, Cotati, CA) is used for sample injection. The water carrier stream merges with the MB reagent and following a mixing coil, the stream enters the segmentor, a common miniature barbed tee made from polypropylene (1/16 in., Ark-Plas, Flippin, AR). Chloroform is pumped by the displacement bottle technique into the tee. From the replacement bottle, either water or chloroform output can be chosen by a 3-way valve, making startup or shutdown and cleaning of the flow system convenient. The flow cell design is illustrated in Fig. 2. One integral piece of 0.38 mm i.d. PTFE tubing is used from the segmentor to the waste and it passes through the detector housing to constitute the flow cell. Thus, intact organic segments, critical to the successful performance of the system, can be maintained throughout. Incident light is brought into the cell by one leg of a bifurcated glass fiber optic bundle

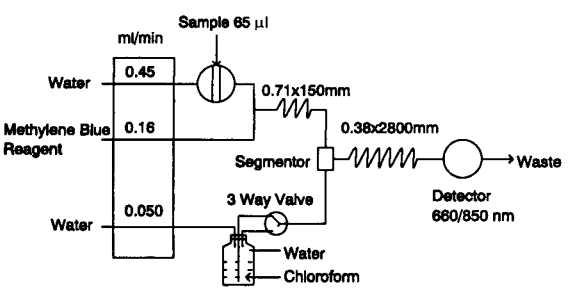

Fig. 1. Schematic flow diagram for the determination of methylene blue active substance.

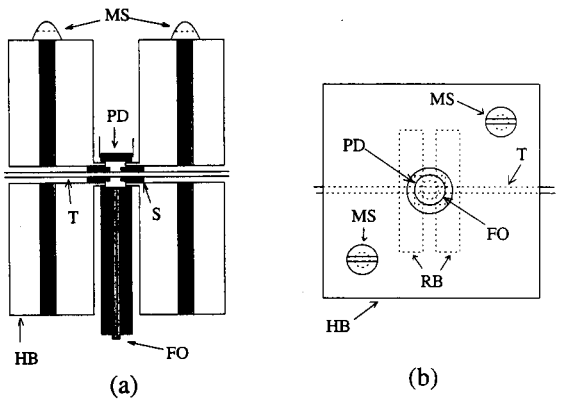

Fig. 2. (a) Vertical and (b) horizontal cross sectional views of the flow cell. MS: machine screws holding aluminum holding blocks HB, T: PTFE tube, PD: photodiode, S: slits composed of razor blades RB, FO: fiber optic.

(bundle diameter 1 mm). A pair of razor blades define the optical slit width, ~ 500 μm, resulting in an illuminated volume of ~ 60 nl. Under the standard operating conditions shown in Fig. 1, individual organic segments are about 1 cm in length and 1 μl in volume; hence, the cell is discriminating enough to detect each phase. When measured with a blue dye such as bromthymol blue that does not transfer to the organic phase when injected as sample, the dispersion coefficient of the manifold (for a 65 μl injected sample and for the aqueous phase only) is 1.8. Under actual operating conditions, the concentration of sample in the organic phase is much higher than the aqueous concentration injected, the exact value is governed by the ratio of the total aqueous phase flow rate to the organic phase flow rate and the system dispersion, discussed later.

The scheme for performing LED-based dual wavelength absorbance measurement is shown in Fig. 3. This is a PC-based version of one of the detection strategies described by Dasgupta et al. [15]. The use of a PC permits a much simpler external electronic interface; further processing of the raw information, such as the recognition of the organic segments and calculation of the peak area etc., can be automatically performed immediately after data collection. The digital outputs of the DAS-16G data acquisition board (Keithley/Metrabyte, Taunton, MA) are used to turn on LED1 (type A1012, peak λ 660 nm, Electronic Goldmine, Phoenix, AZ) and LED2 (type DN 305, peak λ 850 nm, Stanley Electric, Tokyo) through a pair of 2N3565 transistors alternately (ca. 100 Hz). Through bifurcated optical fibers (BFO, type E624, Dolan-Jenner Industries, Lawrence, MA, two of these are coupled end-to-end at the common legs by a connecting sleeve C) one portion of the emitted light is led to the reference photodiode PDR, the other portion is led to the flow cell FC and thence the transmitted light is detected by the signal photodiode PDS (both photodiodes type S2007, Electronic Goldmine). The outputs of the operational amplifiers OPA2107 AP (Burr-Brown, Tucson, AZ) are digitized by the 12 bit A/D converter and all the conversion results obtained (ca. 100 individual data points at 50 kHz A/D conversion rate) are averaged during the period each LED is turned on. The log ratio of the averaged reference output to the averaged signal output, namely the absorbance, is calculated and stored in memory. The function of further software to process this initial data is described in the next section. The software, coupled with an assembly language rou-

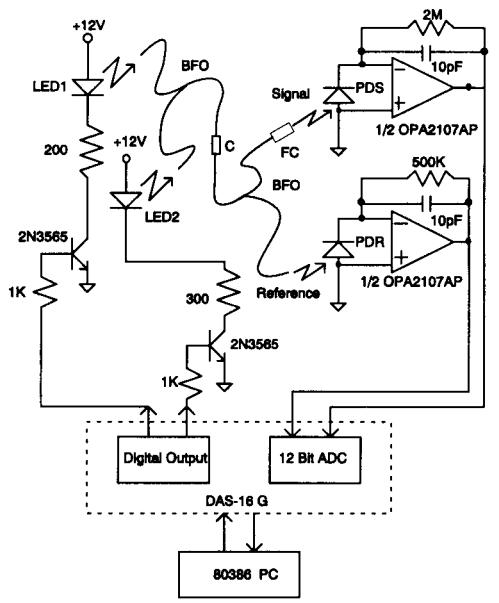

Fig. 3. LED-based dual wavelength photodetector. See text for description.

tine for data acquisition and LED on-off control, is written in C and is available free from the authors for non commercial use.

3. Results and discussion

The determination of MBAS is a challenging analytical problem of considerable environmental significance. Most countries have regulatory limits imposed on the level of anionic surfactants that are permitted in discharged effluents. Ion-pair formation with the cationic dye MB and extraction of the ion-pair into an organic solvent constitutes the accepted method of MBAS determination and standard methods have been formulated on this principle [16]. In recent years, we have made a series of unsuccessful attempts to automate this analysis system by adsorption of the ion-pair on a hydrophobic adsorbent, followed by its elution with a suitable solvent [17]. Such approaches work for synthetic standards (albeit nonlinear calibration curves result) but are ineffective in analyzing real samples which contain other species that inevitably affect the adsorption behavior. Because of the nonlinear calibration behavior, standard addition methods are not easily applicable. We concluded that in this particular analysis system there are a number of pitfalls in substituting a true solvent extraction system with a solid phase extraction scheme as above. It seemed ideal therefore to test the present concept with this very well-established and routinely used MBAS determination principle. For this application, the nonspecific wavelength chosen was in the near infrared, at 850 nm, where MB does not absorb. The second wavelength chosen was 660 nm, close to the peak visible absorption of MB.

3.1. System output and processing of initial results

Raw system output for a 2.5 ppm C-12 LAS is shown in Fig. 4. Two sections of the output, one near the baseline where there is little sample present and a second one near the peak apex where significant amounts of sample are present are magnified (note that the entire abscissa span

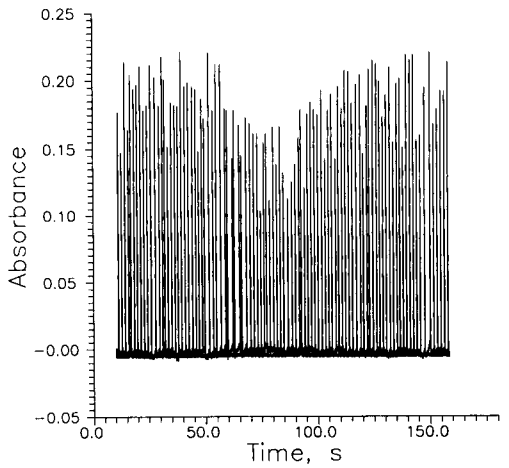

Fig. 4. Raw data output (both 660 nm and 850 nm detectors) for 2.5 ppm C-12 LAS sample. The data covers the injection of a single sample, which is extracted into a multitude of small organic segments. Each pike represents the rear edge of an aqueous segment.

on these figures are 1 s) and are shown respectively as Fig. 5a and b. Note that the small undulations are due to pump pulsation. MB tends to adsorb on the hydrophobic PTFE tubing wall. But as the extractant segment passes through the conduit, it has stronger affinity for the wall sites and displaces the MB. Thus, narrow concentrated zones of MB are formed at the rear end of each aqueous segment. The spikes in the 660 nm detector output in Fig. 5a and b correspond to these concentrated zones; these zones are actually readily visible to the naked eye. Although the MB reagent initially constitutes of a homogeneous

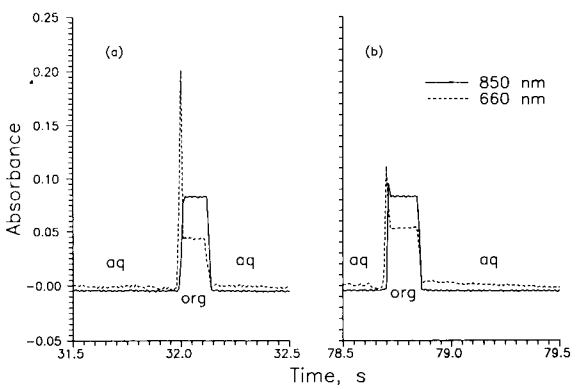

Fig. 5. Small subsections of Fig. 4, (a) near baseline conditions and (b) near the sample peak apex.

reagent in bulk solution, in the actual extraction system the aqueous phase is far from spatially homogeneous at the detection point (unless, of course, so much analyte is present that the MB has been completely removed from the aqueous phase). The presence of an anionic surfactant results in the interphase transfer of some of the MB to the organic phase. Consequently, the precise starting position and the magnitude of the spikes arising from the rear of the aqueous segment are related to the analyte concentration originally present in that segment. It is very apparent from a comparison of Fig. 5a and b that the spikes observed in the 660 nm detector output are very different in magnitude, decreasing with increasing sample concentration. If we reexamine Fig. 4, it will be observed that a decrease in the spike magnitude can be seen for about a 20 s wide region, centered at t ca. 75 s, corresponding to the sample peak. In the present application, because of refractive index effects, the apparent absorbance of the organic phase at either wavelength is very significantly higher than that of the aqueous phase and phase recognition is not difficult based on this criterion. Fig. 4 combines both 660 and 850 nm detector outputs and careful observation will reveal the detection of the organic phase by the 850 nm detector, corresponding to an absorbance of ca. 0.085. On the other hand, in examining Fig. 5, it should be clear that the exact starting position of the organic segments cannot be distinguished exactly by a single measurement wavelength of 660 nm because of the spikes caused by the concentrated methylene blue zones and the variations in them. This problem is solved by the measurement information available at the nonspecific wavelength, 850 nm, at which methylene blue does not absorb. Only the refractive index signal is detected at 850 nm, allowing the precise recognition of the organic segment location and its length. Once these are recognized, the average absorbance for the whole segment is computed by summing and averaging the data (at each terminal end of the segment, 10–20 ms worth of data are not included in the averaging process, to avoid potentially noisy readings close to the interface of the phases. Under the stated experimental conditions, each organic segment requires ~ 100 ms to pass through the detector on the average. During this time, ~ 10 separate sets of readings are taken at each wavelength. Based on the average absorbance and the length for each organic segment, a digital representation of the FIEgram is constructed, using only the data computed for the organic phase segments. A few seconds worth of baseline data on each side of the peak are averaged and used to perform a correction to set the baseline absorbance equal to zero. Fig. 6 shows a set of such superimposed baseline corrected FIEgrams for various concentrations of C-12 LAS standards.

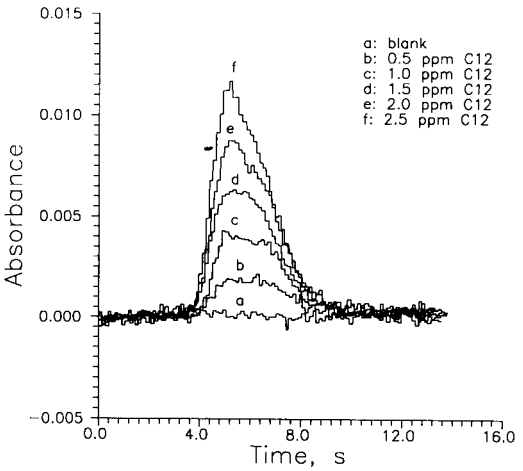

Fig. 6. Reconstructed FIEgram for various concentrations of C-12 LAS, time scale refers only to the accumulated time elapsed during organic phase detection.

A careful evaluation of Fig. 6 or a superposition of Fig. 5a and b will indicate that the segments are not exactly of the same length. Since not only the absorbance of each organic phase segment but also its length is measured accurately, the degree of segmentation uniformity attainable by a simple T-segmentor and peristaltic pumping can be used. For quantitation, because of the improvement in S/N from integration, peak areas provide better LODs than peak heights. We have not performed any peak smoothing prior to area computations and cannot comment if there will be any measurable improvements in attainable LODs if, for example, Savitsky-Golay smoothing [18] is performed prior

to area integration. The total computation time necessary for a 80386 class PC equipped with a 80387 co-processor to generate a FIEgram trace as in Fig. 6 and calculate the peak area requires < 5 s.

3.2. System performance and system characteristics

We have operated the system with a sampling frequency of 20 h^{-1}. However, the possibility of performing up to 40 determinations h^{-1} is suggested by the peak widths observed for the outputs in Fig. 6. Note that with a ratio of the total aqueous phase flow rate (Q_a) to the total organic phase flow rate (Q_o) of ~ 12 (as noted in Fig. 1), the actual data acquisition period for each of the traces in Fig. 6 is ~ 13 $[(Q_a + Q_o)/Q_o]$ times the depicted scale of events (ca. 170 s for each trace, 150 s span shown in Fig. 4). Also during the analysis period, after the new sample was aspirated and fully injected into the system, the conduit connecting the sample container to the injection valve was rinsed with 75% ethanol for 40 s. The surfactant samples do adsorb on the wall of sample introduction conduit. Unless this step is taken, response due to any given sample increases with repeated injections and stable responses are obtained only after about the fourth injection. The fact that reproducible results are obtained with the washing step and that a linear calibration curve is obtained indicates to us that the loss due to adsorption is a first order process, i.e., a constant fraction is lost by adsorption on the tubes. For a 40 cm × 0.38 mm i.d. PTFE conduit through which a C-12 LAS sample is aspirated for ~ 140 s at 0.45 ml/min, ~ 17% appears to be lost by adsorption. The use of metallic aspiration conduits will likely decrease this loss significantly; however, since reproducible results were obtained with the incorporation of the wash step, we did not pursue this aspect further.

A representative typical anionic surfactant, C-12 LAS, shows linear response ($r^2 = 0.99986$, uncertainty of slope 1.05%) with an intercept statistically indistinguishable from zero. Standard method descriptions suggest a linear dynamic range only up to an LAS concentration of ~ 2.5 ppm, calibration was therefore not conducted for concentrations much higher than this. The precision for the measurement of 2.0 ppm C-12 LAS is 1.5% in relative standard deviation. The standard deviation of the blank measurements corresponds to a concentration of 0.01 ppm from which we estimate an LOD of 0.03 ppm C-12 LAS. This is in comparison to an LOD of 0.025 ppm LAS cited for the standard manual MBAS determination method [14], in which 100–400 ml sample is extracted, depending on the expected MBAS concentration. The system was also calibrated with sodium hexadecane sulfonate and Neodol® 45S (a sulfated functionality surfactant with an average chain length of 14.5). Linear calibration plots were obtained with these cases as well; as indicated in the manual standard method, calibration slopes are different for different surfactants.

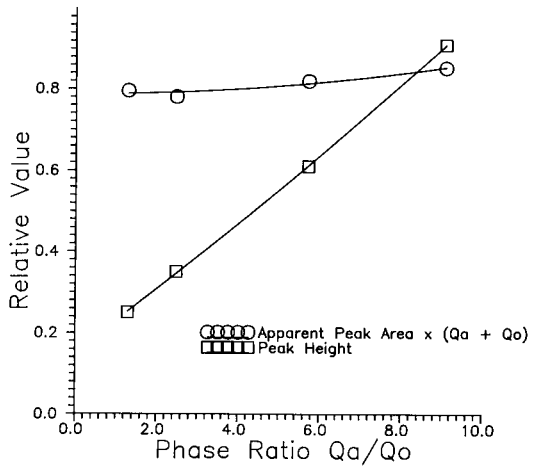

Fig. 7. Effects of flow rate ratio (Q_a/Q_o) on peak area and peak height.

3.3. Effect of flow rates and phase ratio

Fig. 7 shows the influence of changing the phase ratio (aqueous/organic) on peak area and peak height. These experiments were conducted by changing Qo at a constant Qa value of 0.61 ml/min with 2.5 ppm C-12 LAS being the injected sample. The apparent peak areas (with a dimensionality of absorbance × time) are multi-

plied by the total flow rate ($Q_a + Q_o$) to obtain the true peak areas (with a dimensionality of absorbance × volume) that are plotted in Fig. 7. The area values remain essentially unchanged over an order of magnitude variation in the phase ratio, indicating that extraction is essentially quantitative over this whole range. The peak height, on the other hand, increases in the same experiment with increasing phase ratio. Because these experiments were conducted at a constant Q_a, increasing phase ratio also connotes a decrease in total flow rate. We have conducted a limited set of experiments in which the phase ratio was maintained the same as the experimental arrangement shown in Fig. 1 while the total flow rate was varied over a 5-fold range, from 0.33 times to 1.67 times of that depicted in Fig. 1. The peak heights did not markedly change with total flow rate.

3.4. Real samples

Samples of water from a local play a lake and municipal tap water samples were collected. The anionic surfactant content was measured both by direct measurement and by the standard addition method. No significant level of MBAS was found in the tap water. Results obtained for the lake water sample (allowed to settle, the decantate was diluted but not filtered) by direct vs. standard addition method varied up to ±20%. However, in the absence of independent reference results, the accuracy of either method could not be verified. We chose therefore to spike these samples with known quantities of surfactants and again use standard addition and direct measurement methods to determine the spike recovery, after subtracting the original value of the unspiked water sample determined by the corresponding method. The results are shown in Table 1. It would appear that there *are* matrix interferences causing poor recovery in the direct measurement method but that these are adequately compensated for in the standard addition approach. The latter technique is therefore recommended for practical applications; in our experience, there was little to be gained in using more than one standard addition.

3.5. General applicability of concept

Phase recognition in the present application is achieved through the large difference in background absorbance at the nonspecific wavelength that arises because of a refractive index difference. However, this is not an essential requirement to successfully operate the system. All that is required is to use a marker substance that remains in one phase and that can be selectively followed by one measurement channel without interference from the analyte or its reaction product. In so far as optical detection strategies are concerned, ongoing work in this laboratory shows that the detection technique is not limited to the use of LEDs as sources, liquid crystal shutters can be pulsed on and off and used with

Table 1
Analytical recovery from direct and standard addition measurements

Sample matrix	Type and concentration of anionic surfactant spiked	Direct measurement (recovery)	Standard addition measurement (recovery)
Playa lake water	Neodol® 45S 0.5 ppm	0.452 (90.4%)	0.496 (99.2%)
Playa lake water	Neodol® 45S 1.0 ppm	0.914 (91.4%)	0.944 (94.4%)
Playa lake water	C-16 sulfonate 1.0 ppm	0.609 (60.9%)	0.960 (96.0%)
Tap water	Neodol® 45S 0.625 ppm	0.557 (89.1%)	0.611 (97.9%)

continuum sources well into the near UV region. If two different light sources are used with different modulation frequencies, each individual signal can be locked onto, using frequency bandpass filters. There would be essentially no limitation at all on either detection wavelength with such an arrangement. However, in so far as aqueous–organic extraction systems are concerned, a simpler and universally applicable technique may consist of the simultaneous measurement of optical absorbance and electrical conductance, the latter being used for zone recognition; there is always a significant difference in the latter property between aqueous and organic phases, regardless of the individual compositions [4,7,8].

4. Conclusions

The described system provides a new approach to perform FIE determinations. Both the absorbance and the length of each organic segment are detected by the dual-channel measurement system. The amount of analyte in each organic segment can be measured and the area of the reconstructed peak represents the total amount of analyte extracted into organic phase. All of the analyte extracted into organic phase is detected and phase separation is avoided. Hence, the efficiency and reliability of phase separation are no longer germane issues, giving FIE an altogether new dimension of practicality.

5. Acknowledgements

We thank Sheila Dubey, Shell Development Co., for her help and encouragement towards looking for a lasting solution towards automating surfactant determination methods. This research was supported partially by an unrestricted grant from Shell Development Co.

6. References

[1] K. Backstrom, L.-G. Danielsson and L. Nord, Anal. Chim. Acta, 187 (1986) 255.
[2] B. Karlberg and S. Thelander, Anal. Chim. Acta, 98 (1978) 1.
[3] H. Bergamin F°, J.X. Mediiros, B.F. Reis and E.A. Zagatto, Anal. Chim. Acta, 101 (1978) 9.
[4] P.K. Dasgupta and W. Lei, Anal. Chim. Acta, 226 (1989) 255.
[5] K. Kina and N. Ishibashi, Talanta, 25 (1978) 295.
[6] F. Cañete, M. Angel Rios, Luque de Castro and M. Valcarcel, Anal. Chem., 60 (1988) 2354.
[7] W. Lei, P.K. Dasgupta and D.C. Olson, Anal. Chem., 61 (1989) 496.
[8] C.C. Lindgren and P.K. Dasgupta, Talanta, 39 (1992) 101.
[9] Y. Sahleström and B. Karlberg, Anal. Chim. Acta, 179 (1986) 15.
[10] S.J. Gluck, Anal. Chim. Acta, 214 (1988) 315.
[11] C. Thommen, A. Fromageat, P. Obergfell and H.M. Widmer, Anal. Chim. Acta, 234 (1990) 141.
[12] V. Kuban, L.-G. Danielsson and F. Ingman, Anal. Chem., 62 (1990) 2026.
[13] V. Kuban, Anal. Chim. Acta, 248 (1991) 493.
[14] V. Kuban and F. Ingman, Anal. Chim. Acta, 245 (1991) 251.
[15] P.K. Dasgupta, H.S. Bellamy, H. Liu, J.L. Lopez, E.L. Loree, K. Morris, K. Petersen and K.A. Mir, Talanta, 40 (1993) 53.
[16] L.S. Clesseri, A.E. Greenberg and R.R. Trussell (Eds.), Standard Methods for the Examination of Water and Wastewater, American Public Health Association, Washington, DC, Method 5540C. Anionic Surfactants as MBAS, 5-59 - 5-63, 17th edn., 1989,
[17] H. Liu and P.K. Dasgupta, Reports to Shell Development Corporation, 1992–93.
[18] A. Savitsky and M.J.E. Golay, Anal. Chem., 36 (1964) 1627.

ELSEVIER

Analytica Chimica Acta 288 (1994) 247–257

ANALYTICA CHIMICA ACTA

Determination of chromium in different oxidation states by selective on-line preconcentration on cellulose sorbents and flow-injection flame atomic absorption spectrometry

Abdulmagid M. Naghmush, Krystyna Pyrzyńska, Marek Trojanowicz *

Department of Chemistry, University of Warsaw, Pasteura 1, 02-093 Warsaw, Poland

(Received 12th November 1992; revised manuscript received 18th October 1993)

Abstract

For on-line preconcentration of Cr(III) and Cr(VI), several functionalized cellulose sorbents, a chelating resin and conventional ion-exchange resins were examined. Cellulose with phosphonic acid exchange groups was found to be superior for the preconcentration of Cr(III), but a cellulose derivative with quaternary amine groups for the preconcentration of Cr(VI). The effects of most common cations and anions present in natural waters on the sorption of both chromium forms was examined. In the optimized flow-injection manifold for a 50-ml aspirated sample volume the detection limits were calculated to be 0.78 and 1.4 $\mu g\ l^{-1}$ for Cr(III) and Cr(VI), respectively. Preliminary results of the application of the developed method to the determination of chromium speciation in natural water samples are presented.

Key words: Atomic absorption spectrometry; Flow injection; Chromium; Preconcentration; Speciation

1. Introduction

Speciation analysis of trace heavy metals in environmental samples concerns their presence in various oxidation states, in different protonated and polymerized forms, in complexes with various ligands and various degrees of homogeneous and heterogeneous association with constituents of natural samples. For chromium in natural waters, most speciation studies deal with the determination of the total amount of dissolved Cr(III) and Cr(VI), owing to the different interactions of these two forms with living organisms.

In an early review [1], a wide variety of manual procedures for the determination of chromium speciation based on precipitation, liquid–liquid extraction, ion exchange and electrodeposition were surveyed. Examples of such ion-exchange [2] and solid-phase extraction [3] procedures with detection by electrothermal atomic absorption spectrometry (AAS) can also be found in recent publications.

The predominant trend in recently proposed methods for the speciation of chromium is the use of liquid chromatography (LC) and flow methods of analysis. Coupled methods combining

* Corresponding author.

SSDI 0003-2670(93)E0615-E

LC with AAS detection [4,5], direct current plasma atomic emission spectrometric (AES) detection [6,7], inductively coupled plasma (ICP) mass spectrometry [8], with chemiluminescence detection [9,10] and visible spectrophotometry with postcolumn derivatization [11] have been developed.

The main purpose of the use of non-chromatographic flow analysis in speciation studies of trace metals is the possibility of improving the selective preconcentration of a given chromium species on flow-through microcolumns with solid sorbents prior to elution to the detector. Most published work has been focused on the on-line preconcentration of Cr(III). For this purpose a column packed with quinolin-8-ol immobilized on porous glass [12], with an anion-exchange resin and 8-hydroxy-7-iodoquinoline-5-sulphonic acid [13] or *N*-phenylhydroxamic acid resin [14] has been used. Using columns with differently activated alumina, Cr(III) or Cr(VI) can be preconcentrated, which was utilized in flow-injection (FI) ICP-AES [15,16]. Recently a differential FI-AAS determination of Cr(VI) and total chromium was reported, where Cr(VI) was selectively preconcentrated on-line on a C_{18} bonded silica column using sodium diethyldithiocarbamate as chelating agent, whereas the total Cr was determined after oxidation of Cr(III) by potassium peroxodisulphate [17].

The aim of this work was to examine the possibility of using commercial cellulose sorbents with various functional groups for the preconcentration of Cr(III) and Cr(VI) in FI-AAS. For trace metal preconcentration, commercial cellulose sorbents already used were based on triethylamino functional groups (Cellex T) [18,19], the dibasic phosphate ester of cellulose (Cellex P) [20,21] and carboxymethyl groups (Cellex CM) [22]. For the preconcentration of Cr(III) quinolin-8-ol sulphonate cellulose, ethylenediaminetriacetic acid–cellulose [23] and Cellex P [20] have been applied, the last exhibiting much the best retention. A satisfactory preconcentration of Cr(III) was also observed using 2,2′-diaminodiethylamine cellulose filters [24]. In this work, the effectiveness of Cellex P (and other cationic sorbents) and Cellex T (and other anionic sorbents) used in series in a flow cell for preconcentration and determination of Cr(VI) and Cr(III), respectively, was investigated.

2. Experimental

2.1. Apparatus

A Beckman Model 1272 atomic absorption spectrometer equipped with a Unilam air–acetylene burner and a Pye Unicam GRM 1268 graphite furnance was used for AAS measurements.

The flow-injection set-up consisted of an MS/4 Reglo multi-channel peristaltic pump from Ismatec (Zurich), a Model 5020 low-pressure rotary injection valve from Rheodyne (Cotati, CA) and a laboratory-made rotary injection valve. Flow manifolds were assembled using PTFE tubing of 0.8 mm i.d.

A Model OP-211/1 digital pH meter from Radelkis (Budapest) was used for pH measurements and a Model 357 plate shaker from Elpan (Warsaw) for static measurements of retention.

2.2. Reagents

A 1000 mg l^{-1} Cr(III) stock standard solution was obtained from Merck and diluted as required. A 1000 mg l^{-1} Cr(VI) stock standard solution was prepared from analytical-reagent grade potassium chromate from POCh (Gliwice, Poland) and diluted as required. For preparation of all solutions deionized water obtained from a Waters Milli-Q system was used.

As cationic sorbents the following commercially available preparations were used: Cellex P (Bio-Rad Laboratories), which is a highly purified cellulose powder with phosphonic acid exchange groups of ion-exchange capacity 0.80 meq g^{-1}; Cellex CM, (Bio-Rad Laboratories), which is a carboxymethylated cellulose of ion-exchange capacity 0.65 meq g^{-1}; Chelex-100 chelating resin (Bio-Rad Laboratories); and Varion KS cation exchanger (Nitrokemia, Hungary).

As anionic sorbents the following commercially available preparations were used: Cellex T

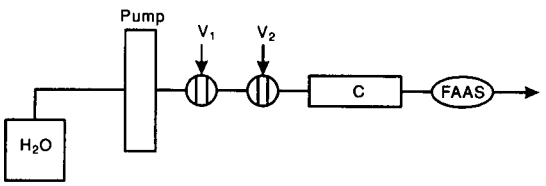

Fig. 1. Schematic diagram of FI-AAS system with one flow-through column used for the optimization of sorption and elution conditions.

(Bio-Rad Laboratories), which is cellulose with quaternary amine functional groups of ion-exchange capacity 0.74 meq g^{-1}; and Varion AT 660 anion exchanger in the chloride form (Nitrokemia) of ion-exchange capacity 3.5 meq g^{-1}.

2.3. On-line preconcentration of chromium species

Optimization of the on-line preconcentration of a particular chromium species was carried out in the single-line flow-injection manifold shown in Fig. 1. Injection valve V_1 was used for the injection of chromium solution and V_2 for the injection of eluent. C is a glass microcolumn packed with an appropriate ion exchanger. Larger sample volumes were continuously aspirated instead of injection with valve V_1.

2.4. Determination of chromium species using a dual-column flow-injection manifold

Cationic and anionic sorbent columns were used to investigate the determination of Cr(III) and Cr(VI) in the same injected sample. For a dual-column system in measurements of Cr concentrations below 0.1 mg l^{-1} using a larger column (45 mm long plastic tip of a 1-ml pipette) it was found that the sequence of placement of the two columns in the system and the order of elution have a great influence on the performance of the system. Hence, in order to find a condition where no Cr(III) is retained on Cellex T and no Cr(VI) is retained on Cellex P, two different configurations of the flow-injection system with two preconcentration columns connected in series were examined. The manifolds used all had the same basic structure, as shown in Fig. 2.

When the Cellex P column was used as the first in the series, Cr(VI) was eluted first and then Cr(III). Eluent for the Cellex T column did not pass through the Cellex P column, and eluent from the Cellex P column was diverted past the Cellex T column. Preconcentration without pH adjustement was performed using 50 ml as solution containing both chromium species at a flow-rate of 6 ml/min.

In the reverse situation, where the Cellex T column was first, preconcentration of 25 ml solution of pH 2.5 containing both chromium species was performed. Three different modes of operation of such a system were examined. First, Cr(III) retained on the Cellex P column was eluted first with HCl, then Cr(VI) from the Cellex T column; the NaOH solution used for Cr(VI) elution does not pass through the Cellex P column. In the second mode, the Cr(III) was again eluted first, then the NaOH solution was also pumped through the Cellex T and the Cellex P columns. In the third situation examined, Cr(VI) retained on the Cellex T column was eluted first and NaOH solution used for elution was passed also through the Cellex P column.

The optimized manifold for determination of both species from the same aspirated sample is shown in Fig. 2. It contains two injection valves, V_1 and V_2, and a two-way switch. The Cellex T column is placed first in the manifold. After the required sample volume has been aspirated, the solution inlet is transferred to the carrier HCl solution of pH 2.5. Both chromium species are simultaneously preconcentrated on the Cellex T and Cellex P columns.

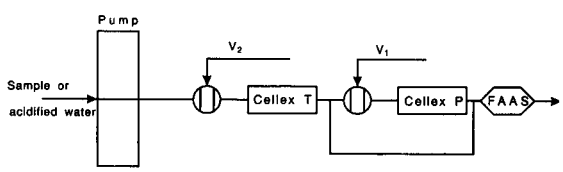

Fig. 2. Schematic diagram of the optimized FI-AAS system with two preconcentration columns for the simultaneous determination of Cr(III) and Cr(VI) species.

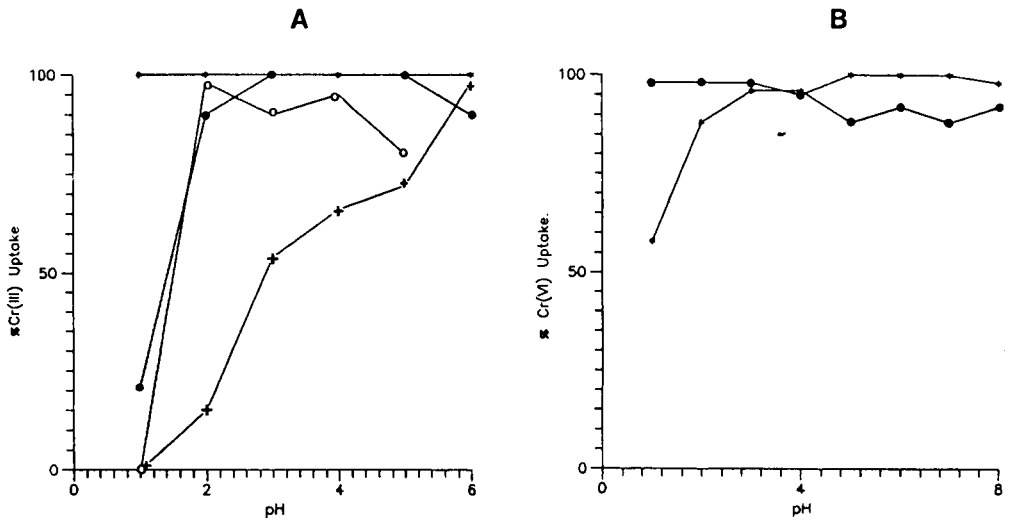

Fig. 3. Effect of pH on sorption under static conditions of (A) Cr(III) on (*) Varian KS, (+) Cellex CM, (●) Cellex P and (○) Chelex 100 and (B) Cr(VI) on (*) Varian AT 660 and (●) Cellex T.

In the elution stage, Cr(III) is eluted first from the Cellex P column by injection of 1 ml of 1 M HCl with valve V_1. Then the two-way switch is opened, and valve V_1 is closed by setting it in the intermittent position. Cr(VI) retained on the Cellex T column is eluted by injection of 1 ml of 1 M NaOH directly to the spectrometer without passing through the Cellex P column.

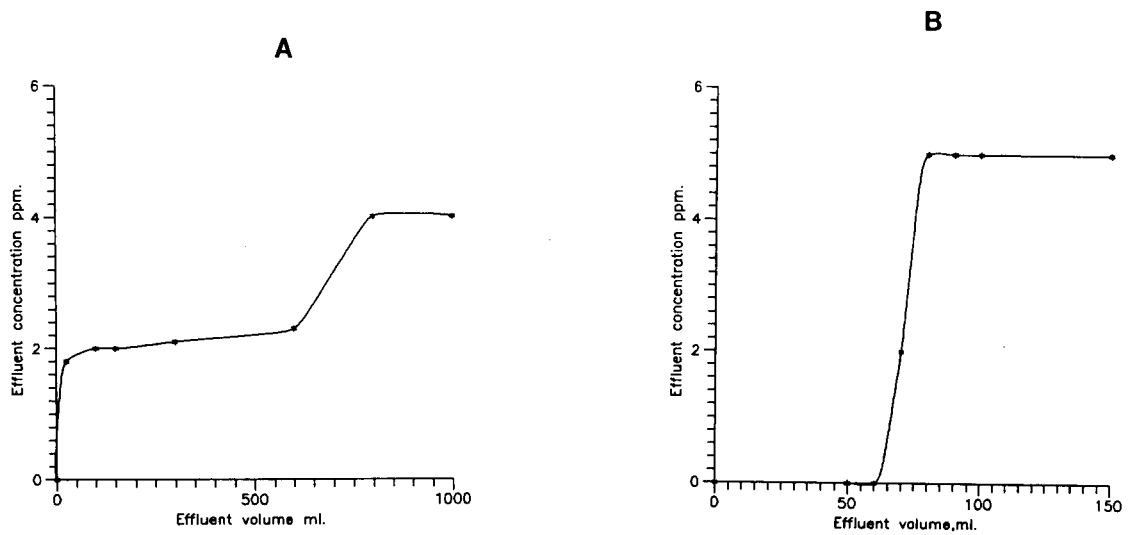

Fig. 4. Breakthrough curves for Cr(III) using 20 × 3 mm i.d. columns with (A) Varian KS and (B) Cellex P obtained for 5.0 mg l^{-1} Cr(III) solution at a flow-rate of 2.0 ml min^{-1}.

3. Results and discussion

3.1. Comparison of selected sorbents for chromium preconcentration

In order to choose the most appropriate sorbent for further on-line application, as a preliminary step a comparison of the retention of chromium species in the batch mode at different pH values was carried out in the flow-injection system shown in Fig. 1 Retention of Cr(III) was examined for two different cellulose sorbents, Cellex CM and Cellex P, the ion exchanger Varian KS and the chelating resin Chelex 100. To 0.2 g of the sorbent 20 ml of solution containing 1 mg of Cr(III) or Cr(VI) were added, the pH of solution was adjusted to the required value with HCl or NaOH and the mixture was shaken for 1 h, then filtered and the chromium content in the filtrate was determined using flame AAS. As can be seen from Fig. 3A, in the widest pH range 100% Cr(III) uptake was observed for Varian KS and Cellex P. For these two sorbents the ion-exchange breakthrough capacity was then examined. In this experiment 5 mg l^{-1} Cr(III) solution was continuously pumped through the microcolumns (20 × 3 mm i.d.) with a given sorbent at a flow-rate 2.2 ml min^{-1} until the concentration of Cr(III) in the effluent was the same as that in feed solutions. The results of these experiments are shown in Fig. 4, indicating a significant difference in the kinetic behaviour of the sorbents. Under the same hydrodynamic conditions the Varian KS bed does not retain all the Cr(III) passing through the column, owing to slow sorption by the ion exchanger (Fig. 4A). Cellex P exhibits much faster Cr(III) binding, the breakthrough curve shows a very sharp increase and its capacity was estimated as 0.15 meq g^{-1} dry resin (Fig. 4B). Because of relatively wide range of available pH and its good kinetic properties Cellex P was selected for further study of on-line Cr(III) preconcentration.

Retention of Cr(VI) was examined for the ion exchanger Varian AT 660 and the cellulose sorbent Cellex T. In this instance also a wider range of almost complete Cr(VI) uptake was observed for the conventional ion exchanger (Fig. 3B), whereas for Cellex T 95% of the Cr(VI) was retained in the pH range 3–4. However, also in this instance the kinetic properties of the cellulose sorbent were more favourable (Fig. 5), and this was the main reason for selecting this sorbent for further study on on-line Cr(VI) preconcentra-

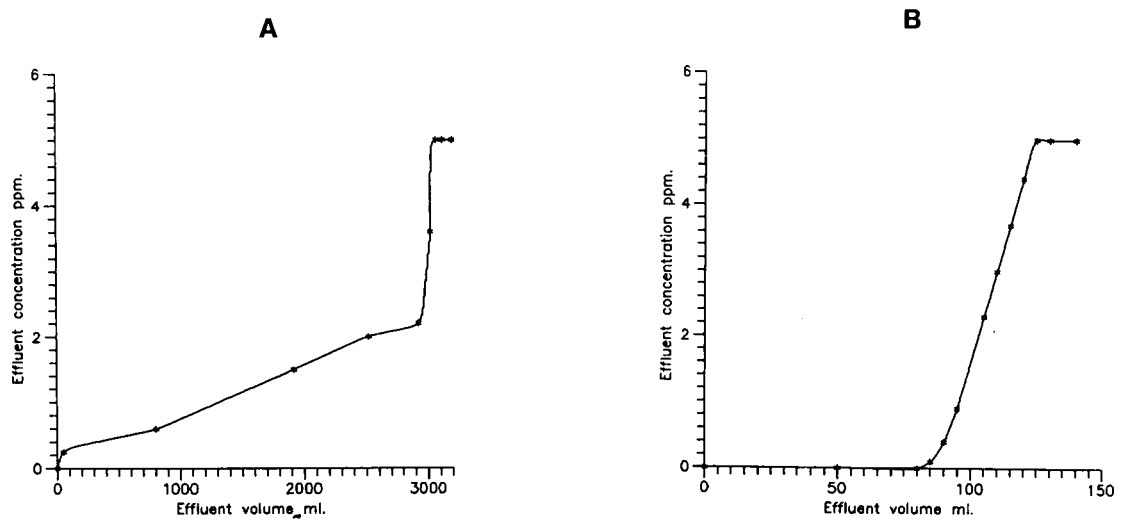

Fig. 5. Breakthrough curves for Cr(VI) using 20 × 3 mm i.d. columns with (A) Varian AT 660 and (B) Cellex T obtained for 5.0 mg l^{-1} Cr(VI) solution at a flow-rate of 2.0 ml/min.

tion. Its capacity was estimated as 0.19 meq g^{-1} dry resin.

3.2. Elution of chromium from cellulose sorbents

Metals retained on solid sorbents are most commonly eluted with mineral acids or strong complexing agents. In this study the effective elution of Cr(III) retained on Cellex P was achieved with both hydrochloric and nitric acid. The effect of HCl concentration on the effectiveness of elution is shown in Fig. 6 (curve 1). Above an HCl concentration of 0.2 M, the signal of eluted Cr(III) was virtually constant for a 1-ml injection volume. On the other hand, in the optimization of the volume of eluent needed for complete elution, it was found that for 1 M HCl used as the eluent, the Cr(III) signal did not increase when 0.5 ml of eluent was used. Also, for the next injection of 2 M HCl no peak for chromium was observed. In most further experiments 0.5 or 1 ml of 1 M HCl was used for Cr(III) elution.

Several reagents were examined for the elution of Cr(VI) retained on Cellex T, such as sodium hydroxide, sodium chloride and ammonia solutions. All of these can elute Cr(VI), but the elution signal observed for chromium after elution with ammonia is much broader than for elution with NaOH or NaCl (Fig. 7), indicating a slower elution process. Higher peaks were observed with NaOH than with NaCl, so the former was selected. As can be seen from curve 2 in Fig. 6, at least a 0.8 M NaOH concentration should be used for complete elution, so in all further experiments 1 M NaOH was used for Cr(VI) elution.

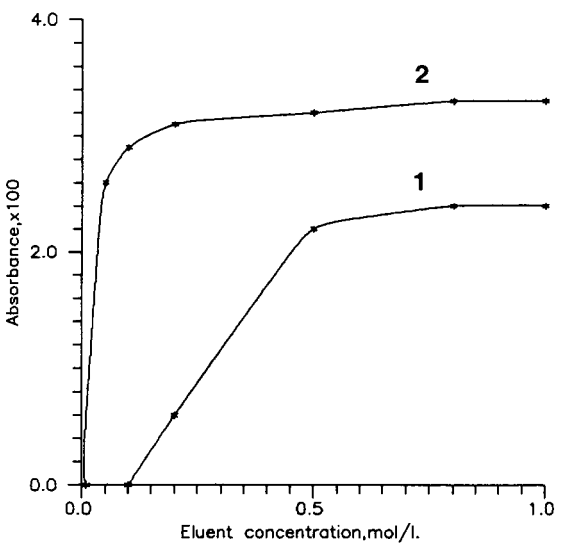

Fig. 6. Effect of eluent concentration on chromium FI-AAS signal magnitude obtained for (1) Cr(III) eluted with HCl and (2) Cr(VI) eluted with NaOH. In all instances 1.0 ml of eluent was injected.

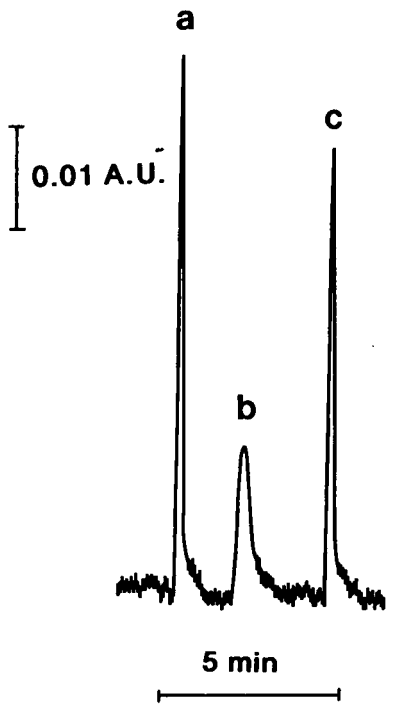

Fig. 7. Examples of peaks recorded with the FI-AAS system for Cr(VI) eluted using 1.0 ml of 1 M solutions of (a) NaOH, (b) NH_3 and (c) NaCl.

3.3. Retention of Cr(III) on Cellex T and Cr(VI) on Cellex P

In order to apply both selected cellulose sorbents to the determination of chromium speciation, Cr(III) should not be retained on Cellex T, and Cr(VI) should not be retained on Cellex P. This was examined by the injection of 1 ml of 1 mg l^{-1} Cr(III) or Cr(VI) solution into the flow system without any preconcentration column or

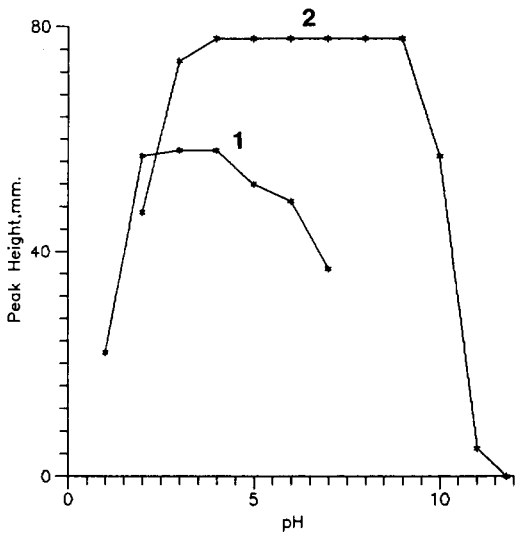

Fig. 8. Effect of pH on retention under dynamic conditions in the FI-AAS system of (1) Cr(III) on Cellex P and (2) Cr(VI) on Cellex T at a flow-rate of 5.0 ml min^{-1}.

with a Cellex T column (5 × 5 mm i.d.) for testing Cr(III) sorption or with the same size Cellex P column for checking Cr(VI) sorption. In both instances the signal magnitudes observed in the system without and with the column were identical, demonstrating that no such interference is observed with the sorbents used.

3.4. Effect of pH and flow-rate on on-line preconcentration

Under the dynamic conditions of on-line preconcentration, the pH range of maximum retention of Cr(III) is shifted towards more acidic solutions in comparison with results obtained in batch experiments. As shown in Fig. 8 (curve 1), the maximum height of the flow-injection peaks resulting from preconcentration of Cr(III) was obtained in the pH range 2–4 and is limited by hydrogen ion competition in more acidic range and the formation of less retained hydroxo complexes of Cr(III) in weakly acidic and neutral media.

The optimum pH range for the on-line preconcentration of Cr(VI) on the Cellex T column is not different to that observed in the batch mode. The maximum flow-injection signal for the elution of preconcentrated Cr(VI) was observed in the pH range 4–9 (Fig. 8).

For the preconcentration of both chromium species the effect of flow-rate in the range 3.5–9.5 ml min^{-1} was examined. For a 5 × 5 mm i.d. column size the same signal magnitude was observed both for Cr(III) and Cr(VI) over the whole flow-rate range examined. For the larger columns used for on-line preconcentration the flow-rate applied usually has to be limited to about 6 ml min^{-1} because of the flow resistance in larger packed columns.

3.5. Calibration characteristics

The responses of the flow-injection system with preconcentration for both chromium species were examined both in terms of chromium concentration in the same injected sample volume and in terms of injected volume of chromium solution of the same concentration.

For Cr(III) preconcentration on Cellex P, 100-ml samples were aspirated at 5 ml min^{-1} at concentrations ranging from 1 to 10 $\mu g\ l^{-1}$. A linear calibration plot was obtained with a correlation coefficient of 0.996 ($n = 5$).

The same satisfactory linearity of response was observed for Cr(VI) preconcentration on the Cellex T column. For aspiration of 100 ml of Cr(VI) solution at concentrations ranging from 1 to 10 $\mu g\ l^{-1}$ at 8 ml min^{-1} a linear calibration plot was again obtained with a correlation coefficient of 0.998 ($n = 10$) and a slope of 87% of that for Cr(III).

3.6. Effect of the presence of other cations on Cr(III) preconcentration

The presence of other cations in the sample often affects the sorption of preconcentrated analytes. For the sorption of Cr(III) on Cellex P this effect was examined under on-line conditions using a 5 × 5 mm i.d. column and aspiration of 50 ml 0.1 mg l^{-1} Cr(III) solution at a flow-rate of 5.0 ml min^{-1} in the presence of excess of various cations (Table 1).

Table 1
Effect of the presence of other cations on the sorption of Cr(III) on Cellex P using a 5×5 mm i.d. column.

Cation	Concentration (mg l^{-1})	Cr(III) recovery (%)
Na^+	1000	100
K^+	50	100
	100	100
	200	104
Ca^{2+}	50	103
	100	107
	200	107
Mg^{2+}	50	96
	100	87
	200	64
Mn^{2+}	5	100
Cu^{2+}	5	56
	5	100 [a]
Al^{3+}	5	100 [a]
Fe^{3+}	5	220

[a] For a 65×5 mm i.d. column.

In the presence of 5 mg l^{-1} Fe(III) a large increase in the chromium signal was observed. An attempt to decrease this interference by the addition of fluoride to the sample solution prior to the preconcentration was not successful and resulted in a significant decrease in the chromium signal. For a larger 25 mm column, up to 10 mg l^{-1} Fe(III) did not affect the chromium signal. Because it was found that under the same conditions Fe(III) is retained and eluted together with Cr, the observed interference has a typical spectral nature. This can be eliminated by changing the measuring conditions from the most sensitive chromium wavelength of 357.9 nm to the less sensitive 425.4 nm. This allows iron(III) interference to be eliminated up to concentrations of 20 mg l^{-1}. With further increases in Fe(III) concentration a decrease in the chromium signal was observed, but at 40 mg l^{-1} Fe(III) 92% of preconcentrated Cr(III) was recovered. Therefore, for practical applications the use of the less sensitive wavelength is recommended for the detection of eluted chromium when the presence of Fe(III) at concentrations above 10 mgl^{-1} can be expected.

No other cations gave rise to interference at concentrations below 20 mg l^{-1}.

3.7. Effect of the presence of common anions on the retention of Cr(VI)

Chloride, nitrate and sulphate were selected as potential interfering anions for Cr(VI) preconcentration on Cellex T. Using a 5 × 5 mm i.d. Cellex T column for preconcentration of Cr(VI) from an aspirated 100 ml of 0.1 mg l^{-1} solution, it was found that up to 100 mg l^{-1} chloride and 20 mg l^{-1} nitrate do not affect the Cr(VI) sorption.

The presence of sulphate significantly decreased the Cr(VI) sorption as at 10 mg l^{-1} sulphate only 75% of the Cr(VI) was retained. A pH study indicated that the optimum pH range is 5–7 in the presence of sulphate, but sorption is incomplete. Satisfactory results were obtained by increasing the column length (Fig. 9). As can be seen in Fig. 10, for aspiration of 100 ml of 5 μg l^{-1} Cr(VI) solution and using a 75 mm Cellex T column, the presence of up to 150 mg l^{-1} chloride, 50 mg l^{-1} nitrate and 100 mg l^{-1} sulphate in the same solution does not affect the Cr(VI) preconcentration.

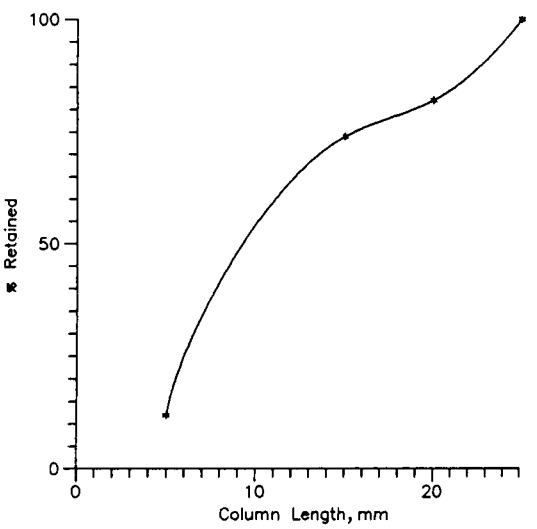

Fig. 9. Effect of Cellex T column length on preconcentration of Cr(VI) from 100 ml of 5.0 mg l^{-1} solution in the presence of 20 mg l^{-1} sulphate at an aspiration flow-rate of 5.0 ml min^{-1}.

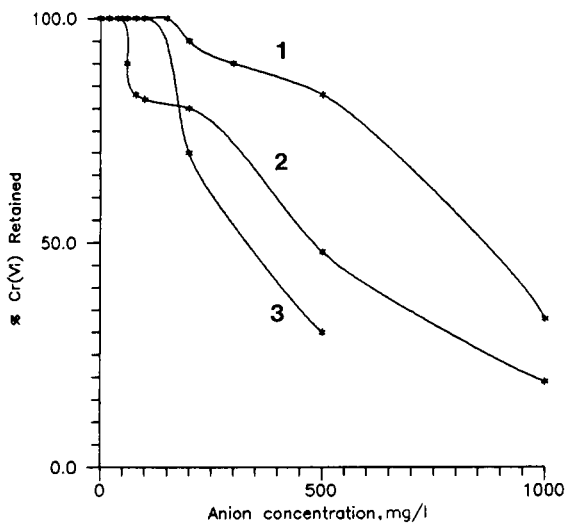

Fig. 10. Effect of the presence of (1) chloride, (2) nitrate and (3) sulphate on the retention of Cr(VI) from 100 ml of 5.0 mg l^{-1} solution at an aspiration flow-rate of 7.6 ml min^{-1} and an elution flow-rate of 3.0 ml min^{-1}.

3.8. Simultaneous preconcentration of Cr(III) and Cr(VI) in a dual-column flow-injection system

When packed flow-through columns, which may change their flow resistance, are used in flow-injection systems, the functioning of a branched manifold with a split sample stream may be very irreproducible. Hence in this study a configuration with two columns in series was preferred, especially as the optimum conditions for the preconcentration of both chromium species are not very different.

As mentioned under Experimental, several different modes of operation of the dual-column system were examined. An important factor for satisfactory functioning of the measuring system is an appropriate sequence of both flow-through columns. For a flow system with the Cellex P column placed first, the signal corresponding to Cr(III) elution is always larger than observed for the same amount of preconcentrated Cr(VI). Also, in spite of the results mentioned above, even when the aspirated sample solution did not contain Cr(III), the elution of the Cellex P column with HCl gave a positive signal, indicating some sorption of Cr(VI) on the Cellex P column. For such a system a carrier solution of pH 4 provided the best results and the optimum sample pH adopted was 5.5.

More satisfactory results were obtained, however, for the flow system with the Cellex T column placed first. When Cr(VI) was eluted first and the eluate passed through the Cellex P column and then Cr(III) was eluted, a double peak was obtained for Cr(VI) elution and the height of the Cr(III) peak was decreased, indicating that Cr(III) was partially eluted with Cr(VI). Unsatisfactory results were also obtained when Cr(III) was eluted first and then the eluent used for Cr(VI) elution was first passed through the Cellex T and then the Cellex P column. In this instance the signal from Cr(III) was decreased, which can be attributed to the interaction of NaOH solution with the Cellex P sorbent, causing an increase in sorbent volume and resulting in a decrease in flow-rate. This was not observed when NaOH did not pass through the Cellex P column and such a mode of operation was considered to be the optimum. The best performance of the system was obtained after adjustment of the pH of sam-

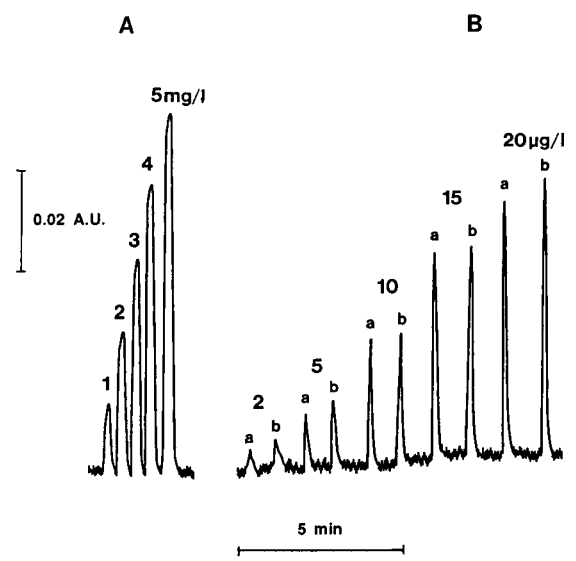

Fig. 11. Comparison of recordings obtained for flame AAS measurements of chromium with (A) conventional aspiration and (B) with the optimized FI-AAS system with preconcentration of (a) Cr(III) and (b) Cr(VI). Aspirated sample volume, 100 ml; flow-rate, 5.0 ml min^{-1}.

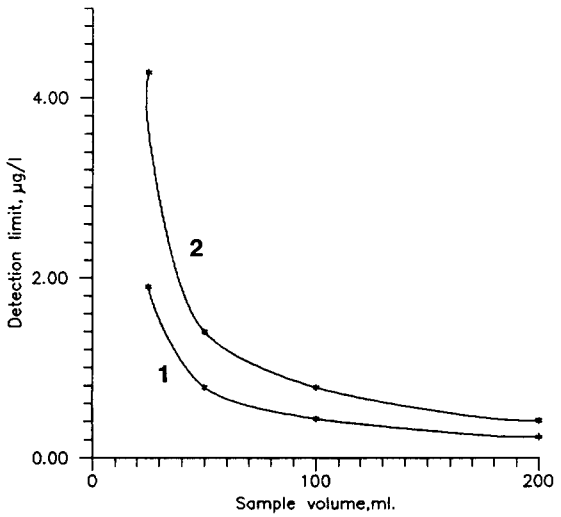

Fig. 12. Effect of the aspirated sample volume at an aspiration flow-rate of 4.0 ml min^{-1} in the optimized FI-AAS system on the detection limits of (1) Cr(III) and (2) Cr(VI).

ple solution to 2.0–2.5. An example of signals recorded under such conditions is shown in Fig. 11.

3.9. Detection limit

Although excellent linearity was found for the dependence of the signal magnitude on the volume of sample of 10 $\mu g\ l^{-1}$ aspirated up to 200 ml, as shown previously for the preconcentration of Cu on ligand-loaded sorbents [25], it does not offer unlimited possibilities to lower the detection limit. The values plotted in Fig. 12 were determined as the concentration corresponding to a signal magnitude equal to three times the standard deviation obtained for ten samples of a given volume. This determination was done at less sensitive chromium line at 425.4 nm. For 50 ml of aspirated solution the detection limits were 0.78 and 1.4 $\mu g\ l^{-1}$ for Cr(III) and Cr(VI), respectively. Using a 200-ml sample volume three times lower values can be obtained. The precision obtained was 2.6% and 4.5% for Cr(III) and Cr(VI), respectively, for $n = 10$ and for 10 $\mu g\ l^{-1}$ of each chromium species.

Table 2
Determination of chromium speciation in natural waters using the optimized flow-injection system with flame AAS detection

Sample	Found by FI-AAS ($\mu g\ l^{-1}$) [a]		Total Cr content by electrothermal AAS ($\mu g\ l^{-1}$)
	Cr(III)	Cr(VI)	
Tap water	4.67±0.12	3.75±0.18	0.48
Well water I	4.69±0.12	4.00±0.20	0.64
Well water II	4.99±0.15	4.25±0.21	0.72
River water I	5.36±0.16	4.50±0.23	1.04
River water II	5.67±0.15	4.50±0.23	1.36

50 ml of sample aspirated at a flow-rate of 3.0 ml min^{-1}. For FI-AAS measurements each sample was spiked with 4.0 $\mu g\ l^{-1}$ Cr(III) and 4.0 $\mu g\ l^{-1}$ Cr(VI).
[a] Mean ± S.D. ($n = 3$).

3.10. Preliminary application to natural water samples

The developed method for the determination of chromium speciation using a dual-column manifold was applied to several samples of natural waters, using an aspiration volume of 50 ml. The collected samples of surface and tap water were filtered using a 0.45-μm filter and acidified to pH 2.5 with HCl. As in most instances the concentration of both chromium forms was very close to the detection limit, all samples were spiked with 4.0 $\mu g\ l^{-1}$ Cr(III) and 4.0 $\mu g\ l^{-1}$ Cr(VI). The results of this preliminary study, presented in Table 2 show moderate agreement with the total content of chromium found by electrothermal AAS. In all the natural samples examined chromium (III) predominates, which is in agreement with earlier results of chromium speciation studies in natural water by other workers [2,17].

4. Conclusions

Functionalized cellulose sorbents were found to be more appropriate for the on-line preconcentration of Cr(III) and Cr(VI) in a flow-injection system than conventional cation or anion exchangers or a chelating resin. Although the detection limits for both chromium forms were worse than reported recently [17], an advantage

of the developed system is that both Cr(III) and Cr(VI) forms can be determined in the same aspirated sample volume without any sample pretreatment.

5. References

[1] B. Griepink, Pure Appl. Chem., 56 (1984) 1477.
[2] C.A. Johnson, Anal. Chim. Acta, 238 (1990) 273.
[3] M.T. Morocco, G.P. Newman A. Syty, J. Anal. At. Spectrom., 5 (1990) 29.
[4] A. Syty, R.G. Christensen T.C. Rains, At. Spectrosc., 7 (1986) 89.
[5] A. Syty, R.G. Christensen T.C. Rains, J. Anal. At. Spectrom., 3 (1988) 193.
[6] V.B. Lewis, S.H. Nam I.T. Urasa, J. Chromatogr. Sci., 27 (1989) 468.
[7] S. Ahmad, R.C. Murthy S. Chandra, Analyst, 115 (1990) 287.
[8] R. Roehl M.M. Alforque, At. Spectrosc., 11 (1990) 210.
[9] T. Williams, P. Jones L. Ebdon, J. Chromatogr., 482 (1989) 361.
[10] B. Gammelgaard, O. Jons B. Nielsen, Analyst, 117 (1992) 637.
[11] E. Pobozy, M. Trojanowicz P.R. Worsfold, Anal. Lett., 25 (1992) 1373.
[12] E.B. Milosavljevic, L. Solujic, J.H. Nelson J.L. Hendrix, Mikrochim. Acta, Part III, (1985) 353.
[13] V. Porta, C. Sarzanini E. Mentasti, Mikrochim. Acta, Part III, (1989) 247.
[14] A. Shah S. Devi, Anal. Chim. Acta, 236 (1990) 469.
[15] A.G. Cox, I.G. Cook C.W. McLeod, Analyst, 110 (1985) 331.
[16] A.G. Cox C.W. McLeod, Anal. Chim. Acta, 179 (1986) 487.
[17] M. Sperling, X. Yin B. Weltz, Analyst, 117 (1992) 629.
[18] K. Słonawska K. Brajter, J. Anal. At. Spectrom., 4 (1989) 653.
[19] K. Brajter K. Słonawska, Mikrochim. Acta, Part I (1989) 137.
[20] K. Brajter K. Słonawska, Fresenius' Z. Anal. Chem., 320 (1985) 142.
[21] K. Brajter K. Słonawska, Water Res., 11 (1988) 1413.
[22] K. Pyrzyńska, Anal. Chim. Acta, 238 (1990) 285.
[23] N. Prakash, G. Csanady, M.R.A. Michaelis G. Knapp, Mikrochim. Acta, Part III, (1989) 257.
[24] J.A. Smits R.E. van Grieken, Anal. Chem., 52 (1980) 1479.
[25] A.M. Naghmush, M. Trojanowicz E. Olbrych-Śleszyńska, J. Anal. At. Spectrom., 7 (1992) 323.

ELSEVIER

Analytica Chimica Acta 288 (1994) 259–264

ANALYTICA CHIMICA ACTA

Pentachlorophenol preconcentration using quinolin-8-ol immobilized on controlled-pore glass and flow spectrophotometric determination

C. Moreno-Román, M.R. Montero-Escolar, M.E. León-González *, L.V. Pérez-Arribas, L.M. Polo-Díez

Departamento de Química Analítica, Facultad de Ciencias Químicas, Universidad Complutense de Madrid, 28040 Madrid, Spain

(Received 6th June 1993)

Abstract

A pentachlorophenol preconcentration method using a microcolumn (20 × 2.5 mm i.d.) filled with quinolin-8-ol (oxine) immobilized on controlled-pore glass (CPG) is proposed. The method is based on retention at pH 1 and elution at pH 3 with acetonitrile–water (80 + 20). Maximum retention of pentachlorophenol was 180 μg per gram of oxine–CPG. The breakthrough volume was 100 ml. The good ability for retention and elution allows the flow spectrophotometric determination of microgram amounts of pentachlorophenol. The calibration graph was linear from 4.0 to 25 μg for a sample volume of 100 ml, the repeatability using a single column for 12 μg of pentachlorophenol was 1.2% (R.S.D., $n = 4$), and the reproducibility between five different microcolumns for the same concentration level was 1.6%. The 3σ detection limit was 2.5 μg and a preconcentration factor of 250-fold was obtained. Common cations and other phenols do not interfere significantly.

Key words: Flow systems; UV–Visible spectrometry; Pentachlorophenol; Preconcentration; Waters

1. Introduction

Phenols in general are an important group of compounds to be monitored in surface water, waste water and leachate, and an automated on-line system would give valuable data in many situations. In particular, chlorophenols and nitrophenols are used as pesticides, bactericides, wood preservatives and synthetic intermediates. Moreover, chlorophenols are also byproducts of the chlorine bleaching process used in pulp and paper mills. The efficiency of a bio-oxidation waste water treatment plant can be monitored by observing how it handles low-level concentrations of pentachlorophenol; this phenol is more difficult to biodegrade than most other phenols, and its increase in the plant effluent may indicate decreased efficiency and a potential problem [1]. Moreover, chlorophenols have been investigated as an indicator parameter for polychlorinated dibenzodioxins and furans from municipal waste combustion [2]. Several on-line determinations of phenols have been reported recently [1,3].

* Corresponding author.

SSDI 0003-2670(93)E0616-F

The US Environmental Protection Agency recommends a maximum level of 1 $\mu g\ ml^{-1}$ of total phenolic compounds in water supplies [4] for analysis at this concentration level it is necessary to preconcentrate the sample before detection [1,5] for sensitivity enhancement. The use of solid materials for the retention of analytes or interferences in a liquid sample passing through them is a common alternative to sample pretreatment on account of the advantages offered. Quinolin-8-ol (oxine) has been used in immobilized form for the preconcentration of trace levels of metal ions [6–8]; other applications of immobilized oxine include the liquid chromatographic separation of metal ions [9] and the metal-assisted separation of phenols [10]. Controlled-pore glass (CPG) has been the support of choice in some of these applications because immobilization reactions on the glass surface are relatively simple [11]. Also, CPG exhibits the good mechanical strength and swelling stability required for flow systems.

The purpose of this work was to study the retention of phenols, and especially pentachlorophenol, for preconcentration on oxine immobilized covalently on CPG, and spectrophotometric detection in a continuous-flow system.

2. Experimental

2.1. Equipment

The system consisted of a Wiz programmable peristaltic pump connected to a column filled with oxine immobilized on CPG, a Hewlett-Packard HP 8452A diode-array spectrophotometer equipped with a 1-cm path length silica flow cell and a PTFE reaction coil. The spectrophotometer was interfaced to an HP Vectra AT computer and an HP Think Jet printer.

2.2. Reagents

All chemicals were of analytical-reagent grade and purified water was obtained using a Milli-Q apparatus (Millipore). Pentachlorophenol (99% pure, Carlo Erba), 2,4,6-trichlorophenol (99% pure, Carlo Erba), 2,4-dichlorophenol (99% pure, Aldrich Chemie), 4-chloro-3-methylphenol (99%, Aldrich Chemie), 2-nitrophenol (> 99% pure, Fluka), 4-nitrophenol (> 99% pure, Fluka), 3-nitrophenol (Carlo Erba), 2,4-dinitrophenol (99.4% pure, Chem Service), 4,6-dinitro-2-methylphenol (98% pure, Chem Service) and 2,4-dimethylphenol (90% pure, Merck) were used for preparing 125 mg l^{-1} stock standard solutions in 1.0×10^{-3} M sodium hydroxide solution. (Aminophenyl)trimethoxysilane (95% pure, ABCR) was supplied as mixed isomers and stored under refrigeration. Controlled-pore glass (CPG-240-200, Sigma) was boiled in 5% nitric acid for 30 min, filtered on a glass filter, washed with deionized water and dried in an oven at 95°C.

2.3. Immobilization procedure and storage

Immobilization on CPG was achieved following the procedure described by Marshall and

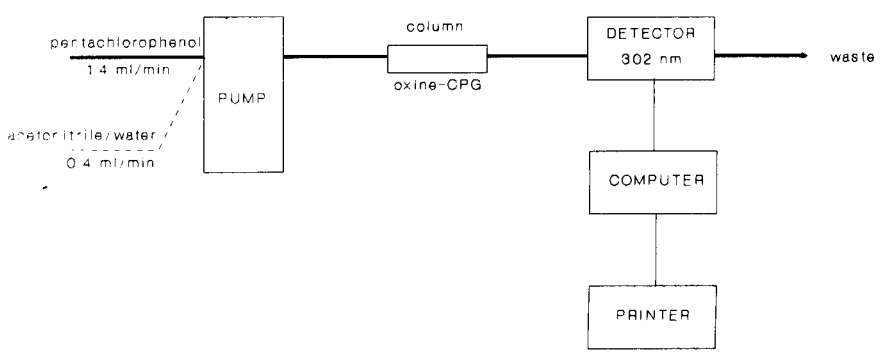

Fig. 1. Flow system for determination of pentachlorophenol.

Mottola [11]. The product was packed in a glass microcolumn (20 × 2.5 mm i.d.) so that the length of the immobilized oxine zone was 15 mm. The column filled with the immobilized oxine was stored in a refrigerator at 4°C and pH 1. The dried material was stored in a desiccator.

The efficiency of the immobilization procedure was evaluated indirectly. The difference between the initial oxine concentration added to the diazonium salt–CPG and the final concentration in the waste was measured spectrophotometrically in a buffered solution (pH 9, 0.1 M NH_4Cl–NH_3) at 360 nm in the presence of 1.0×10^{-2} M Al^{3+}.

2.4. Flow determination of pentachlorophenol

Calibration was achieved by pumping aliquots of solutions containing pentachlorophenol in the 4–25 μg in 100 ml volume range at 1.4 ml min^{-1} through the microcolumn filled with oxine–CPG at pH 1. Once pentachlorophenol had been retained on the column, after selection of the second channel in the pump, elution was effected with an acetonitrile–water (80:20) at pH 3, the flow-rate being 0.4 ml min^{-1}. Spectrophotometric measurements of the peak height were made at 302 nm against a blank solution (Fig. 1).

3. Results and discussion

3.1. Immobilization efficiency

In order to determine the amount of oxine immobilized on CPG, the waste liquid from the immobilization procedure was collected. The concentration of oxine was evaluated by formation of the aluminium–oxinate complex at pH 9.2 and spectrophotometric measurement at 360 nm. The amount of oxine immobilized was about 130 mg per gram of CPG.

3.2. Stability

The hydrolytic stability of the immobilized oxine–CPG was studied in the pH range 1–12. The material is very stable in strongly acidic solutions. A slight coloration of the effluent is observed at pH > 4.8. At pH > 9 the yellow effluent becomes dark yellow with a maximum at 380 nm that may be due to the hydrolysis of the azo bond (the oxine absorbance maximum at this pH is at 308 nm).

Regarding stability, no significant change in the retention of phenols has been observed over a 5-month storage period.

Table 1
Results of optimization of working conditions for the flow system

Variable	Range studied	Value selected
pH (retention)	1.0–12.8	1.0
Flow-rate (retention) (ml min^{-1})	0.4–2.9	1.4
Eluent	Acetonitrile–water Methanol–water Ethanol–water Acetone–water	Acetonitrile–water
Eluent composition (v/v)	50 + 50–80 + 20	80 + 20
pH (elution)	2–12	3
Flow-rate (elution) (ml min^{-1})	0.4–1.3	0.4
Sample volume (ml)	10–500	100
Pentachlorophenol per gram of oxine–CPG (μg)	1–200	180 [a]

[a] Maximum at which the column is saturated with pentachlorophenol.

3.3. Selection of working conditions

Hydrodynamic and chemical variables affecting the flow system were studied by UV–visible absorbance measurements between 190 and 800 nm with a diode-array spectrophotometer. Table 1 shows the range and characteristics tested and the values selected for pentachlorophenol. The retention of pentachlorophenol from aqueous solutions in the microcolumn was evaluated at different pH values. At low pH (between 1 and 3), the retention was > 97%, whereas at pH 7 only 7% of the pentachlorophenol was retained. At pH > 9, the effluent on becomes yellow-orange with an absorbance maximum at 380 nm and pentachlorophenol is not retained in the microcolumn. Under the acidic retention conditions used, the phenols are not ionized and at least three types of interactions may be involved in the retention of the phenolic compounds: hydrogen-bonding, π–π and dispersion interactions.

The influence of the flow-rate on the retention of pentachlorophenol was evaluated between 0.4 and 2.9 ml min^{-1}. At flow-rates higher than 1.4 ml min^{-1} the retention decreased, being only of about 88% at 2.9 ml min^{-1}. For flow-rates between 0.4 and 1.4 ml min^{-1} the retention was higher than 98%; therefore, 1.4 ml min^{-1} was chosen for further studies.

Once the pH and flow-rate conditions for retention had been established, several parameters affecting the elution were studied. Several organic solvent–water mixtures were evaluated as eluents for pentachlorophenol. Ethanol–water and methanol–water mixtures produced a yellow effluent with maximum absorbance at 380 nm, which interfered, making the spectrophotometric evaluation of the eluate difficult. Acetone–water mixtures produced small bubbles in the system and hence gave rise to irreproducible results. Several acetonitrile–water mixtures were tested; a 50 + 50 mixture yielded only a recovery of 56%, whereas an 80 + 20 mixture yielded recoveries > 92%.

The effect of pH on elution with acetonitrile–water (80 + 20) was studied in the range 3–12. At pH < 3 the recovery was low, and at pH above 7 the effluent again became yellow-orange with maximum absorbance at 380 nm. At pH 3 the highest recovery (ca. 92%) was achieved. The elution flow-rate was studied between 0.4 and 1.3 ml min^{-1}; for flow-rates higher than 0.4 ml min^{-1} the recovery decreased, so this value was selected for further studies. In the elution process a well defined peak appeared, showing the good elution characteristics.

The maximum amount of pentachlorophenol retained by the column per gram of oxine–CPG was established as 180 μg. The breakthrough volume was determined by studying spectrophotometrically the recovery of 10 μg of pentachlorophenol in volumes between 10 and 500 ml. The volume of 100 ml was chosen as optimum because higher volumes yielded lower recoveries (71% was obtained for 250 ml).

To study the stability of the pentachlorophenol retained on the column, 100 ml of solution containing 20 μg of pentachlorophenol at pH 1 were pumped through the column. The column with the retained pentachlorophenol was kept in a refrigerator for 4 days; subsequently, pentachlorophenol was eluted with acetonitrile–water (80 + 20) at pH 3 and the recovery was > 98%. Under the conditions established, it was possible to use the column to make about ten determinations of pentachlorophenol with recoveries of ca. 96%. This behaviour shows the reversibility of the retention–elution process.

3.4. Analytical characteristics

The linear calibration range was 4.0–25 μg for a sample volume of 100 ml. The 3σ detection limit was 2.5 μg. The repeatability for use of one microcolumn, expressed as relative standard deviation, was 1.2% for 12 μg of pentachlorophenol (four determinations). The reproducibility between five different microcolumns for the same amount (12 μg) was 1.6%. A preconcentration factor of 250-fold was obtained for an initial sample volume of 100 ml (the final volume was about 0.4 ml).

3.5. Interferences

The effect of several metal ions on the peak height in the elution of pentachlorophenol was

studied. Metal ions such as aluminium, calcium and magnesium do not interfere in the determination of 20 μg of pentachlorophenol under the conditions established up to a concentration level of 100 μg ml^{-1}.

The influence of the presence of other phenols was studied; Table 2 shows the percentage retention of 20 μg of each phenol by the column under the conditions optimized for pentachlorophenol. The relationship between the structure of particular phenols and the retention is not clear, but the presence of chlorosubstituents results in higher retention; hence the retention of pentachlorophenol is higher than that of 2,4,6-trichlorophenol, and the retention of the latter is higher than that of 2,4-dichlorophenol. Retention of nitrophenols depends on the number of substituents and their relative positions in the aromatic ring. Nitrosubstituents in the *ortho* or *para* position results in substantially increased retention relative to 3-nitrophenol. However, an increase in the number of nitrosubstituents produced a decrease in retention. Further, the presence of a methyl group resulted in a greater electron density in the aromatic ring and hence π–π interactions, and also dispersion interactions, were enhanced. Indeed, 4,6-dinitro-2-methylphenol was more strongly retained than 2,4-dinitrophenol.

To study the selectivity, the effect of 10 μg of different chlorophenols, methylphenols and nitrophenols on the absorbance of 10 μg of pentachlorophenol at 302 nm was studied; the results were compared with those obtained by mixing solutions containing 10 μg of pentachlorophenol and 10 μg of the other phenols in a final volume of 10 ml under the chemical conditions proposed for the flow determination of pentachlorophenol (Table 3). Except for 2,4,6-trichlorophenol, the level of interference is clearly decreased owing to the different retentions of the individual phenols and the different absorption maxima, as can be seen in Table 2. Phenols such as 4-nitrophenol and 2-nitrophenol produce very a high absorbance but, owing to their retention by the column of oxine–CPG, the interference in the determination of pentachlorophenol is very low.

Table 2
Retention of different phenols in the oxine–CPG column

Phenol	λ(max) (nm)	Retention (%) [a]
2,4,6-Trichlorophenol	290	84.2
2,4-Dichlorophenol	286	6.1
2-Nitrophenol	348	44.4
3-Nitrophenol	326	9.3
4-Nitrophenol	282	43.8
2,4-Dinitrophenol	262	20.9
4-Chloro-3-methylphenol	280	14.0
4,6-Dinitro-2-methylphenol	272	46.7
2,4-Dimethylphenol	276	24.0

[a] Under the same conditions as pentachlorophenol.

Table 3
Influence of different phenols on the spectrophotometric determination of pentachlorophenol

Phenol	Interference (%)	
	Without column	In the proposed flow method
2,4,6-Trichlorophenol	8.0	6.0
2,4-Dichlorophenol	–	–
4-Chloro-3-methylphenol	–	–
2,4-Dinitrophenol	62	15
4,6-Dinitro-2-methylphenol	37	14
4-Nitrophenol	481	–
3-Nitrophenol	83	–
2-Nitrophenol	66	18
2,4-Dimethylphenol	–	–

4. Conclusions

Oxine immobilized on CPG shows a good ability to preconcentrate pentachlorophenol. Oxine–CPG can be packed in a microcolumn and used in flow systems, allowing preconcentration and further spectrophotometric determination of pentachlorophenol at low concentrations. The stability of the material makes the off-line sampling and later determination in the laboratory possible. In addition, the immobilization procedure is inexpensive and simple.

5. Acknowledgements

The financial support of the Spanish DGICYT, project PB89-109, is gratefully acknowledged.

6. References

[1] R.G. Melcher, D.W. Bakke and G.H. Hughes, Anal. Chem., 64 (1992) 2258.
[2] T. Öberg and J. Berström, Chemosphere, 19 (1989) 337.
[3] E. Rodríguez-Gonzalo, J.L. Pérez-Pavón, J. Ruzicka and G.D. Christian, Anal. Chim. Acta, 259 (1992) 37.
[4] Environmental Protection Agency, Manual of Methods for Chemical Analysis of Water and Wastes, Office of Technology Transfer, Washington, DC, 1974.
[5] G.W. Patton, L.L. McConnell, M.T. Zaranski and T.F. Bidleman, Anal. Chem., 64 (1992) 2858.
[6] G. Persaud and F.F. Cantwell, Anal. Chem., 64 (1992) 89.
[7] P.Y.T. Chow and F.F. Cantwell, Anal. Chem., 60 (1988) 1569.
[8] M.R. Weaver and J.M. Harris, Anal. Chem., 61 (1989) 1001.
[9] M.-S. Kuo and H.A. Mottola, Anal. Chim. Acta, 120 (1980) 255.
[10] G.J. Shahwan and J.R. Jerozek, J. Chromatogr., 256 (1983) 39.
[11] M.A. Marshall and H.A. Mottola, Anal. Chem., 55 (1983) 2089.

ELSEVIER

Analytica Chimica Acta 288 (1994) 265–269

ANALYTICA CHIMICA ACTA

Determination of escin based on its inhibitory action on lactose crystallization

F. Grases *, L. García-Ferragut, A. Costa-Bauzá, R. Prieto, J.G. March

Department of Chemistry, University of Balearic Islands, 07071 Palma de Mallorca, Spain

(Received 5th April 1993)

Abstract

A sensitive and simple kinetic turbidimetric method for the determination of escin, based on its inhibitory action on the crystallization of lactose, is presented. Supersaturated solutions of lactose were prepared by addition of acetone to a stable aqueous lactose solution. The induction period of the crystallization process was measured turbidimetrically in the absence and presence of escin. The method was applied to the determination of escin in pharmaceutical products.

Key words: Turbidimetry; Crystallization; Escin; Lactose; Pharmaceuticals

1. Introduction

The crystallization of organic substances is affected by the presence of traces of other organic molecules with chemical structures partly identical with or only slightly different from that of the bulk component of the crystal [1]. These effects must be assigned to the selective interaction of the foreign molecule at specific points of the crystallizing substance, causing marked changes in the crystallization rate. These processes are highly sensitive and selective and for this reason they have found application in analytical chemistry [2–6]. These processes permit an appropriate substrate to be designed to be used to determine a given analyte. In this work, lactose was used as the crystallizing substrate to determine escin, a saponin commonly found in plants with diverse applications in pharmaceutical preparations and cosmetics.

To date, the most common methods for the determination of escin involve chromatographic procedures, and thin-layer chromatographic [7–9] and liquid chromatographic [10,11] methods have been described. A radioimmunoassay has also been proposed [12].

2. Experimental

2.1. Reagents

Saccharides were purchased from Sigma, escin from Fluka and the solvents (ethanol, propan-2-ol and acetone) from Merck. Solutions of lactose

* Corresponding author.

SSDI 0003-2670(93)E0617-G

and escin were prepared weekly in doubly distilled water and stored in a refrigerator.

2.2. Apparatus

Turbidimetric measurements were performed using a Metrohm Model 662 photometer equipped with a light-guide measuring cell and using monochromatic light (500 nm). The crystallization processes were carried out in a cylindrical glass flask (height 5 cm, diameter 2.4 cm) that was magnetically stirred (500 rpm) and maintained at constant temperature (25 ± 0.2°C). The absorbance–time curve was printed by a chart recorder.

2.3. Procedure

A 0.020-ml volume of 23.75 g l^{-1} lactose, escin solution as necessary for a final concentration between 0.1 and 0.6 μg ml^{-1} and water to achieve a volume of 0.150 ml were placed in the crystallization flask, Then 12 ml of acetone were added and the chart recorder and magnetic stirrer were switched on. From the resulting absorbance–time curve (see Fig. 5), the induction period (time elapsed before absorbance began to increase due to the appearance of solid phase) was measured and used to prepare the calibration graph. Each measurement took ca. 5 min.

2.4. Application

To test the applicability of the proposed method, it was applied to the determination of escin in pharmaceutical products. The following previous treatments were performed:

(a) Circovenil fuerte (Wyeth-Orfi) in tablet form was first ground, then the powder was maintained in aqueous suspension for 2 h and finally filtered (0.45 μm) before analysis after appropriate dilution.

(b) Feparil (Madaus Cerafarm), lyophilized: an aqueous solution of the lyophilized sample was used for determination.

(c) Uralyt Urato (Madaus Cerafarm), granulated: owing to the presence of salts (as sodium citrate) in this product and in order to avoid crystallization of such salts on adding acetone, the escin was extracted from the granulated material with acetone for 2 h, the suspension was centrifuged, then the method was applied to a diluted sample. Considering the solubility of escin in acetone, total extraction was assumed.

3. Results and discussion

On the basis of structural analogies between lactose and escin (see Fig. 1), and considering that lactose is a common commercially available sugar, it was selected as the precipitating substrate to determine escin. Supersaturated solutions of lactose were obtained by changing the solvent composition. Thus, the addition of an organic solvent to stable aqueous solutions of this sugar allowed unstable supersaturated solutions to be obtained. Several organic solvents were used for comparison. As can be seen in Fig. 2, the precipitation curve obtained when acetone was used as an organic solvent was the best for analytical purposes. Hence the induction period was easily measured when this solvent was used in the presence of low concentrations of lactose. When ethanol or propan-2-ol was used, however, a high concentration of lactose was necessary to obtain precipitation, so that the induction period was

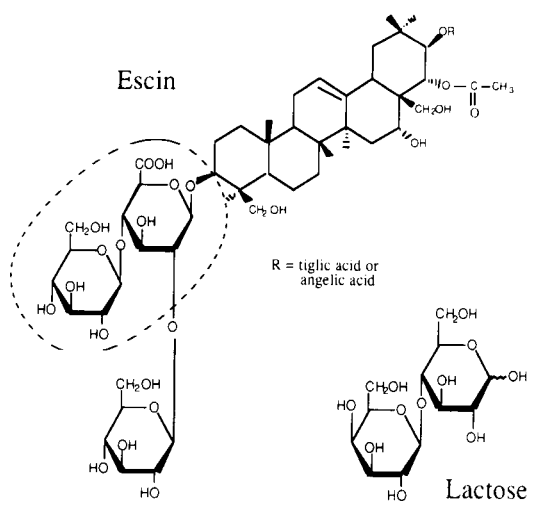

Fig. 1. Structures of lactose and escin.

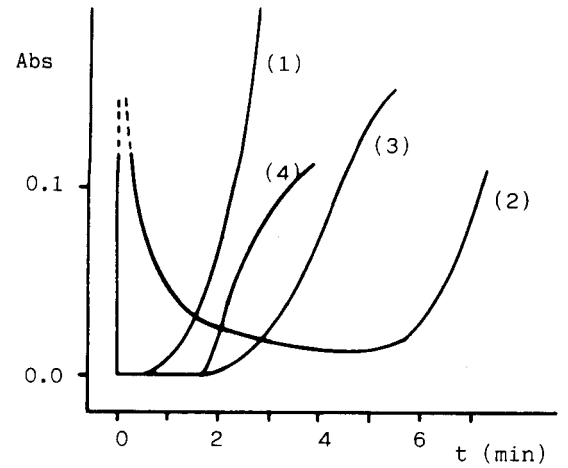

Fig. 2. Turbidimetric curves (absorbance vs. time) corresponding to lactose precipitation from supersaturated solutions under different conditions. Temperature, 25°C; stirring rate, 500 rpm. Curves: 1 = 1180 μg ml^{-1} lactose, solvent ethanol–water (99.17 + 0.83, v/v); 2 = 1180 μg ml^{-1} lactose, solvent propan-2-ol–water (99.17 + 0.83, v/v); 3 = 98 μg ml^{-1} lactose, solvent acetone–water (99.17 + 0.83, v/v); 4 = 39 μg ml^{-1} lactose, solvent acetone–water (98.77 + 1.23 v/v).

evaluated with greater difficulty. Consequently, acetone was chosen as the solvent.

3.1. Study of the variables

In order to select optimum conditions for the determination of escin, the influence of several variables on the inhibitory effect of escin on the crystallization of lactose was studied: concentration of the precipiting substrate, acetone–water relationship, temperature and stirring rate.

Fig. 3 shows the influence of percentage of water on the precipitation of lactose. As can be seen, in both the absence and presence of escin, the induction periods were longer when a higher percentage of water was present. Nevertheless, the inhibitory effect of escin (difference between curves 1 and 2) was slightly affected by the percentage of water and 1.23% of water was chosen as the optimum because slight variations in water content at this value did not significantly influence the results.

The initial lactose concentration clearly affected the inhibitory action of escin on lactose precipitation (Fig. 4). Thus, the lower the concentration of lactose, the greater was the inhibitory action of escin. This can be explained considering that by increasing the amount of the crystallized phase the number of specific points on the crystallizing substance to which the inhibitor can bind is increased, and consequently the sensitivity of the inhibitory action would decrease. A 39 μg ml^{-1} concentration of lactose was chosen as optimum. No lower lactose concentrations were tested because of the problems of detection of the solid phase, as under such conditions only small amounts of lactose are precipitated.

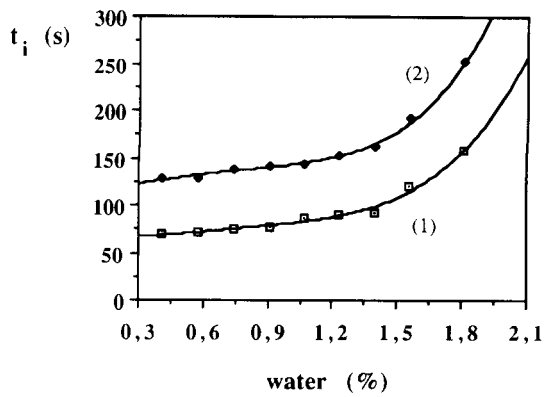

Fig. 3. Influence of the water–acetone composition on the induction period when precipitating 39 μg ml^{-1} lactose. Temperature, 25°C; stirring rate, 500 rpm. (1) In the absence of escin; (2) in the presence of 0.29 μg ml^{-1} escin.

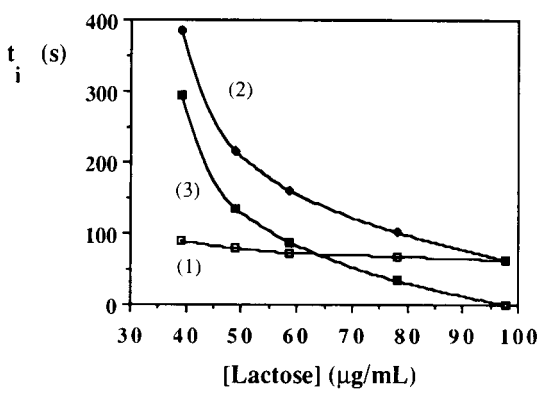

Fig. 4. Influence of the concentration of lactose on the inhibition of the escin in 98.77% acetone. (1) In the absence of escin; (2) in the presence of 0.29 μg ml^{-1} escin; (3) difference between (2) and (1). Temperature, 25°C; stirring rate, 500 rpm.

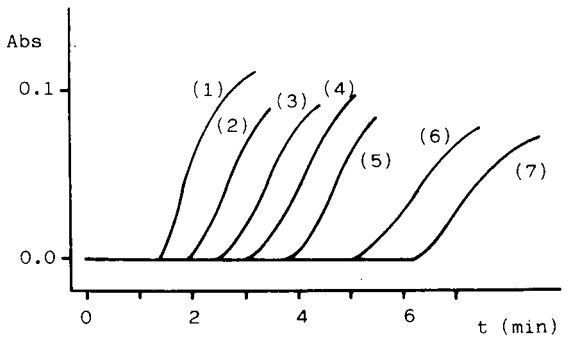

Fig. 5. Turbidimetric curves (absorbed light vs. time) corresponding to precipitation of 39 μg ml^{-1} lactose in 98.77% acetone in the absence and presence of escin. Temperature, 25°C; stirring rate, 500 rpm. Escin concentration (μg ml^{-1}): (1) 0; (2) 0.10; (3) 0.19; (4) 0.29; (5) 0.38; (6) 0.48; (7) 0.57.

No significant influence of temperature (in the range 20–30°C) and stirring rate (200–600 rpm) were observed, but both should be kept constant during analysis in order to avoid unexpected variations.

3.2. Characteristics of the method

In order to obtain the calibration graph, absorbance–time curves (Fig. 5) obtained under selected conditions and in the presence of different amounts of escin were used. A plot of the logarithm of the induction period versus escin concentration was linear, having a least-squares regression with the following equation:

$$\ln t_i - \ln t_i^0 = 0.019 + 2.442[\text{escin}]$$

where t_i (s) is the induction period in the presence and t_i^0 that in the absence of escin and [escin] is the escin concentration in μg ml^{-1}. It was considered that the induction period was the time necessary for the formation of the solid phase to be detectable. The correlation coefficient was 1.00 ($n = 6$).

Table 1
Tolerance levels for several saccharides in the determination of 0.29 μg ml^{-1} escin

Saccharide	Maximum tolerated amount (μg/ml) [a]
Fructose, galactose	25 [b]
Glucose	16
Lactose	3
Melibiose	2.5
Sucrose, trehalose, maltose	2
Raffinose	1.5
Stachyose	0.1

[a] Error $\leqslant$ 2.5%.
[b] Highest assayed amount.

Reproducibility was evaluated from eight replicates of the reference (without escin) and ten replicates of a sample containing 0.29 μg ml^{-1} escin. The standard errors were 1.83% and 2.99%, respectively.

To evaluate the selectivity of the proposed method, the effects of several saccharides whose chemical structures were related to lactose were studied in order to establish the tolerance levels (Table 1). As can be seen, the tested substances, depending on the concentration, exerted some inhibitory effects, thus giving positive interferences. In contrast, additional lactose produced a diminution of the induction period, and thus gave a negative interference.

It is interesting to observe how the inhibitory capacity of the saccharides (interferences) is related to their structural complexity, in the sequence monosaccharide < disaccharide < trisaccharide < tetrasaccharide, likewise demonstrating that when a moiety of the inhibitor sub-

Table 2
Determination of escin in pharmaceutical products

Product	Calibration graph [a] (%)	Standard addition (%)	Reported (%)
Circovenil fuerte (Wyerth-Orfi)	3.7 ± 0.1	3.9	4.0
Feparil (Madaus Cerafarm)	101.0 ± 1.2	99.4	100.0
Uralyt Urato (Madaus Cerafarm)	0.033 ± 0.0004	0.035	0.039

[a] Average of five determinations.

stance is identical with or very similar to the bulk component of the crystallizing substance, its inhibitory action increases with increasing the complexity and molecular weight of the complementary part.

3.3. Application

The results obtained using direct calibration and standard addition methods for each pharmaceutical sample are given in Table 2. The determined values are in good accordance with the reported concentrations.

4. Acknowledgements

Financial support by the Dirección General de Investigación Científica y Técnica (grant PB 92-0249) is gratefully acknowledged.

References

[1] L. Addadi, Z. Berkovitch-Yellin, I. Weissbuch, J. van Mil, L.J.W. Shimon, M. Lahav and L. Leiserowitz, Angew. Chem., Int. Ed. Engl., 24 (1985) 466.
[2] F. Grases and P. March, Anal. Chim. Acta, 219 (1989) 89.
[3] F. Grases, A. Costa-Bauzá and J.G. March, Analyst, 116 (1991) 59.
[4] F. Grases and J.G. March, Trends Anal. Chem., 10 (1991) 190.
[5] F. Grases, A. Costa-Bauzá and J.G. March, Analusis, 21 (1993) 95.
[6] F. Grases and C. Genestar, Talanta, 40 (1993) 1589.
[7] E. Uberti, E.M. Martinelli and G. Pifferi, Fitoterapia, 61 (1990) 57.
[8] B. Renger, K. Wenz and W. Ziegenbalg, Lab. 2000, 2 (1988) 12.
[9] B. Renger, J. Planar Chromatogr. Mod. TLC, 3 (1990) 160.
[10] M. Burnouf-Radosevich and N.E. Delfel, J. Chromatogr., 368 (1986) 433.
[11] N. Picerno, Cosmet. Toiletries, 11 (1990) 50.
[12] T. Lehtola and A. Huhtikangas, J. Immunoassay, 11 (1990) 17.

ELSEVIER

Analytica Chimica Acta 288 (1994) 271–278

ANALYTICA CHIMICA ACTA

Ionization constants of pH reference materials in acetonitrile–water mixtures up to 70% (w/w)

J. Barbosa *, J.L. Beltrán, V. Sanz-Nebot

Department of Analytical Chemistry, University of Barcelona, Avda. Diagonal 647, 08028 Barcelona, Spain

(Received 13th August 1993; revised manuscript received 21st October 1993)

Abstract

Ionization constants of pH reference materials in acetonitrile–water mixtures containing 30, 40, 50 and 70% (w/w) acetonitrile were obtained. The ionization constant values determined were: pK_1 and pK_2 for tartaric and phthalic acid; pK_1, pK_2 and pK_3 for citric acid and pK_1 for boric and acetic acid. These values are essential to determine the standard reference value, pH_S, for various standard reference buffer solutions. In the total composition range studied, pK values were linearly correlated with the mol fraction of acetonitrile and with the reciprocal of the dielectric constant of solvent mixtures. Considering the unlimited number of solvent mixtures, a multilinear regression procedure was applied to correlate pK values with % (w/w) and % (v/v) of acetonitrile, and the methodology of linear solvation energy relationships (LSERs) was used to relate pK data with solvatochromic parameters of acetonitrile–water mixtures.

Key words: Ionization constants; Reference materials, pH; LSERs

1. Introduction

Nowadays, reversed-phase liquid chromatography (RPLC) seems to be the most popular technique for the separation of ionogenic substances. In addition to other advantages, this effective technique uses readily available and inexpensive polar mobile phases, mainly mixtures of water with methanol or acetonitrile as organic solvents. However, it must be emphasized that the interpretation of the ionization effect in non-aqueous mobile phases, such as acetonitrile–water mixtures, is difficult because of many problems connected with the pH measurements in the solvent systems and the lack of ionization constant data, pK, in these media [1,2].

Usually, interpretation of chromatographic behaviour of substances is made assuming that the pH and pK data used for the mobile phase are the same as, or linearly correlated with, those in the aqueous fraction, in which case errors due to medium effects [3] contribute to the uncertainty in the true pH and pK values. In acetonitrile–water mixtures, considerable variations can be observed and pH and pK values cannot be as-

* Corresponding author.

SSDI 0003-2670(93)E0606-8

sumed to be independent or linearly correlated with composition of solvent mixtures [2,4].

Determination of accurate pH values of standard reference solutions is the key to solving pH measurement problems in aqueous–organic solvent mixtures such as acetonitrile–water [3,5]. The following internationally recognized operational equation is used for electrometric pH measurements [6]:

$$pH_X = pH_S + \frac{E_S - E_X}{g}$$

where E_X and E_S denote the emf measurements made in cell A on the sample solutions at unknown pH_X and on the standard buffer at known pH_S, and $g = (\ln 10)RT/F$.

The composition of cell A can be described as: Reference electrode | Salt bridge | Sample solution at pH_X or buffer solution at pH_S in acetonitrile–water | H^+-responsive electrode.

Ionization constant values for the involved equilibria of pH reference materials in acetonitrile–water mixtures are necessary to assign reference pH values to standard buffer solutions in acetonitrile–water mixtures.

pK values of pH reference materials in acetonitrile–water mixtures up to 70 wt.%, which is the upper limit for the absence of ionic association in such mixed solvents [7], were hitherto missing, although pK_1 values for phthalic acid are available in the literature [4], and pK_2 values for phosphoric acid in acetonitrile–water mixtures and pK values of different pH reference materials in 10% acetonitrile–water mixtures were determined previously work [2,8]. These pK values can give valuable information concerning the behaviour of substances in acetonitrile–water mobile phases used in RPLC and permit evaluations of pH_S standards for pH measurements in these solvents.

The present work concerns the determination of pK values of pH reference materials [9] in 30, 40, 50 and 70% (w/w) acetonitrile–water mixtures according to the rules and procedures recently endorsed by IUPAC [5]. The ionization constant values determined in the present work were: pK_1 and pK_2 for tartaric and phthalic acid; pK_1, pK_2 and pK_3 for citric acid and pK_1 for boric and acetic acid. These are the required pK values for subsequent standard pH_S evaluations. Also, in order to obtain pK values in whichever of the unlimited number of the possible binary solvent acetonitrile–water mixtures, relationships between pK values and different characteristics of the solvent mixtures were examined and the methodology of linear solvation energy relationships (LSERs) [2,10,11] were used to correlate pK values with solvent dipolarity/polarizability (π^*), solvent hydrogen bond donating acidity (α) and solvent hydrogen bond accepting basicity (β).

2. Experimental

2.1. Apparatus

emf values for the potentiometric cell were measured with a CRISON 2002 potentiometer (± 0.1 mV) using a Radiometer G202C glass electrode and a Ag/AgCl reference electrode prepared according to the electrolytic method [12]. In the experimental work described, three different Radiometer G202C glass electrodes were used in acetonitrile–water media and the obtained pK results did not differ significantly. Obviously, changing the glass electrode involves a new standardization of the potentiometric cell [12]. The glass electrodes were stored in water when not in use and soaked for 15–20 min in acetonitrile–water before potentiometric measurements.

The reference electrode was stable for three months of continuous work and during the whole time the standard potential, $E°$, remained essentially constant (standard deviation, $s < 1.3$ mV).

The stabilization criterion for the emf readings was a stability of 0.2 mV within 150 s; if the stabilization was not achieved after 20 min, a new addition of titrant was made. The system gave stable and reproducible potentials within 5 min.

The cell was thermostated externally at 25 ± 0.1°C. The potentiometric assembly was automatically controlled with a PC microcomputer.

2.2. Reagents

Analytical reagent grade chemicals either from Merck (pro analysi) or Carlo Erba (RPE grade) were used. Stock 0.1 M potassium hydroxide (Carlo Erba, RPE) solutions were prepared with an ion-exchange resin [13] to avoid carbonation and were standardized titrimetrically with potassium hydrogenphthalate. While using 70% (w/w) acetonitrile–water, the concentration of KOH solutions was 0.02 M because of lower solubility in the mixture. All the solutions were prepared by mixing doubly distilled freshly boiled water and acetonitrile (Merck, chromatography grade)

2.3. Procedures

The pK values have been determined from titration of appropriate solutions of acid species of the buffer in 30, 40, 50 and 70% (w/w) acetonitrile–water mixtures using KOH solutions in the same solvent as the titrant and approximately 5×10^{-4} M KCl solution for the correct response of electrode system. pK values as proscribed by IUPAC specific standardization rules [9] have been obtained from systematic measurements of the emf of cell B: Pt | Ag | AgCl | HA + A + KCl in acetonitrile–water | Glass electrode (GE). HA and A are the acidic and basic species respectively involved in the dissociation equilibrium studied. A typical cell for determination of pK_1 and pK_2 values of tartaric acid with the mixed electrolyte is cell C: Pt | Ag | AgCl | Tartaric acid + potassium hydrogentartrate + KCl in acetonitrile–water | GE. The key Nernstian function of the reversible emf E values of cell B is:

$$(E^\circ - E)/g = \mathrm{p}(a_{H^+}a_{Cl^-}) = \mathrm{pH} + \mathrm{p}a_{Cl^-} \qquad (1)$$

where $g = (\ln 10)RT/F$. Eq. 1 requires knowledge of the relevant values of the standard emf E° of cell B; these E° values covering acetonitrile–water mixtures containing up to 70% (w/w) acetonitrile at 298.15K were determined as previously [12]. Taking into account the general expression for the dissociation equilibria studied

$$K = \frac{c_A y_A c_{H^+} y_{H^+}}{c_{HA} y_{HA}} \qquad (2)$$

the functional Eq. 3, which permits pK calculation, is obtained:

$$\frac{E^\circ - E}{g} + \log\frac{c_{HA} y_{HA} c_{Cl^-} y_{Cl^-}}{c_A y_A} = \mathrm{p}K \qquad (3)$$

where c_{HA} and c_A are the molar concentrations of acidic and basic species respectively, and c_{Cl^-} is the molar concentration of the mixed electrolyte KCl, and y_x the molar activity coefficient of species x.

In cases of p$K < 5$ computation of c_{HA} and c_A values required knowledge of c_{H^+} which is in turn function of the molar activity coefficients y, and this can be calculated through an extrathermodynamic assumption, i.e., a form of the classical Debye-Hückel equation,

$$py = \frac{AI^{1/2}}{(1 + a_o BI^{1/2})} \qquad (4)$$

where A and B are the Debye-Hückel constants, a_o is the ion size parameter in the solvent mixture and I is the ionic strength.

In compliance with IUPAC rules [5,14] the value of the $a_o B$ product in Eq. 4 is assigned at temperature $T = 298.15$K by an extension of the Bates-Guggenheim convention [5,6], in terms of

$$(a_o B)_T = 1.5(\epsilon^W \rho^S / \epsilon^S \rho^W)_T^{1/2} \qquad (5)$$

where ϵ is the dielectric constant, ρ the density and the superscripts W and S refer to pure water and to the appropriate solvent mixture, respectively. All these quantities have been reported previously [2,12].

Calculation of py_{Cl^-} through Eq. 4 requires knowledge of the ionic strength I of the HA + A + KCl mixed electrolyte solution, but I is, in turn, a function of the H^+ concentration, c_{H^+} which is expressed by

$$\mathrm{p}c_{H^+} = \frac{E^\circ - E}{g} - \mathrm{p}c_{Cl^-} - \mathrm{p}(y_{H^+} y_{Cl^-}) \qquad (6)$$

Thus, determination of pK values requires an iterative cycle for each point of the potentiometric titration at which E is measured.

Initially one takes $I = c_A + c_{Cl^-}$ and obtains y_{Cl^-} values by Eq. 4, for their subsequent insertion in Eq. 6 to obtain $\mathrm{p}c_{H^+}$ values and a better

value of I and so on, until constancy of I values is obtained.

The two equilibria of phthalic acid can be independently considered but this is definitely not the case for tartaric and citric acid, whose equilibria overlap, and to carry out their pK value calculations, it is not possible to neglect the rest of the ionization constant values.

In order to determine pK_1 and pK_2 values for tartaric acid and pK_1, pK_2 and pK_3 values for citric acid a program in PASCAL, pKPOT, is used [8,15].

3. Results and discussion

Different emf measurement series for cell B and pK calculations from Eq. 3 at various concentrations of acidic, HA, and basic, A, species were made for each reference material [6] studied

Table 1
pK values of acetic and boric acid in 30% (w/w) acetonitrile–water

Acetic acid						
V_o	V_e	C_t	[KCl]	E^o	pH	pK_a
20	1.31	0.0994 M	3.67×10^{-4} M	426.57		
V	E	[HA] ($\times 10^{-3}$ M)	[A] ($\times 10^{-3}$ M)	y		
0.10	−48.9	5.96	0.52	0.958	4.56	5.66
0.20	−66.8	5.45	0.99	0.949	4.85	5.64
0.30	−79.2	4.94	1.48	0.942	5.06	5.63
0.40	−89.1	4.43	1.96	0.936	5.22	5.63
0.50	−97.9	3.92	2.43	0.930	5.36	5.63
0.60	−105.9	3.42	2.90	0.925	5.49	5.63
0.70	−113.8	2.93	3.36	0.920	5.61	5.62
0.80	−122.0	2.44	3.82	0.916	5.74	5.63
0.90	−130.9	1.95	4.28	0.912	5.89	5.63
1.00	−141.3	1.47	4.73	0.909	6.06	5.63
1.10	−154.9	0.99	5.18	0.906	6.28	5.65
						pK_a = 5.63
						s = 0.01
						n = 11

Boric acid						
V_o	V_e	C_t	[KCl]	E^o	pK_{ap}	pK_a
20	1.65	0.0994 M	3.67×10^{-4} M	426.57	14.97	
V	E	[HA] ($\times 10^{-3}$ M)	[A] ($\times 10^{-3}$ M)	y	pH	
0.10	−320.2	7.67	0.49	0.959	9.17	10.38
0.20	−339.6	7.14	0.98	0.950	9.49	10.37
0.30	−352.2	6.61	1.47	0.942	9.70	10.38
0.40	−361.9	6.09	1.95	0.936	9.86	10.38
0.50	−369.8	5.58	2.42	0.930	9.98	10.38
0.60	−376.9	5.07	2.90	0.925	10.10	10.38
0.70	−383.6	4.56	3.36	0.920	10.21	10.38
0.80	−390.0	4.06	3.82	0.916	10.31	10.38
0.90	−396.1	3.57	4.28	0.912	10.41	10.37
1.00	−402.3	3.08	4.73	0.909	10.51	10.37
1.10	−408.2	2.59	5.18	0.905	10.61	10.35
1.20	−414.6	2.11	5.63	0.902	10.71	10.33
1.30	−421.2	1.63	6.07	0.899	10.82	10.30
						pK_a = 10.36
						s = 0.02
						n = 13

Table 2
pK values of pH reference materials in acetonitrile–water mixtures up to 70% at 298.15K (values in parentheses are standard deviations, $30 < n < 60$)

Substance		% (w/w) of acetonitrile					
		0	10	30	40	50	70
Tartaric acid	pK_1	3.03	3.27 (0.02)	3.73 (0.01)	4.00 (0.01)	4.29 (0.02)	5.17 (0.02)
	pK_2	4.36	4.57 (0.01)	5.02 (0.04)	5.30 (0.05)	5.57 (0.02)	6.52 (0.03)
Citric acid	pK_1	3.13	3.40 (0.05)	3.81 (0.03)	4.06 (0.03)	4.31 (0.02)	5.00 (0.03)
	pK_2	4.76	5.01 (0.03)	5.50 (0.03)	5.81 (0.02)	6.08 (0.02)	7.03 (0.04)
	pK_3	6.40	6.68 (0.04)	7.29 (0.02)	7.63 (0.02)	7.91 (0.03)	8.86 (0.02)
Boric acid	pK_1	9.24	9.57 (0.05)	10.40 (0.04)	10.81 (0.03)	11.25 (0.03)	11.84 (0.09)
Phthalic acid	pK_1	2.95	3.15 (0.02)	3.60 (0.03)	3.82 (0.03)	4.08 (0.03)	4.77 (0.02)
	pK_2	5.41	5.77 (0.04)	6.86 (0.03)	7.31 (0.02)	7.75 (0.02)	9.06 (0.04)
Acetic acid	pK_1	4.75	4.97 (0.04)	5.63 (0.03)	5.99 (0.02)	6.41 (0.03)	7.57 (0.03)

in 30, 40, 50 and 70 wt.% acetonitrile–water mixtures.

To simplify the tabulation and as an example, emf experimental values for only one titration of acetic acid and one titration of boric acid in 30% (w/w) acetonitrile–water are shown in Table 1, where V_0 is the initial solution volume, V_e the equivalence volume, c_t the titrant concentration, [KCl] the initial KCl concentration and E^0 the standard emf of the cell. For each point of titration, E is the emf value measured, [HA] the concentration of acidic species, [A] the concentration of basic species and y the molar activity coefficient. The ionization constant values determined for the involved equilibria for pH standard reference solutions in 30, 40, 50 and 70% (w/w) acetonitrile–water are collected in Table 2, together with the literature pK values in water [16,17] and the pK values determined previously in acetonitrile–water with 10% (w/w) acetonitrile content [8].

Because of the very large number of possible acetonitrile–water mixtures, determination of pK values at each distinct solvent composition would mean an unlimited number of potentiometric measurements. So, in order to predict the pK

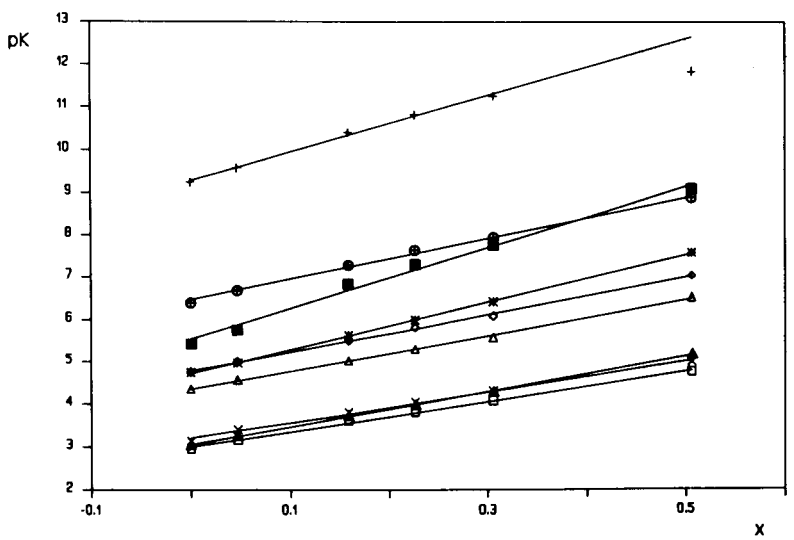

Fig. 1. Plot of pK values vs. the mol fraction of acetonitrile, x. (□) pK_1 and (■) pK_2 for phthalic acid; (▲) pK_1 and (△) pK_2 for tartaric acid; (+) pK_1 for boric acid; (×) pK_1, (◇) pK_2 and (crossed circle) pK_3 for citric acid; (*) pK_1 for acetic acid.

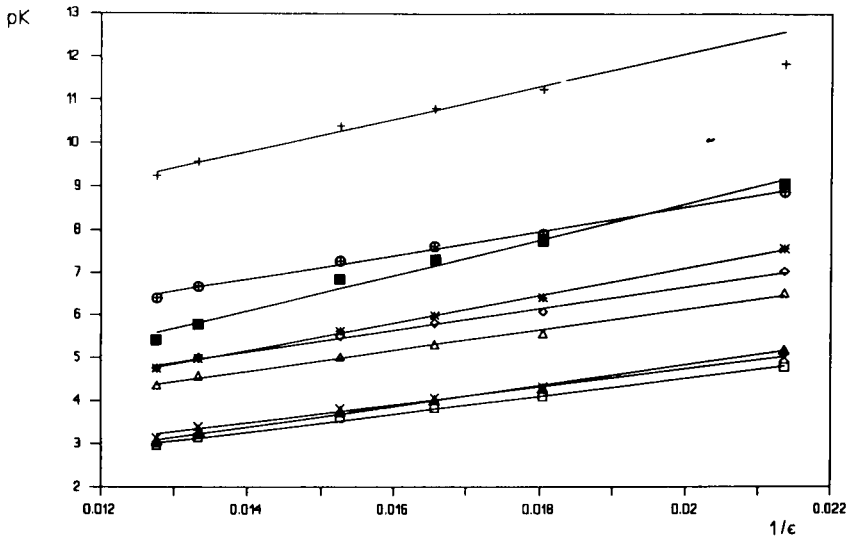

Fig. 2. Plot of pK values vs. the reciprocal of the relative permittivity of solvent mixture, $1/\epsilon$. Key to symbols as in Fig. 1.

values in all the possible acetonitrile–water mixtures up to a percentage of acetonitrile of 70% (w/w), relationships between the different sets of results and the solvent mixtures properties have been studied.

Thus, pK values were plotted against the mol fraction of acetonitrile x, $1/\epsilon$ values and π^* values, which are known over the entire range of composition [11,12]. Plot of pK values against the mol fraction of acetonitrile (Fig. 1) or against the values of the reciprocal of the relative permittivity (Fig. 2) of the solvent mixture, show linear relationships over the whole experimental range of acetonitrile content studied. This fact and the unlinearity showed by the plots of solvatochromic parameters (α, ß and E_T^N) vs. pK values, suggests

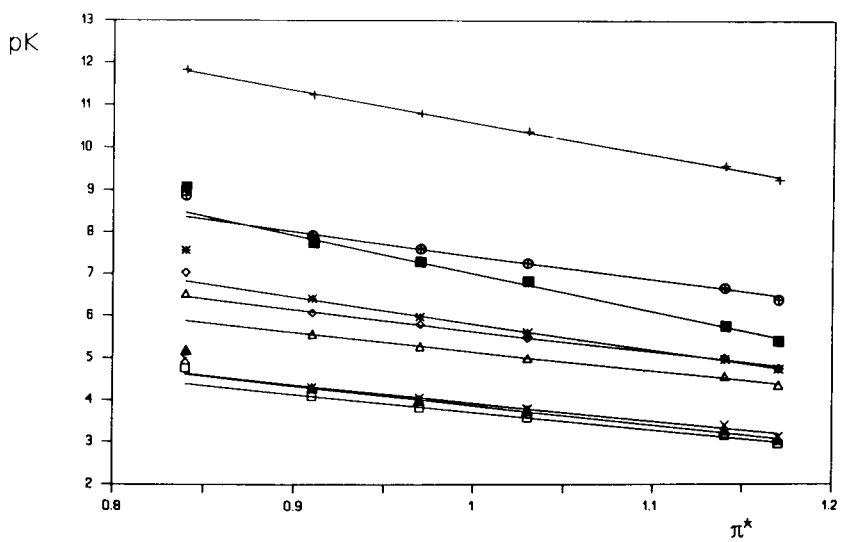

Fig. 3. Plot of pK values vs. Kamlet-Taft π^* polarizability-dipolarity parameters of solvent mixtures. Key to symbols as in Fig. 1.

Table 3
Equations corresponding to plots of pK values vs. mol fraction, x, vs. the reciprocal of the dielectric constant, $1/\epsilon$, and vs. the Kamlet-Taft solvatochromic parameter, π^* (correlation coefficient r refers to 6 data points)

Substance	pK against x		pK against $1/\epsilon$		pK against π^*	
Tartaric acid	$pK_1 = 3.05 + 4.16x$	$r = 0.999$	$pK_1 = 0.02 + 240.19/\epsilon$	$r = 0.998$	$pK_1 = 8.54 - 4.67\pi^*$	$r = 0.998$
	$pK_2 = 4.35 + 4.21x$	$r = 0.999$	$pK_2 = 1.29 + 242.67/\epsilon$	$r = 0.997$	$pK_2 = 9.69 - 4.53\pi^*$	$r = 0.999$
Citric acid	$pK_1 = 3.20 + 3.62x$	$r = 0.998$	$pK_1 = 0.57 + 208.56/\epsilon$	$r = 0.996$	$pK_1 = 8.25 - 4.32\pi^*$	$r = 0.995$
	$pK_2 = 4.78 + 4.42x$	$r = 0.999$	$pK_2 = 1.57 + 254.64/\epsilon$	$r = 0.998$	$pK_2 = 10.59 - 4.95\pi^*$	$r = 0.998$
	$pK_3 = 6.46 + 4.82x$	$r = 0.998$	$pK_3 = 2.95 + 278.25/\epsilon$	$r = 0.996$	$pK_3 = 13.14 - 5.73\pi^*$	$r = 0.997$
Acetic acid	$pK_1 = 4.73 + 5.59x$	$r = 0.999$	$pK_1 = 0.66 + 322.48/\epsilon$	$r = 0.999$	$pK_1 = 12.09 - 6.27\pi^*$	$r = 0.999$
Boric acid	$pK_1 = 9.27 + 6.67x$	$r = 0.998$	$pK_1 = 4.49 + 379.55/\epsilon$	$r = 0.994$	$pK_1 = 18.18 - 7.60\pi^*$	$r = 0.999$
Phthalic acid	$pK_1 = 2.99 + 3.57x$	$r = 0.999$	$pK_1 = 0.39 + 205.86/\epsilon$	$r = 0.998$	$pK_1 = 7.93 - 4.22\pi^*$	$r = 0.998$
	$pK_2 = 5.53 + 7.21x$	$r = 0.995$	$pK_2 = 0.28 + 416.11/\epsilon$	$r = 0.993$	$pK_2 = 16.05 - 9.03\pi^*$	$r = 0.997$

that the electrostatic interactions are more important in these mixtures than any other solute–solvent interaction, as those derived from hydrogen-bond formation and those derived from modifications in the solvation shell with varying solvent composition.

If the results obtained for pK values are plotted against the π^* values (Fig. 3) linear relationships only up to acetonitrile contents around 50% (w/w) are seen, but for higher acetonitrile contents linearity is lost. This fact is in accordance with the interpretation of Cheong and Carr [11]. The changes in observed π^* values operate through the dielectric properties of the local medium around the solute, but there is a significant qualitative similarity in the shape of the plots of π^* and $1/\epsilon$ vs. composition in acetonitrile–water mixtures up to an acetonitrile content of 50% (w/w).

Table 3 shows the equations for all the linear relationships obtained, together with their linear regression coefficients. For boric acid, the pK value at 70% (w/w) acetonitrile, has not been included in the equation calculations because of

Table 4
Relationships between pK values and weight, w, and volume, v, percentages of acetonitrile in admixtures with water (r as in Table 3)

Substance		
Tartaric acid	$pK_1 = 3.06 + 1.51 \times 10^{-2}w + 2.10 \times 10^{-4}w^2$	$r = 0.999$
	$pK_1 = 3.07 + 8.46 \times 10^{-3}v + 2.43 \times 10^{-4}v^2$	$r = 0.998$
	$pK_2 = 4.39 + 1.24 \times 10^{-2}w + 2.52 \times 10^{-4}w^2$	$r = 0.998$
	$pK_2 = 4.40 + 5.86 \times 10^{-3}v + 2.80 \times 10^{-4}v^2$	$r = 0.997$
Citric acid	$pK_1 = 3.16 + 1.77 \times 10^{-2}w + 1.18 \times 10^{-4}w^2$	$r = 0.999$
	$pK_1 = 3.17 + 1.16 \times 10^{-2}v + 1.57 \times 10^{-4}v^2$	$r = 0.998$
	$pK_2 = 4.79 + 1.62 \times 10^{-2}w + 2.20 \times 10^{-4}w^2$	$r = 0.999$
	$pK_2 = 4.80 + 9.17 \times 10^{-3}v + 2.56 \times 10^{-4}v^2$	$r = 0.998$
	$pK_3 = 6.42 + 2.30 \times 10^{-2}w + 1.67 \times 10^{-4}w^2$	$r = 0.999$
	$pK_3 = 6.43 + 1.49 \times 10^{-2}v + 2.18 \times 10^{-4}v^2$	$r = 0.998$
Boric acid	$pK_1 = 9.20 + 4.33 \times 10^{-2}w - 7.38 \times 10^{-5}w^2$	$r = 0.999$
	$pK_1 = 9.20 + 3.26 \times 10^{-2}v + 3.11 \times 10^{-5}v^2$	$r = 0.999$
Phthalic acid	$pK_1 = 2.97 + 1.63 \times 10^{-2}w + 1.34 \times 10^{-4}w^2$	$r = 0.999$
	$pK_1 = 2.97 + 1.03 \times 10^{-2}v + 1.71 \times 10^{-4}v^2$	$r = 0.999$
	$pK_2 = 5.39 + 4.14 \times 10^{-2}w + 1.51 \times 10^{-4}w^2$	$r = 0.999$
	$pK_2 = 5.40 + 2.86 \times 10^{-2}v + 2.46 \times 10^{-4}v^2$	$r = 0.999$
Acetic acid	$pK_1 = 4.76 + 1.88 \times 10^{-2}w + 3.03 \times 10^{-4}w^2$	$r = 0.999$
	$pK_1 = 4.77 + 9.66 \times 10^{-3}v + 3.49 \times 10^{-4}v^2$	$r = 0.999$

the deviation from linearity due to the poor stability of the emf measurements in boric acid solutions at 70% (w/w) acetonitrile.

In order to check the internal consistency of the results obtained a multilinear regression procedure is applied. The usual concentration by volume % (v/v), v, or % (w/w), w, values are the independent variables and second order polynomials shown in Table 4 are obtained.

To provide an independent interpretation of pK results, the linear solvation energy relationship (LSER) method, based on the Kamlet-Taft multiparameter scales [10], has been used. The solvatochromic LSER approach of Kamlet and Taft seeks to relate as a dissociation constant value, XYZ, with three types of terms as shown below, based on the differential evaluation of solvent dipolarity/polarizability, π^*, solvent hydrogen bond donating acidity, α, and solvent hydrogen bond accepting basicity, ß,

$$XYZ = XYZ_o + a\alpha + b\beta + s\pi^* \quad (7)$$

a, b and s represent the susceptibilities of XYZ to changing solvent solvatochromic properties [18]. Values of the Kamlet-Taft solvatochromic parameters π^* [11], α [19] and ß [20] for acetonitrile–water mixtures are known. As a result of application of LSER method to pK values determined in this work, the relationships shown in Table 5 are obtained. These equations allow us to know the pK values for the acid–base equilibria of standard buffers in any acetonitrile–water mixture, from a relatively small set of experimental data.

Table 5
Linear solvation energy relationships for pK values of pH reference materials (for definition of symbols, see text)

Substance		
Tartaric acid	$pK_1 = 11.74 - 10.05\pi^* + 3.42\alpha - 2.89\beta$	$r = 0.992$
	$pK_2 = 13.23 - 10.62\pi^* + 3.87\alpha - 3.03\beta$	$r = 0.990$
Citric acid	$pK_1 = 10.60 - 7.97\pi^* + 2.30\alpha - 2.37\beta$	$r = 0.995$
	$pK_2 = 13.94 - 10.54\pi^* + 3.53\alpha - 2.97\beta$	$r = 0.991$
	$pK_3 = 16.06 - 10.36\pi^* + 2.87\alpha - 2.61\beta$	$r = 0.992$
Boric acid	$pK_1 = 18.57 - 7.77\pi^* + 0.61\alpha - 0.68\beta$	$r = 0.999$
Phthalic acid	$pK_1 = 10.15 - 7.88\pi^* + 2.30\alpha - 2.01\beta$	$r = 0.994$
	$pK_2 = 19.09 - 13.72\pi^* + 2.79\alpha - 2.59\beta$	$r = 0.993$
Acetic acid	$pK_1 = 16.15 - 13.52\pi^* + 4.63\alpha - 3.31\beta$	$r = 0.993$

4. Acknowledgements

The financial support of the DGICYT (project PB91-0262) is gratefully acknowledged.

5. References

[1] T. Mussini, P. Longhi, S. Rondinini, M. Tettamanti and A.K. Covington, Anal. Chim. Acta, 174 (1985) 331.
[2] J. Barbosa and V. Sanz-Nebot, Mikrochimica Acta, in press.
[3] T. Mussini and F. Mazza, Electrochimica Acta, 32 (1987) 855.
[4] S. Rondinini and A. Nese, Electrochim. Acta, 32 (1987) 1499.
[5] S. Rondinini, P.R. Mussini and T. Mussini, Pure Appl. Chem., 59 (1987) 1549.
[6] A.K. Covington, R.G. Bates and R.A. Durst, Pure Appl. Chem., 57 (1985) 531.
[7] P. Longhi, P.R. Mussini, T. Mussini and S. Rondinini, J. Chem. Eng. Data, 34 (1989) 64.
[8] J. Barbosa, S. Butí and V. Sanz-Nebot, Talanta, in press.
[9] R.G. Bates, Crit. Rev. Anal. Chem., 10 (1981) 247.
[10] M.I. Kamlet, J.L.M. Abboud, M.H. Abraham and R.W. Taft, J. Org. Chem., 48 (1983) 2877.
[11] W.J. Cheong and P.W. Carr, Anal. Chem., 60 (1988) 820.
[12] J. Barbosa and V. Sanz-Nebot, Anal. Chim. Acta, 244 (1991) 183.
[13] J.E. Powell and M.A. Hiller, J. Chem. Educ., 34 (1957) 330.
[14] T. Mussini, A.K. Covington, P. Longhi and S. Rondinini, Pure Appl. Chem., 57 (1985) 865.
[15] J. Barbosa, J.L. Beltran and V. Sanz-Nebot, Talanta, submitted for publication.
[16] G. Kortum, W. Vogel and K. Andrussow, Dissociation Constants of Organic Acids in Aqueous Solution, IUPAC, Butterworths, London, 1961.
[17] D.D. Perrin, Dissociation Constants of Inorganic Acids and Bases in Aqueous Solution, IUPAC, Butterworths, London, 1969.
[18] C. Reichardt, Solvent and Solvent Effects in Organic Chemistry, VCH, Weinheim, 1988.
[19] J.H. Park, M.D. Jang, D.S. Kim and P.W. Carr, J. Chromatogr., 513 (1990) 107.
[20] T.M. Krygowski, P.K. Wrona, U. Zielkowska and C. Reichardt. Tetrahedron, 41 (1985) 4519.

ELSEVIER

Analytica Chimica Acta 288 (1994) 279–284

ANALYTICA CHIMICA ACTA

SSDI 0003-2670(94)00024-G

BOOK REVIEWS

Michael D. Morris (Ed.), *Microscopic and Spectroscopic Imaging of the Chemical State* (*Practical Spectroscopy A Series*, Vol. 17), Marcel Dekker, New York, 1993 (ISBN 0-8247-9104-5). viii + 493 pp. Price US$175.00.

Techniques for imaging analysis have evolved tremendously over the past decade. They allow the study of the spatial distribution of impurities in non-homogeneous samples and have many applications in the life sciences, earth sciences, and materials science. There is now a large range of atomic and molecular imaging methods available with spatial resolution from mm to atoms. These methods make use of a wide variety of combinations of excitation methods and spectroscopies and depend heavily on computer methods for data acquisition, storage and display. It is quasi-impossible for an individual to have experience in more than a few of these methods and a comprehensive multi-author source book on this subject, hence, fills a need.

This book is limited to spectroscopic imaging methods of the chemical state, i.e., these methods which provide molecule specific detection as opposed to the more readily available methods with atomic imaging potential. In twelve chapters a number of imaging techniques based on electronic and vibrational spectroscopy, nuclear and electron paramagnetic resonance, x-ray absorption and fluorescence, mass spectrometry, scanning tunneling and atomic force spectroscopy, near-field optical microscopy and chemical sensors are briefly summarised. The book starts with a few concise chapters on the fundamental underlying aspects of light microscopy and computer imaging methodology.

The editor did a good job: the range of methods treated is well chosen and the authors of the different chapters are leaders in their particular fields. There is practically no overlap between the different contributions and figures and layout are clear and well presented. The editor's own writing effort, however, was strictly limited to a very brief preface of slightly more than one page. A longer introductory overview covering the many common aspects of the imaging methods and a concluding chapter with at least some indications on what to expect as highlights in these methodologies for the near future would certainly have been of interest for many readers. The index, obviously an important item for multi-technique reference work, also is a weak spot; it could have been better designed and made more substantial.

The book is a useful reference text for both analytical chemists and for those applying the methods for their applications.

F. Adams

William D. Ehmann and Diane E. Vance, *Radiochemistry and Nuclear Methods of Analysis*, Wiley, Chichester, 1991 (ISBN 0-471-60076-8). xviii + 531 pp. Price £41.50.

The need for yet another book on nuclear science may be questioned, but the present text is justified by its readability and its relevant extensions outside the remit of the title, although there are a few deficiencies within the remit. A wealth of history, some of it anecdotal, should appeal to the market at which the book is aimed, namely a one-semester introductory course at undergraduate or graduate level. Within the fourteen chapters, the usual topics to be found in textbooks of

radiochemistry are dealt with clearly: some, such as radioactivation analysis, are covered extensively. Also of interest to the analytical chemist is the ion-beam analysis chapter in which the meanings of PIXE and other acronyms are made clear.

All aspects of radioanalytical chemistry known to the reviewer are treated. A whole chapter is devoted to nuclear dating with near-exhaustive coverage of methods. The chapter on cosmic radiochemistry conveys mind-boggling information, such as that the Planck era occupied 10^{-43}s after the "big bang", and provides a balance to the more mundane aspects of nuclear science. In the final chapter (Particle Generators) the section on nuclear reactors is less than complete. The potentialities of nuclear fusion are not discussed and the UK advanced gas cooled reactor receives scant mention, understandably perhaps in an American book. Some mention of nuclear accidents, their causes and effects, would have been appropriate: also in a book of this type, some discussion of future developments in the nuclear industry is desirable. A major omission in the text is any reference to the chemistry of the heavy radioelements: one would expect something at least about the separation of uranium and plutonium. But these shortcomings are minor. With a "terms to know" list, a reading list and exercises at the end of each chapter, and with appendixes on statistics, data sources, nuclear properties and physical constants, the book is not only a worthwhile student text (for whom its price may be prohibitively high, however) but also a useful general source of reference.

Colin G. Taylor

H.M. Stahr, *Analytical Methods in Toxicology*, Wiley, New York, 1991 (ISBN 0-471-85136-1). xxxvi + 328 pp. Price £82.00.

This book is an extremely useful practical manual for analytical toxicologists and chemists. It provides detailed, tried and tested methods for a wide range of analytes in most of the types of samples used by toxicologists. The introductory pages discuss safety, the importance of good sample collection, the use of radioisotopes and the nomenclature used.

The main part of the book is split into sections which broadly depend on the type of analyte. The sections are inorganic and other analysis, mycotoxin analysis, pesticide analysis, rodenticide analysis, the analysis of antibiotics, drugs, vitamins and feed additives and miscellaneous methods. Each method starts with a brief abstract and then follows with detailed descriptions of the reagents and apparatus needed for the method and the procedure. The calculations required to provide the final result are given and then sections on general considerations, accuracy, precision and interferences, and references are given, depending on the method. Specific safety precautions are provided for particularly hazardous analyses such as the determination of mycotoxins.

A large appendix section provides some theory and description of instrumental techniques, details about quality assurance and record keeping, and practical information such as how to clean glassware. Useful tables are also included.

Although I have not had an opportunity to try out the methods, they are all quite straightforward and could be easily followed with the details provided. The advantage of the book is that it provides a wide range of methods for the specific area of toxicology. The author is a very experienced analytical toxicologist from the Chemistry Laboratory, Veterinary Diagnostic Laboratory at Iowa State University and the methods in this book are those that have been tried and tested in this laboratory. The sensible and practical approach to safety throughout the book will be particularly valued by practicing analytical toxicologists.

Instrumental methods are included but the most modern techniques, which are highly applicable such as inductively coupled plasma atomic emission and mass spectrometry, and capillary zone electrophoresis, are not included. These omissions, however, are understandable because the instrumentation is expensive and new instrumental methods are not usually accepted by regulatory agencies until they are extremely well established. Otherwise the use of normality instead of molarity may cause confusion for some young

chemists and the inclusion of some typographical errors such as the title "Gas Chromatrophs" on p. 292 is unfortunate.

My criticisms of the book are few and I would highly recommend it to practical chemists and toxicologists.

G.M. Greenway

Stephen G. Schulman (Ed.), *Molecular Luminescence Spectroscopy. Methods and Applications:* Part 3, Wiley, New York, 1993 (ISBN 0-471-51580-9). xii + 467 pp.

This third volume comprises nine chapters on diverse aspects of luminescence. The first is a rather brief (23 pp.) account of chemiluminescence by Nakashima and Imai, and is followed by a most useful discussion of fluorescent probes for local physical and structural parameters (60 pp.) by Valleur, and a comprehensive description of photochemical fluorometry by Aaron (47 pp.). A short (16 pp.) chapter on organized bile salt media for luminescence analysis (McGown) and a detailed description of the very interesting phenomenon of spectral hole burning (80 pp., Holliday and Wild) precede the currently topical account of near-infrared luminescence spectroscopy (23 pp., Akiyama) and a useful description of microspectrofluorimetry on supported planar membranes (53 pp., Tamm and Kalb). The book concludes with a brief account of clinical applications of fluorescence spectroscopy, including fluoroimmunoassay (15 pp., Schenk) and a welcome extensive review of laser excited molecular fluorescence (121 pp., Hofstraat, Gooijer and Velthorst). This last article includes descriptions of the lasers and the detection systems used, applications to various types of analytes, low temperature spectroscopy and flow cytometry.

This is a well-produced text, which covers many of the topics of current interest in analytical luminescence, and is a worthy addition to the well-received previous volumes in this series.

Alan Townshend

W. Bertsch, G. Holzer and C.S. Sellers, Chemical Analysis for the Arson Investigator and Attorney, Hüthig, Heidelberg, 1993 (ISBN 3-7785-1890-9). xiii + 525 pp. Price DM198.00.

This monograph aims to present timely technical information to chemists and laboratory personnel and to provide a technical background for the community of fire loss adjustors, investigators, attorneys and judges, most of whom have had little education in chemistry. The authors have thus taken on a novel, difficult and challenging task, one which essentially requires two books within one text.

Chapter I, "Fire Investigation, Accelerants and Chemical Analysis. How do the pieces of the puzzle get together?", provides an overview of the entire field of chemical analysis as it relates to the determination of accelerants in fire debris. Chapter 2 "Fire Matter and Accelerants" deals with basic chemistry and physics of fire per se. Chapter 3 "Laboratory Methods", is a comprehensive review of accelerant recovery from debris and chromatography with particular reference to selective detectors. This is primarily directed at experts as are chapters 4 and 5, "Methods Development, Quality Assurance and Laboratory Protocol" and "Evaluation and Interpretation of Data", respectively. This latter section has a most useful introduction to pattern recognition techniques.

Considerable and successful efforts at bridge building have been made between expert and laypersons by extensive cross referencing and the provision of a comprehensive glossary and a library of chromatograms of the common types of accelerants encountered in practice. The authors are to be congratulated on the technical content and on the success of their approach, which will aid communication between technical experts and those involved in aspects of the investigative and judicial processes following accidental or deliberate fires as well as be invaluable in the training of new entants to the subject area.

D. Thorburn Burns

G. Kateman and L. Buydens, *Quality Control in Analytical Chemistry*, Wiley, New York, 2nd edn., 1993 (ISBN 0-471-55777-3). xvii + 317 pp. Price £49.50.

The first edition of this book, in 1981, broke new ground in the way that analytical measurements were viewed. This second edition provides the extension of these fundamental ideas especially in the context of good laboratory practice. A good measure of the thoroughness of a revised edition is the number of references included after the first edition publication date; in this instance it is 36%. The topics covered include sampling, quality of analytical procedures, quality control, filtering, data handling and pattern recognition. Laboratory organisation and management is considered briefly also in the context of cost benefit of analytical measurements. Much of the book is written in terms of mathematical and statistical parlance. However, it is not so daunting as to make it unreadable to the non-specialist. It provides a bridge between those who have an interest but little detailed knowledge of chemometrics and the specialist literature. This book should find a place on every analytical chemist's bookshelf who is seriously involved in maximising the benefit of analytical measurements within their organisation. In a book of only 317 pages there are some areas which deserved more attention; CUSUM analysis in particular. However, this is an excellent, well produced source work at a reasonable price.

C. Burgess

Gabor Patonay (Ed.), *HPLC Detection. Newer Methods*, VCH, Weinheim, 1992 (ISBN 3-527-28219-X). xii + 236 pp. Price DM158.00.

This collection of review articles describes detection methods that have been proposed as improvements to the established spectroscopic detectors. After a chapter on the concepts behind the assessment of detectors and the use of laser based systems, chapters describe long-lived luminescence and chemiluminescence methods and near-infrared spectroscopy. Tran discusses photothermal detectors, including the thermal lens detector (much acclaimed some years ago as the end to all detector problems). A chapter on FT-IR detection covers both on-line and solvent elimination methods.

Each chapter describes the background to the techniques and some examples of model applications. They each end on an optimistic note, the methods offer "promise", "wide application" is "imminent", "brought ... to the stage of viability" but frequently have to admit that problems have befallen their general acceptance.

Chapters by Wang on electrochemical detection (hardly a "new technique") and by Tomer on LC–MS look at techniques which are accepted but are not as widely used as their potential suggests. The final chapter by Albert and Bayer discusses LC–NMR, which has needed the advent of high field instruments to make it viable.

The chapters are introductions rather than comprehensive reviews although the theoretical background is usually well covered. As always with a book on an advancing field it is disappointed to find that it has taken a considerable time between preparation and publication, overall there are few 1990 or later references.

Roger M. Smith

L. Huber and S.A. George (Eds.), *Diode Array Detection in HPLC* (*Chromatographic Science Series*, Vol. 62), Marcel Dekker, New York, 1993 (ISBN 0-8247-8947-4). vii + 400 pp. Price US$150.00.

Commercial diode array detectors for LC first became available in the early 1980s and the ability to generate multivariate data from flowing streams rapidly and reliably led to their immediate acceptance for routine use. From the chromatographers viewpoint diode array technology offered a relatively low cost system that could be used for, e.g., peak identification and purity determination, full spectrum or multiple wavelength acquisition and three-dimensional detection.

The attractions of peak identification and purity determination are considered sufficiently important for a substantial chapter to be devoted to the subject in this book. It is a well written and comprehensive account that discusses topics such as derivative spectra and resolution very clearly with the aid of excellent figures. This follows on from a brief introduction to historical developments in diode array detection and a general discussion of its advantages.

The next chapter considers the use of chemometrics in conjunction with diode array detection, particularly with regard to the quantification of analytes in the presence of an unknown matrix. Factor analysis is the principal technique discussed in general terms with a brief explanation of approaches such as rank annihilation factor analysis and the generalized rank annihilation method for the quantification of components in unresolved peaks.

Due to the rapid emergence of the technique in the 1980s there is now a large database of applications in the literature. Half of the book is therefore devoted to a wide ranging survey of applications classified by area, e.g., clinical/toxicology, environmental, petrochemicals, biomolecules and food and beverages. Each example is accompanied by chromatograms and/or spectra that are in keeping with the high quality of presentation achieved throughout. The references for the application chapters give the reader a comprehensive database but include a high percentage of manufacturers' application notes.

The final two chapters provide useful practical information on optimization of the detection system and its use for automated routine analysis.

In summary the material is clearly and logically presented and there is a good balance between general discussion of the technique and practical details of specific applications. The book is Vol. 62 in the *Chromatographic Science Series* and is recommended as a valuable reference source for both technical information and potential uses.

Paul J. Worsfold

Norberto A. Guzman, *Capillary Electrophoresis Technology* (*Chromatographic Science Series,* Vol. 64), Marcel Dekker, New York, 1993 (ISBN 0-8247-9042-1). xv + 857 pp. Price US$165.00.

Capillary electrophoresis is currently the analytical separation technique that analytical scientists are most keen to learn about, and, if possible to apply, because of its high resolution, sensitivity and versatility. The present, large text provides the information required, in a series of thirty chapters, written by an international panel of experts. The contents are divided into five parts, viz. overview (3 chapters), the buffer system (4), the capillary column (5), instrumentation (7) and applications (11), including chiral separations, DNA sequencing, clinical diagnostics and forensic science. The book ends with a comprehensive subject index. Its appearance is timely, and will provide a wealth of information, both for the established practitioner in capillary electrophoresis, and the newcomer.

Hans-Peter Thier and Jochen Kirchoff (Eds.), *DFG Pesticides Commission. Manual of Pesticide Residue Analysis*, Vol. II, VCH, Weinheim, 1992 (ISBN 3-527-27017-5). xvi + 483 pp. Price DM168.00.

This volume is a direct continuation of Vol. I. Thirty-two methods for the determination of individual pesticides, five new and two updated methods for various classes of pesticides, and six methods for multiresidue analysis of water are described. All methods have been validated by at least one independent laboratory. Also included is a description and applications of the automated multiple development TLC technique, further descriptions of clean-up procedures, including solid-phase extraction, a means of deriving the limits of detection and determination based on the calibration curve concept, and four pages of electron impact mass spectrometric peaks and intensities. The book concludes with indexes of pesticides, metabolites and related compounds, analytical matrices, suppliers and authors.

Grenville Holland and Andrew N. Eaton (Eds.), *Applications of Plasma Source Mass Spectrometry II*, The Royal Society of Chemistry, Cambridge, 1993 (ISBN 0-85186-465-1). ix + 243 pp. Price £45.00.

These are the Proceedings of the *3rd International Conference on Plasma Source Mass Spectrometry*, held at Durham, UK, 13–18 September 1992. It comprises 26 presentations, covering a variety of topics, including isotopic analysis, glow discharge and environmental applications. The last paper, by Alan Gray, is entitled "So where do we go from here", and identifies six areas that are likely to provide important advances in the near future. The articles are prepared very clearly in camera-ready format. There is a brief subject index.

International Union of Pure and Applied Chemistry, Physical Chemistry Division, *Quantities, Units and Symbols in Physical Chemistry*, Blackwell, Oxford, 2nd edn., 1993 (ISBN 0-632-03583-8). ix + 167 pp. Price £14.95.

This "Green Book" is a slightly revised and appreciably extended version of its much valued predecessor, and provides an agreed basis for the quantities, units and symbols used in physical chemistry and, by implication, those other areas on which physical chemistry impinges. There are major changes to the sections on quantum mechanics and quantum chemistry, electromagnetic radiation and chemical kinetics. There is a new section on dimensionless quantities, and there are extensive indexes of abbreviations and acronyms, symbols and subjects. In total it is an indispensable companion to physical chemistry, and is perhaps one of the clearest demonstrations of the value of IUPAC activities.

ELSEVIER

Analytica Chimica Acta 288 (1994) 285–286

ANALYTICA CHIMICA ACTA

AUTHOR INDEX

ELSEVIER

Analytica Chimica Acta 288 (1994) 287

ANALYTICA CHIMICA ACTA

Erratum corrected 14 Jun 94/AP

Some processes occurring in graphite furnaces used for electrothermal atomic absorption spectrometry in the presence of organic chemical modifiers, *Analytica Chimica Acta*, 284 (1993) 367–377, by A.B. Volynsky, S.V. Tikhomirov, V.G. Senin and A.N. Kashin

p. 367, 11th line of the Abstract, and p. 368, 14th line, left column: analyser should read atomizer.

p. 368, 5th line of the Experimental section: "graphite-coated" should be deleted.

p. 375, 7th and 9th line of the right column: m_{crit} should read $m_{crit}g$. It represents the weight of the particles that can be kept at the liquid–gas boundary.

SSDI 0003-2670(94)00046-O

Calendar of forthcoming meetings

★ *indicates new or amended entry*

May 8-13, 1994
Minneapolis, MN, USA
HPLC '94. 18th International Symposium on High Performance Liquid Chromatography. *Contact:* Janet E. Cunningham, Barr Enterprises, P.O. Box 279, Walkersville, MD 21793, USA. Tel.: (301) 898-3772; Fax: (301) 898-5596.

★ ***May 9-11, 1994***
Basel, Switzerland
International Conference on Pharmaceutics — Validation of the Pharmaceutical Process. *Contact*: Technomic Publishing AG, Missionsstrasse 44, CH-4055 Basel, Switzerland. Tel.: 061/43 52 26; Fax: 061/43 52 59.

May 16-19, 1994
Ottawa, Ont., Canada
24th International Symposium on Environmental Analytical Chemistry. *Contact:* Dr. M. Malaiyandi, CAEC, Chemistry Department, Carleton University, Ottawa, Ont., Canada K1S 5B6; Fax: +1 613 788-3749; or Dr. J.F. Lawrence, Food Research Division, Banting Research Centre, Health and Welfare Canada, Ottawa, Ont., Canada K1A 0L2; Fax: +1 613 941-4775.

★ ***May 16-20, 1994***
Montreux, Switzerland
ISM '94 — 13th International Symposium on Microchemical Techniques; and SAS '94 — 2nd Symposium on Analytical Sciences. *Contact*: D'Conference 94, 7, rue d'Argout, 75002 Paris, France.

★ ***May 17, 1994***
Teddington, UK
Near Infra-Red Standards. Ultraviolet Spectrometry Group Meeting and Exhibition. *Contact*: Tom Frost, Analytical Development Dept., Wellcome Foundation, Dartford DA1 5AH, UK. Tel.: +44 322 223488, ext. 1970; Fax: +44 322 289285.

May 22-26, 1994
Venice, Italy
ESEAC '94. 5th European Conference of Electroanalysis. *Contact:* Prof. Salvatore Daniele, Department of Physical Chemistry, The University of Venice, Calle Larga S. Marta 2137, I-30123 Venice, Italy. Tel. +39 41 5298503; Fax: +39 41 5298594.

★ ***May 23-25, 1994***
Les Diablerets, Switzerland
The Seventh International Symposium on Polymer Analysis and Characterization (ISPAC-7). *Contact*: ISPAC Registration, 815 Don Gaspar, Sante Fe, NM 87501, USA. Tel: +1 (505) 989-4735; Fax: +1 (505) 989-1073 or Dr. M. Rinaudo, CERMAV-CNRS, B.P. 53X, 38041 Grenoble Cedex, France. Tel: +33 76541145; Fax: +33 76547203.

★ ***May 24-27, 1994***
Toronto, Canada
An International Symposium on Metals and Genetics. *Contact*: Prof. B. Sarkar, Dept. of Biochemistry, The Hospital for Sick Children, 555 University Avenue, Toronto, Ont., Canada M5G 1X8.

May 29-June 3, 1994
Chicago, IL, USA
42nd ASMS Conference on Mass Spectrometry and Allied Topics. *Contact:* Judith A. Sjoberg, ASMS, 815 Don Caspar, Santa Fe, NM 87501, USA. Tel.: +1 505 989-4517; Fax: +1 505 989-1073.

May 30-June 1, 1994
Bergen, Norway
SSIR 94. Scandinavian Symposium on Infrared and Raman Spectroscopy. *Contact*: Dr. Alfred A. Christy, Department of Chemistry, Allegt. 41, University of Bergen, N-5007 Norway. Tel.: +47 55 213363; Fax: +47 55 329058); or Laila Kyrkjebø, Department of Chemistry, University of Bergen. Tel.: +47 55 213342.

May 30-June 3, 1994
Nagoya, Japan
Pyrolysis 94. 11th International Symposium on Analytical and Applied Pyrolysis. *Contact:* Dr. H. Ohtani, Department of Applied Chemistry, Nagoya University, Nagoya 464-01, Japan. Tel.: +81 52-7815111, ext. 4664/3560; Fax: +81 52-7814895.

May 31-June 3, 1994
Bruges, Belgium
Second International Symposium on Hormone and Veterinary Drug Residue Analysis. *Contact:* Prof. C. van Peteghem, Symposium Chairman, Faculty of Pharmaceutical Sciences, University of Ghent, Harelbekestraat 72, B-9000 Ghent, Belgium. Tel.: +32 9-221 8951 ext. 235; Fax: +32 9-220 5243.

June 1-3, 1994
New Orleans, LA, USA
Biosensors '94. 3rd World Congress on Biosensors. *Contact:* Kay Russell, Elsevier Advanced Technology, Mayfield House, 256 Banbury Road, Oxford OX2 7DH, UK. Tel.: +44 865 512242; Fax: +44 865 310981.

June 5-7, 1994
Bruges, Belgium
VIth International Symposium on Luminescence Spectrometry in Biomedical Analysis — Detection Techniques and Applications in Chromatography and Capillary Electrophoresis. *Contact:* Prof. Dr. Willy R.G. Baeyens, Symposium Chairman, University of Ghent, Pharmaceutical Institute, Dept. of Pharmaceutical Analysis, Lab. of Drug Quality Control, Harelbekestraat 72, B-9000 Ghent, Belgium. Tel.: +32 9-2214175; Fax: +32 9-2218951.

June 8–11, 1994
Toledo, Spain
Flow Analysis VI. 6th International Conference on Flow Analysis. *Contact:* M. Valcarcel or M.D. Luque de Castro, Flow Analysis VI, Departmento de Química Analítica, Facultad de Ciencias, E-14004 Córdoba, Spain. Tel.: +34 57 218616; Fax: +34 57 218606.

June 12–15, 1994
Washington, DC, USA
1994 PREP Symposium and Exhibit. International Symposium on Preparative Chromatography. *Contact:* 1994 PREP Symposium Manager, c/o Barr Enterprises, 10120 Kelly Road, P.O. Box 279, Walkersville, MD 21793, USA. Tel.: +1 301 898-3772; Fax: +1 301 898-5596.

June 13–15, 1994
Lund, Sweden
FFF'94. 4th International Symposium on Field-Flow Fractionation. *Contact:* The Swedish Chemical Society, The Analytical Section, Wallingatan 24, 3tr, S-11124 Stockholm, Sweden. Fax: +46 46104525.

★ ***June 15–18, 1994***
Loen, Norway
Second International Symposium on Specification of Elements in Toxicology and In Environmental and Biological Sciences. *Contact*: Yngvar Thomassen (Symposium Chairman), National Institute of Occupational Health, P.O. Box 8149 DEP, N-0033 Oslo, Norway. Tel: +47 22466850; Fax: +47 22603276.

★ ***June 19–21, 1994***
Loen, Norway
5th Nordic Symposium on Trace Elements in Human Health and Disease. *Contact*: Yngvar Thomassen (Symposium Secretary), National Institute of Occupational Health, P.O. Box 8149 DEP, N-0033 Oslo, Norway. Tel: +47 22466850; Fax: +47 22603276.

June 19–24, 1994
Bournemouth, UK
20th International Symposium on Chromatography. *Contact:* The Executive Secretary, Chromatographic Society, Suite 4, Clarendon Chambers, 32 Clarendon Street, Nottingham NG1 5JD, UK. Tel.: +44 603-500596; Fax: +44 602-500614.

June 20–22, 1994
Valladolid, Spain
ESOPS-11. 11th European Symposium on Polymer Spectroscopy. *Contact:* J.M. Pastor, ESOPS-11, Física de la Materia Condensada, Facultad de Ciencias, Universidad de Valladolid, 47005 Valladolid, Spain. Tel.: +34 83 423194; Fax: +34 83 423192 or 423013.

June 20–23, 1994
Ringe, NH, USA
2nd Oxford Conference on Spectroscopy. *Contact:* Dr. Art Springsteen, Labsphere Inc., P.O. Box 70, North Sutton, NH 03260, USA. Tel.: +1 603 927-4266; or Dr. C. Burgess, Glaxo Manufacturing Servies, Harmire Road, Barnard Castle, Co. Durham, DL12 8DT, UK. Tel. +44 833-692490; Fax: +44 833-692774.

June 28–29, 1994
Singapore
CHEMSPEC ASIA 94. Exhibition and Conference. *Contact:* Jane Malcolm-Coe, PR & Publicity Manager, FMJ International Publications Ltd., Queensway House, 2 Queensway, Redhill, Surrey RH1 1QS, UK. Tel.: +44 737 768611; Fax: +44 737 761685.

★ ***July 3–7, 1994***
Veldhoven, The Netherlands
International Chemometrics Research Meeting. *Contact:* Laboratory for Analytical Chemistry, Faculty of Science, Catholic University of Nijmegen, Toernooiveld 1, 6525 ED Nijmegen, The Netherlands.

★ ***July 6–11, 1994***
Strasbourg, France
Reactivity in Organized Microstructures: New Materials. *Contact*: The Executive Director of the Programme: Dr. Josip Hendekovic, European Science Foundation, 1 quai Lezay-Marnésia, 67080 Strasbourg Cedex, France. Tel.: +33 88 76 71 35; Fax: +33 88 36 69 87.

★ ***July 10–13, 1995***
Vancouver, Canada
Vth COMTOX Symposium on Toxicology and Clinical Chemistry of Metals. *Contact*: F. William Sunderman Jr., M.D., Departments of Laboratory Medicine and Pharmacology, University of Connecticut Medical School, P.O. Box 1292, Farmington, CT 06034-1292, USA. Tel: (203) 679-2328; Fax: (203) 679-2154.

July 10–15, 1994
Merseburg, Germany
16th International Symposium on the Organic Chemistry of Sulfur. *Contact:* Dr. Schukat, Department of Chemistry, Martin Luther University Halle-Wittenberg, Geusaer Straße, D-06217 Merseburg, Germany. Tel.: +49 3461/462086; Fax: +49 3461/462370.

July 11–14, 1994
Norwich, UK
Spectroscopy Across the Spectrum IV: Techniques and Applications of Analytical Spectroscopy. *Contact:* Dr. D.L. Andrews, Hon. Secretary, Spectroscopy Across the Spectrum IV, School of Chemical Sciences, University of East Anglia, Norwich NR4 7TJ, UK.

★ ***July 17–22, 1994***
Paris, France
ICEM 13. 13th International Congress on Electron Microscopy. *Contact*: Secretariat ICEM 13, 67, rue Maurice Günsbourg, 94205 Ivry sur Seine Cedex, France.

July 20–22, 1994
Hull, UK
7th Biennial National Atomic Spectroscopy Symposium. *Contact:* Dr. Steve Haswell, School of Chemistry, University of Hull, Hull HU6 7RX, UK. Tel: +44 482-465469.

July 31–August 5, 1994
Ottawa, Ont., Canada
8th International Symposium on Molecular Recognition and Inclusion. *Contact:* Mrs. Hguette Morin-Dumais, 8th ISMRI, Steacie Institute for Molecular Sciences, National Research Council Canada, Room 1157, 100 Sussex Drive, Ottawa, Ont., Canada K1A 0R6. Tel.: +1 613 990-0936; Fax: +1 613 954-5242; E-mail: ismri@ned1.sims.nrc.ca.

August 2–6, 1994
Changchun, P.R. China
The Second Changchun International Symposium on Analytical Chemistry (CISAC). *Contact:* Prof. Qinhan Jin, Department of Chemistry, Jilin University, Changchun 130023, P.R. China. Tel.: 0431-822331, ext. 2433; Fax: 0431-823907.

August 22–26, 1994
Hong Kong
ICORS '94. XIV International Conference on Raman Spectroscopy. *Contact:* Prof. Nai-Teng Yu, ICORS '94, c/o De-

partment of Chemistry, The Hong Kong University of Science and Technology, Clear Water Bay, Kowloon, Hong Kong.

August 23–26, 1994
Guildford, UK
QSA-8. International Conference on Quantitative Suface Analysis: Techniques and Applications. *Contact:* Doreen Tilbrook, Division of Materials Metrology, National Physical Laboratory, Teddington, Middlesex TW11 0LW, UK.

★ ***August 23–28, 1994***
Sapporo, Japan
International Trace Analysis Symposium '94 (ITAS '94). *Contact*: Prof. Hiroto Watanabe, Laboratory of Analytical Chemistry, Faculty of Engineering, Hokkaido University, Sapporo 060, Japan. Tel.: +81 11-716-2111, ext. 6743; Fax: +81 11-726-4454.

★ ***August 24–26, 1994***
York, UK
International Symposium on Capillary Electrophoresis (jointly with the Chromatographic Society and the British Electrophoresis Society). *Contact*: Dr. T.L. Threlfall, Industrial Liason Executive, Department of Chemistry, University of York, York, YO1 5DD, UK. Tel: +44 904 432576 or 904 432511; Fax: +44 904 432516.

September 11–16, 1994
Essen, Germany
EUCMOS XXII. XXII European Congress on Molecular Spectroscopy. *Contact:* Congress Secretariat, Gesellschaft Deutscher Chemiker, Abt. Tagungen, P.O. Box 900440, W-6000 Frankfurt 90, Germany. Tel.: +49 69 7917-366; Fax +49 69 7917-475; Telex 4 170 497 gdch d. *(Further details published in Vol. 272, No. 2).*

September 12–14, 1994
Paris, France
Workshop on Biosensors and Biological Techniques in Environmental Analysis. *Contact:* Prof. M.-C. Hennion, ESPCI, Lab. Chimi Analytique, 10 rue Vauquelin, 75005 Paris, France.

★ ***September 12–15, 1994***
Portland, OR, USA
108th AOAC International Annual Meeting and Exposition. *Contact*: Margaret Ridgell, AOAC International, 2200 Wilson Blvd., Suite 400, Arlington, VA 22201-3301, USA. Tel.: +1 703-522-3032; Fax: +1 703-522-5458.

September 12–17, 1994
Madrid, Spain
Frontiers in Analytical Chemistry: Surface and Interface Analysis. A course organized with the ERASMUS Network "Analytical Chemistry". *Contact:* Prof. Dr. A. Sanz-Medel, Universidad di Oviedo, Quimica Fisica e Analitica, E-33006, Oviedo, Spain. Tel.: +34 8 510-3474; Fax: +34 8 50-3480.

September 18–22, 1994
Chambéry, Savoy, France
14th International CODATA Conference. Data and Knowledge in a Changing World: The Quest for a Healthier Environment. *Contact:* Prof. J.-E. Dubois, ITODYS, Université Paris 7, 1 rue Guy de la Brosse, 75005 Paris, France. Fax: +33 1 42881466. E-mail: codata@paris7.jussieu.fr (Internet).

★ ***September 19–22, 1994***
Turin, Italy
International Ion Chromatography Symposium 1994. *Contact*: Century International, P.O. Box 493, Medfield, MA 02052, USA. Tel.: +1 508/359-8777; Fax: +1 508/359-8778.

September 21–23, 1994
Stockholm, Sweden
5th International Symposium on Pharmaceutical and Biomedical Analysis: *Contact:* Swedish Academy of Pharmaceutical Sciences, P.O. Box 1136, S-111 81 Stockholm, Sweden. Tel.: +46 8 245085; Fax: +46 8 205511.

September 22–24, 1994
Constanta, Romania
12th Conference on Analytical Chemistry. *Contact:* Dr. Gabirel-Lucian Radu, Romanian Society of Analytical Chemistry, 13 Blvd. Carol I, Sector 3, 70346 Bucharest, Romania.

★ ***September 25–30, 1994***
Goa, India
ISMEBC '94. International Conference on Molecular Electronics and Biocomputing. *Contact*: Dr. Ratna S. Phadke, Scientific Secretary for ISMEBC '94, Chemical Physics Group, Tata Institute of Fundamental Research, Homi Bhabha Road, Bombay 400 005, India. Tel: +91 (22) 215 2971; Fax: +91 (22) 215 2110 e-mail: mebc@tifrvax.bitnet mebc@tifrvax.tifr.res.in.

★ ***September 25–30, 1994***
Bristol, UK
1994 European Workshop in Chemometrics. *Contact*: Janice Green, School of Chemistry, University of Bristol, Cantock's Close, Bristol BS8 1TS, UK. Tel: +44 (0)272 303030 ext. 4421 (ansaphone) or +44 (0)272 303672; Fax: +44 (0) 272 251295.

★ ***September 26–28, 1994***
Basel, Switzerland
Chemometrics: Multivariate Analysis and Design in Chemical Research and Development. *Contact*: S. Morgenthaler, ASS, EPFL, Dept. de Mathématiques, CH-1015 Lausanne, Switzerland.

October 3–7, 1994
St. Peterburg, Russia
ISCMS '94. International Symposium: Chromatography and Mass Spectrometry in Environmental Analysis. *Contact:* ISCMS '94, Dr. Alexander Rodin, State Institute of Applied Chemistry, Dobrolubov Ave. 14, 197198, St. Petersburg, Russia. Tel.: +7 812 2389786; Fax: +7 812 2338989; Telex: 121345 ptb sigma.

★ ***October 11–13, 1994***
Amsterdam, The Netherlands
6th International Colloquium Solid Sampling with Atomic Spectroscopy. *Contact*: Prof. Dr. R.F.M. Herber, Coronel Laboratory, University of Amsterdam, Meibergdreef 15, 1105 AZ Amsterdam, The Netherlands.

October 17–19, 1994
Strasbourg, France
3rd International Symposium on Supercritical Fluids: Thermodynamics, Physico-chemical Properties, Technology and Applications. *Contact:* ISASF, Mle. Brionne, ENSIC, P.O. Box 451, F-54001 Nancy Cedex, France. Tel.: +33 83175003; Fax: +33 83350811.

★ ***October 31–November 2, 1994***
Minneapolis, USA
Anabiotec '94. 5th International Symposium on Analytical Methods, Systems and Strategies in Biotechnology. *Con-*

tact: Anabiotec Conference Secretariat, Elsevier Advanced Technology, Mayfield House, 256 Banbury Road, Oxford, OX2 7DH, U.K., Tel: +44 (0)865 512242, Fax: +44 (0)865 310981.

November 9–11, 1994
Montreux, Switzerland
11th Montreux Symposium on Liquid Chromatography–Mass Spectrometry (LC/MS; SFC/MS; CE/MS; MS/MS). *Contact:* M. Frei-Häusler, Postfach 46, CH-4123 Allschwil 2, Switzerland. Tel.: +41 61-4812789; Fax: +41 61-4820805.

November 21–22, 1994
Enschede, The Netherlands
μTAS'94. Workshop on Micro Total Analysis Systems. *Contact:* Dr. Albert van den Berg, University of Twente, MESA Research Institute, P.O. Box 217, 7500 AE Enschede, The Netherlands. Tel. +31 53 892 691; Fax: +31 53 309 547.

March 6–10, 1995
PITTCON '95. Pittsburgh Conference on Analytical Chemistry and Applied Spectroscopy. *Contact:* Pittsburgh Conference, Suite 332, 300 Penn Center Blvd., Pittsburgh, PA 15235-9962, USA.

May 9–12, 1995
Jülich, Germany
6th International Hans Wolfgang Nürnberg Memorial Symposium on Metal Compounds in Environment and Life, 6: Analysis, Speciation and Specimen Banking. *Contact:* Dr. H.W. Dürbeck, Institute of Applied Physical Chemistry, Research Center, Jülich (KFA), P.O. Box 1913, D-5170 Jülich, Germany.

June 5–8, 1995
Singapore
Fifth Symposium on Our Environment and First Asia-Pacific Workshop on Pesticides. *Contact:* The Secretariat, 5th Symposium on Our Environment, c/o Department of Chemistry, National University of Singapore, Kent Ridge, Rep. Singapore 0511. Fax: +65 779-1691.

July 9–15, 1995
Hull, UK
SAC 95. *Contact:* Analytical Division, The Royal Society of Chemistry, Burlington House, Piccadilly, London W1V 0BN, UK. Tel.: +44 71 437-8656; Fax: +44 71 734-1227.

August 27–September 1, 1995
Leipzig, Germany
CSI XXIX. Colloquium Spectroscopicum Internationale XXIX. *Contact:* Gesellschaft Deutscher Chemiker, Abt. Tagungen, P.O. Box 90 04 40, D-60444 Frankfurt/ Main, Germany.

August 27–September 1, 1995
Budapest, Hungary
10th International Conference on Fourier Transform Spectroscopy. *Contact:* Mrs. Klára Láng/Mr. Attila Varga, Conference Office, Roland Eötvös Physical Society, P.O. Box 433, H-1371 Budapest, Hungary. Tel./Fax: +36 1 201-8682.

September 4–5, 1995
Paris, France
Sample Handling of Pesticides in the Aquatic Environment. Short course preceding the 5th Workshop on Chemistry and Fate of Modern Pesticide. *Contact:* Prof. M.-C. Hennion, ESPCI, Lab. Chimi Analytique, 10 rue Vauquelin, 75005 Paris, France.

September 6–8, 1995
Paris, France
5th Workshop on Chemistry and Fate of Modern Pesticides. *Contact:* Prof. M.-C. Hennion, ESPCI, Lab. Chimi Analytique, 10 rue Vauquelin, 75005 Paris, France.

September 12–15, 1995
Leuven, Belgium
5th International Symposium on Drug Analysis. *Contact:* Prof. J. Hoogmartens, Drug Analysis '95, Institute of Pharmaceutical Sciences, Van Evenstraat 4, B-3000 Leuven, Belgium. Tel.: +32 16 283440; Fax: +32 16 283448.

Announcement of meeting

ANABIOTEC '94 5th INTERNATIONAL SYMPOSIUM ON ANALYTICAL METHODS, SYSTEMS AND STRATEGIES IN BIOTECHNOLOGY, MINNEAPOLIS, USA, OCTOBER 31–NOVEMBER 2, 1994

Since its inception Anabiotec has acted as a forum for the appraisal of new and exciting research developments in the analytical chemistry of biological systems.

The analytical chemistry of extremely complex matrices involving species of biological origin is a rapidly developing research frontier. The problems of identification and quantification in mixtures range from *in vivo* determination of glucose to detection of cells in a fermentation vessel. It is clear that these analytical demands present enormous challenges to the analytical chemist, biochemist and biotechnologist alike.

The increasing synergy between the fields of analytical chemistry, biochemistry, clinical chemistry and biotechnology necessitates a forum such as Anabiotec where all involved can appreciate the importance of biocomplexity and the op-

portunities for its continued evolution. Accordingly, an exciting feature of this Symposium is the opportunity to bring together individuals from academia and industry, with emphasis being placed on active participation and discussion to promote the maximum exchange of information.

Anabiotec '94 is a three-day event consisting of plenary sessions, selected original papers, posters and an exhibition. Topics scheduled for discussion include:

— New instruments and techniques for analytical biochemistry
— Monitoring of industrial scale processes such as fermentation technology
— Strategies for clinical diagnosis, including biosensor formats

For further information please contact: Anabiotec Conference Secretariat, Elsevier Advanced Technology, Mayfield House, 256 Banbury Road, Oxford, OX2 7DH, UK. Tel.: +44 (0)865 512242; Fax: +44 (0)865 310981.

Announcements are included free of charge. Information on planned events should be sent well in advance (preferably 6 months or more) to:
ACA Newsbrief,
Elsevier Science B.V.,
P.O. Box 330,
1000 AH Amsterdam,
The Netherlands
Fax: (+31) 20 5862 459

ELECTROCHEMICAL SENSORS

SYMPOSIUM

DEDICATED TO THE MEMORY OF PROFESSOR

WILHELM SIMON

15–18 September, 1994
Mátrafüred, Hungary

Organized by
the Electroanalytical Committee
of the Hungarian Academy of Sciences
the Research Group for Technical Analytical Chemistry
of the Hungarian Academy of Sciences

Sponsored by
the Hungarian Academy of Sciences
the National Committee for Technological Development
the Federation of the European Chemical Societies

The Symposium on ELECTROCHEMICAL SENSORS dedicated to the memory of the late Professor Wilhelm SIMON will be organized by the Electroanalytical Committee of the Hungarian Academy of Sciences at Mátrafüred (in a hilly area 100 km North-East of Budapest), Hungary on September 15–18, 1994.

TOPICS

1. New sensing devices
2. Modified electrodes, microelectrodes
3. Novel techniques and applications

ADDRESS OF THE ORGANIZING COMMITTEE

Dr. Andrea Hrabéczy
Organizing Committee,
Symposium on Electrochemical Sensors
Institute for General and Analytical Chemistry,
Technical University Budapest
H–1502 Budapest, Szent Gellért tér 4., HUNGARY

Announcement from the Publisher

Elsevier Science encourages submission of articles on floppy disk.

All manuscripts may now be submitted on computer disk, with the eventual aim of reducing production times still further.

- The preferred storage medium is a 5¼ or 3½ inch disk in MS-DOS format, although other systems are welcome, e.g. Macintosh.
- After **final acceptance**, your disk plus one final, printed and exactly matching version (as a printout) should be submitted together to the editor. **It is important that the file on disk and the printout are identical.** Both will then be forwarded by the editor to Elsevier.
- Illustrations should be provided in the usual manner.
- Please follow the general instructions on style/arrangement and, in particular, the reference style of this journal as given in 'Instructions to Authors'.
- Please label the disk with your name, the software & hardware used and the name of the file to be processed.

Contact the Publisher for further information:

Elsevier Science
Analytica Chimica Acta
P.O. Box 330
1000 AH Amsterdam, The Netherlands
Phone: (+31-20) 5862 791 Fax: (+31-20) 5862 459

ELSEVIER SCIENCE

Experimental Design: A Chemometric Approach

Second, Revised and Expanded Edition

By **S.N. Deming** and **S.L. Morgan**

Data Handling in Science and Technology Volume 11

Now available is the second edition of a book which has been described as
"...an exceptionally lucid, easy-to-read presentation... would be an excellent addition to the collection of every analytical chemist. I recommend it with great enthusiasm."
(Analytical Chemistry).
N.R. Draper reviewed the first edition in Publication of the International Statistical Institute
"...discussion is careful, sensible, amicable, and modern and can be recommended for the intended readership."

The scope of the first edition has been revised, enlarged and expanded. Approximately 30% of the text is new. The book first introduces the reader to the fundamentals of experimental design. Systems theory, response surface concepts, and basic statistics serve as a basis for the further development of matrix least squares and hypothesis testing. The effects of different experimental designs and different models on the variance-covariance matrix and on the analysis of variance (ANOVA) are extensively discussed. Applications and advanced topics (such as confidence bands, rotatability, and confounding) complete the text. Numerous worked examples are presented.

The clear and practical approach adopted by the authors makes the book applicable to a wide audience. It will appeal particularly to those with a practical need (scientists, engineers, managers, research workers) who have completed their formal education but who still need to know efficient ways of carrying out experiments. It will also be an ideal text for advanced undergraduate and graduate students following courses in chemometrics, data acquisition and treatment, and design of experiments.

Contents:

© 1993 454 pages Hardbound
Price: Dfl. 310.00 (US$ 177.25)
ISBN 0-444-89111-0

ELSEVIER SCIENCE

ORDER INFORMATION
ELSEVIER SCIENCE B.V.
P.O. Box 330
1000 AH Amsterdam
The Netherlands
Fax: (+31-20) 5862 845

For USA and Canada
P.O. Box 945
Madison Square Station
New York, NY 10159-0945
Fax: (212) 633 3680

US$ prices are valid only for the USA & Canada and are subject to exchange rate fluctuations; in all other countries the Dutch guilder price (Dfl.) is definitive. Customers in the European Union should add the appropriate VAT rate applicable in their country to the price(s). Books are sent postfree if prepaid.

CHEMOMETRICS TUTORIALS II

edited by **R.G. Brereton**, University of Bristol, Bristol, UK, **D.R. Scott**, U.S. Environmental Protection Agency, Research Triangle Park, NC, USA, **D.L. Massart**, Vrije Universiteit Brussel, Brussels, Belgium, **R.E. Dessy**, Virginia Polytechnic Institute, Blackburg, VA, USA, **P.K. Hopke**, Clarkson University, Potsdam, NY, USA, **C.H. Spiegelman**, Texas A&M University, College Station, TX, USA and **W. Wegscheider**, Universität Graz, Graz, Austria

The journal Chemometrics and Intelligent Laboratory Systems has a specific policy of publishing tutorial papers (i.e. articles aiming to discuss and illustrate the application of chemometric and other techniques) solicited from leading experts in the varied disciplines relating to this subject. This book comprises reprints of tutorials from Volumes 6-11 of this journal, covering the period from mid 1989 to late 1991. The authors of the papers include analytical, organic and environmental chemists, statisticians, pharmacologists, geologists, geochemists, computer scientists and biologists, which reflects the strong interdisciplinary communication. The papers have been reorganized into major themes, covering most of the main areas of chemometrics.

This book is intended both as a personal reference text and as a useful background for courses in chemometrics and laboratory computing.

1992 x + 314 pages
Paperback
Price: US $ 156.50 / Dfl. 250.00
ISBN 0-444-89858-1

ORDER INFORMATION

For USA and Canada
ELSEVIER SCIENCE

Judy Weislogel
P.O. Box 945
Madison Square Station,
New York, NY 10160-0757
Tel: (212) 989 5800
Fax: (212) 633 3880

In all other countries
ELSEVIER SCIENCE

P.O. Box 211
1000 AE Amsterdam
The Netherlands
Tel: (+31-20) 5803 753
Fax: (+31-20) 5803 705

US$ prices are valid only for the USA & Canada and are subject to exchange rate fluctuations; in all other countries the Dutch guilder price (Dfl.) is definitive. Books are sent postfree if prepaid.

ELSEVIER
SCIENCE

PUBLICATION SCHEDULE FOR 1994

	S'93	O'93	N'93	D'93	J	F	M	A	M			
Analytica Chimica Acta	281/1 281/2 281/3	282/1 282/2 282/3	283/1 283/2	283/3 284/1 284/2	284/3 285/1–2 285/3	286/1 286/2 286/3	287/1–2 287/3 288/1–2	288/3 289/1 289/2	289/3 290/1–2 290/3			
Vibrational Spectroscopy		6/1			6/2		6/3		7/1			

INFORMATION FOR AUTHORS

Detailed "Instructions to Authors" for *Analytica Chimica Acta* was published in Volume 256, No. 2, pp. 373–376. Free reprints of the "Instructions to Authors" of *Analytica Chimica Acta* and *Vibrational Spectroscopy* are available from the Editors or from: Elsevier Science B.V., P.O. Box 330, 1000 AH Amsterdam, The Netherlands. Telefax: (+31-20) 5862459.

Manuscripts. The language of the journal is English. English linguistic improvement is provided as part of the normal editorial processing. Authors should submit three copies of the manuscript in clear double-spaced typing on one side of the paper only. *Vibrational Spectroscopy* also accepts papers in English only.

Rapid publication letters. *Letters* are short papers that describe innovative research. Criteria for letters are novelty, quality, significance, urgency and brevity. Submission data: max. of 2 printed pages (incl. Figs., Tables, Abstr., Refs.); short abstract (e.g., 3 lines); *no* proofs will be sent to the authors; submission on floppy disc; *no* revision will be possible.

Abstract. All papers and reviews begin with an Abstract (50–250 words) which should comprise a factual account of the contents of the paper, with emphasis on new information.

Figures. Figures should be prepared in black waterproof drawing ink on drawing or tracing paper of the same size as that on which the manuscript is typed. One original (or sharp glossy print) and two photostat (or other) copies are required. Attention should be given to line thickness, lettering (which should be kept to a minimum) and spacing on axes of graphs, to ensure suitability for reduction in size on printing. Axes of a graph should be clearly labelled, along the axes, outside the graph itself. All figures should be numbered with Arabic numerals, and require descriptive legends which should be typed on a separate sheet of paper. Simple straight-line graphs are not acceptable, because they can readily be described in the text by means of an equation or a sentence. Claims of linearity should be supported by regression data that include slope, intercept, standard deviations of the slope and intercept, standard error and the number of data points; correlation coefficients are optional. Photographs should be glossy prints and be as rich in contrast as possible; colour photographs cannot be accepted. Line diagrams are generally preferred to photographs of equipment. Computer outputs for reproduction as figures must be good quality on blank paper, and should preferably be submitted as glossy prints.

Nomenclature, abbreviations and symbols. In general, the recommendations of IUPAC should be followed, and attention should be given to the recommendations of the Analytical Chemistry Division in the journal *Pure and Applied Chemistry* (see also *IUPAC Compendium of Analytical Nomenclature, Definitive Rules*, 1987).

References. The references should be collected at the end of the paper, numbered in the order of their appearance in the text (*not* alphabetically) and typed on a separate sheet.

Reprints. Fifty reprints will be supplied free of charge. Additional reprints (minimum 100) can be ordered. An order form containing price quotations will be sent to the authors together with the proofs of their article.

Papers dealing with vibrational spectroscopy should be sent to: Dr J.G. Grasselli, 150 Greentree Road, Chagrin Falls, OH 44022, U.S.A. Telefax: (+1-216) 2473360 (Americas, Canada, Australia and New Zealand) or Dr J.H. van der Maas, Department of Analytical Molecular Spectrometry, Faculty of Chemistry, University of Utrecht, P.O. Box 80083, 3508 TB Utrecht, The Netherlands. Telefax: (+31-30) 518219 (all other countries).

0003-2670/94/$07.00

This issue is printed on acid-free paper.

PRINTED IN THE NETHERLANDS

Analytical Applications of Circular Dichroism

Edited by **N. Purdie** and **H.G. Brittain**

Techniques and Instrumentation in Analytical Chemistry Volume 14

Circular dichroism is a special technique which provides unique information on dissymmetric molecules. Such compounds are becoming increasingly important in a wide variety of fields, such as natural products chemistry, pharmaceutics, molecular biology, etc. The content of this book has been selected in order to feature the unique aspects of circular dichroism, and how these strengths can be of assistance to workers in the field.

Substantial discussions have been provided regarding the particular phenomena associated with dissymmetric compounds which give rise to the circular dichroism effect. Reviews are also given of the type of instrumentation available for the measurement of these effects. A number of chapters cover the wide range of applications illustrating the power of the method.

Owing to its broad appeal, the book will be of interest to workers in all areas of chemistry and pharmaceutical science.

Contents:

© 1994 360 pages Hardbound
Price: Dfl. 355.00 (US $ 202.75)
ISBN 0-444-89508-6

ORDER INFORMATION

For USA and Canada
ELSEVIER SCIENCE INC.
P.O. Box 945
Madison Square Station
New York, NY 10160-0757
Fax: (212) 633 3880

In all other countries
ELSEVIER SCIENCE B.V.
P.O. Box 330
1000 AH Amsterdam
The Netherlands
Fax: (+31-20) 5862 845

US$ prices are valid only for the USA & Canada and are subject to exchange rate fluctuations; in all other countries the Dutch guilder price (Dfl.) is definitive. Customers in the European Community should add the appropriate VAT rate applicable in their country to the price(s). Books are sent postfree if prepaid.

ELSEVIER SCIENCE B.V.

0003-2670(19940411)288:3;1-8